APPENDIX IR13-1 NATIONAL RESEARCH COUNCIL CANADA PHYSICAL MODEL STUDY REPORT

ALBERTA TRANSPORTATION SPRINGBANK OFF-STREAM RESERVOIR PROJECT
RESPONSE TO CEAA INFORMATION REQUEST PACKAGE 3, AUGUST 31, 2018

Appendix IR13-1 National Research Council Canada Physical Model Study Report
May 2019

Stantec

NATIONAL RESEARCH COUNCIL CANADA

Physical Model Study of the Springbank Off-stream Storage Project Diversion Structure on the Elbow River

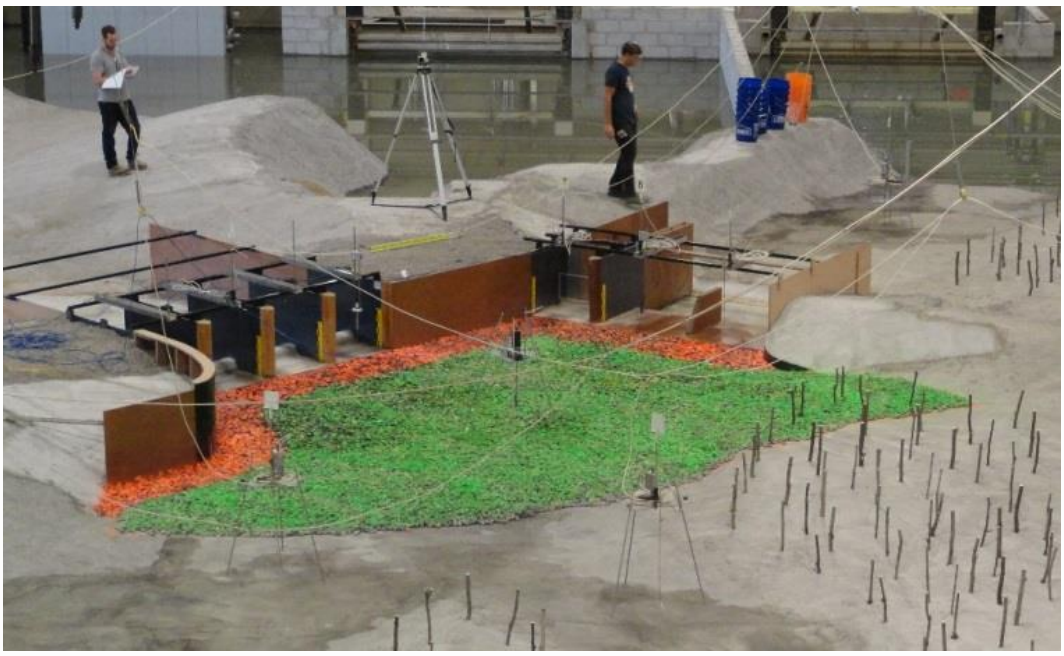

Paul Knox, Andrew Cornett, Mitchel Provan

Ocean, Coastal and River Engineering

NRC Technical Report: OCRE-TR-2016-028

December 2016

National Research Council Canada | Conseil national de recherches Canada

Canada

ABSTRACT

Stantec Consulting (Stantec) was retained by the government of Alberta to complete the engineering design for a new flood diversion channel and off-stream storage reservoir on the Elbow River as part of the Springbank Off-stream Storage Project. As part of the design effort, physical model studies were required to evaluate the performance of the preliminary design in operational and extreme conditions. Of particular interest are the interactions with water-borne sediments and debris. A physical hydraulic model of the proposed sluiceway for the diversion inlet structure and service spillway for the main channel of the river was constructed at an undistorted geometric scale of 1:16 in the facilities of the National Research Council – Ocean, Coastal and River Engineering (NRC-OCRE) research laboratory located in Ottawa, Canada. The purpose of the physical model study was to investigate the performance of the proposed civil works under a given range of design conditions supplied by Stantec. A large quantity of information was obtained on the performance of the diversion inlet and service spillway, the water levels and velocities encountered in the river and floodplain, the fate of the river sediments, and the interaction of tree debris with the proposed structures during floods.

TABLE OF CONTENTS

LIST OF TABLES

Page

LIST OF FIGURES

Page

1 INTRODUCTION

Stantec Consulting (Stantec) was retained by the government of Alberta to complete the engineering design for a new flood diversion channel and off-stream storage reservoir on the Elbow River as part of the Springbank Off-stream Storage Project. As part of the design effort, the National Research Council of Canada's Ocean Coastal and River Engineering Portfolio (NRC-OCRE) was commissioned by Stantec to conduct a physical model study to support the design of the diversion inlet and service spillway as well as some of the civil works adjacent to the structures. The scope of NRC-OCRE's work included the design, construction, and outfitting of a three-dimensional physical model of a portion of the floodplain and river at the site, model versions of the proposed diversion inlet and service spillways structures (concrete aprons, retaining walls, gate structures, energy dissipation features and stilling basins), the floodplain berm, and a portion of the downstream diversion channel and main river channel. The performance of the structures to pass design flood flows was of interest, in particular their interactions with water-borne sediments and debris.

2 PROJECT BACKGROUND

2.1 Site Conditions

The Elbow River flows through southwest Calgary and is susceptible to flooding with catastrophic results. During the flood of June 2013, the peak flow rate of the Elbow River entering the Glenmore Reservoir reached approximately 1240m^3/s. The capacity of the river without taking flooding precautions is 180m^3/s. Assessments made by the City of Calgary estimates that there is up to $942 million at risk in the event of a 1-in-200 year flood. As part of a flood mitigation study, the Springbank Off-stream Storage Project was conceived to divert part of the flows of the Elbow River during floods into an off-stream storage reservoir where the flood water would be stored and released gradually back into the Elbow River after the flood has passed.

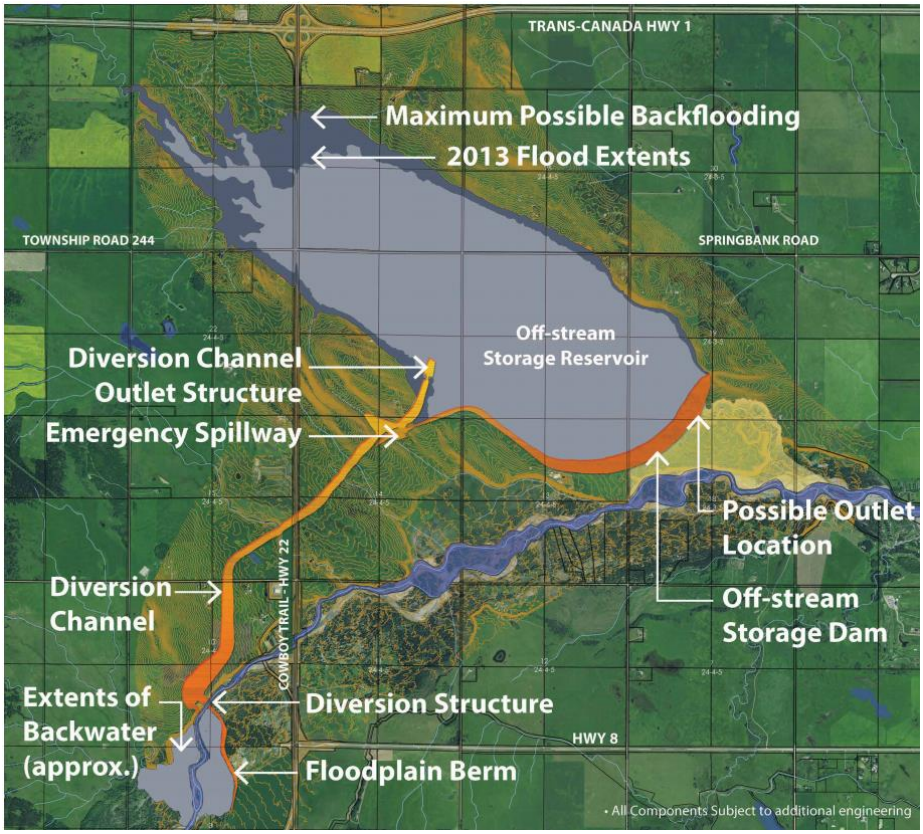

Figure 1. Location of Springbank Off-stream Storage Project (Government of Alberta, 2016)

2.2 Proposed Structures

The proposed structures include a gated diversion inlet structure that intersects the Elbow River, a diversion channel excavated through the adjacent land to transport the flow to the off-stream storage reservoir, a gated service spillway that would control the flow through the Elbow River at the diversion junction and a floodplain berm that lines the south-east portion of the upstream floodplain. The physical model study investigated two design layouts for the diversion inlet and service spillway – the initial proposed design, and one that was revised based on the results and observations seen during the testing phase of the study. The model was used to determine the gate settings for various flow rates, as well as improve several features of each design to better handle the flow, sediment loads, or woody debris.

2.2.1 *Initial Design*

The original designs for the diversion inlet and service spillway are shown in Figure 2 to Figure 6. The diversion inlet structure featured four 10m wide bays separated by 2m wide piers, radial gates to control the flow, and energy dissipation chute blocks through the stilling basin. There were two structures to control the flow of the main river channel – a 10m wide sluiceway featuring a radial gate, and a 31m wide service spillway with Obermeyer style crest gates. There were curved retaining walls on the west side of the diversion inlet and also on the east side of the service spillway (fronting

the floodplain berm). A 31.63m straight-line retaining wall joined the diversion inlet to the service spillway. Fronting the entire set of structures was a 10m wide riprap bed intended to protect against scour.

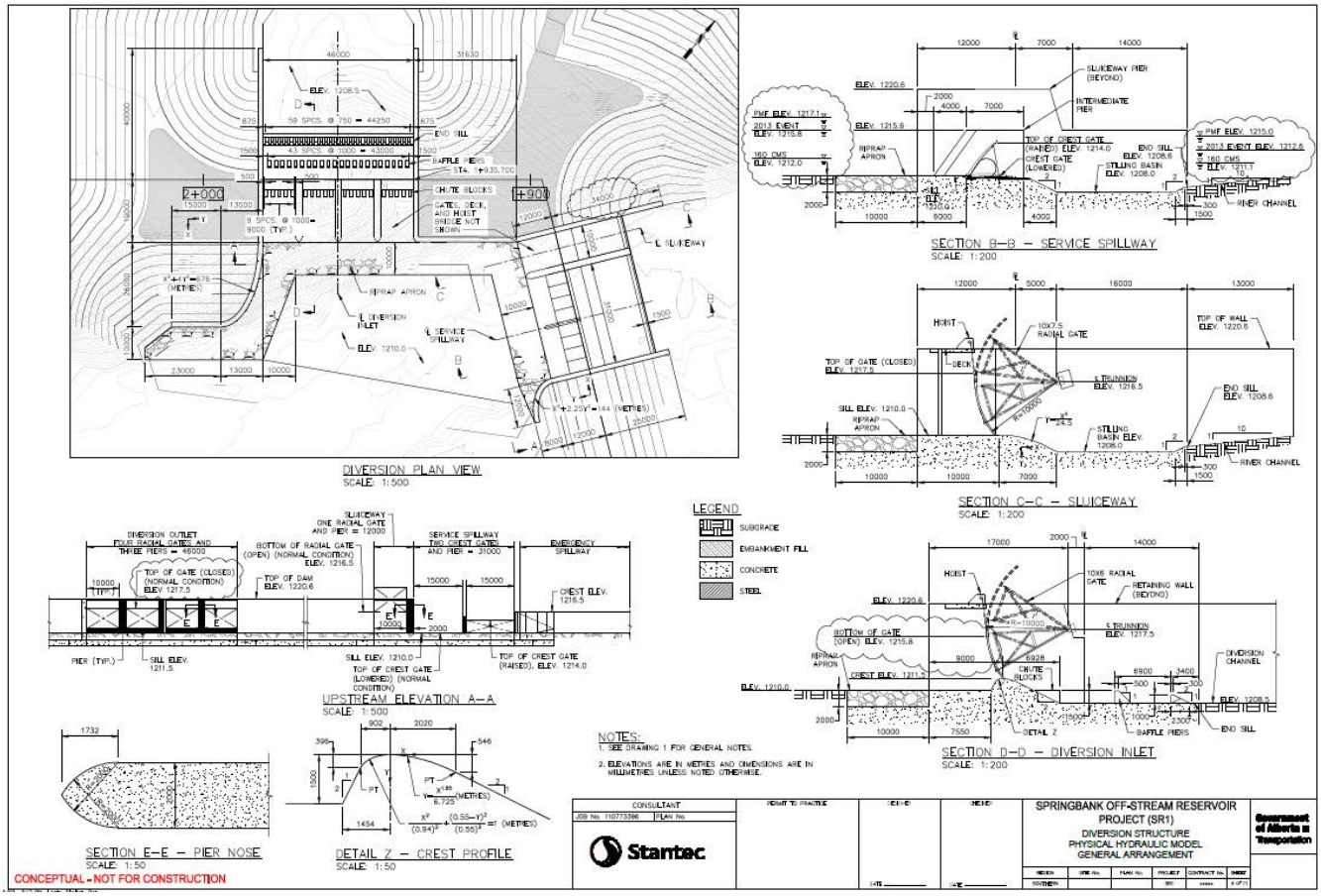

Figure 2. General arrangement drawing of the initial diversion inlet structure and service spillway.

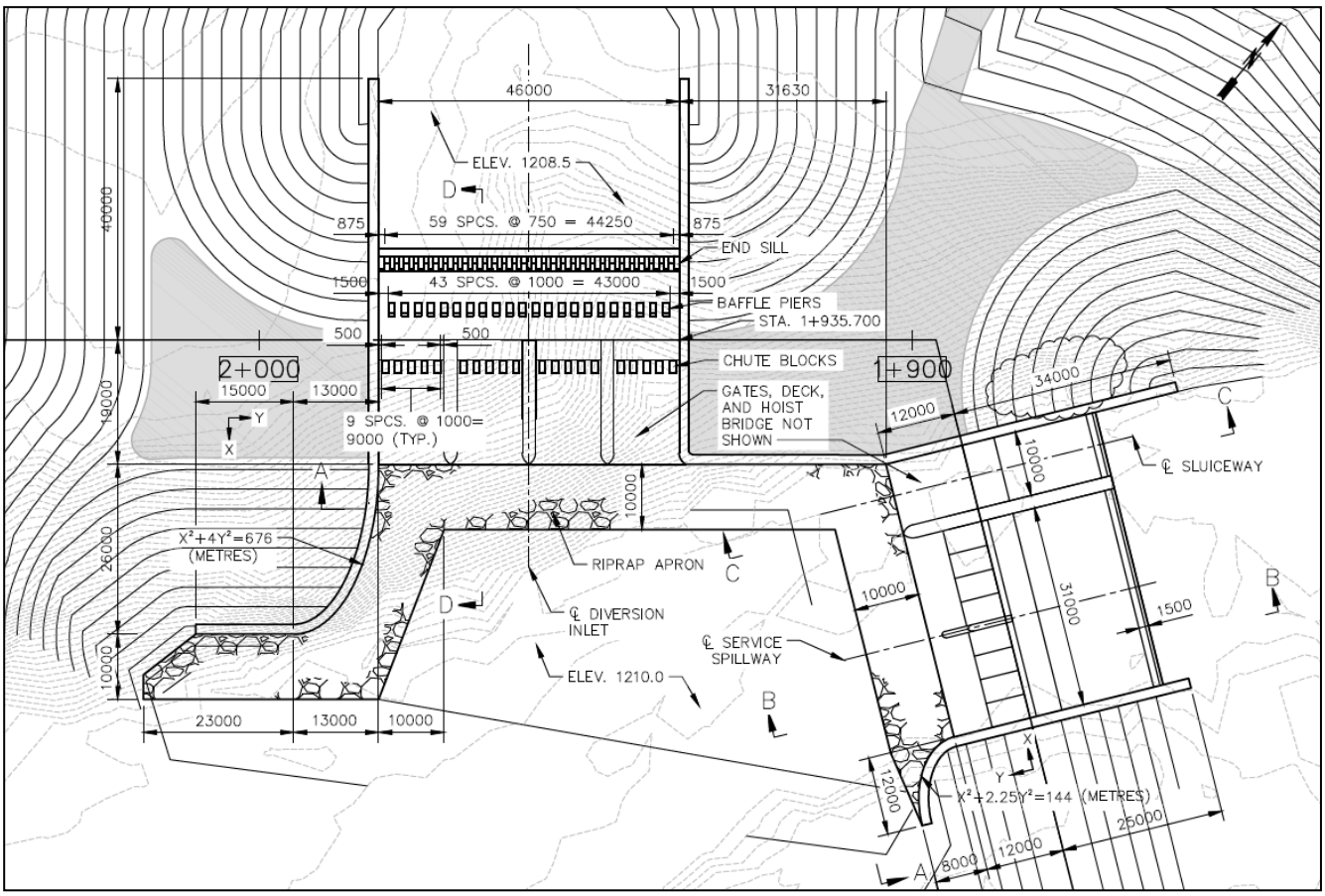

Figure 3. Plan view of the initial diversion inlet structure and service spillway.

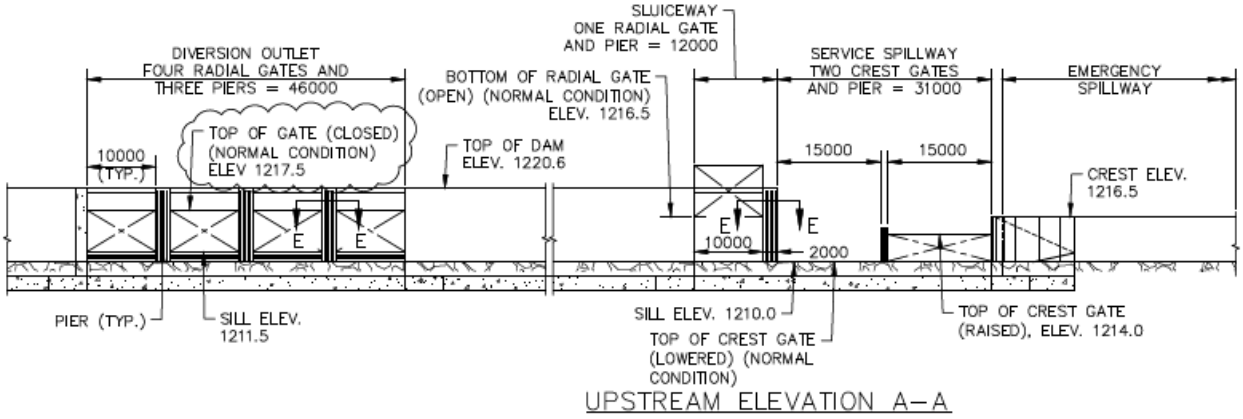

Figure 4. Profile view of the initial diversion inlet structure and service spillway design.

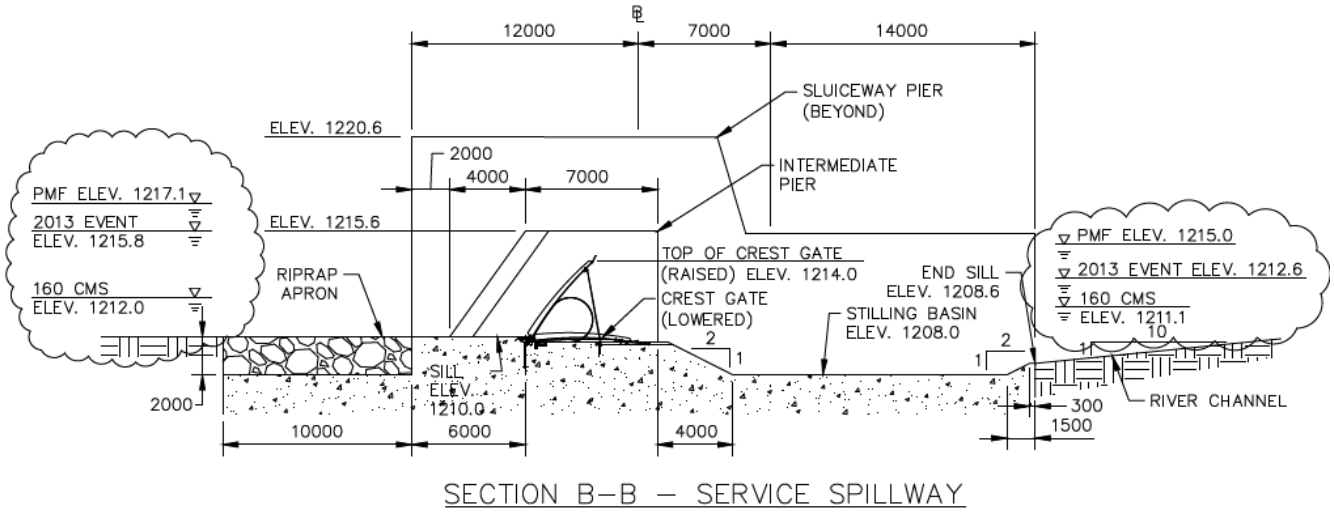

SECTION B–B – SERVICE SPILLWAY

Figure 5. Section view of the initial service spillway design.

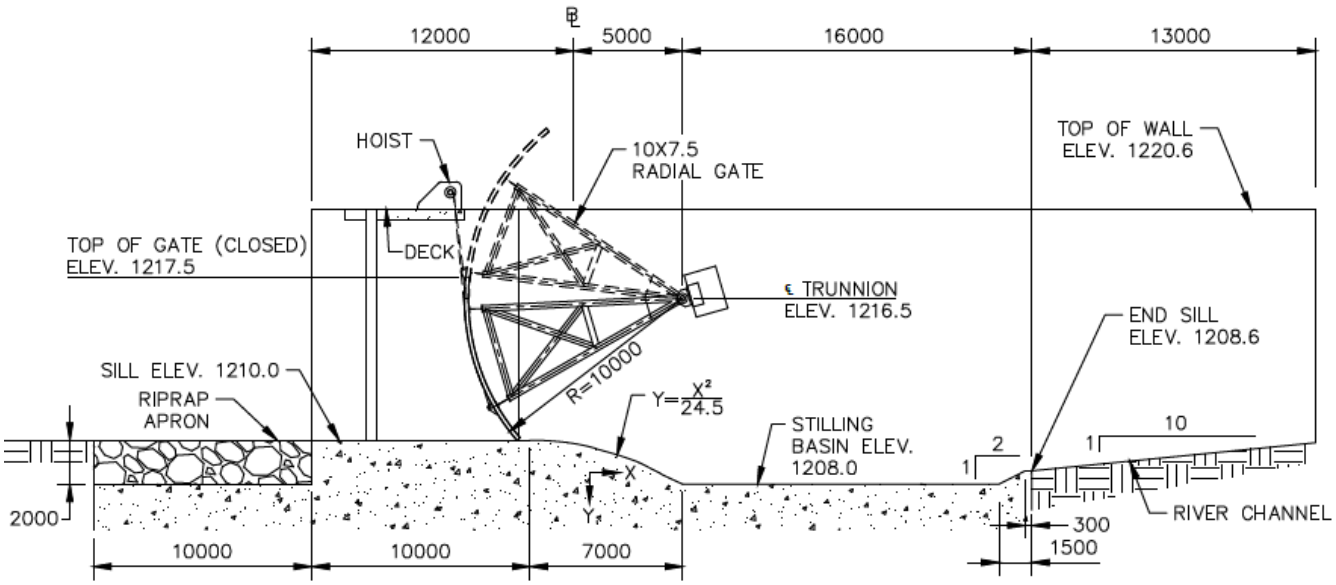

SECTION C–C – SLUICEWAY

Figure 6. Section view of the initial design sluiceway bay for the service spillway.

2.2.2 *Revised Design*

Based on the observations and results of the early physical model test runs, the design of the diversion inlet and service spillway structures were revised with an aim to improve the hydrodynamics as well as the capability of the structures to handle tree debris. The revised designs for the structures are shown in Figure 7 to Figure 12 with the main changes to the designs being:

- The four 10m wide bays of the diversion inlet were modified to feature two 20m wide bays separated by a larger 4m wide pier. The effective width for the flow remained unchanged between the original and revised design (40m).
- The 4m central pier on the diversion inlet was outfitted with removable pier noses to investigate the performance of different nose shapes and profiles.
- The radial gates on the diversion inlet structure were replaced with vertical lift gates.
- The radial gate sluiceway section of the service spillway was removed.
- The main river channel was controlled by two Obermeyer crest gates separated by a central pier wall. The left hand side (when viewing the structure looking downstream) of the service spillway was 24m wide, and the right hand side bay was 18m wide. The Obermeyer gates worked independently of each other.
- The service spillway structure was shifted 30m upstream of its original location (along the centreline of the structure), as was the floodplain berm on the east side of the service spillway. The central retaining wall dividing the diversion inlet from the service spillway was therefore much smaller than the previous design, and was curved in plan shape (this wall was straight in the original design).
- The retaining walls on the left hand side of the diversion inlet and right hand side of the service spillway were modified to improve the entrance flow characteristics.
- The breast walls in the diversion inlet bays were modified during the testing from a flat profile, to a curved profile that could more easily pass debris.
- Six variations of debris barriers were installed in the optimized design model to assess their performance at controlling the movement of woody debris through the structures.

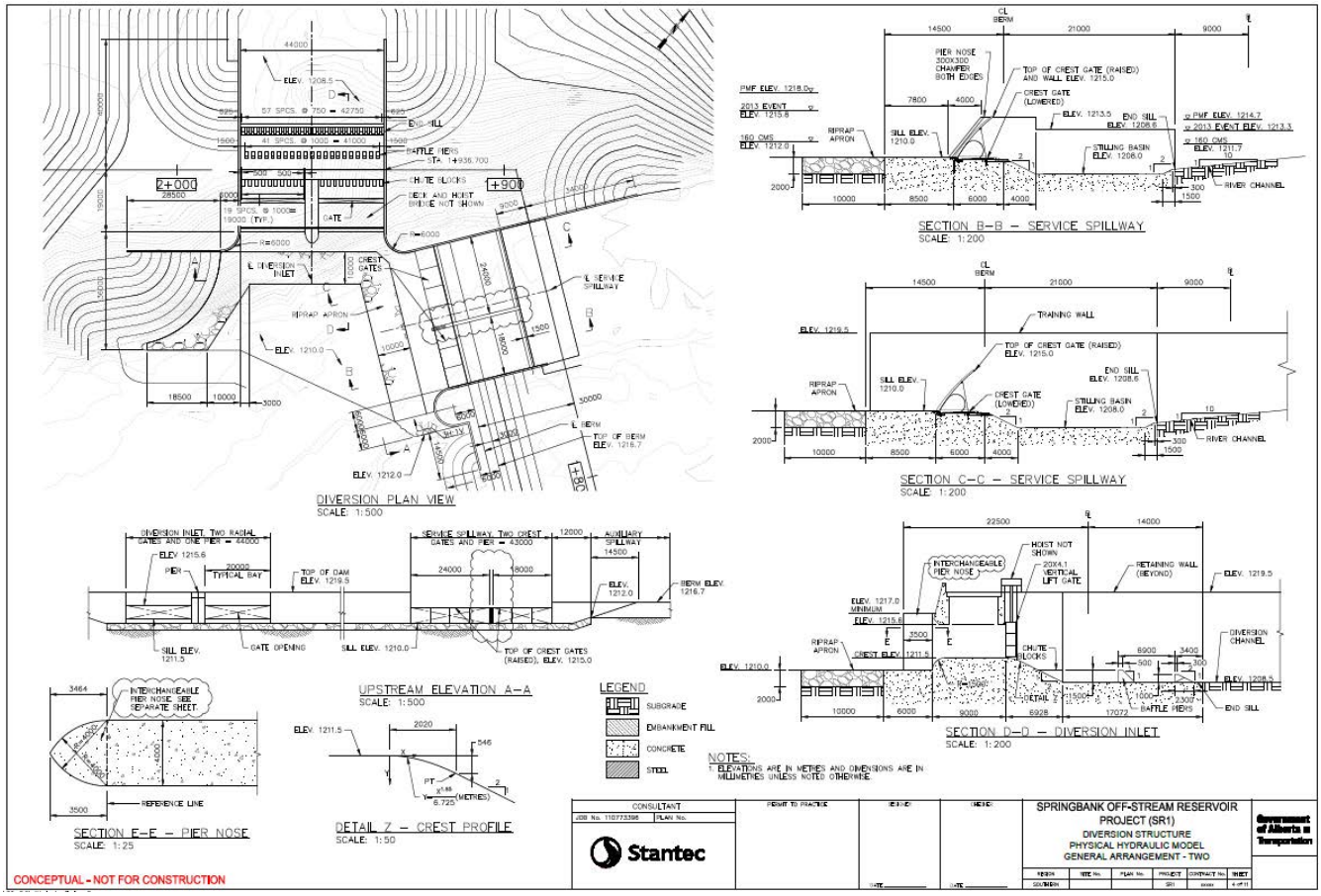

Figure 7. General arrangement drawing of the revised diversion inlet structure and service spillway.

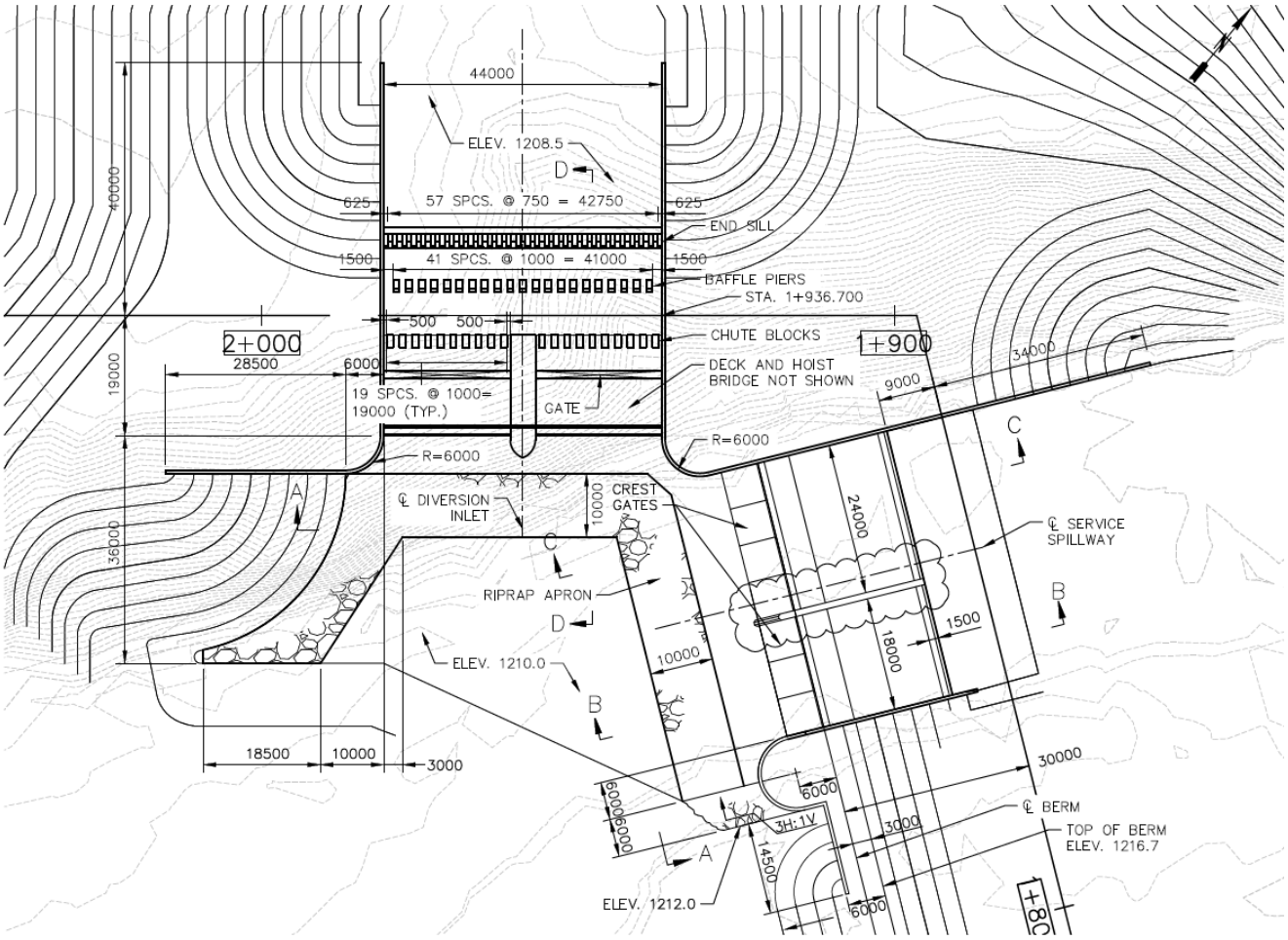

Figure 8. Plan view of the revised diversion inlet structure and service spillway.

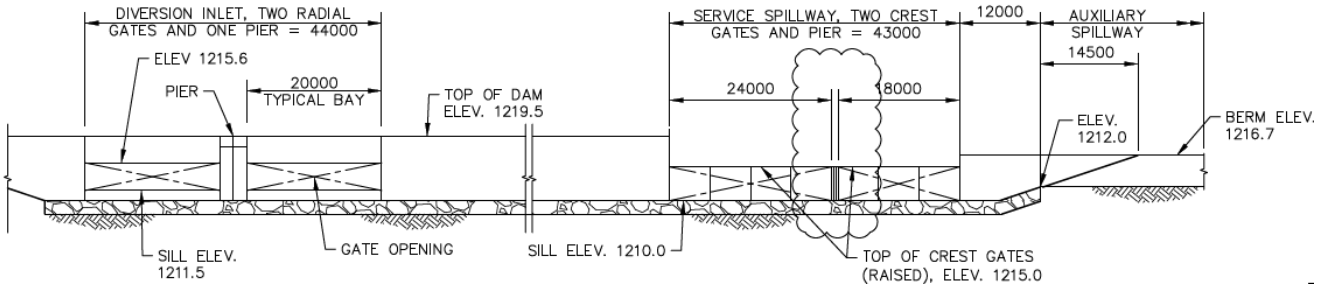

Figure 9. Profile view of the revised diversion inlet structure and service spillway.

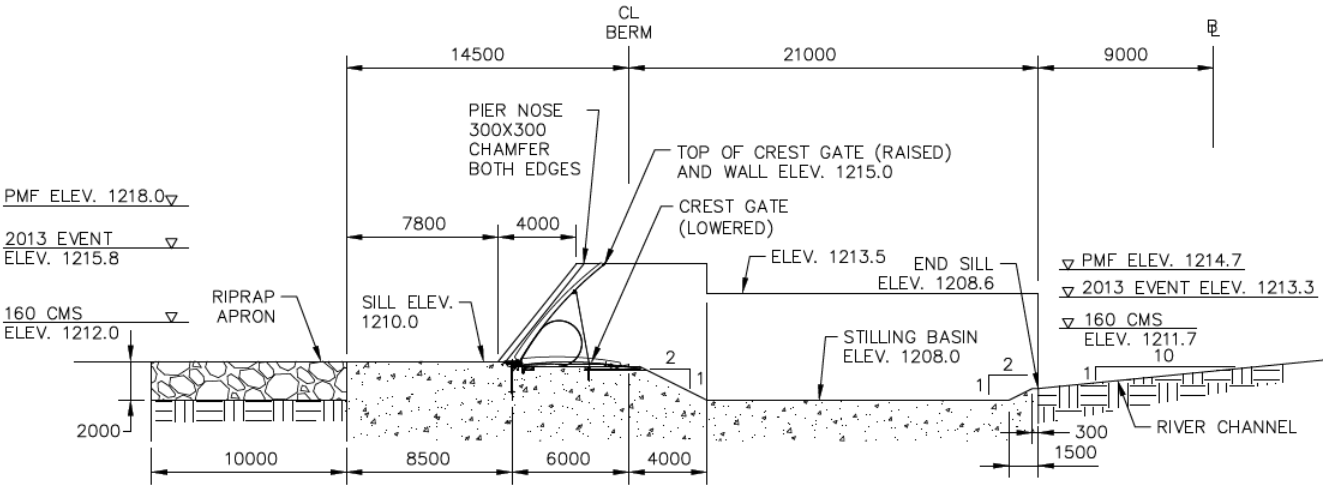

Figure 10. Section view B-B of the service spillway.

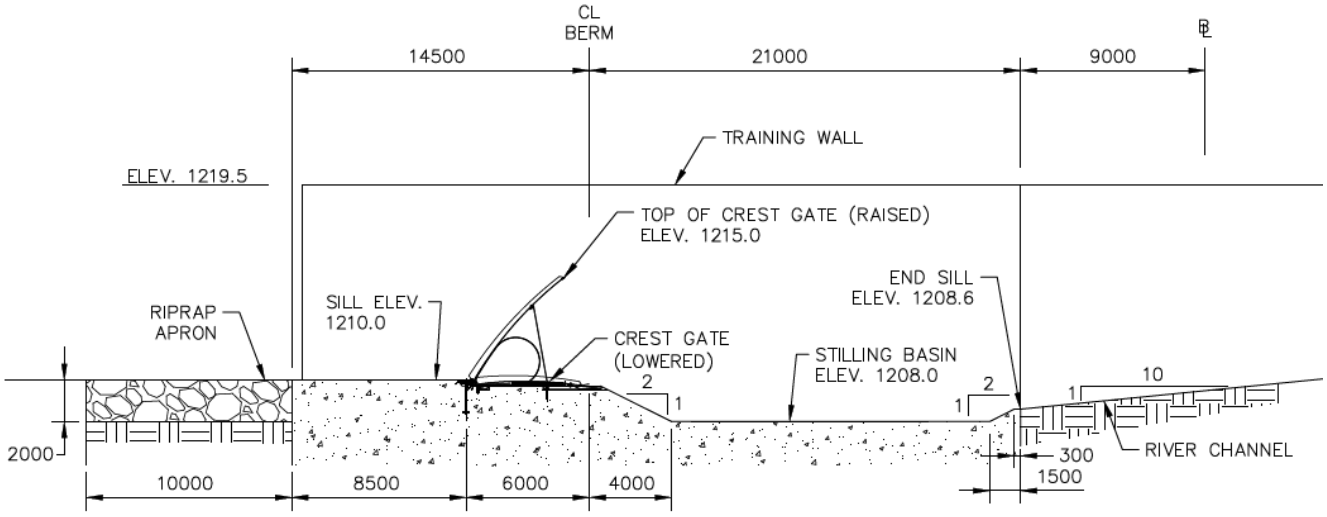

Figure 11. Section view C-C of the service spillway.

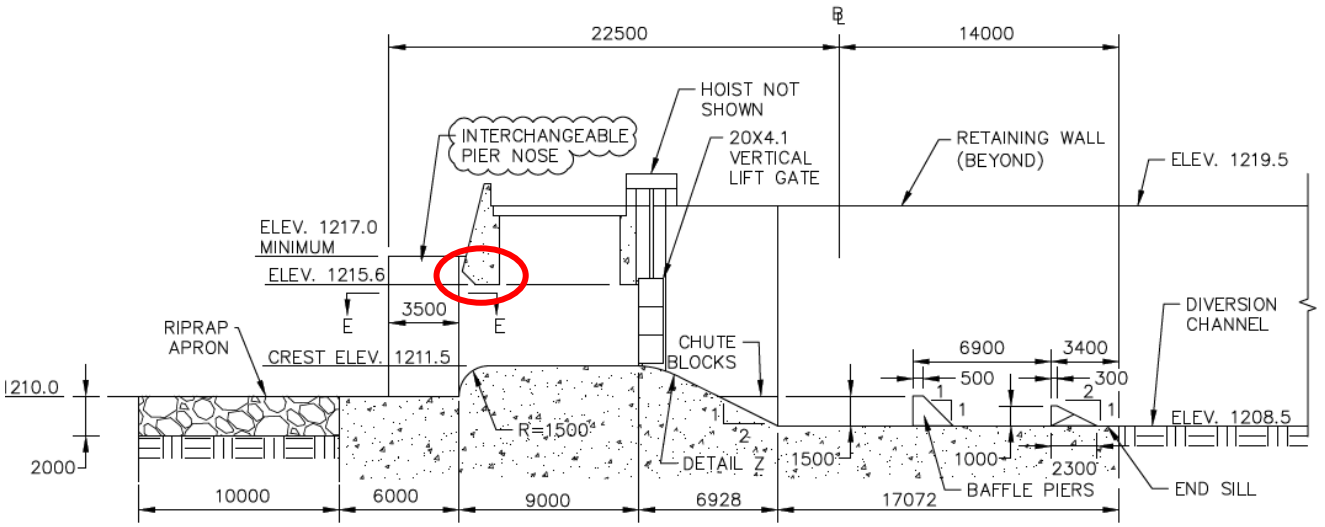

Figure 12. Section view of the diversion inlet structure. Note, the red ellipse highlights the breast wall, which was further modified to a curved profile in the model during the testing.

3 THE PHYSICAL MODEL

3.1 NRC-OCRE Large Area Basin and High Discharge Flume

The Springbank model was situated in NRC-OCRE's Large Area Basin (LAB). The rectangular multi-use LAB facility is located indoors, has interior dimensions of 50m-long by 30m-wide, can accommodate water depths of up to 1.4m (4.5ft), and can be filled and drained quickly when desired. The facility is typically used to conduct large three-dimensional physical model studies of:

- Hydrodynamics in marinas, ports and harbours;
- Moored ship behaviour and response to waves, currents and winds;
- Coastal processes and near-shore circulation;
- Sediment transport, beach response and shoreline developments;
- Open channel flows in estuaries, rivers, canals and inland waterways;
- Wave interaction with coastal and maritime structures and
- Scour, erosion and mitigation methods.

The basin is easily accessible to heavy construction equipment, and the water is supplied from storage reservoir sumps beneath the basin floor. For riverine physical models like the Springbank project, the Large Area Basin is connected to another physical modelling facility - the High Discharge Flume.

NRC-OCRE's High Discharge Flume (HDF) is used to simulate a wide range of open channel flows and study problems in rivers, canals and other inland waterways. Studies in this facility typically focus on the interaction of currents and high-speed flows with a wide range of coastal, riverine and offshore structures. The HDF can also be equipped with a drop gate structure used to simulate the dynamic effects of dam breaks or tsunami waves. The facility is 10m x 2.7m x 1.4m deep and is made of stainless steel. The flume provides a steady flow in an open channel with continuously adjustable discharge from 0 to 1.6 m^3/s (0 to 60 cfs). The discharge is controlled by two pumps, one with a

variable pitch, and the water level can be controlled by an adjustable sluice gate located near the downstream exit.

A schematic showing the HDF and the LAB in NRC-OCRE's Ottawa laboratory is shown in Figure 13.

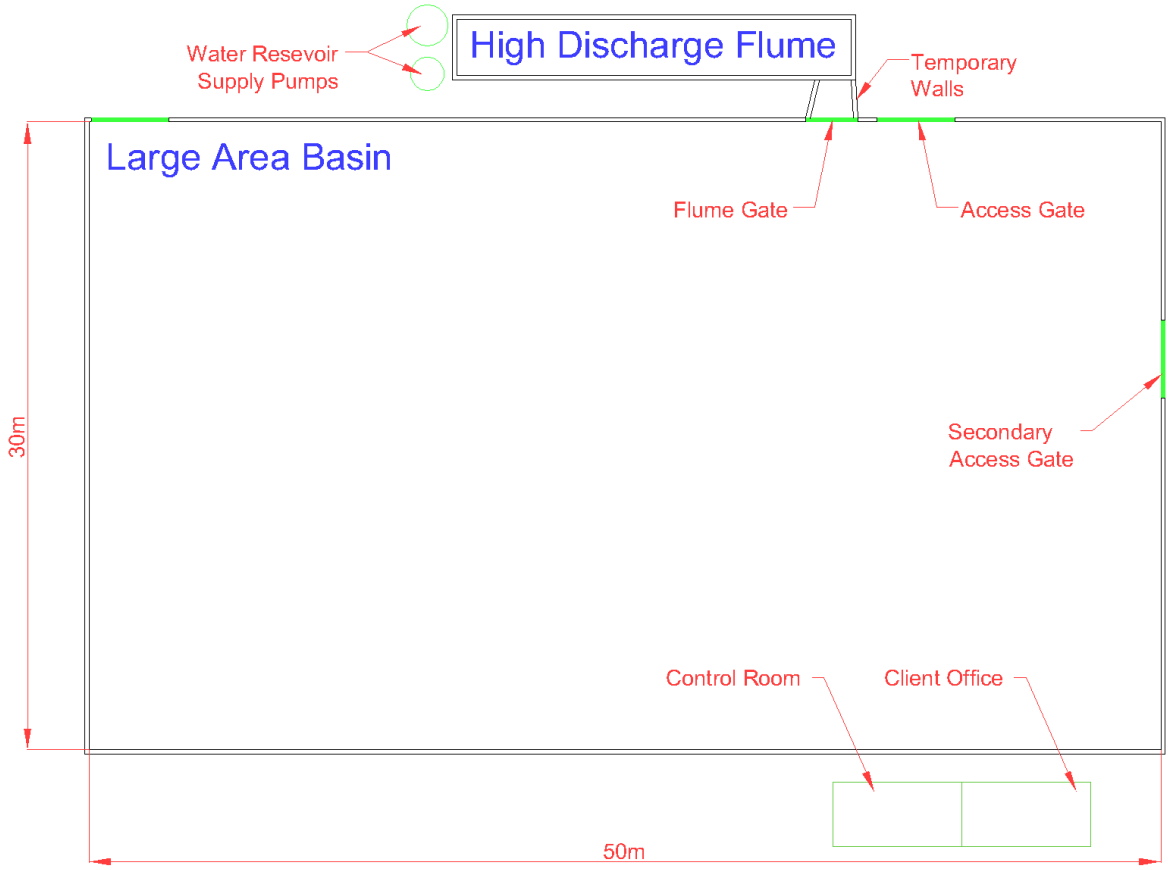

Figure 13. Schematic of NRC-OCRE's Large Area Basin and High Discharge Flume facilities.

3.2 Scaling Considerations

The selection of a suitable geometric scale is a key element in the design of any physical model. Mobile-bed models are especially sensitive in this regard. Although many factors are considered, the decision hinges on establishing a compromise between two important and conflicting requirements:

- minimizing scale effects, particularly with respect to the simulation of sediment transport processes, by selecting the largest model scale possible; and
- working within constraints related to the dimensions and capabilities of key equipment such as the test facility, the pumps used to generate flows, and the sensors used to monitor conditions in the model.

For models with mobile, erodible beds, these erodible materials must be carefully selected to ensure that they provide a reasonable representation of prototype behaviour. While large scale models are generally more realistic, they are also more expensive to build and operate.

The Springbank model was designed and constructed as an undistorted model with a length scale of 1:16. This scale represents a reasonable compromise between minimizing scaling and boundary effects, while maximizing the extent of the model domain and the accuracy of the sedimentary processes being modeled. All lengths in the model (horizontal and vertical) were 16 times less than the corresponding lengths at full scale. At 1:16 scale, the LAB facility represents an 800m-long by 480m-wide rectangle.

All aspects of the model, except for the mobile-bed sediment, were designed using Froude scaling criterion which assumes that gravitational and inertial forces are dominant in comparison to viscous forces. Froude scaling provides a set of scaling laws that dictate the proper relationship between quantities measured in the model, such as flows and velocities, and the same quantities at full scale. These scaling laws are derived from the similarity of the Froude number, which represents the ratio between gravitational and inertial forces. Setting the scale factor for the Froude number (λ_{Fr}) equal to unity ensures that the relative strengths of inertial and gravitational forces are the same in the model as they are at full scale. This similarity in Froude number, combined with geometric similitude, ensures that the model provides a reliable physical representation of flow patterns that occur in nature.

Scale factors for relevant parameters in the present study are presented in Table 1. Note, stated quantities and measurements in this report are in full scale units unless stated otherwise.

Variable	Scale factor	Typical value at full scale	Corresponding model value
Length	$\lambda_l = 16$	10.0 m	0.625 m
Time	$\lambda_t = \sqrt{\lambda_l} = 4$	10.0 sec	2.5sec
Velocity	$\lambda_u = \frac{\lambda_l}{\lambda_t} = 4$	1.0 m/s	0.25 m/s
Acceleration	$\lambda_a = \frac{\lambda_l}{\lambda_t^2} = 1.0$	9.81 m/s^2	9.81 m/s^2
Froude Number	$\lambda_{Fr} = \frac{\lambda_u}{\sqrt{\lambda_g \lambda_l}} = 1.0$	1.0	1.0
Reynolds Number	$\lambda_{Re} = \frac{\lambda_u \lambda_l}{\lambda_\nu} = 4$	2,000,000	500,000
Density of water	$\lambda_{\rho_w} = 1.0$	1,000 kg/m^3	1,000 kg/m^3
Mass	$\lambda_M = \lambda_l{}^3 \lambda_\rho$ $= 4096\lambda_\rho$	1 tonne	244 g

Table 1. Scale factors for key project variables.

3.2.1 *Bed Shear Stress in Steady Flow*

Granular materials on a riverbed are transported downstream when the shear stress exerted by the flow on the bed τ, exceeds the critical shear stress τ_c. In steady flow the bed shear stress is calculated according to

$$\tau = \rho C_D \bar{U}^2$$

where ρ is the fluid density, $\bar{U}$ is the depth-averaged current speed and C_D is the dimensionless drag coefficient, given by:

$$C_D = \left[\frac{0.4}{\ln(h/z_0)-1}\right]^2$$

in which h is the mean water depth and z_0 is a length characterizing the roughness of the bed sediments. The bed roughness length can be calculated as

$$z_0 = \frac{k_s}{30} = \frac{2.5D_{50}}{30}$$

where D_{50} is the median diameter of the sediment.

3.2.2 *Mobility Threshold for Granular Materials*

The Sheilds parameter θ, provides a means of expressing the shear stress acting on a riverbed in non-dimensional form:

$$\theta = \frac{\tau}{(\rho_s - \rho)gD_{50}}$$

Similarly, the dimensionless grain size D_* provides a means of expressing the sediment size in non-dimensional form:

$$D_* = D_{50}\left(\frac{(\rho_s/\rho - 1)g}{\nu^2}\right)^{1/3}$$

in which D_{50} is the median grain size, ρ_s is the sediment density, ρ is the fluid density and ν is the kinematic viscosity of the fluid. Soulsby (1997) proposed the following expression to describe the critical value of θ corresponding to the mobility threshold for non-cohesive granular materials:

$$\theta_c = \frac{0.3}{1+1.2D_*} + 0.055\left[1 - \exp(-0.02D_*)\right]$$

This expression for θ_c fits well to experimental data and is identical to the Shields curve for $D_* > 10$ (see Figure 14). Theory, supported by numerous experiments, suggests that sediments will be stable for $\theta < \theta_c$, and will be mobile for $\theta > \theta_c$. In reality, the transition from a stable condition to a mobile condition occurs over a range of θ around θ_c. The fact that the experimental data on the threshold of motion of granular materials is moderately scattered supports this view. Within the mobile regime,

the rate of sediment transport is generally proportional to the excess shear stress acting on the bed, or the difference between θ and θ_c.

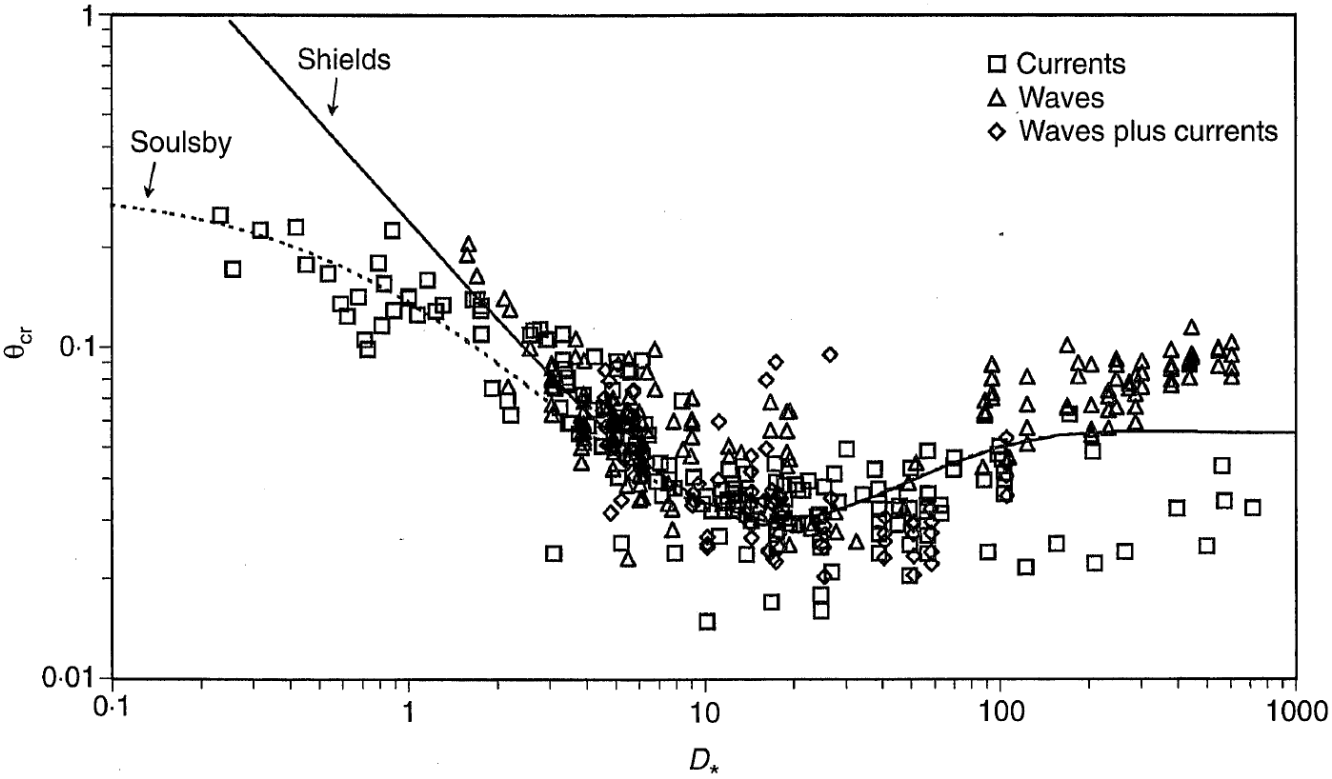

Figure 14. Mobility threshold for sediments (from Soulsby 1997).

Soulsby (1997) also proposed the following formula (valid for $D > 0.01$m) to predict the smallest size of rock that will remain immobile for a given steady flow of water:

$$D_c = \frac{0.25\overline{U}^{2.8}}{h^{0.4}\left[g\left(\rho_s/\rho - 1\right)\right]^{1.4}} \qquad \text{for} \quad D > 0.01m$$

Figure 15 shows the threshold current speed plotted as a function of sediment size for various water depths. This figure can be used to guide the initial selection of riprap for a horizontal bed, once the depth averaged velocity and water depth are known. However, the reader should note that this figure does not take into account any possible flow disturbance and amplification of bed shear stress around structures such as piers, piles, caissons, sluice gates, etc. Whitehouse (1998) reports shear stress amplification factors around structures on the order of between 2 and 6. In other words, the shear stress on the bed near a structure can be up to 6 times larger than the far field shear stress. In such situations, the initial selection of riprap or armour stone should be verified through physical model tests.

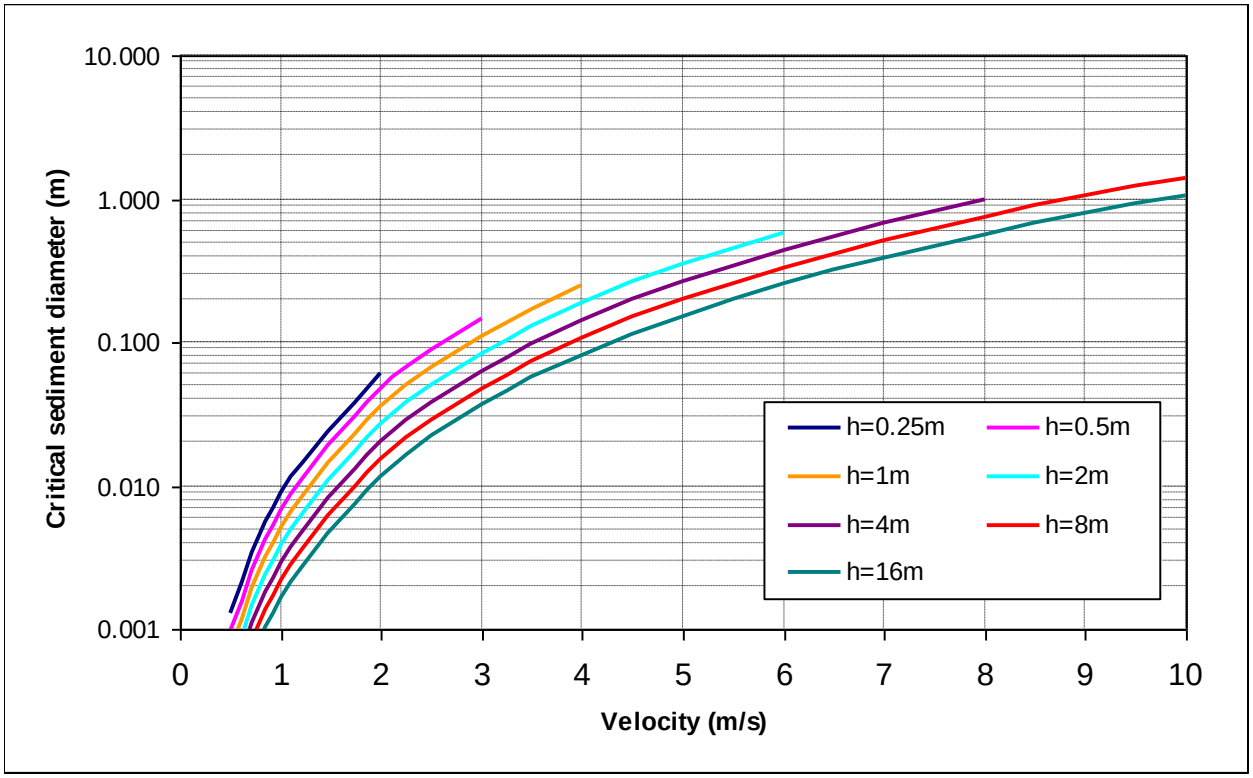

Figure 15. Threshold current speed for mobility of gravels in steady flows.

Granular materials on a riverbed are transported downstream when the shear stress exerted by the flow on the bed τ, exceeds the critical shear stress τ_c. In steady flow the bed shear stress is calculated according to

$$\tau = \rho C_D \overline{U}^2$$

where ρ is the fluid density, $\bar{U}$ is the depth-averaged current speed and C_D is the dimensionless drag coefficient, given by:

$$C_D = \left[\frac{0.4}{\ln(h/z_0) - 1} \right]^2$$

in which h is the mean water depth and z_0 is a length characterizing the roughness of the bed sediments. The bed roughness length can be calculated as

$$z_0 = \frac{k_s}{30} = \frac{2.5 D_{50}}{30}$$

where D_{50} is the median diameter of the sediment.

3.2.3 *Scaling of Mobile Bed Material*

Stantec provided measured grain size distributions at the study site. The typical grain size distribution from these data was used as the prototype grain size distribution (Figure 16).

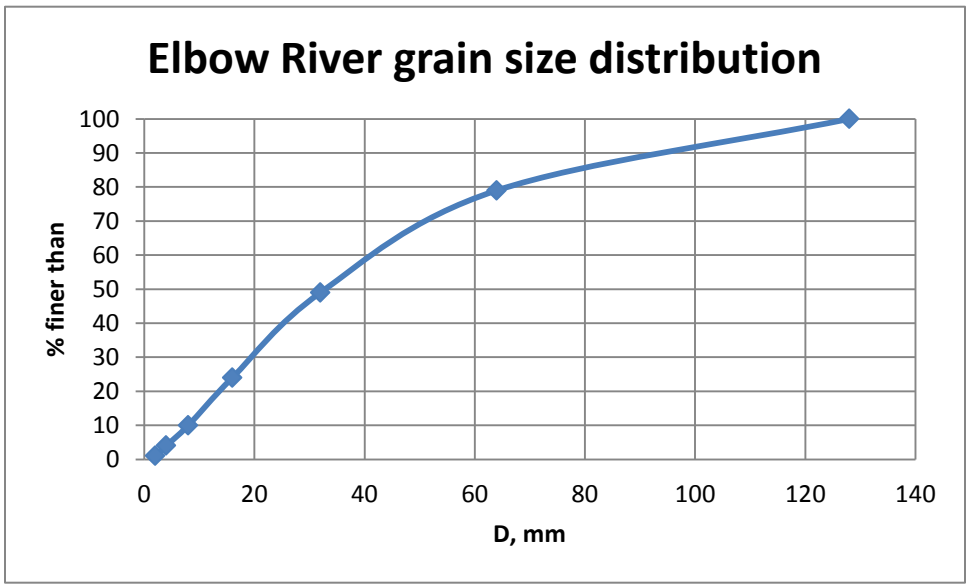

Figure 16. Typical grain size distribution at the Elbow River study site.

The model scale of 1:16 was used for preliminary dimensional scaling of the bed sediments to be used for mobile bed model runs. The mobility of the 1:16 grain size distribution was evaluated based on the non-dimensional Shields criterion in both model and prototype: D_* was calculated for D_{90}, D_{50}, D_{24}, and D_{10} in both model and prototype, and hence θ_c for each fraction was calculated in model and prototype. To calculate θ_c, bed shear stress was calculated using the depth slope product ($\tau = \rho g Y S$), with S= the reach average bed slope of 0.0064, and Y the flow depth during the Q=320 m^3/s flow stage ($Y_{prototype}$=2m, Y_{model}=0.13 m). For the finer fractions ($D \leq D_{50}$), D_{model} was increased slightly to ensure that [$\theta_{prototype} - \theta_{c,prototype} = \theta_{model} - \theta_{c,model}$], i.e., to ensure all fractions had the same mobility in model as in the prototype. Due to the relatively coarse bed sediments in the Elbow River, and the relatively large model scale, little adjustment was required. For example, $D_{50,model}$ was increased from 0.0020 m to 0.0022 m, and $D_{10,model}$ was increased from 0.00050 m to 0.00051 m. The resulting model grain size distribution is shown in Figure 17.

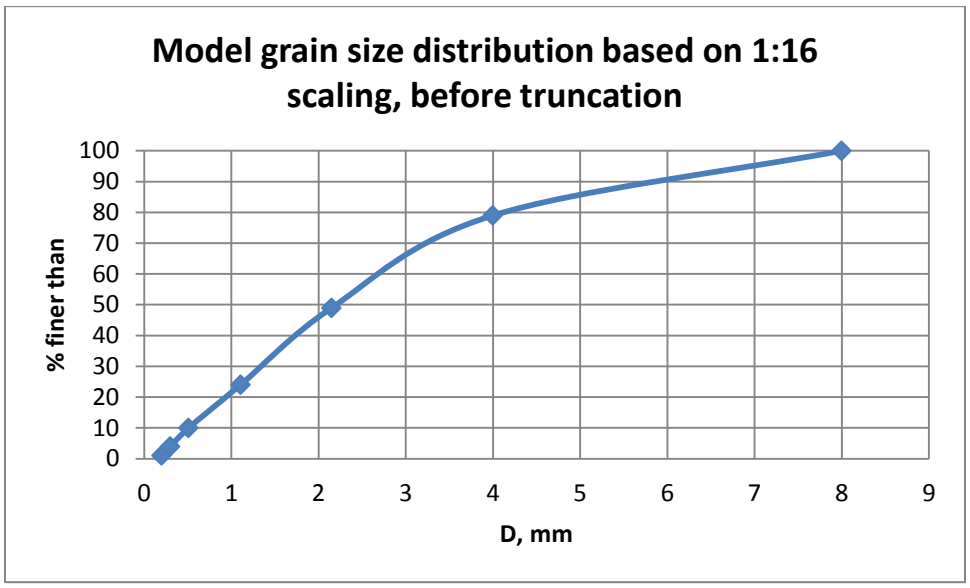

Figure 17. Model scale (1:16) grain size distribution, adjusted slightly to ensure same mobility in model as prototype based on Shields scaling.

However, the total bed material load during the larger flow events was deemed to be too large for the physical model. Furthermore, the transport, erosion, and deposition behaviour of the coarser fraction was deemed to be of the greatest interest. Consequently, the model grain size distribution was truncated near the $D_{50,model}$ at 2mm. The final model grain size distribution is shown in Figure 18. This figure shows the target gradation from theory (blue) as well as the model material selected that reasonably represented the target curve (green).

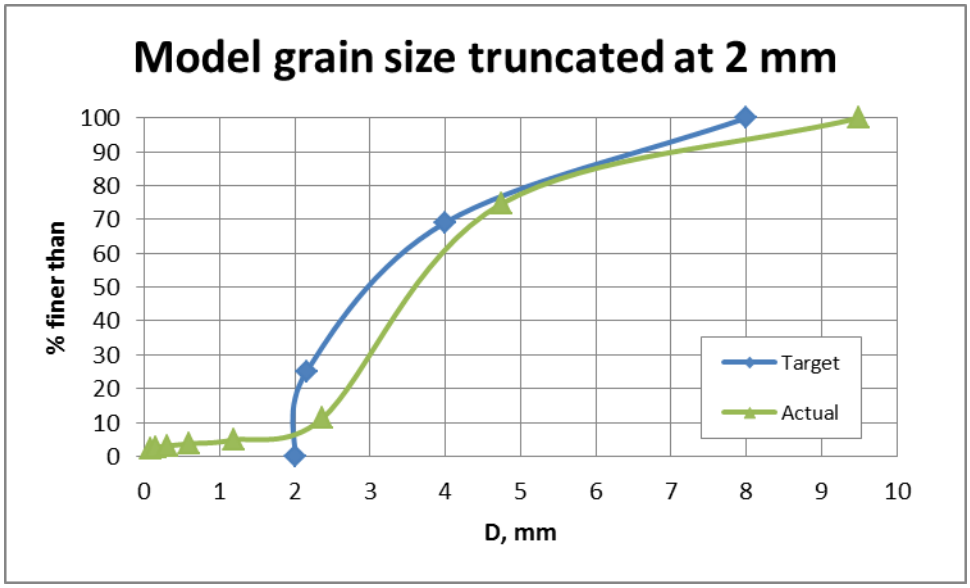

Figure 18. Final model grain size distribution, based on model (1:16) scaled grain size distribution, adjusted slightly to ensure same mobility in model as prototype based on Shields scaling, and truncated at 2 mm.

3.3 Model Layout and Design

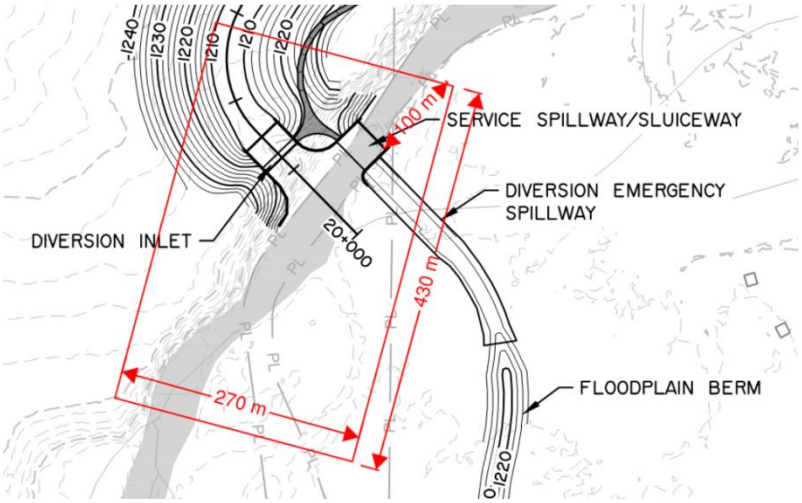

Figure 19. Extent of the physical model domain requested by Stantec.

The extent of the physical model domain requested by Stantec is shown in Figure 19. The model constructed in the LAB included a larger area than that originally requested; in particular it included more of the upstream floodplain so as to represent the incoming flood flows more realistically. An undistorted physical model of the hydraulics and sedimentary processes at the diversion inlet at a length scale of 1:16 was constructed. As described in Section 3.2, the 1:16 length scale was chosen to minimize scale effects and maximize the reliability of the physical model as much as possible. Modelling laws derived from Froude scaling were used to relate conditions in the model to those at full scale. However, the sediments used in the model were selected to replicate the mobility of the prototype sediment, and not just the grain size.

The physical model was constructed in the 50 m by 30 m Large Area Basin (LAB). The physical model included realistic scaled simulations of the bathymetry and topography of the river reach (including a portion of the floodplain), the diversion channel, and the proposed sluiceway and service spillway structures. The bathymetry and topography were modelled as a rigid surface formed in grout (see Section 3.4.1). Where appropriate, the concrete grout was given a stiff broom finish to roughen the bottom of the river channel, diversion channel and floodplain to approximate the hydraulic roughness of the prototype channels. Also, where the prototype floodplain was tree-covered, model trees were cast into the concrete at a specified placement density to simulate the prototype landscape. Near the diversion inlet and service spillway structures, the riprap scour protection apron was modelled with appropriately scaled (M_{50} = 440kg) model stone to investigate its stability under flood conditions. A variable-pitch pump drawing from a large sump was used to supply a steady (adjustable) discharge into the upstream end of the model (via the High Discharge Flume), and a pair of adjustable weirs were used to control the water level at the downstream end of both the river and diversion channels (see Section 3.4.2). After flowing over the weirs, the water returned to the water reservoir sumps. A collection of flow straighteners were utilized to dampen spurious flow circulations at the upstream boundary. Various flood flows up to the 1240 m^3/s event were simulated by regulating the inflow discharge via the pump controller, and the downstream water levels were controlled with the weirs. The sluice and crest gates in the new control structures (see Section 3.4.3) were opened or closed as desired to simulate various operational scenarios. The water flowed through the model in a realistic

manner, and the model provided an excellent means of verifying the performance and optimising the design of the proposed structures, including the risks of sediment deposition and blockage due to floating debris. Scaled replicas of woody debris (logs, trees) were modelled to match debris characterisations and loading estimates provided by Stantec (see Section 3.4.4). The debris was added near the upstream model boundary and allowed to drift downstream, possibly grounding in shallows or snagging in the sluiceway or service spillway. A range of granular sediments were utilized in the model to replicate the mobility of the sediments available in the natural river bed (see Section 3.4.5). These sediments were either pre-loaded on the river bottom, or added to the flow using mechanical spreaders. The layout of the physical model is shown in Figure 20 and Figure 21 as well as the photographs of Figure 22 to Figure 26.

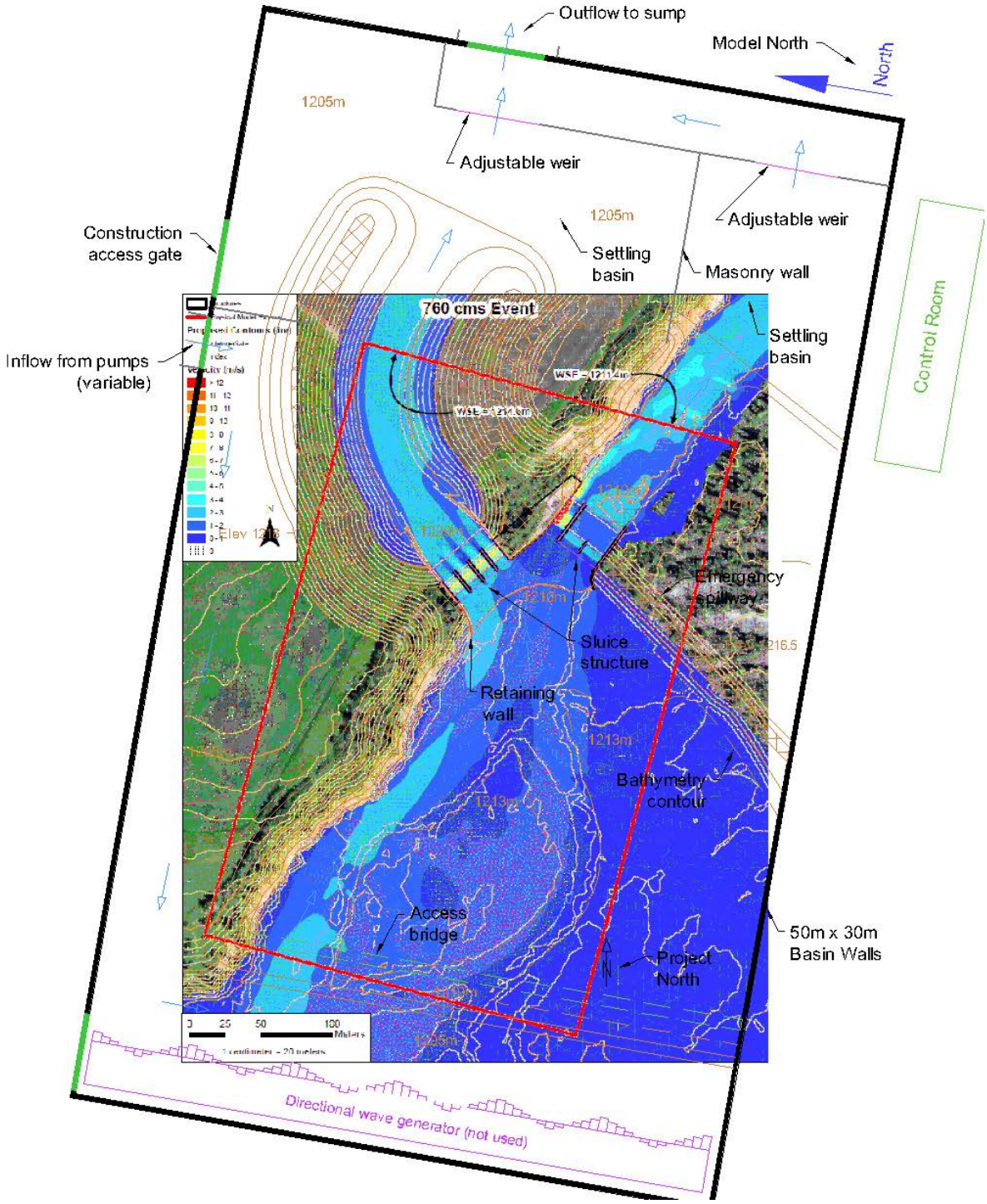

Figure 20. Plan view of the physical model overlain with Stantec numerical modelling results.

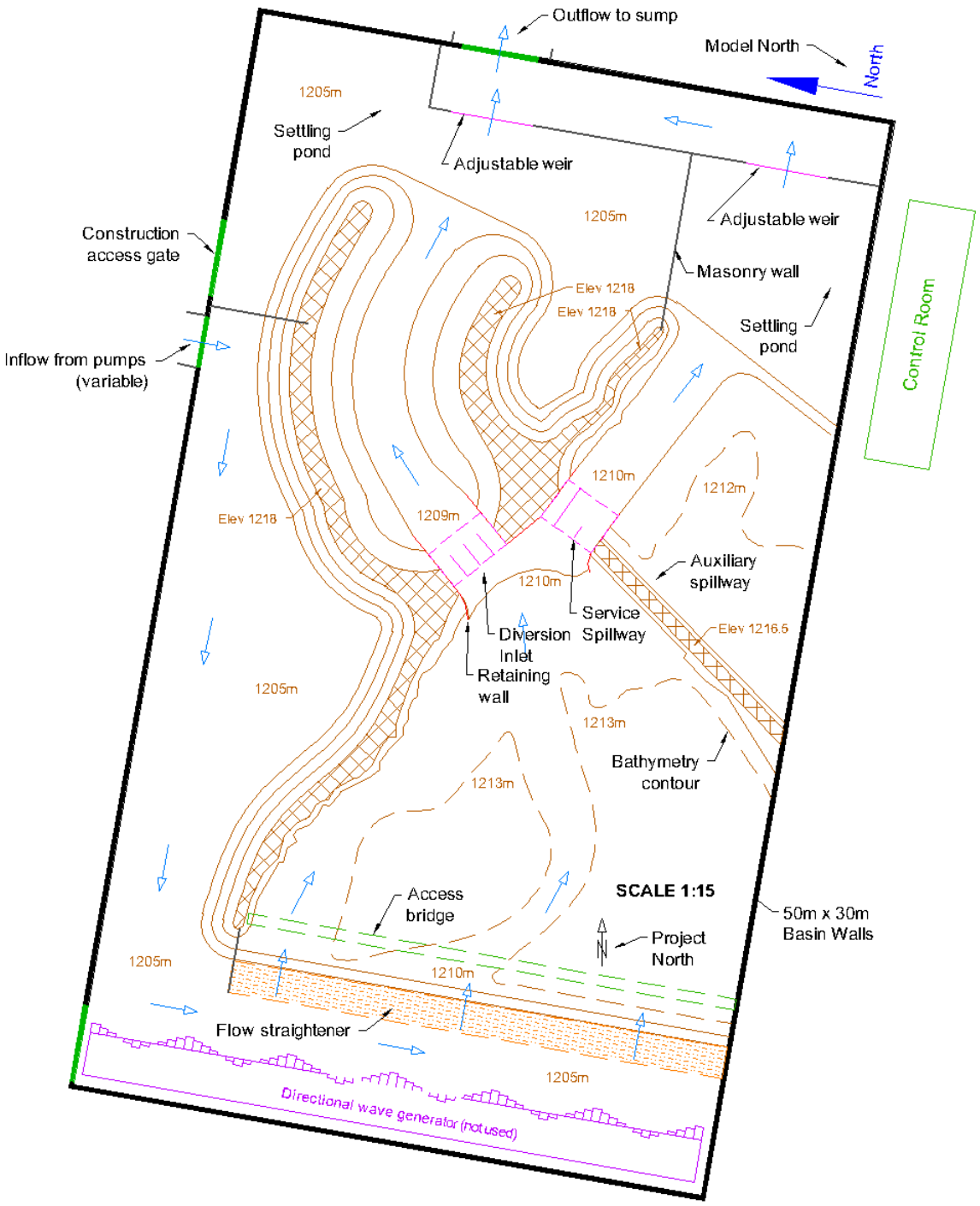

Figure 21. Plan view of the physical model.

Figure 22. Photograph of the physical model after construction – looking downstream.

Figure 23. Photograph of the physical model after construction – looking downstream.

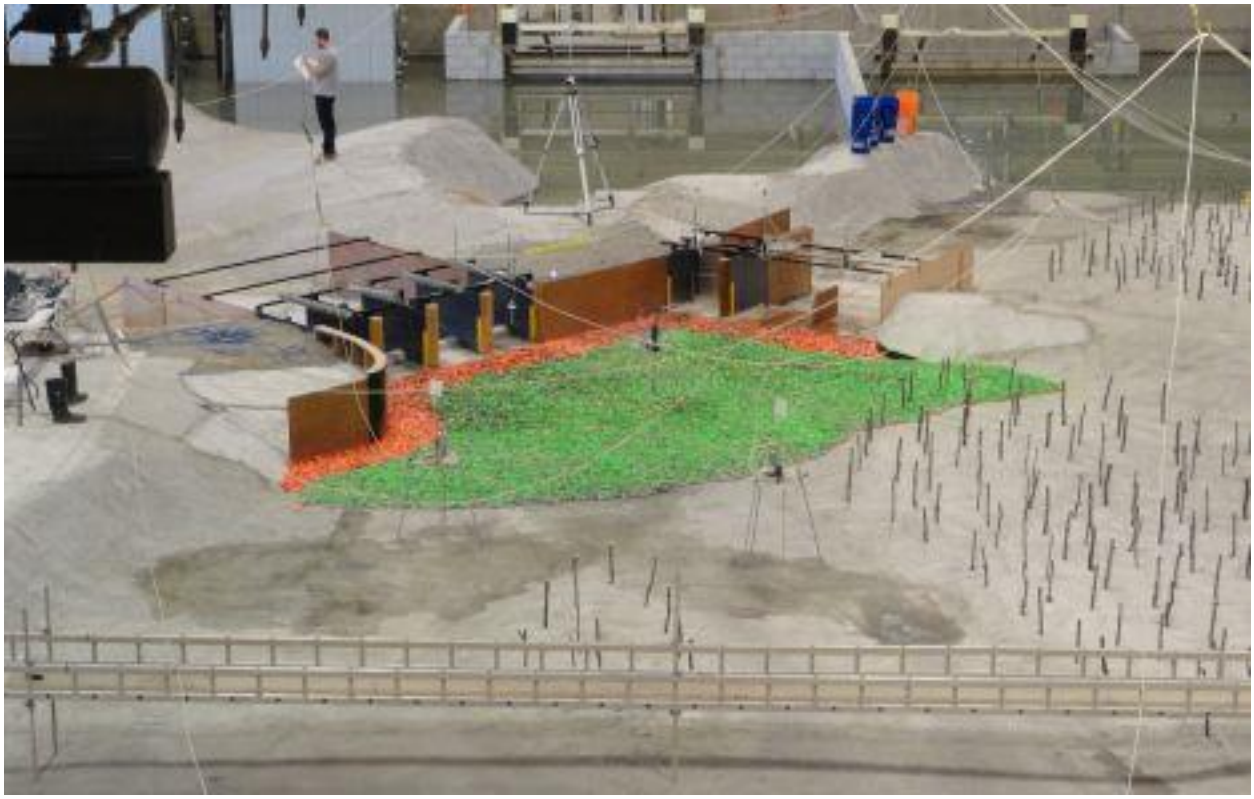

Figure 24. Photograph of the physical model after construction – looking downstream.

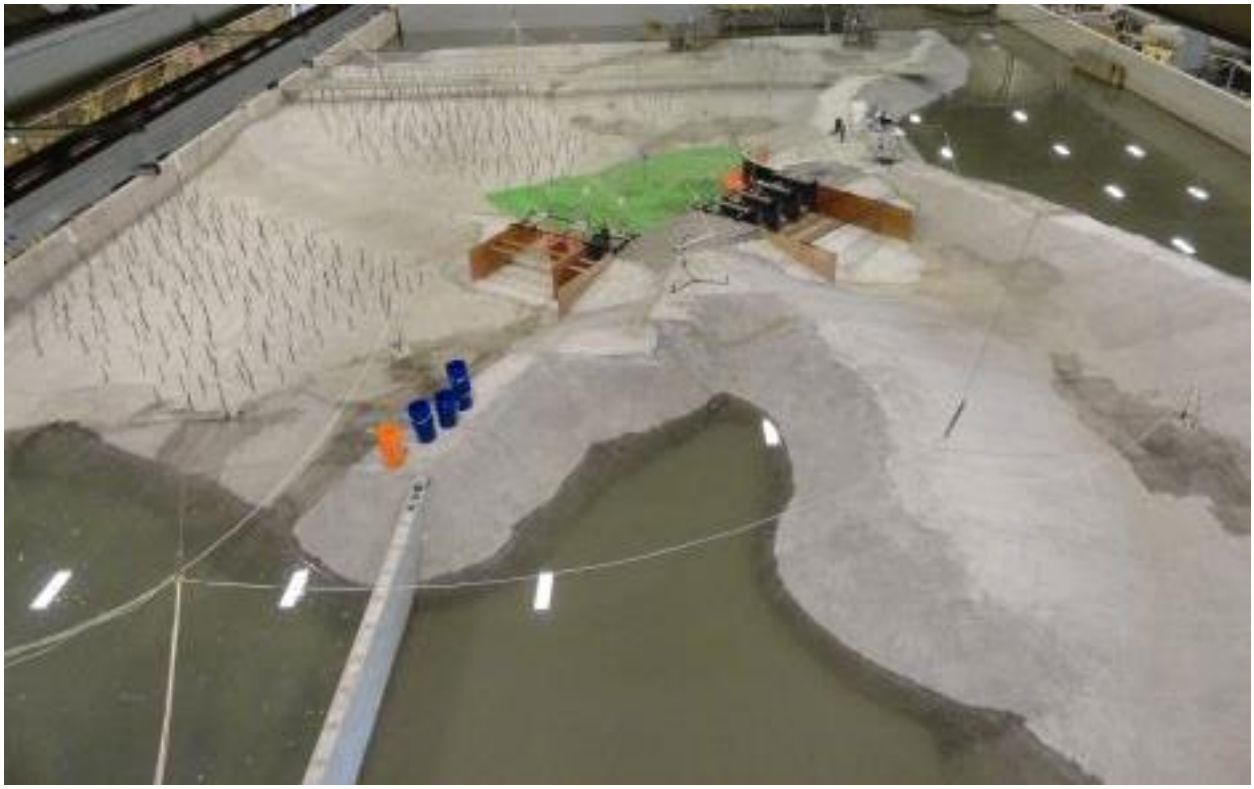

Figure 25. Photograph of the physical model after construction – looking upstream.

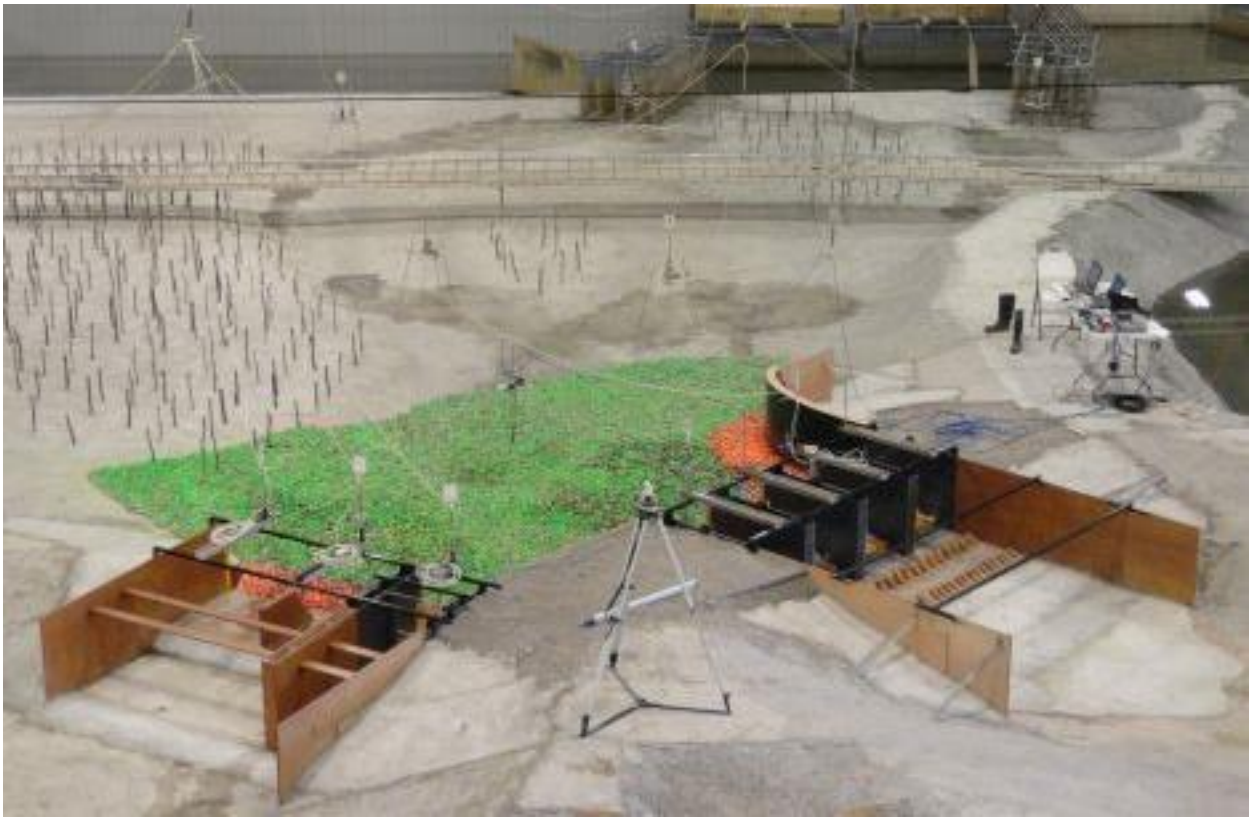

Figure 26. Photograph of the physical model after construction – looking upstream.

3.4 Model Construction

3.4.1 *Concrete Bathymetry/Topography*

The concrete bathymetry was constructed using a series of fibreboard templates erected at 1m intervals (model scale, or MS) throughout the model domain. The templates, used to represent cross-sections of the riverbed, were cut to an accuracy of $\pm$2mm MS and were supported on the basin floor by a grid of pads leveled to within $\pm$1mm MS. Heavy construction equipment was used to fill the templates with clear gravel once secured on top of the leveled pads. The clear gravel was then compacted with a plate tamper such that the final surface rested approximately 5cm MS below the top edge of the templates. Fine aggregate concrete was then placed on top of the gravel base and power screeded to match the elevations of the templates. Once cured, a smooth finish was achieved using a combination of hand- and mechanical-trowelling, and a roughened finish (where applicable) was achieved using a stiff broom finish on the curing concrete. Photographs showing some of the stages of the bathymetry construction are shown in Figure 27 to Figure 32.

This construction technique has been developed and perfected at NRC-OCRE over the past 30 years. The skilled technicians undertaking this work have a well-proven track record of reproducing complex bathymetries with a high level of precision and accuracy. The resulting bathymetry is generally accurate to $\pm$5mm MS, which is equivalent to $\pm$13.75cm at full scale.

Figure 27. Fibreboard templates were erected and backfilled with fine gravel.

Figure 28. Heavy construction equipment was used to fill templates.

Figure 29. Heavy construction equipment was used to pour concrete.

Figure 30. The concrete was screeded to match the template surfaces.

Figure 31. The concrete was broom finished to roughen the surface, and model trees were inserted into the wet concrete to model forested regions of the floodplain.

Figure 32. Model trees in the curing concrete.

The concrete bathymetry for an area close to the diversion inlet and service spillway/sluiceway was lowered to 0.5m below the actual surface level. In this area, scaled mobile river sediments were placed to investigate their mobility and the potential for erosion, scour, and accretion in the model. This mobile-bed area is shown below in Figure 33 and Figure 34. During test series where investigating sediment transport was not desired, the mobile bed area was filled with 210kg riprap stone.

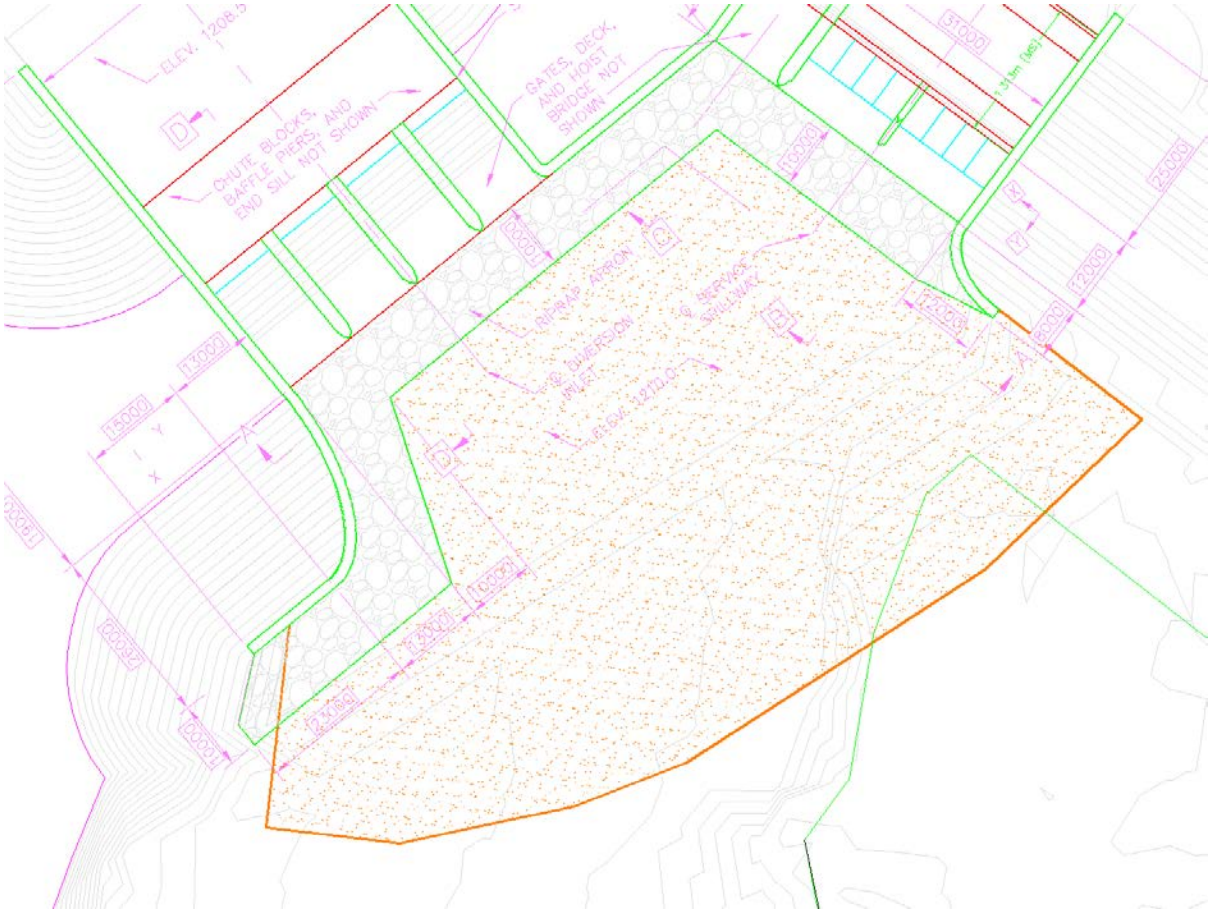

Figure 33. Drawing showing the extents of the lowered concrete where mobile bed material was used (orange hatching).

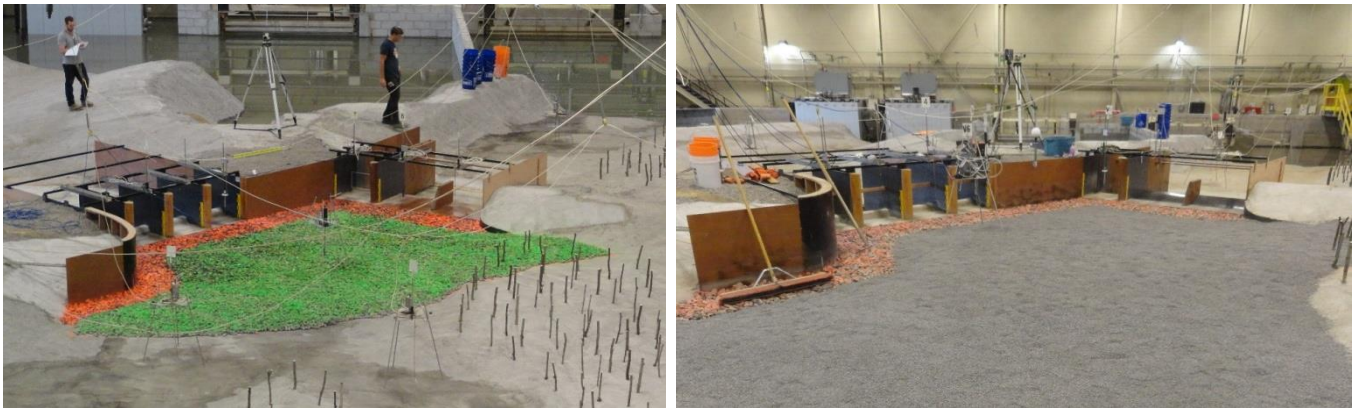

Figure 34. Left – mobile bed area of the model was filled with 210kg (green) riprap stone during clear water or debris tests. Right – model river sediments placed in the mobile bed area.

3.4.2 *Water Supply and Water Level Control*

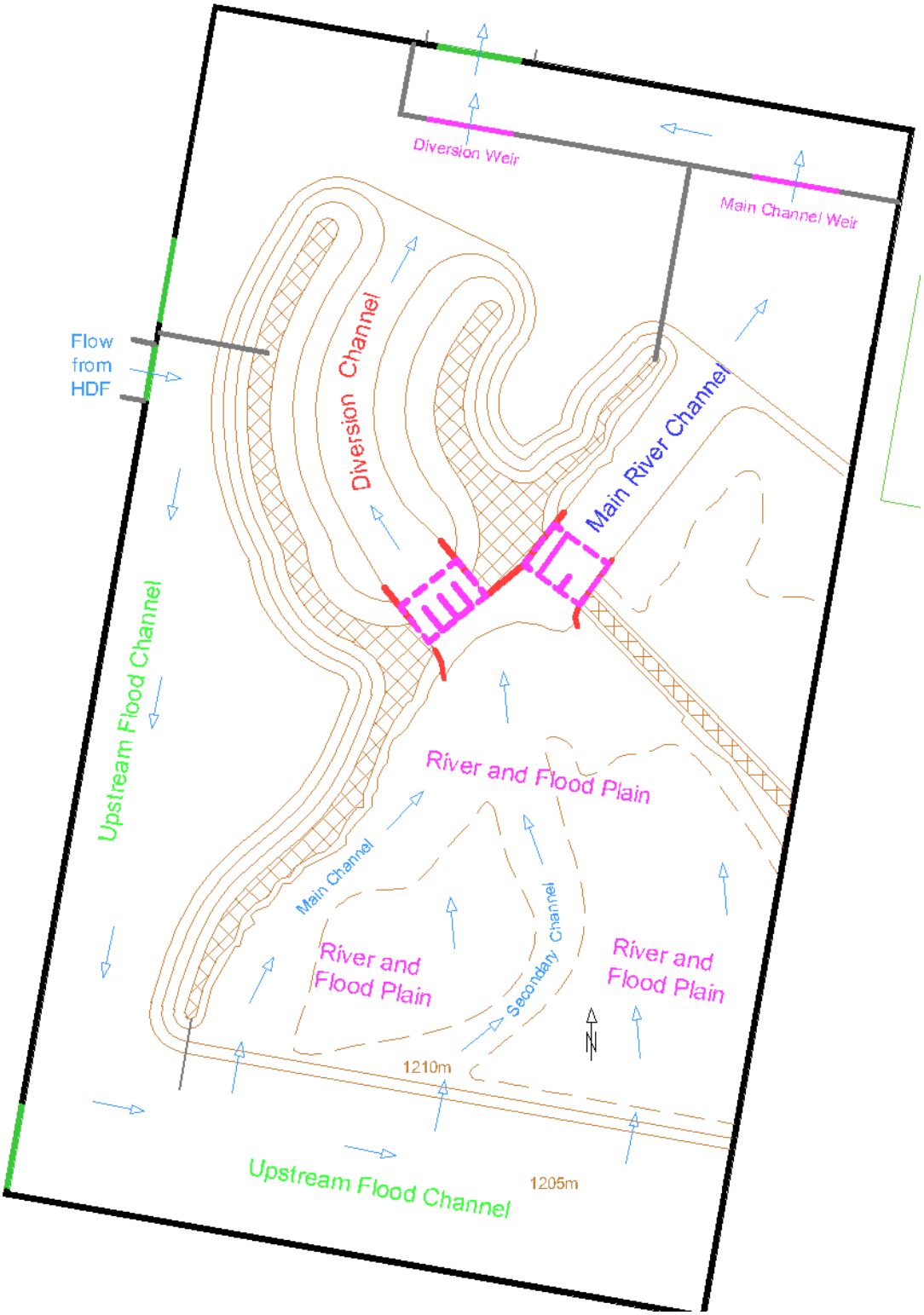

Figure 35. Simplified schematic showing the flow through the model.

A schematic showing the flow through the Springbank model is shown in Figure 35. The flow was supplied from the underground water storage reservoir (sump) and pumped into the HDF using a variable pitch pump. The flow was controlled by adjusting the vane pitch on the pump control panel. The HDF was connected to the LAB with masonry walls. Due to the high ground from the concrete bathymetry and temporary masonry walls installed in the LAB, the model was partitioned into four main areas: the upstream flood channel, the river and floodplain, the diversion channel (and settling pool), and the main river channel (and settling pool). The flow entered into the LAB and flooded the upstream flood channel. Once the volume of water was high enough, the river and floodplain began to flood and the flow was directed though the diversion inlet and service spillway structures by the topography. Flow through the diversion inlet flowed along the model diversion channel before dropping into a settling pool, and finally flowing over the diversion control weir. The tail-water elevation in the diversion channel was controlled by adjusting the level of the diversion weir. Similarly, the flow through the sluiceway/ service spillway flowed along the model river channel into a settling basin and over the main channel control weir. The control weirs are shown in Figure 36. Once the water spilled over the two weirs it was returned to the water reservoir sump for recirculation into the model (via the HDF). The water level elevations upstream of the diversion inlet and service spillway were controlled by the flow and the diversion/sluiceway/spillway gate settings.

Figure 36. Diversion channel control weir (left) and main channel control weir (right).

3.4.3 *Structures*

The original and revised designs for the hydraulic structures were presented in Section 2.2. From these designs, simplified model versions were developed that represented the hydraulic characteristics of the prototypes, yet were designed to easily accommodate changes in the model. The walls of the diversion inlet or service spillway structures were made from either PVC or marine plywood, and the bases were made from plate steel and concrete. Details of both the original and revised design are presented in the following sections.

3.4.3.1 Original Design

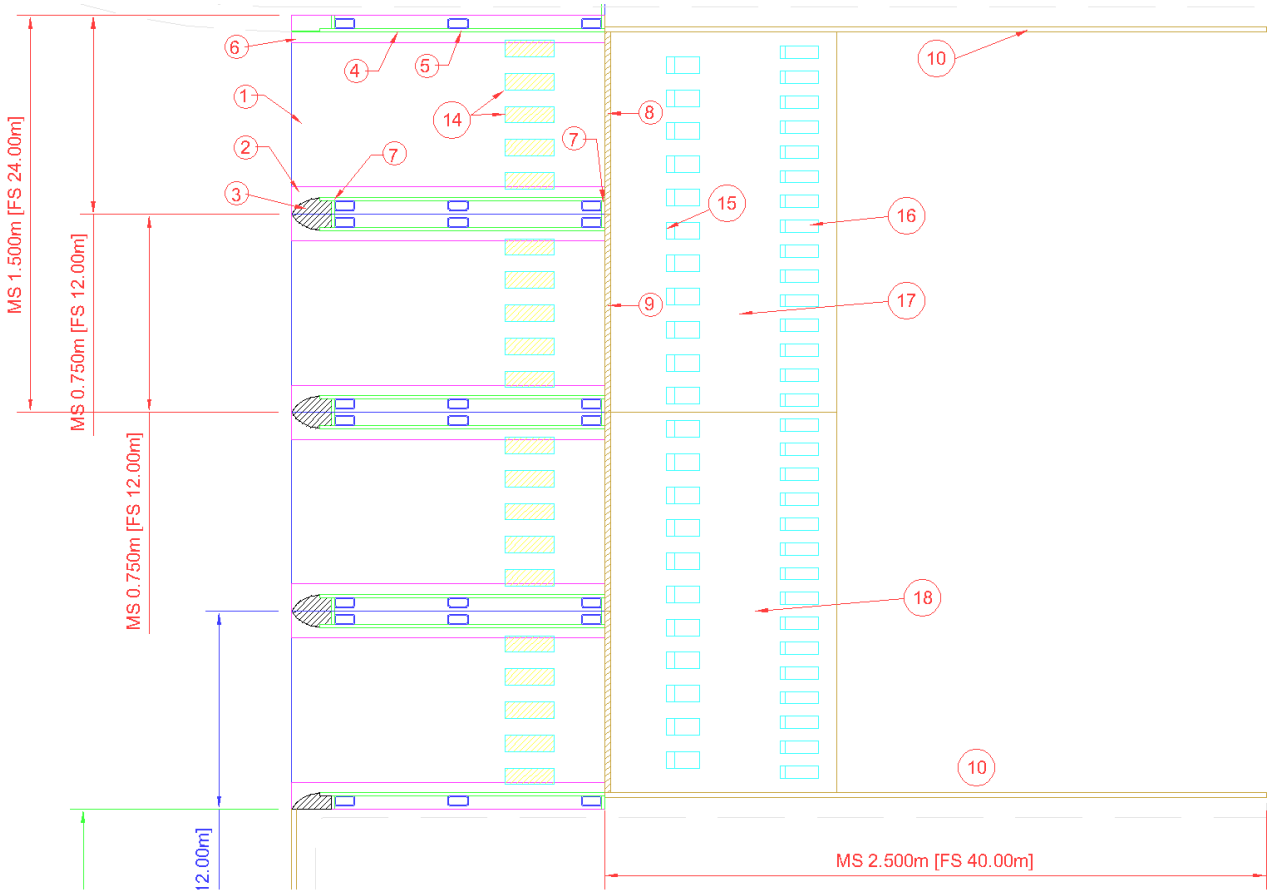

Figure 37. Example of a general assembly construction drawing of the model diversion. Note, MS and FS refer to Model Scale and Full Scale, respectively.

The prototype designs for the hydraulic structures were transferred to model scale (1/16th the size) and construction shop drawings were developed by NRC-OCRE and approved by Stantec. Figure 37 presents an example of a shop drawing of the diversion. The location of all the structures and features in the model were laid out with precision using a total station. The retaining walls and side walls of the structures were made from marine plywood, PVC, or sheet metal.

The diversion inlet structure was constructed on a ½" steel baseplate, and the central piers were made from hollow structural steel that was welded to the baseplate, and the piers were clad with PVC. The pier noses were precision milled from hardwood to match the prototype designs. The concrete apron of the diversion inlet was made from concrete grout, and its construction was guided by the use of a template to precisely match the profile curves. Wooden chute blocks were cut and fastened to the concrete apron of the diversion inlet apron and stilling basin. The gates for the diversion inlet were not modelled in the original design - if the model diversion inlet was to be closed, marine plywood was fastened to the back of the pier to stop the flow through the diversion inlet bays. Photographs showing some of the stages of construction for the original diversion inlet structure are shown in Figure 38 to Figure 42.

Figure 38. Left: diversion inlet pier struts and base plates installed in the basin. Right: precision milled hardwood pier noses after manufacture.

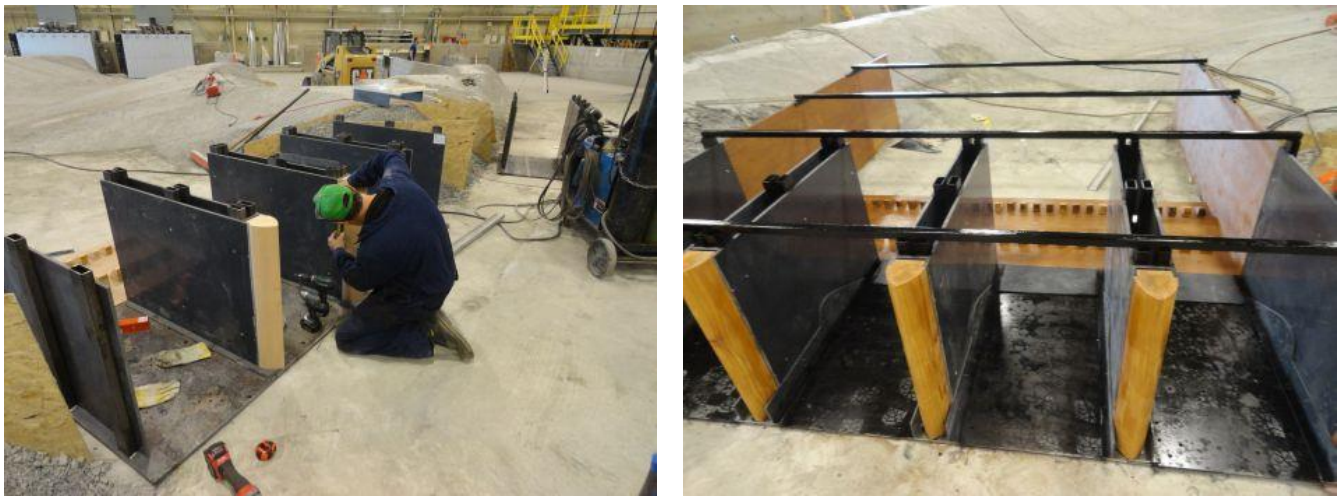

Figure 39. Left: installing the pier noses. Right: installing the support struts, rear retaining walls and rear stilling basin chute blocks.

Figure 40. Left: forming the concrete apron. Right: concrete apron and front chute blocks installed.

Figure 41. Left: retaining walls made from plywood and sheet metal. Right: installing the riprap apron material and the plywood retaining wall that spans between the diversion inlet and the sluiceway.

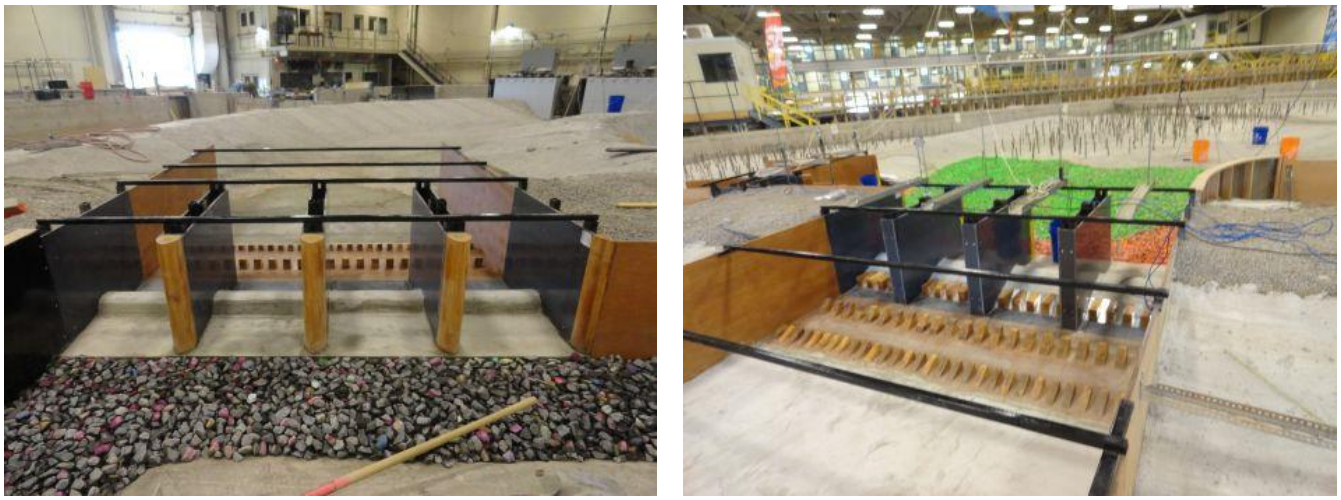

Figure 42. Left: diversion inlet looking downstream. Right: diversion inlet looking upstream (the 440kg riprap and 210kg riprap used in the mobile bed portion of the model was painted to aid in movement detection).

The sluiceway and service spillway were constructed similarly to the diversion. The sluiceway section was built on a steel baseplate with hollow structural steel members cladded with PVC sheet to form the interior pier. The sluiceway concrete apron was cast in concrete to match the curved profile of the design. The radial sluiceway gate was modelled with a lift gate made from clear acrylic plastic. The bottom 1m of the lift gate was cut to match the curved radial gate profile to give the flow through the opening the proper character. The base of the service spillway was made from plywood, as was the angled central pier that divided the Obermeyer crest gates. The sluiceway pier was constructed on a ½" steel baseplate, clad with PVC, and fitted with the precision milled hardwood pier nose. The concrete apron of the diversion inlet was made from concrete grout, and its construction was guided by the use of a template to precisely match the profile. Obermeyer gates set to specific elevations were pre-constructed from sheet metal facing supported by wooden ribs, and the gates were screwed to the service spillway base to allow rapid installation and removal in the model. A wooden end sill was fastened to the concrete apron of the sluiceway/service spillway stilling basin. Photographs showing some of the stages of construction for the original diversion inlet structure are shown in Figure 43 to Figure 45.

Figure 46 and Figure 47 show front and rear views of the original design after construction.

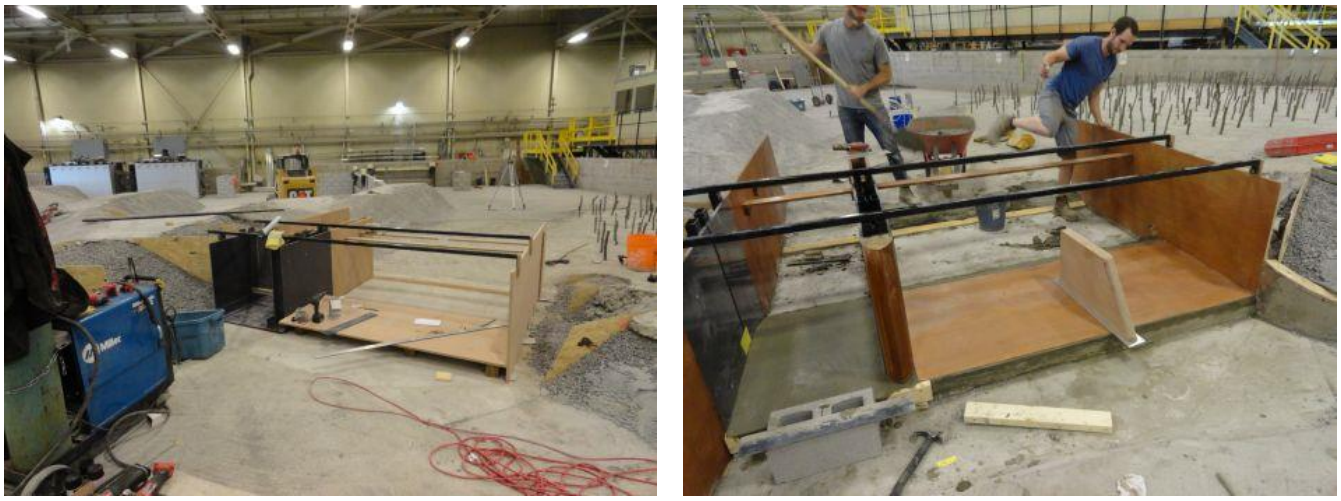

Figure 43. Left: sluiceway and service spillway installation in the model. Right: pouring the concrete apron through the sluiceway, installing the pier nose and the angled central pier on the service spillway.

Figure 44. Left: the riprap apron was installed, and the (black) curved retaining wall on the RHS of the service spillway was tapered to match the profile of the floodplain berm. Right: view of the finished sluiceway with the clear plastic gate lowered and riprap painted orange.

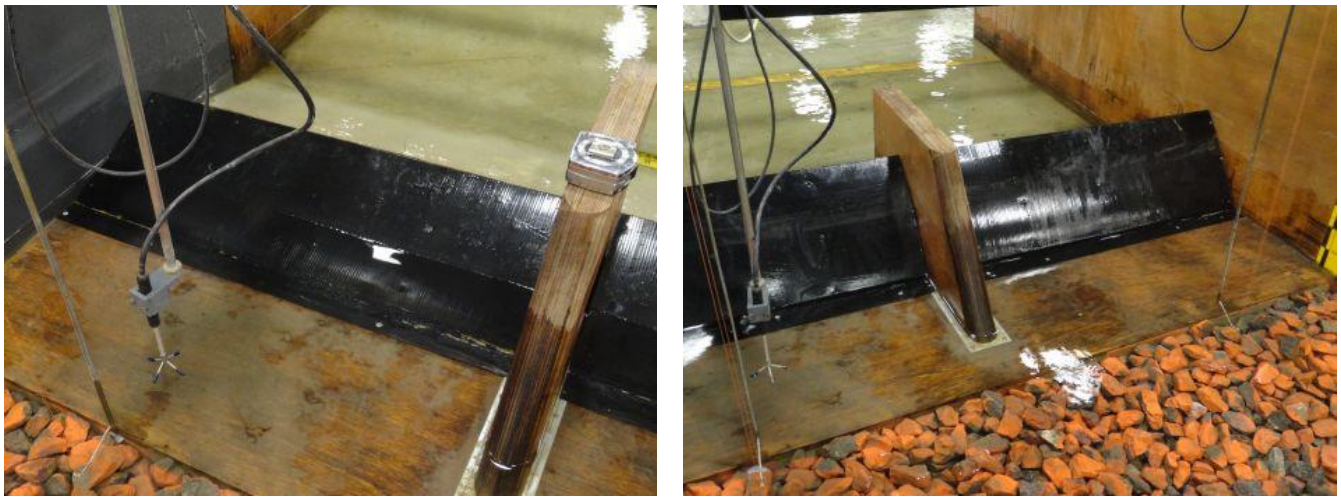

Figure 45. Obermeyer gates were made from sheet metal plate fastened to curved ribs to match the gate profile.

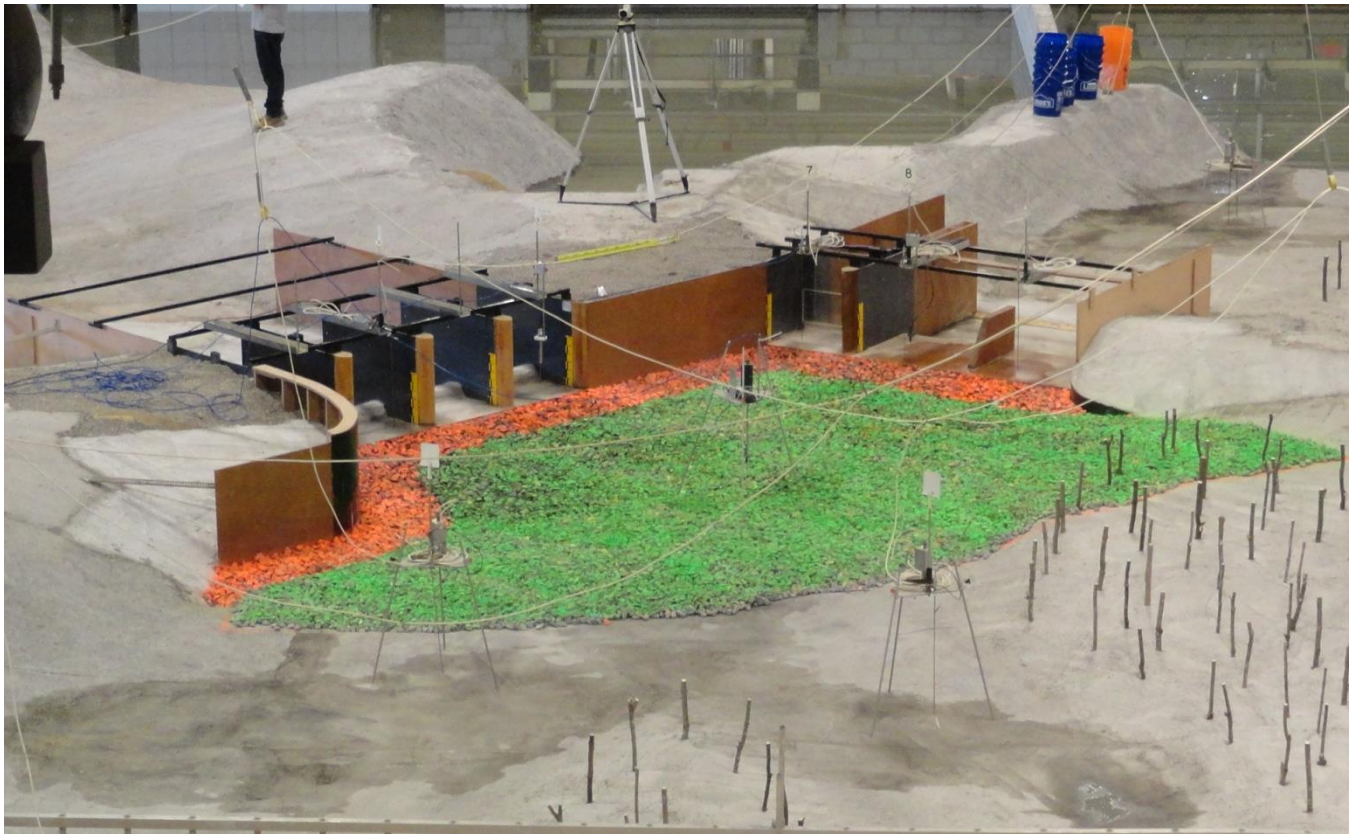

Figure 46. Front view of the original design for the diversion inlet and sluiceway/service spillway structures in the model. For the initial tests where mobile sediments were not investigated, the mobile bed area was filled with 210kg riprap and painted green.

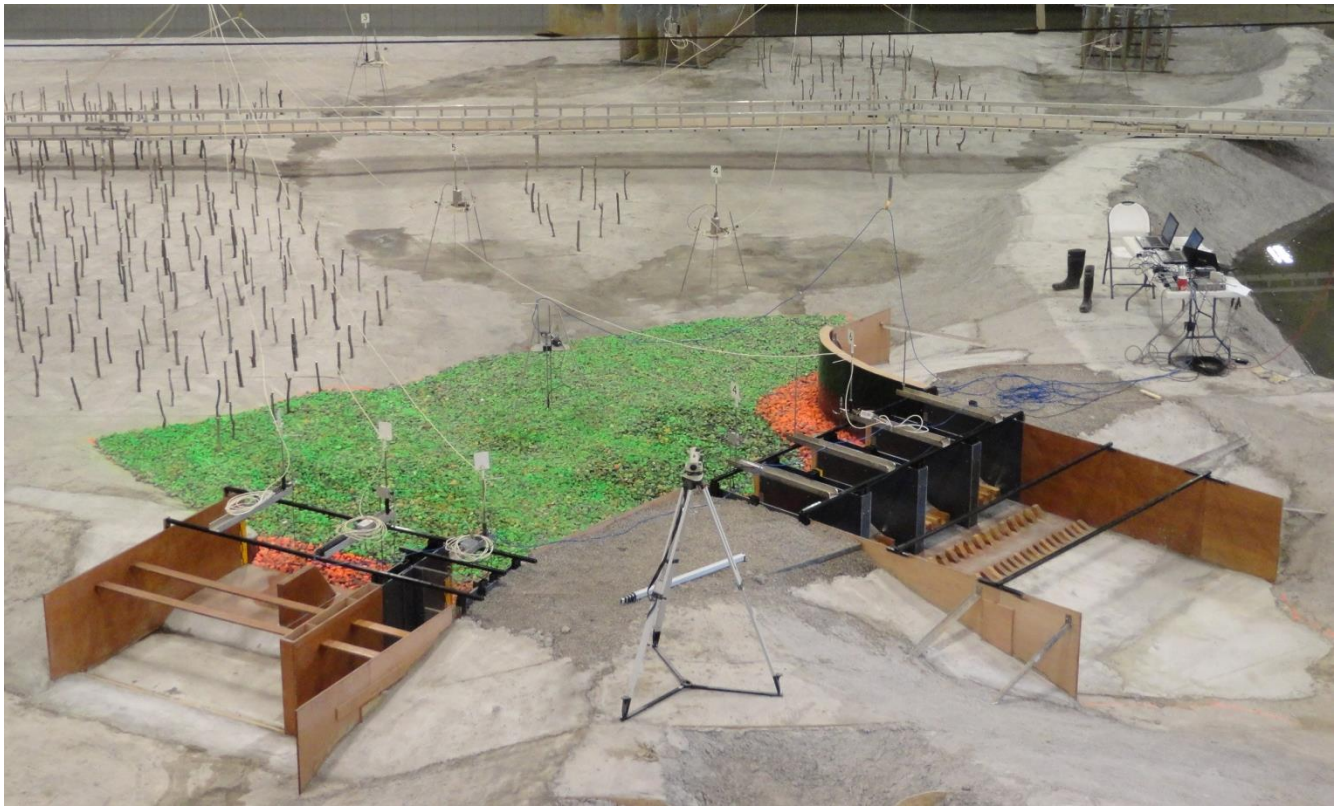

Figure 47. Rear view of the original diversion inlet and sluiceway/service spillway structures.

3.4.3.2 Revised Design

As described in Section 2.2.2, the original design was revised by reducing the number of diversion inlet bays, re-aligning the service spillway, and removing the sluiceway. As before, the prototype designs were transferred to model construction and shop drawings and approved by Stantec. The main construction features remained the same – the straight sections of the structure walls were made from PVC and marine plywood, and the curved walls were made from sheet metal.

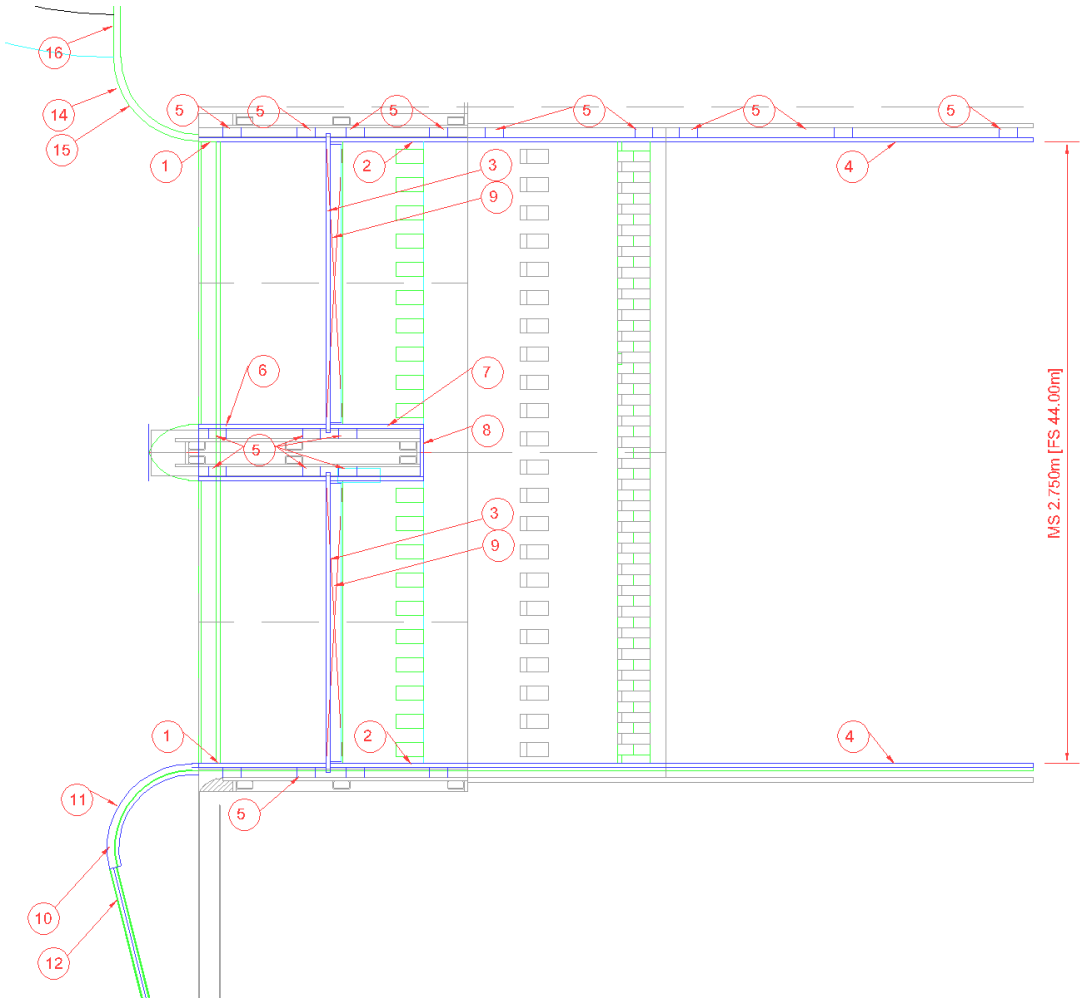

Figure 48. Example of a general assembly construction drawing of the revised model diversion inlet.

The model diversion inlet structure still used the same design basis with the structure and central pier mounted on a baseplate. The original design side walls had inserts installed to make the total diversion inlet breath opening narrower. The wider central pier had steel support members clad with PVC and an allowance for four different types of pier noses to be quickly installed during the testing. The diversion inlet lift gate was modelled with marine plywood, and as before the concrete apron was modelled with concrete and the chute blocks were made from hardwood and fastened to the concrete apron and stilling basin. Photographs showing some of the stages of construction for the revised diversion inlet structure are shown in Figure 49 to Figure 53.

Figure 49. Installation of the narrower sidewalls, curved retaining walls, and preparations for pouring the concrete apron at the diversion.

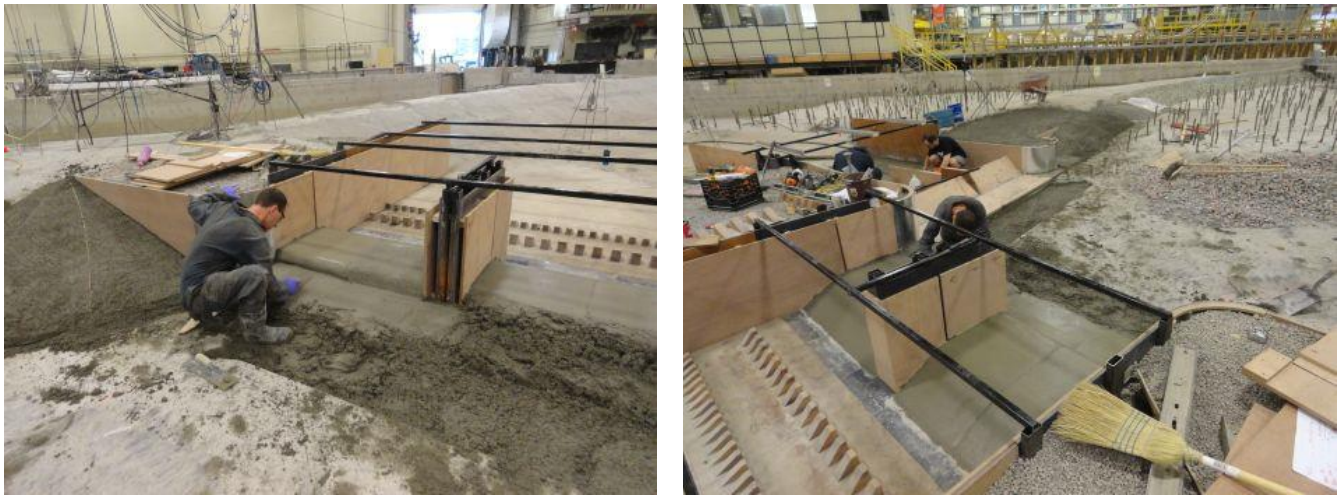

Figure 50. Pouring the concrete for the embankment, diversion inlet apron, and the bottom of the new riprap pit.

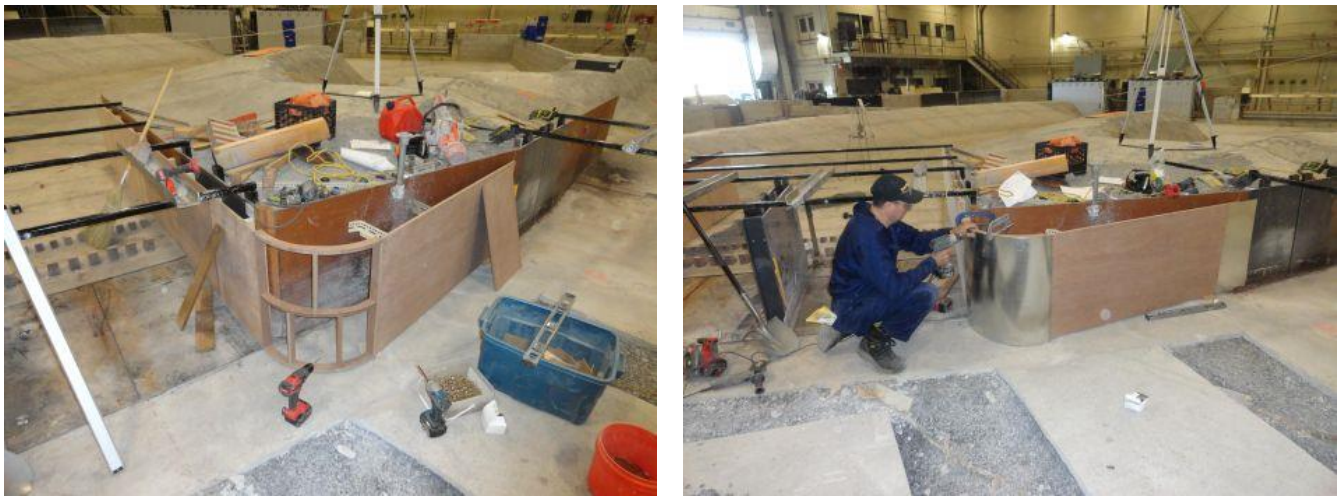

Figure 51. Installing the modified central retaining wall between the diversion inlet and service spillway.

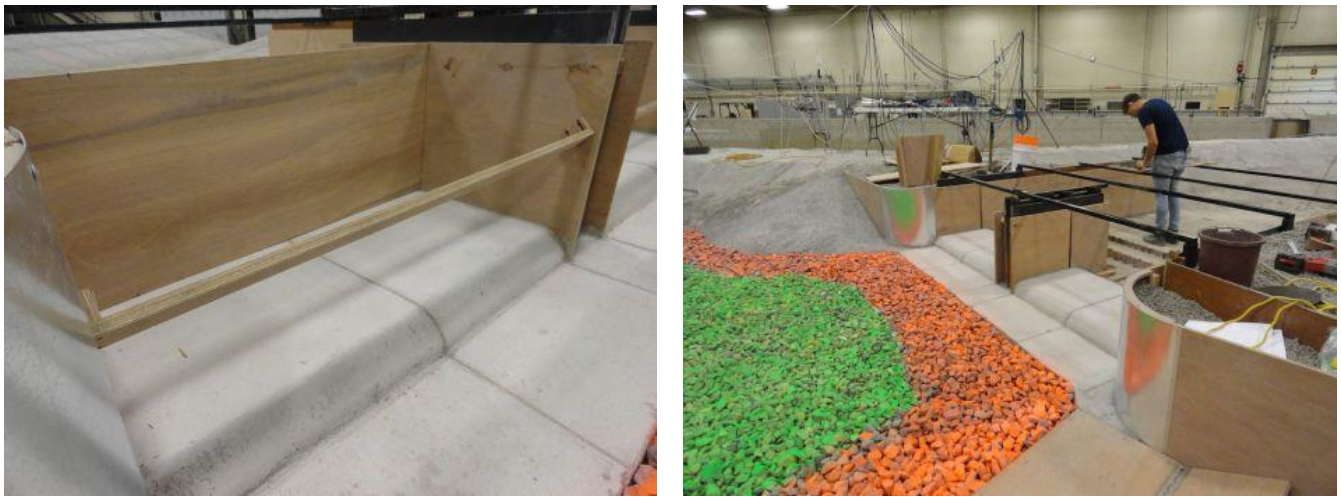

Figure 52. Left: diversion inlet concrete apron and breast wall (the lift gate is closed). Right: installation of the 440kg riprap (orange) and the 210kg riprap stone used to model the mobile-bed portion of the model (green).

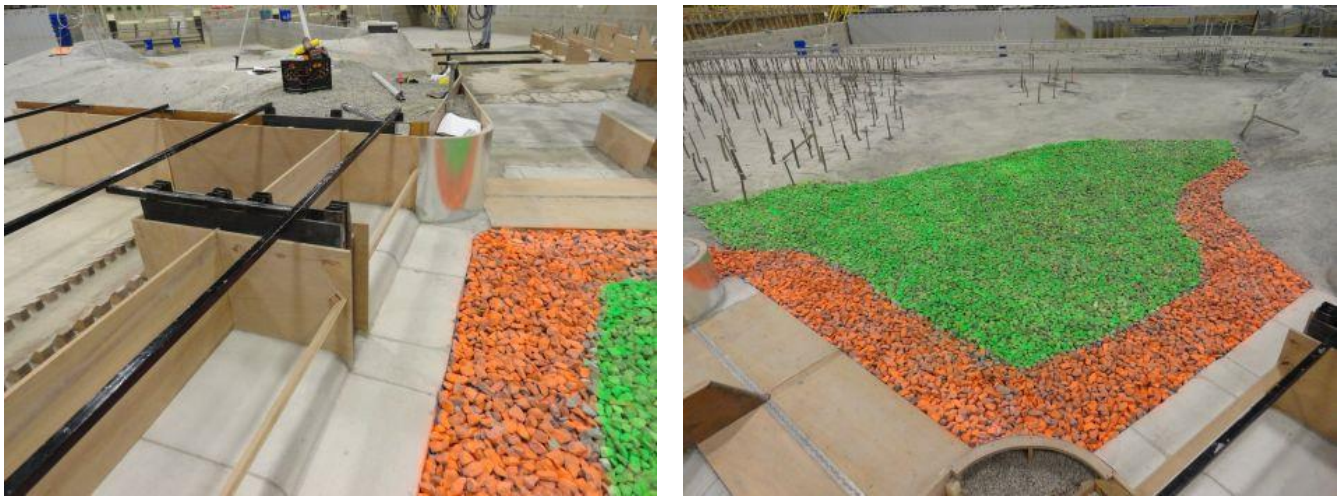

Figure 53. Left: diversion inlet structure with lift gates lowered (no pier nose installed yet). Right: Upstream view of the floodplain as viewed from the revised structures.

3.4.3.3 Revised Design – Pier Nose Designs

The performance of four different pier noses was investigated on the 4m wide central pier of the revised diversion inlet structure. The pier noses were designed to be interchangeable while the model flow was running, and they were swapped in-out during the debris tests to investigate the potential for the debris to catch on the nose of the pier. The main features of the designs were:

- Pier Nose 1 – curving arrowhead plan shape, apex 3.5m from the front edge of the diversion, 8m tall (see Figure 54).
- Pier Nose 2 – same curving arrowhead plan shape, apex 9.5m from the front edge of the diversion, 8m tall (see Figure 55).
- Pier Nose 3 – same curving arrowhead plan shape, adverse 1:4 slope placing the apex 8m from the front edge of the diversion inlet at the top and 6m at the bottom, 8m tall (see Figure 56).
- Pier Nose 4 – circular 1.8m diameter plan shape on the nose, 2:1 sloping profile, and was slightly shorter at 7m high off the concrete apron (see Figure 57).

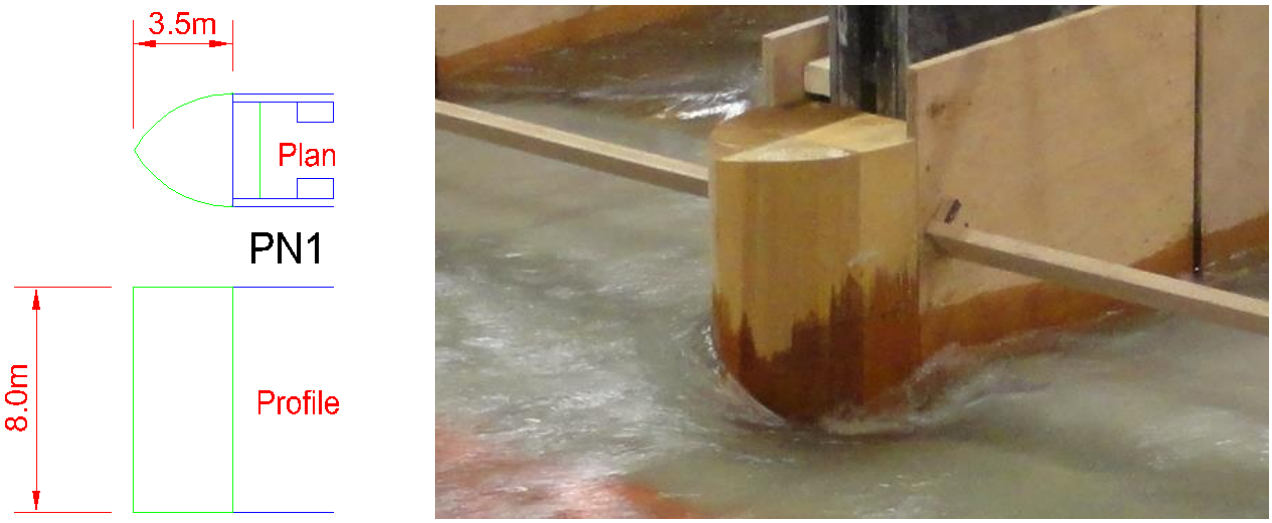

Figure 54. Pier Nose 1 design schematic and implementation in the model.

Figure 55. Pier Nose 2 design schematic and implementation in the model.

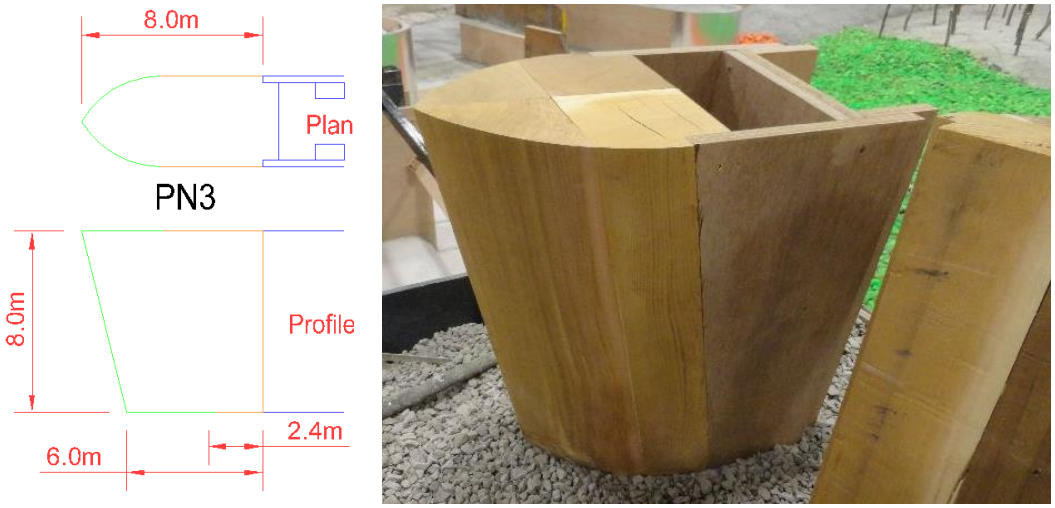

Figure 56. Pier Nose 3 design schematic and photograph before installation.

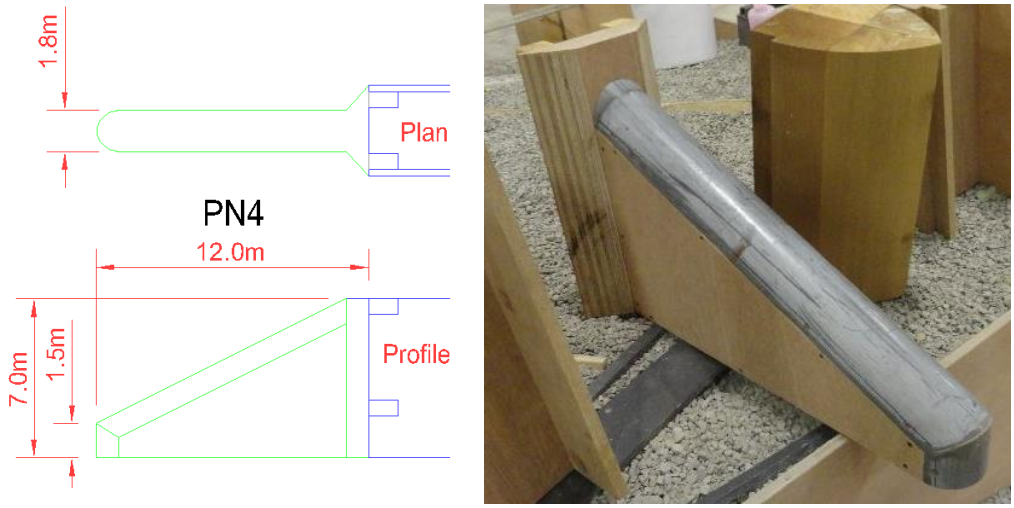

Figure 57. Pier Nose 4 design schematic and photograph before installation.

3.4.3.4 Revised Design – Debris Barrier Designs

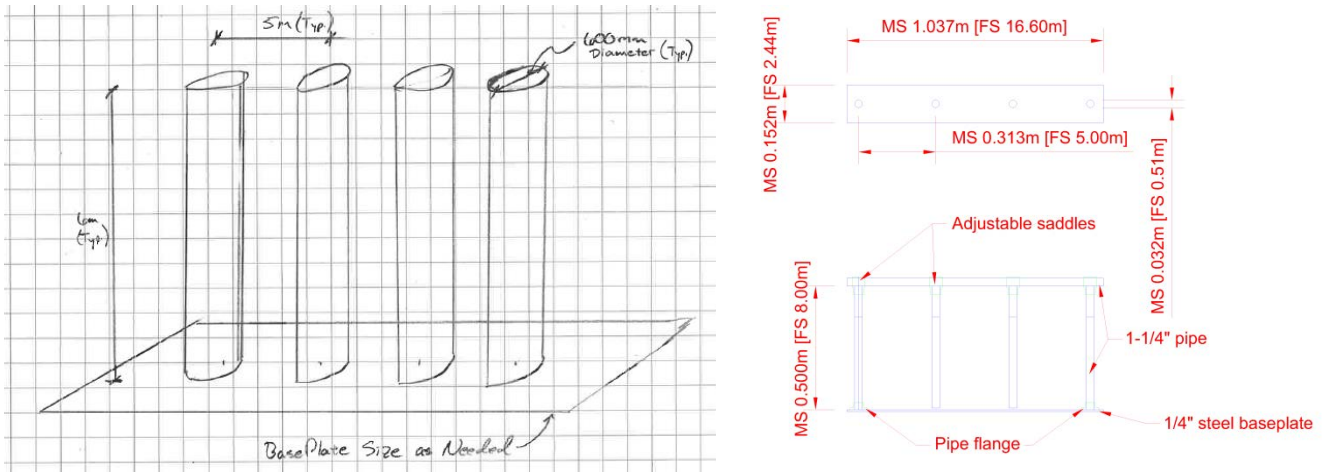

Figure 58. Debris Barrier A-D design schematic and model shop drawings (FS dimension are in Full Scale).

The performance of six different debris barriers (A-F) fronting the diversion inlet structure and their ability to collect tree debris that was inserted from various locations on the upstream floodplain was investigated. Debris barriers A-D used larger piers and were located inside or very near the diversion inlet structure, while barriers E and F used smaller piers on tighter spacing and were installed further up the floodplain.

The design for debris barriers A-D included 600mm diameter piles, 6m tall, and spaced on 5m centers (see Figure 58, left). These debris barriers were modelled with 510mm piles (slightly smaller due to available materials in stock to expedite construction and testing), 8m tall (to accommodate possible height changes), and on 5m center spacing (see Figure 58, right). The layouts for the debris barriers differed slightly, and the main features of the designs were:

- Debris barrier A – two sets of four 600mm diameter piles spaced on 5m (centers) and 6m tall, each set of four were placed in the diversion inlet bays (see Figure 59).
- Debris barrier B – eight 600mm diameter piles spaced on 5m (centers) and 6m tall, each set of four were placed in a line starting at the LHS of the diversion inlet (see Figure 60).
- Debris barrier C – eight 600mm diameter piles spaced on 5m (centers) and 6m tall, similar alignment to barrier B but with a slightly larger gap at the LHS of the diversion inlet (see Figure 61).
- Debris barrier D – nine 600mm diameter piles spaced on 5m (centers) and 6m tall, each set of four were placed in a line starting at the RHS of the diversion inlet (see Figure 62).

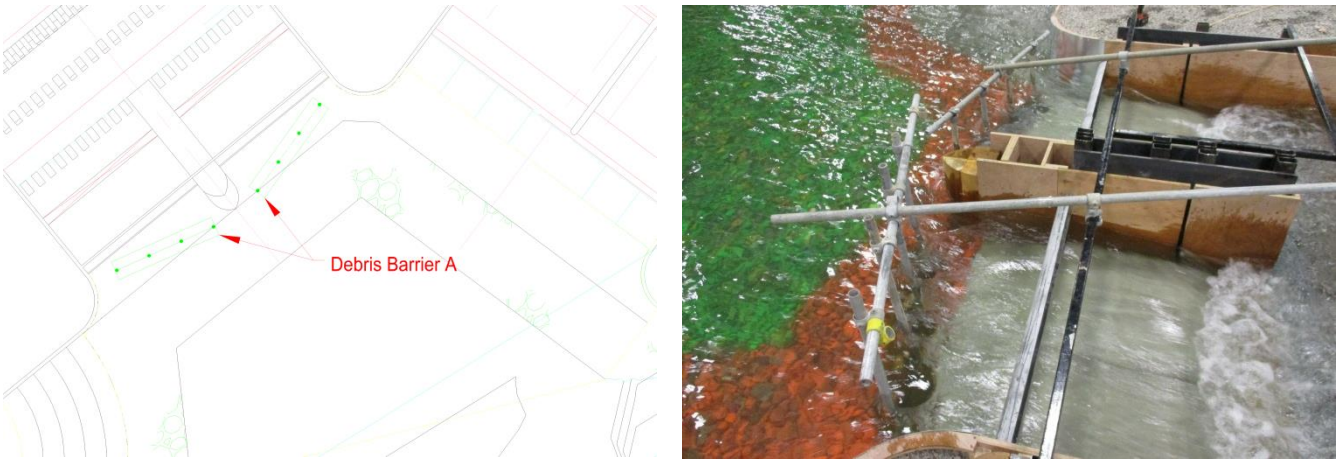

Figure 59. Debris Barrier A layout schematic and implementation in the model.

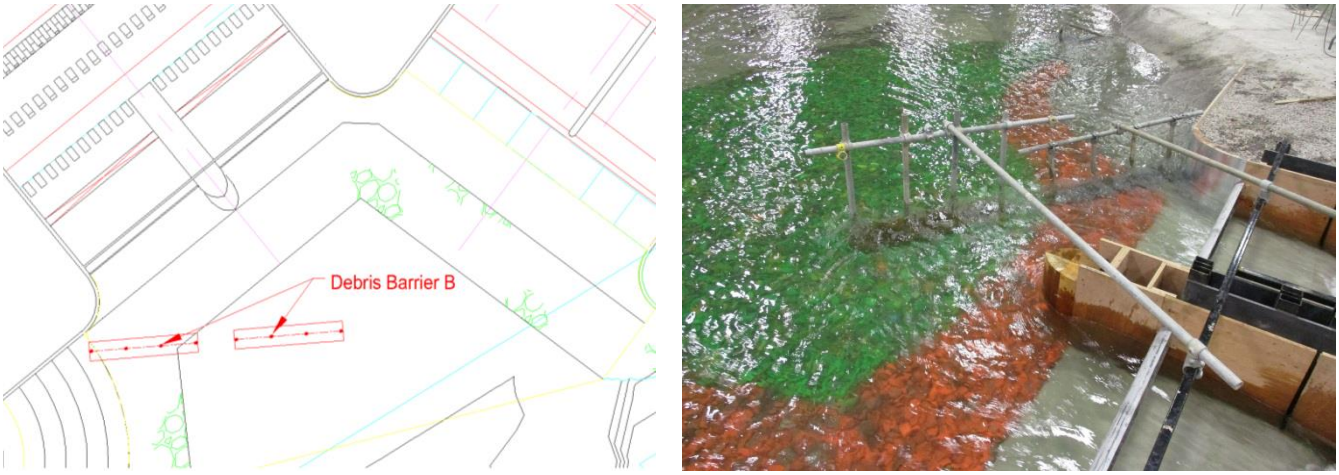

Figure 60. Debris Barrier B layout schematic and implementation in the model.

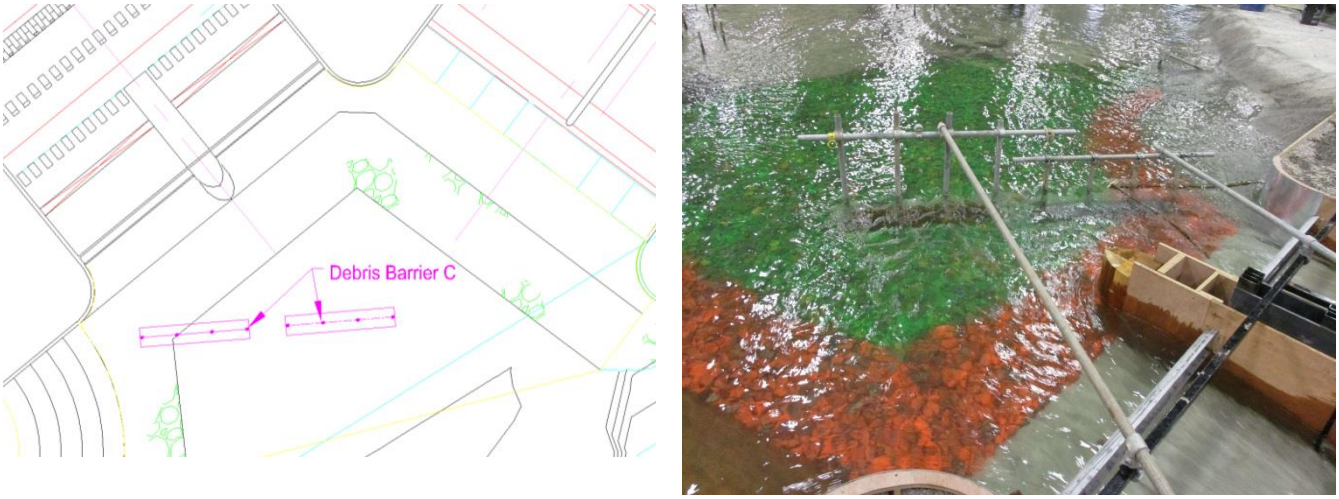

Figure 61. Debris Barrier C layout schematic and implementation in the model.

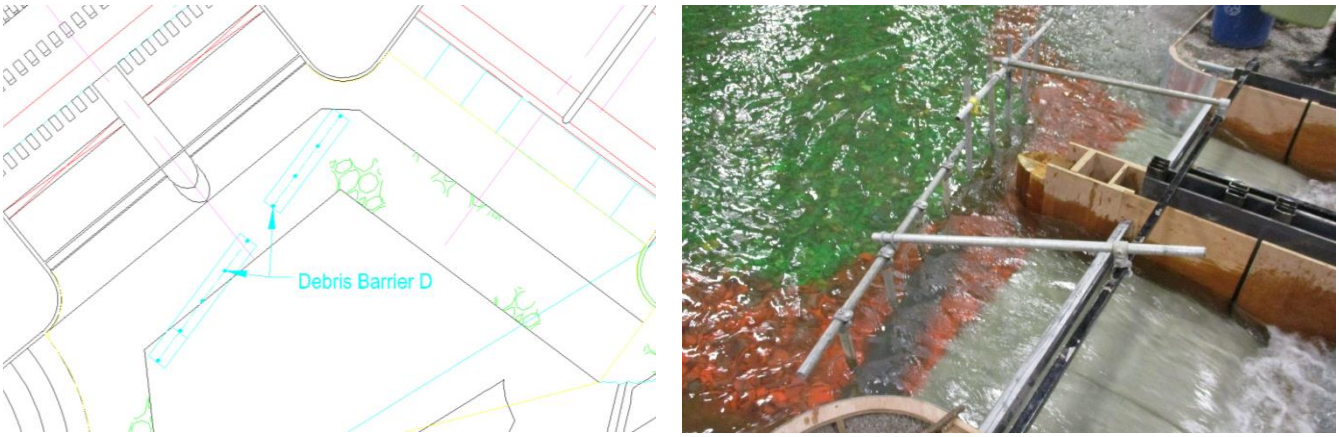

Figure 62. Debris Barrier D layout schematic and implementation in the model.

Debris barriers E and F were much different from A-D in that they stretched from the curved retaining wall between the diversion inlet and service spillway much further (~160m) upstream into the floodplain.

Debris barrier E (see Figure 63) featured three straight legs: moving from upstream, leg AB was 46m long, leg BC was 41m, and leg CD was 90m. The profile designs for the barrier are shown in Figure 64. The wall was to be made from pipe piles 300mm in diameter and spaced on 2m centers, and guide rails made from timber were to be set at elevations of 1216m, 1215m, 1214m and 1213m. These designs were replicated to scale in the model, and Figure 65 shows the barrier being constructed.

Debris barrier F was similar to E, with guide rails between elevations of 1213m and 1216m, however the guide rails were set on a tighter spacing (0.5m) and the alignment stayed closer to the left bank of the river channel to provide less obstruction (refer to Figure 66 and Figure 67).

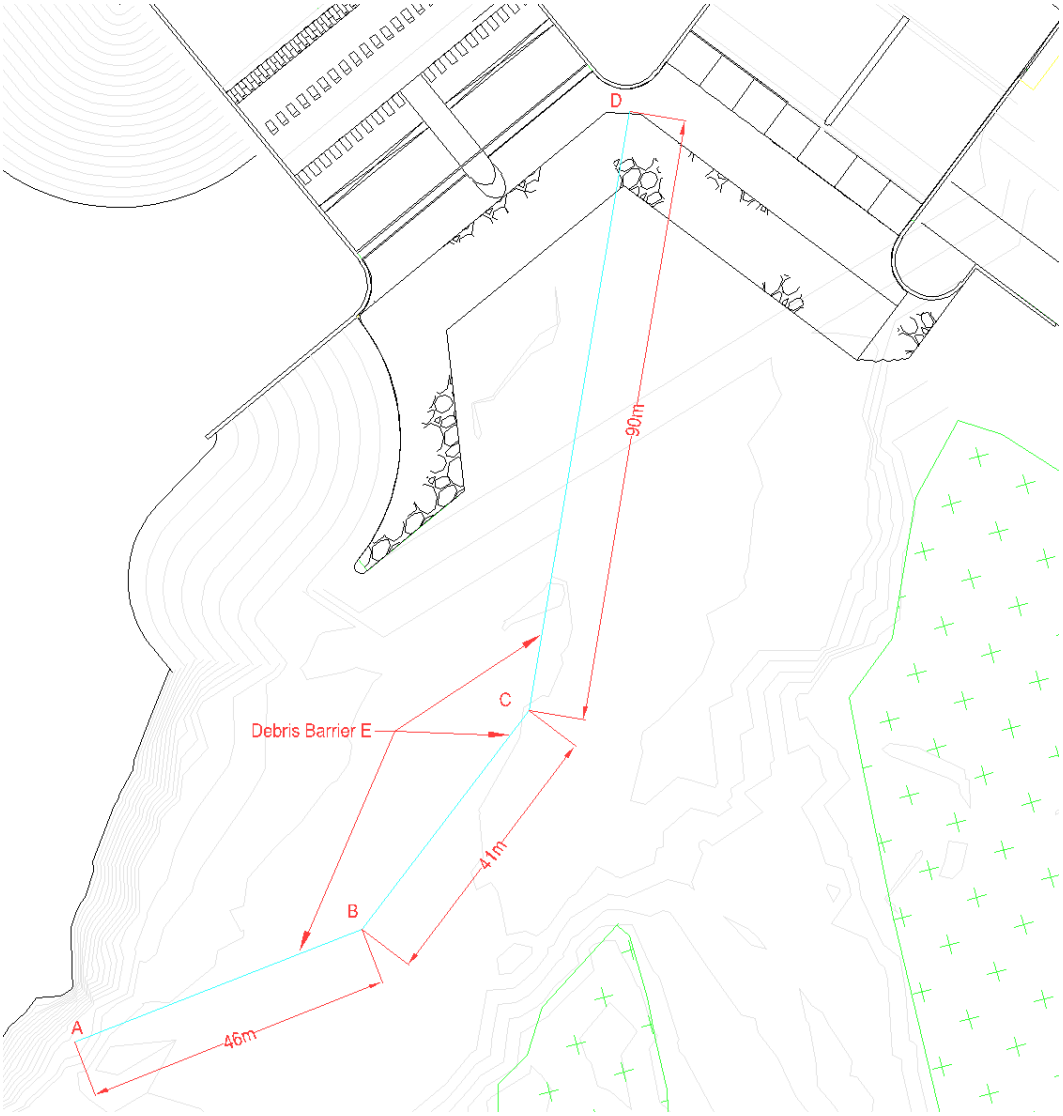

Figure 63. Debris Barrier E layout schematic.

Figure 64. Debris Barrier E design sketches.

Figure 65. Debris Barrier E implementation in the model.

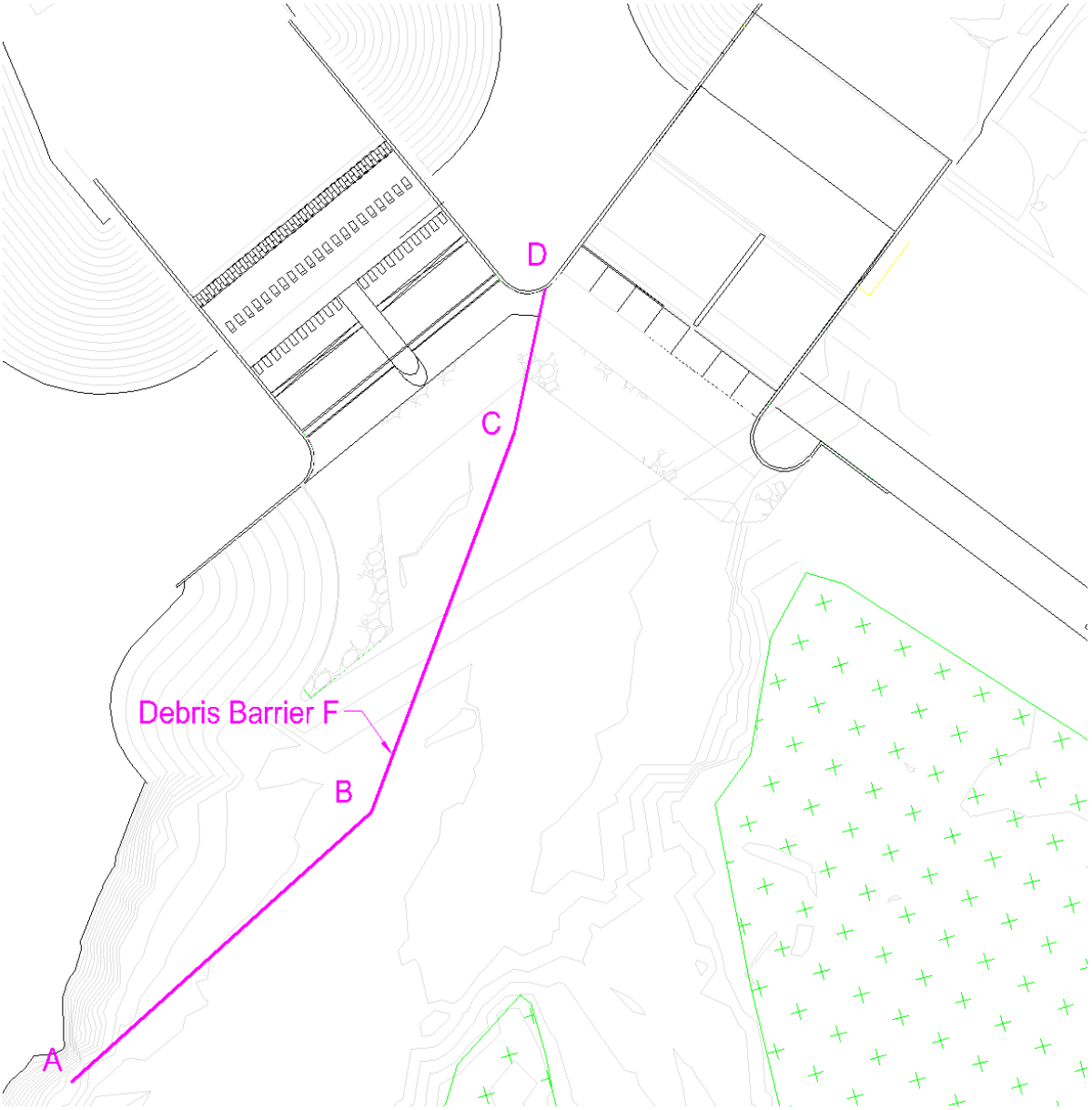

Figure 66. Debris Barrier F layout schematic.

Figure 67. Debris Barrier F construction in the model.

3.4.4 *Trees and Woody Debris*

During extreme flooding events, a large amount of woody debris can be transported down the Elbow River. One of the key facets of the physical model was to investigate and improve the performance of the diversion inlet and service spillway structures with woody debris in the flow. Stantec provided information from a survey of the trees and woody debris along an 8km reach of the Elbow River that indicated the following:

- 63% of the logs had a root wad at the base
- Mean length was 16.5m, and standard deviation was 4m
- Mean large end diameter was 0.44m
- Mean small end diameter was 0.14m

Rather than model the debris with straight wooden dowels, actual tree branches complete with bends and knots were utilized for added realism. Over 200 specimens of model woody debris with a mean diameter of 0.4m to 0.5m were collected, prepared, and used in the modelling. 70% of the model woody debris was 16m long, while 30% were 21m long. 60% of all woody debris had a root wad attached to the base. The model root wads were constructed from two thin timber boards, 1.6m long, stapled to the bottom of the tree in an X-pattern. Trees were deployed into the primary and secondary channels in the model floodplain. A typical debris run at a given flow condition involved releasing single trees, followed by packs of four, ten, and forty trees. Their behaviour and pathway through the floodplain, as well as their interaction with the model structures were observed.

The standing forests in the model floodplain were also modelled using tree branches to the same size specifications. The model trees were cast directly into the concrete with a random placement density specified by Stantec of one tree every $50m^2$. Figure 68 to Figure 70 present photographs documenting the preparation and use of the woody debris in the model.

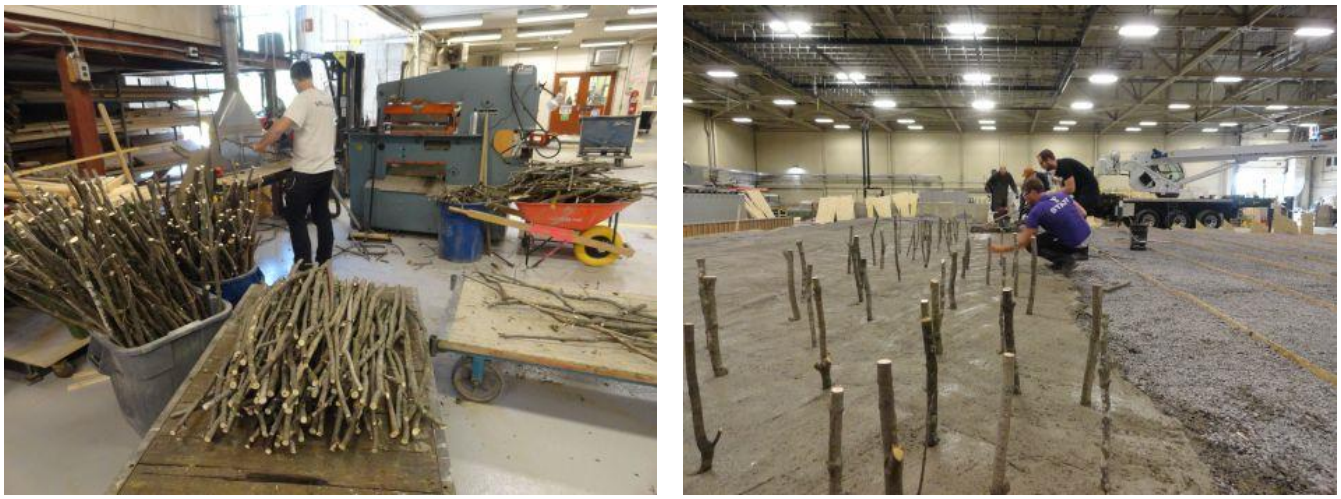

Figure 68. Left - woody debris preparation, right – standing trees cast into the model concrete.

Figure 69. Left – trees cast into the concrete representing the forested floodplain, right – debris rafts in the model including debris with root wad X's at their base.

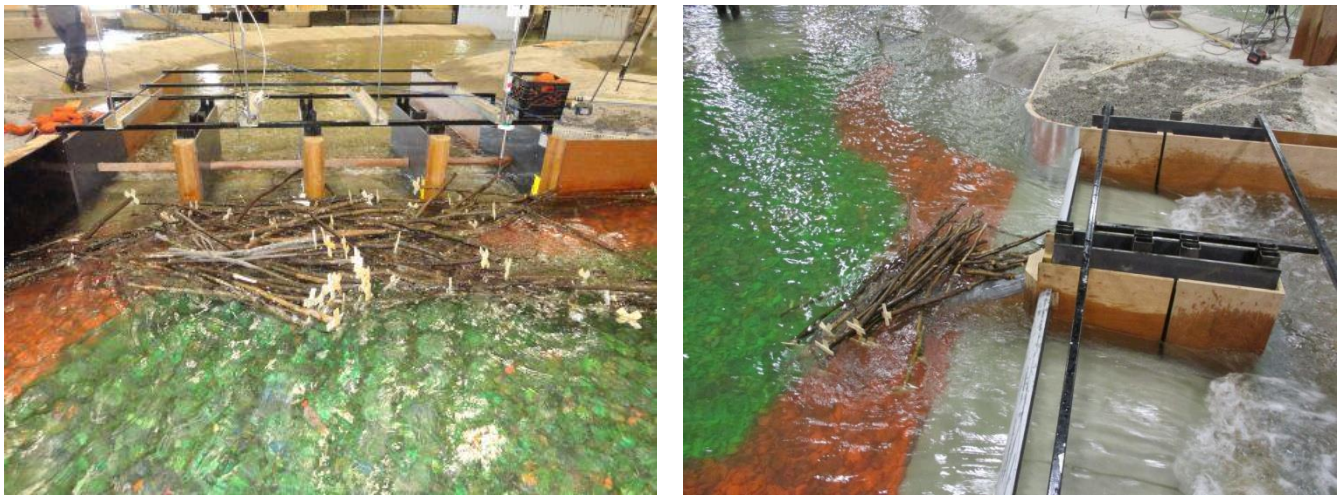

Figure 70. Woody debris interacting with the structures: left – the original diversion, right – the revised diversion inlet with pier nose 4.

3.4.5 *Mobile Bed Sediments*

In order to match the very high sediment loads in the river, motorized spreaders were used to seed the flow with the model sediment (refer to Section 3.2.3 for the model sediment scaling). The spreaders were borrowed from the City of Ottawa (they are normally used to spread road salt) and mounted on steel support frames. Three different spreaders were used for this study and were given the following names: battery spreader, 3360 spreade and B750 spreader (shown in Figure 71). The loading rate of each spreader was calibrated prior to testing to match the sediment loading rates provided by Stantec. The calibration process included filling a spreader with a known quantity of sediment and running the spreaders until they were empty. The spreader motor and conveyor belt did not have a throttle, so the delivery rate was adjusted via the gate opening (small, medium or large) at the end of the conveyor. The delivery rates for all three spreaders for the various gate openings are shown in Table 2. Based on the calibration results the spreaders had loading rates ranging from 280 kg/s to 1800 kg/s (full scale).

Figure 71. Rock Spreader B075.

Model Scale					Full Scale
Hopper	Opening	Stone Weight (Kg)	Time (s)	Loading Rate (kg/s)	Loading Rate (kg/s)
Battery	Large	349.4	228	1.53	1569
	Medium	374	359	1.04	1067
	Small	360.8	1305	0.28	283
3360	Large	367.2	214	1.72	1757
	Medium	368.4	295	1.25	1279
	Small	350.6	seized	NA	
B750	Large	376.8	214	1.76	1803
	Medium	371.8	306	1.22	1244
	Small	367.2	571	0.64	659

Table 2. Spreader Calibration Results.

For the sediment testing runs, each spreader was set up in one of three locations in the upstream floodplain for the 320 m^3/s, 760 m^3/s and 1240 m^3/s flood events (refer to Figure 72). The 320 m^3/s flow condition test run used the battery spreader in location 1. For the 760 m^3/s flow, the battery spreader was moved to location 3 and the B750 spreader was placed in location 1. The 1240 m^3/s

used the same spreader configuration as the 760 m^3/s test with the addition of the 3360 spreader in location 2.

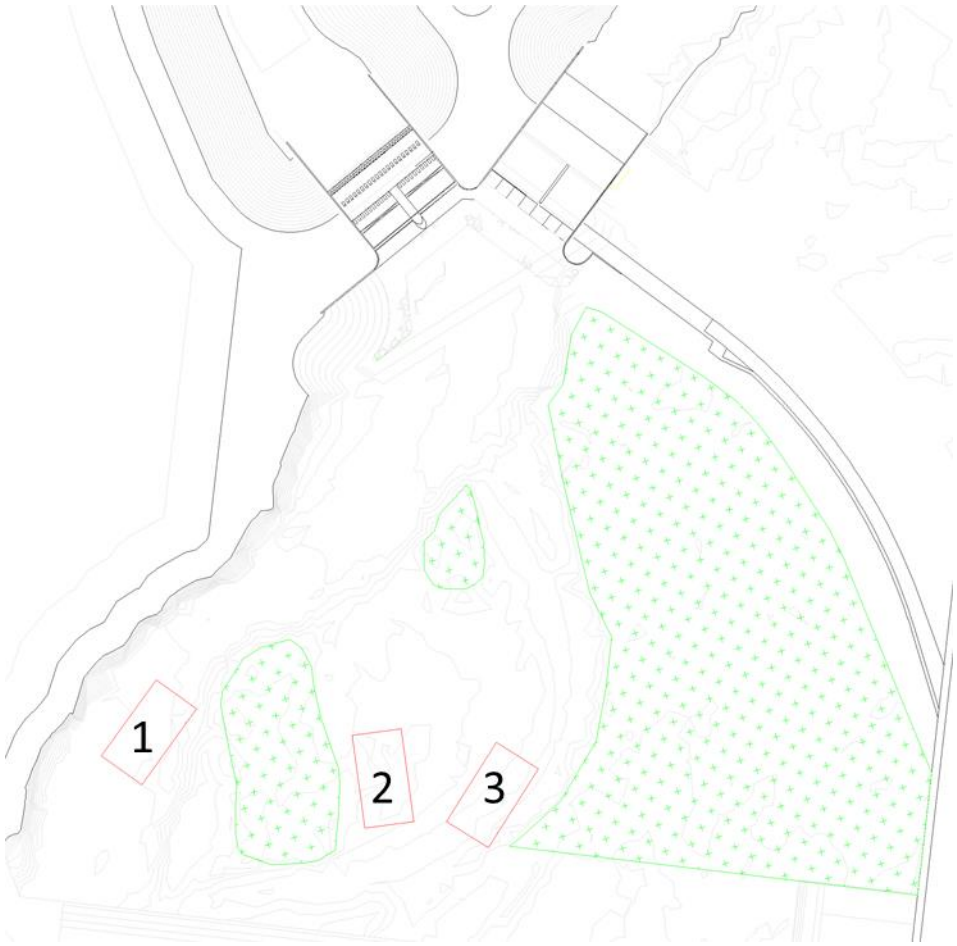

Figure 72. Spreader Locations.

Before the first sediment test, the model was preloaded with sediment along the main channel, secondary channel and in the forebay (see Figure 73). The preloaded sediment was 1m deep in front of the structures and 0.5m deep along the main and secondary channels.

Figure 73. Preloaded sediment in the main channel and secondary channel (left) and in front of the structures (right).

3.5 Instrumentation Systems, Monitoring and Observation

The model was equipped with instruments and video cameras for measuring water levels and velocities in multiple locations of interest. Water level and velocity gauges were deployed through the model domain and adjusted during the modelling to areas of local interest. Two video cameras and two fixed still photography overhead cameras were mounted in the ceiling providing overhead views to track the trajectory of floating debris, floating tracers and coloured dye injected into the model. Also, cameras mounted on tripods were used to video and photograph the performance of the structures. These tools were used to document the water levels, velocities, circulation patterns, and sediment and debris interactions near the new structures for each flow condition. The discharge in the diversion channel and the downstream river channel were measured from the head over the two downstream weirs. There were five different configurations for all of the instruments in the model. These are shown in Figure 74 to Figure 77, and the layout used for each test series is shown in Table 3.

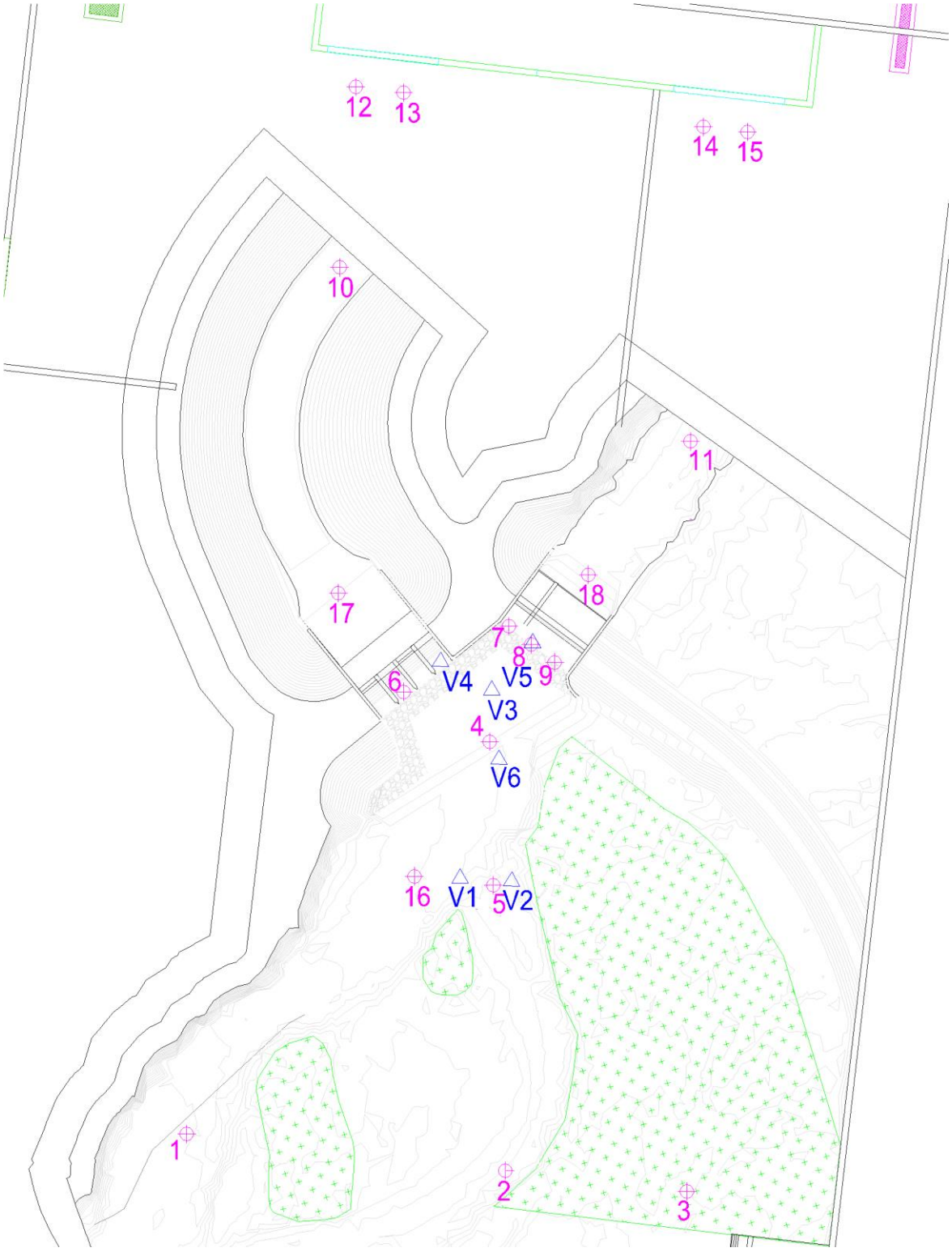

Figure 74. Instrumentation layout 2 – water level probes are shown in pink and velocity probes are shown in blue.

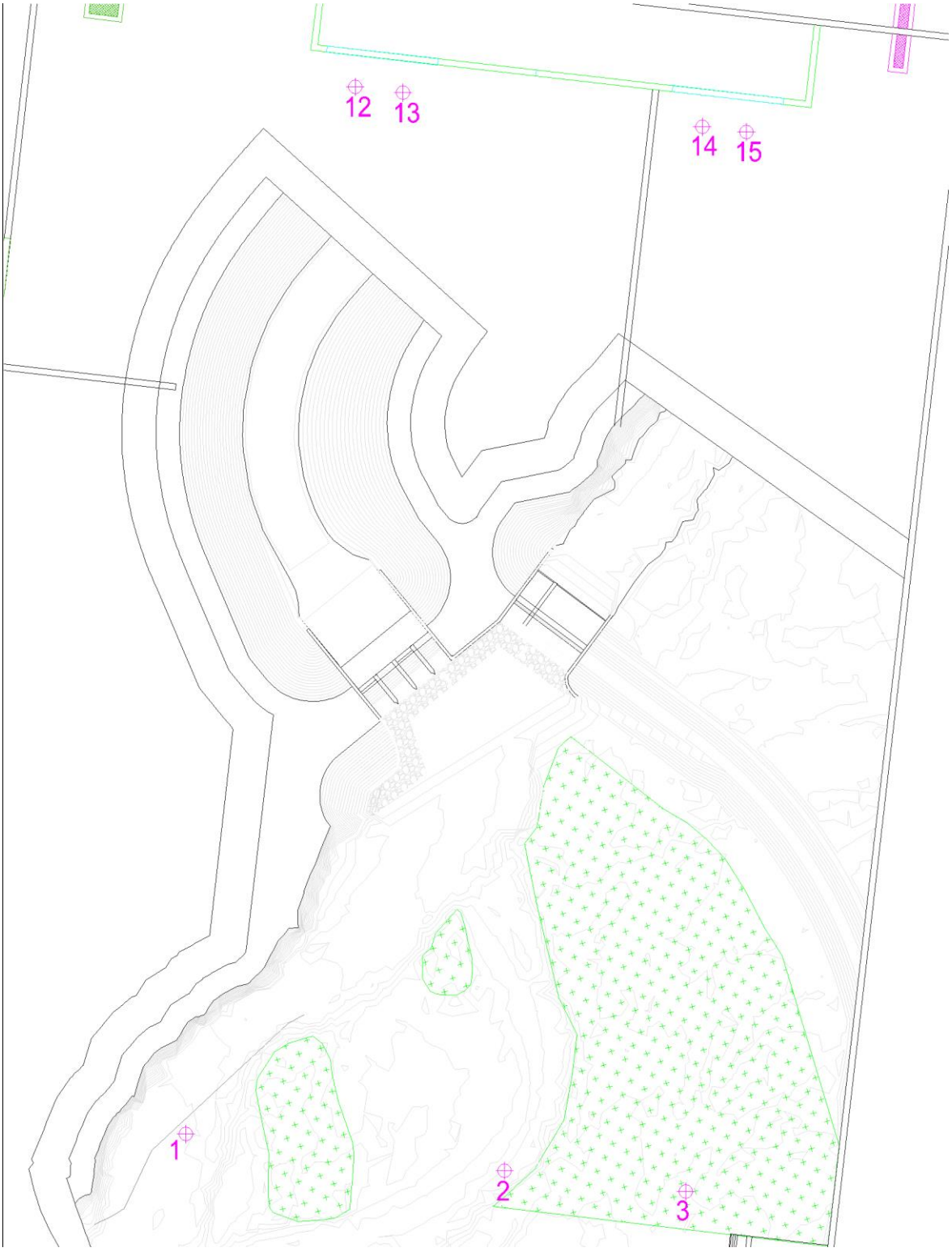

Figure 75. Instrumentation layout 3 – water level probes are shown in pink and velocity probes are shown in blue.

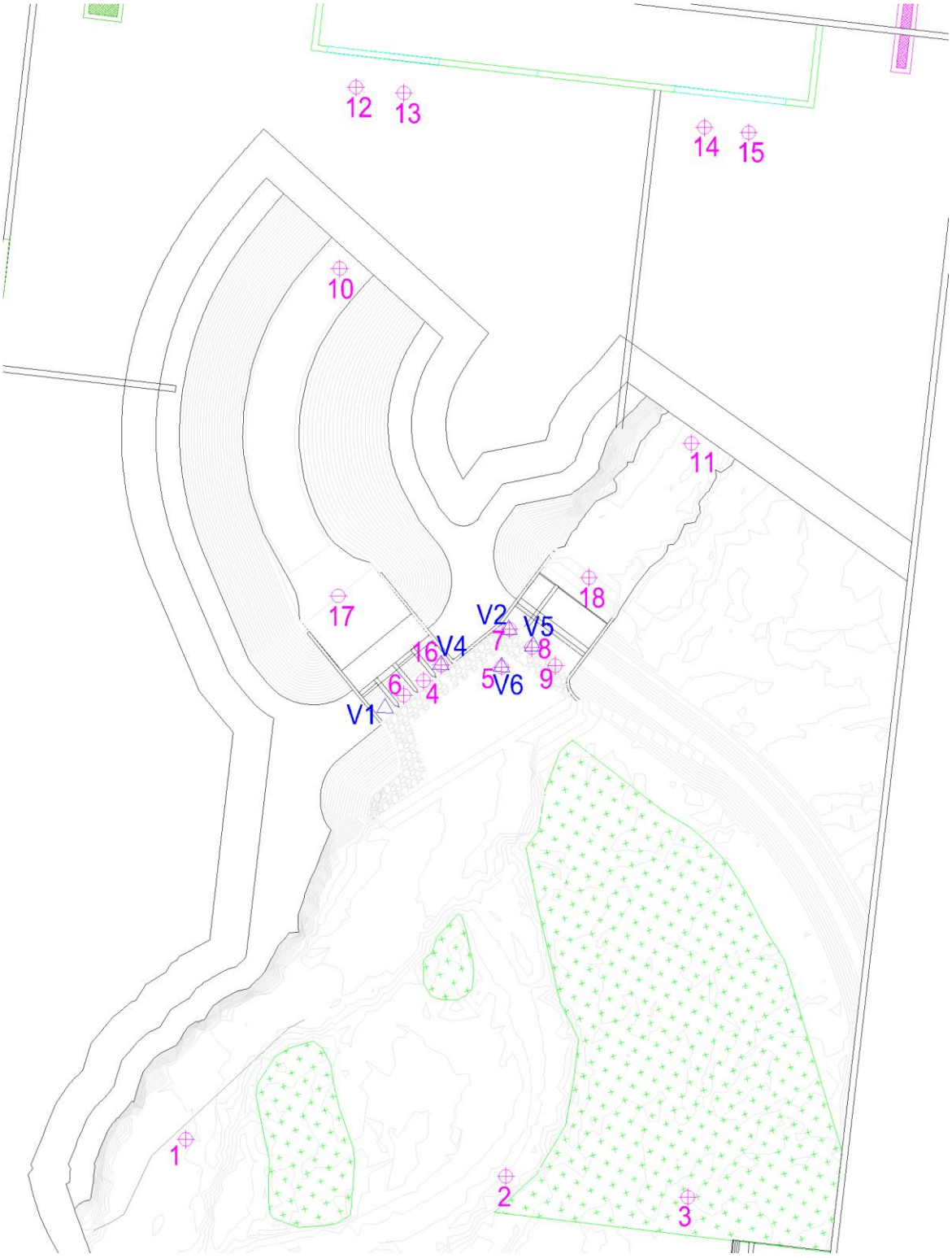

Figure 76. Instrumentation layout 4 – water level probes are shown in pink and velocity probes are shown in blue.

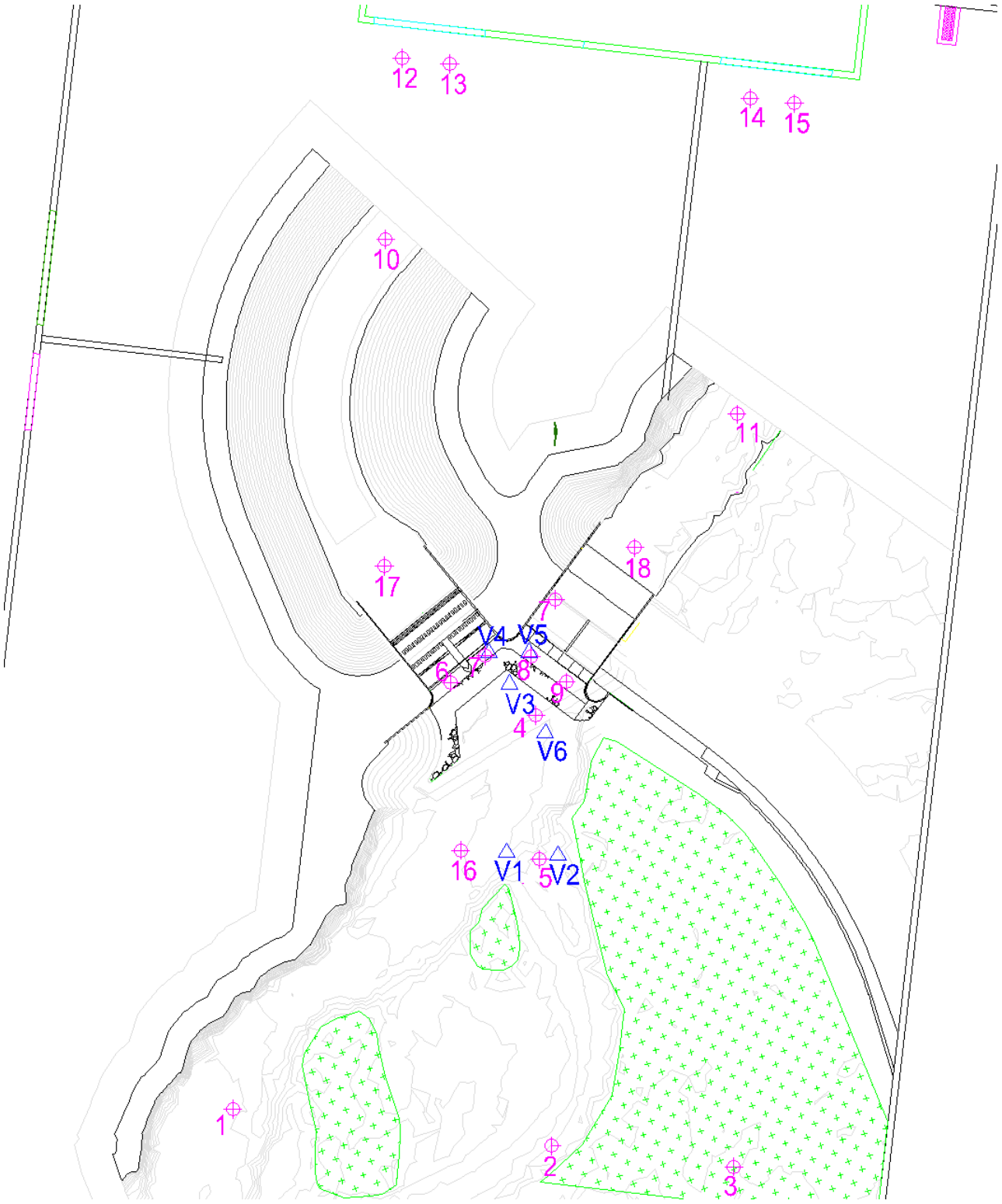

Figure 77. Instrumentation layout 5 – water level probes are shown in pink and velocity probes are shown in blue.

3.5.1 *Water Levels*

Water levels in the model were measured at many different locations using 18 capacitance-type water level gauges developed by Akamina Technologies (see Figure 78). These probes operate by sensing the change in capacitance that occurs as a portion of the insulated wire becomes submerged. The signal is directly proportional to the percentage of the wire that is wetted, regardless of whether the wetting is continuous (caused by "green water") or intermittent (as in the case of spray). This type of gauge has been shown to exhibit a highly linear and stable relationship between water level and voltage. They typically feature calibration errors of less than 0.5% over a 100mm calibration range. This error represents an accuracy of ±0.5mm at model scale or ±8mm at full scale. The water level probes were calibrated several times throughout the test program by changing their elevation with respect to a fixed water level. The calibration constants remained stable throughout the test program.

There were four main water level gauge layouts used for the study, as shown in Figure 74 - Figure 77.

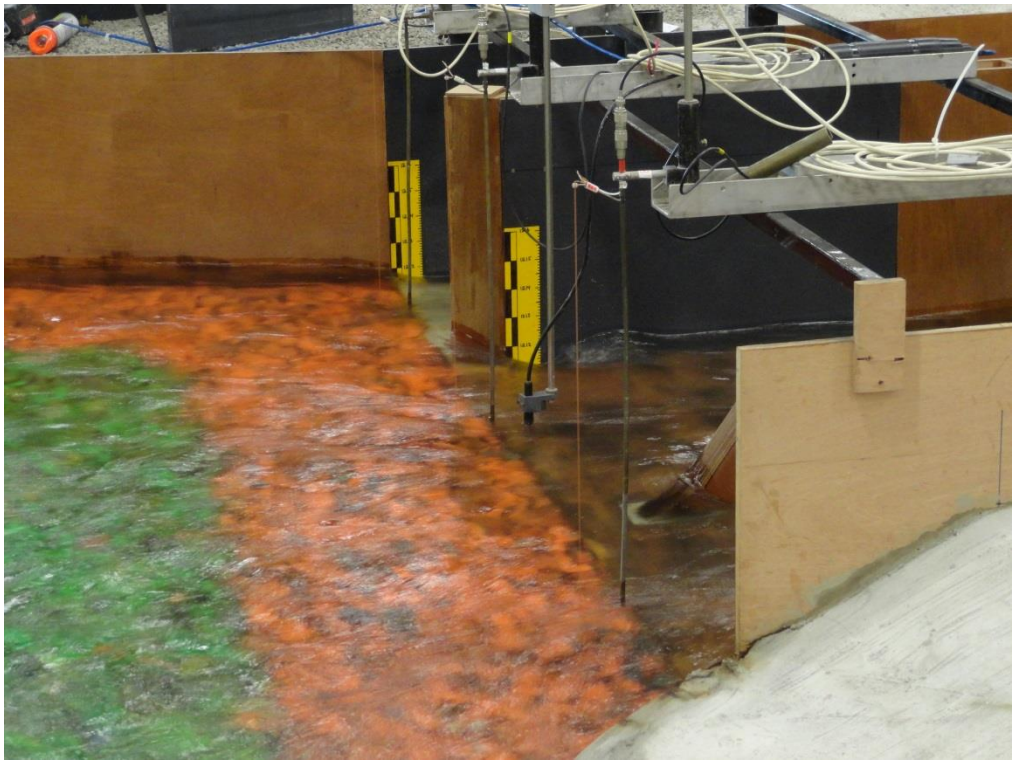

Figure 78. Capacitance water level gauges.

3.5.1 *Discharge*

The discharge was measured using the water level gauges at the two weirs, one for the main channel and one for the diversion channel, located downstream where the water exits the model. The weirs were set to specified elevations to match the tail-water conditions in the river channels given by Stantec. Four water level gauges (two for each weir) were used to record the water levels at each weir. Knowing the weir elevation and the water level at the weirs, the discharge was calculated based on the sharp-crested weir equation:

$$Q = 1.84 \times B \times H^{1.5}$$

Where B is the width of each weir (49.581m) and H is the head above the crest of the weir (as measured by the sensors).

3.5.2 *Velocities*

Two different types of instruments were used to measure velocities within the model, four 2-axis electromagnetic current meters developed by Alec Technologies and two 3-axis acoustic Doppler velocimeters made by Vectrino (ADV's) were utilized (see Figure 79). The height of the current meters above the river bottom was adjusted to be mid-depth for each flow condition. However the ADV sensors require 5cm (model scale) depth below the sensor for accurate readings, therefore they were not used during some of the lower flows since the depths were insufficient.

Flow patterns along the river channels and around the structures were also assessed by tracking floating drogues and plumes of coloured dye injected into the model. Time-lapse photography was employed using an overhead camera to capture the location and motion of individual drogues or dye. Time-averaged mean velocities were then estimated by noting the time required for the drogue to travel a known distance.

Note that the three methods for measuring the current fields were useful for describing the currents at different elevations in the water column. The drogues and dye tended to measure the near surface currents; while the probes measured the flow velocities at mid-depth of the water column.

Figure 79. Three-axis acoustic Doppler velocimeter (left) two-axis electromagnetic current meter (right).

3.5.3 *Mobile Bed Changes*

A FARO 3D laser scanner (see Figure 80) was used to measure the elevation of the mobile bed before and after each sediment run. The FARO scanner uses a laser to take detailed measurements of millions of points in order to capture three-dimensional environments. After each sediment run, multiple scans were completed at different locations around the mobile bed. Each scan captured approximately 5.6 million points at a resolution of 6.1mm between points at 10m from the scanner.

The multiple scans were stitched together to produce a single image of the mobile bed. Using the captured three-dimensional images, erosion/accretion patterns and volumetric sediment motion quantities were calculated by subtracting the pre and post sediment run FARO scans.

Figure 80. FARO 3D Laser Scanner.

3.5.4 *Data Acquisition System*

A data acquisition system converts analog voltage signals from the various sensors deployed in the model into digital form for storage in a computer data file. Analog signals from each sensor were routed to a set of signal conditioning units equipped with separate amplifiers and anti-aliasing filters for each channel. From the signal conditioning units, the analog signals were routed through BNC Interface units to data acquisition cards housed inside a high-speed PC. Two model 6031E cards, supplied by National Instruments Inc., were used for this study. Each card features up to 32 channels of differential input, 16-bit resolution, and a maximum sampling rate of $1x10^5$ samples/sec. The data acquisition system was controlled using NDAC software developed by NRC-OCRE. For this particular study, data from both the water level gauges and current meters was acquired at a sampling frequency of 50Hz and 200Hz, respectively.

3.6 GEDAP

NRC-OCRE's GEDAP software was used for all data analysis. GEDAP is a general-purpose software system for the synthesis, analysis and management of laboratory data that also includes modules for real-time experiment control and data acquisition functions. Standard GEDAP time-domain and frequency-domain analysis algorithms were applied to analyse in considerable detail the water levels, velocities and flows measured in the model.

The following parameters (among others) were obtained from time-domain analysis of the measured water level and velocity records:

Mean average of the recorded data (water levels, velocities or flows);

Min minimum of the recorded data (water levels, velocities or flows);

Max maximum of the recorded data (water levels, velocities or flows);

Std Dev standard deviation of the recorded data (water levels, velocities or flows);

RMS root mean square of the recorded data (water levels, velocities or flows);

Figure 81 shows an example of the water level plot used in this study. It shows the water level time histories measured at eight water level gauges and lists some key derived parameters describing the water levels at each location. All of the water level data collected during the study was analysed and plotted in this manner, and the results were shared with Stantec on a regular basis.

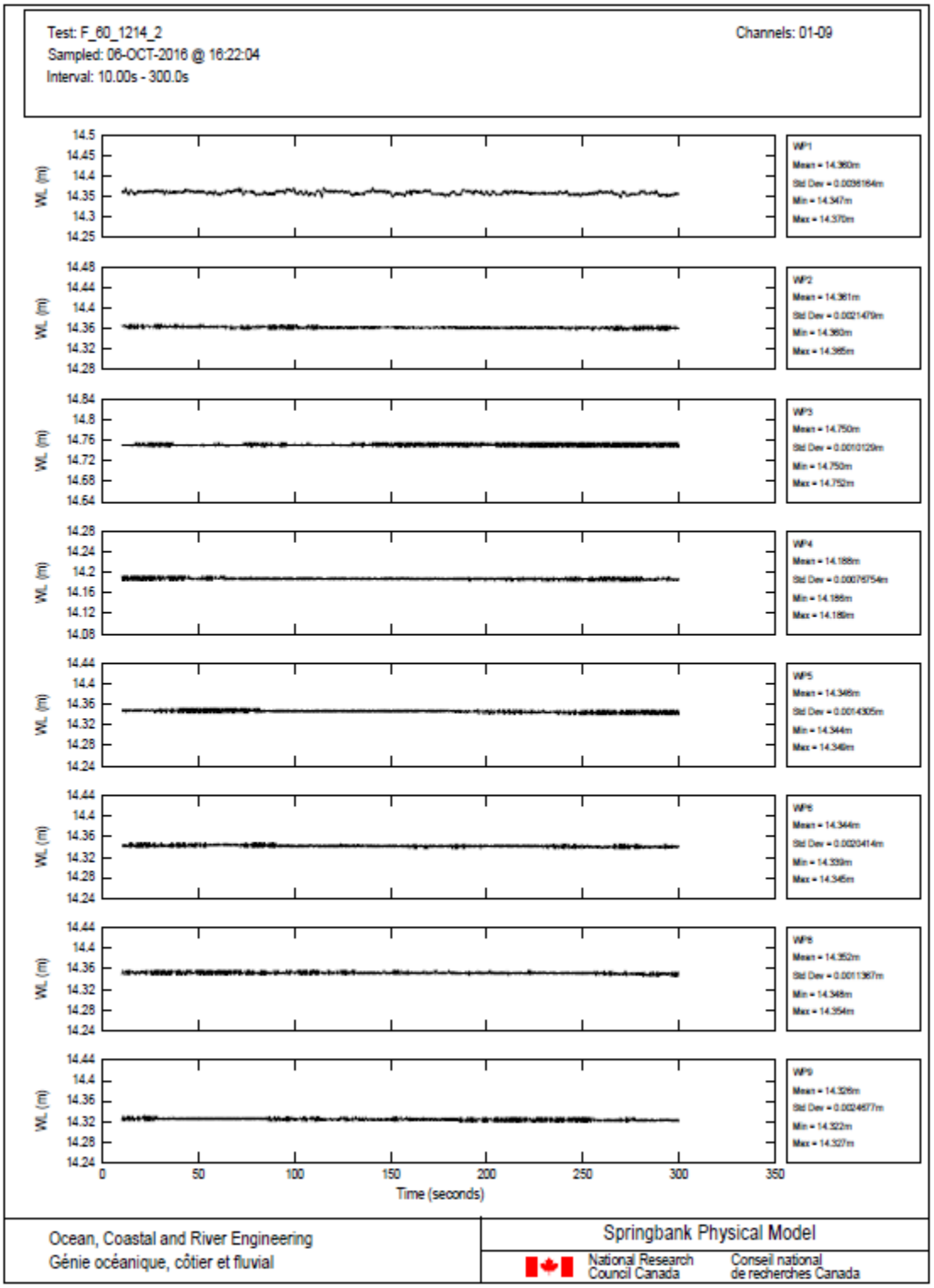

Figure 81. Typical water level analysis plot used in this study.

3.7 Analysis of Currents

The velocity vector at a point in space can be defined as ***U****(t) = (u,v,w)* where *u(t)*, *v(t)* and *w(t)* are the components parallel to the x-, y- and z-axes. For this study, the measured velocities were analysed and reported using a local coordinate system.

The velocity measurements obtained in this study were analysed with the help of GEDAP programs and procedures. The various steps in the analysis process were as follows.

- The first step was to convert the measured velocities into the proper coordinate system.
- Next, to remove high-frequency noise, the time series were passed through a digital low-pass filter with a cut-off frequency set to 0.5 Hz full scale.
- Next, new time series were computed representing the direction and magnitude of the low-frequency, high-frequency and complete velocity fields. The velocity magnitude or flow speed was computed as:

$$|U_h|(t) = \sqrt{u^2(t) + v^2(t)} \tag{12}$$

  while the direction was obtained as:

$$\theta_{U_h}(t) = \tan^{-1}\left(\frac{v(t)}{u(t)}\right) \tag{13}$$

- Next, a statistical analysis program was applied to compute key statistics for the time series data.
- Key statistics and parameters from the analysis were collected in a single ASCII file that was subsequently imported into a spreadsheet program.
- Finally, several plots were generated to visually illustrate the velocity data for each test. Figure 82 shows an example of the velocity data plot that was used in this study. It shows the time histories for several measured and derived parameters (in black), the low-frequency part of each signal (in red), along with several key statistics

All of the velocity data collected during the study was analysed and plotted in this manner, and the results were shared with Stantec on a regular basis.

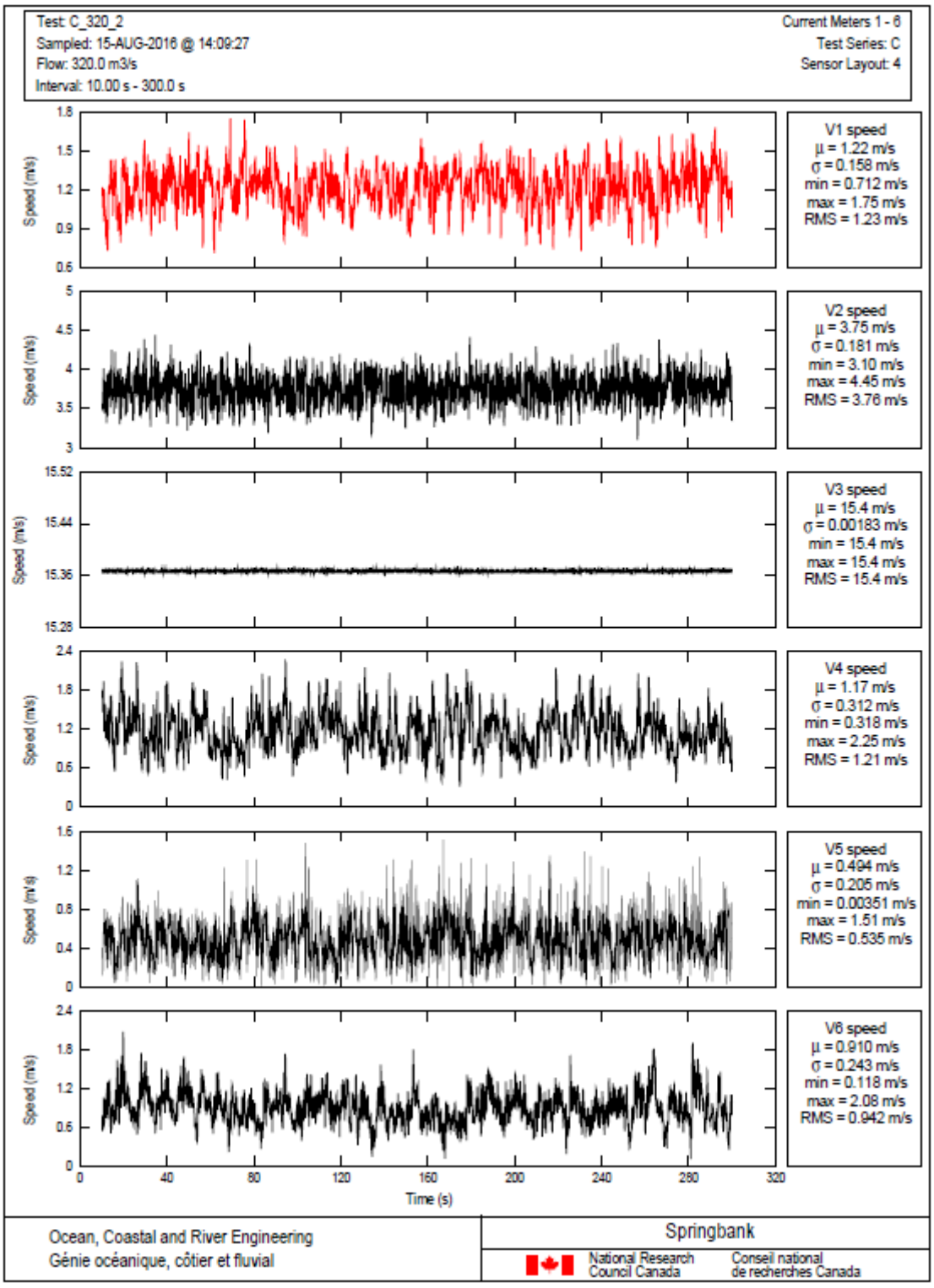

Figure 82. Typical velocity analysis plot used in this study.

3.8 Video and Photography

Digital photographs were taken to document all stages of the model study, including the model during each test. Still cameras were mounted in the laboratory rafters and time-lapse photography (on 2sec intervals) was used to document the fate of drogues and debris through the model domain. Also, a digital camera was used to photograph the model close-up, and also provide some video clips at points of interest. All tests were filmed by four overhead digital video cameras mounted in the rafters. The video stream from these cameras was made accessible to project team members and stakeholders through a password-protected web-page so that they could observe the testing from remote locations.

4 TEST PROGRAM

The test program for the Springbank physical model study included over 400 unique tests divided into seven distinct test series (herein referred to as TS). Testing began on July 20th, 2016 and concluded on November 15th, 2016. During each test series, the model flow conditions were set at the pump, the sluice gates and crest gates were set at the diversion inlet and service spillway to deliver the proper flow split through the structures, and the downstream weir elevations were set to deliver the proper tail water levels while measurements and observations were made. Different types of tests were conducted during the course of the modelling:

- Calibration tests: designed to develop the settings for the pumps and weirs to deliver the proper flow and water level conditions in the model.
- Clear water tests: designed to collect velocity and water level information throughout the entire model domain for the different model configurations and gate settings.
- Sediment tests: designed to indicate potential erosion and accretion issues in the floodplain and near the structures.
- Debris tests: designed to describe the pathways of woody debris through the floodplain, diversion inlet and service spillway. The debris tests were also utilized to develop barriers intended to collect and/or deflect the debris, as well as evaluate pier nose alternatives at the structures.
- Rating curve tests: designed to develop the relationship of flow over the service spillway and the corresponding upstream water level elevation for the various crest gate elevation settings.

Each of the combinations of flow, structure settings, and tail-water settings specified for use in the physical model study were prescribed by Stantec and were assigned a unique test name. In general, a new test series began whenever the model setup was modified significantly (e.g. a design change for the diversion inlet or service spillway) or whenever the primary focus or objective of the testing changed (i.e. assessment of hydrodynamic conditions, sediment transport, or debris behaviour). The test program is summarized in Table 3.

The design of the prototype structures are described in Section 2.2, and the various model structure layouts are described below in Section 3.4.3. The sequence of the testing, including the flow conditions, structure gate settings, sediment loading rates, and debris loading rates for each test series were prescribed by Stantec with input from NRC-OCRE.

The observations and results of each test series are described below in Section 5.

Test Series	Instrumentation Setup	Summary
Cal	1 and 2	Calibrating the model to give the proper flow rates and water level elevations.
A	2	Clear water tests - measuring flows, water levels and velocities for various gate settings. Mapping surface current pathways with drogues.
B	3	Debris tests - inserted woody debris and tracked their pathways through the model.
C	4	Sediment tests - pre-loaded the mobile bed area of the model with sediment and added sediment to the model to investigate areas of erosion and accretion.
D	3	New structure designs. Debris tests - inserted woody debris and tracked their pathways through the model. Revised diversion inlet pier noses and debris barriers.
E	5	New structure designs. Clear water tests - measuring flows, water levels and velocities for various gate settings. Mapping surface current pathways with drogues.
F	5	Rating curve tests - developing the rating curves for the service spillway crest gates.
G	3	Debris tests with a large floodplain debris barrier.
H	3	Debris tests with a large floodplain debris barrier.

Table 3. Test program summary.

Test	Target Flow (m^3/s)	Diversion Inlet		Service Spillway			Sluiceway
		Gate Setting	Target Flow (m^3/s)	Left Crest Gate Elevation	Right Crest Gate Elevation	Target Flow (m^3/s)	Sluice Gate Elevation
A_60_1	60	Lowered	0	1210	1210	60	Raised
A_160_1	160	Lowered	0	1210	1210	160	Raised
A_320_1	320	Raised	160	1212	1212	160	1212.1
A_760_1	760	Raised	600	1214	1214	160	1210.7
A_1240_1	1240	Raised	600	1211.8	1211.8	640	Raised

Table 4. Testing program for Test Series A.

Test	Target Flow (m^3/s)	Debris Barrier	Diversion Inlet		Service Spillway			Sluiceway
			Gate Setting	Target Flow (m^3/s)	Left Crest Gate Elevation	Right Crest Gate Elevation	Target Flow (m^3/s)	Sluice Gate Elevation
B_760_1	760	None	Raised	600	1214	1214	160	1210.7
B_760_2	760	None	Raised	600	1214	1214	160	1210.7
B_1240_1	1240	None	Raised	600	1211.8	1211.8	640	Raised

Table 5. Testing program for Test Series B.

Test	Target Flow (m^3/s)	Sediment Spreaders		Diversion Inlet		Service Spillway			Sluiceway
		Main Channel	Secondary Channel	Gate Setting	Target Flow (m^3/s)	Left Crest Gate Elevation	Right Crest Gate Elevation	Target Flow (m^3/s)	Sluicegate Elevation
C_320_1	320	Battery spreader; medium opening	None	Raised	160	1212	1212	160	1212.1
C_760_1	760	B750 spreader; small opening	Battery spreader; medium opening	Raised	600	1214	1214	160	1210.7
C_1240_1	1240	B750 spreader; medium opening 3360 spreader; medium opening	Battery spreader; medium opening	Raised	600	1211.8	1211.8	640	Raised

Table 6. Testing program for Test Series C.

Test	Target Flow (m^3/s)	Debris Barrier	Pier Nose	Diversion Inlet		Service Spillway			Notes
				Gate Setting	Target Flow (m^3/s)	24m Left Crest Gate Elevation	18m Right Crest Gate Elevation	Target Flow (m^3/s)	
D_760a_PN1_1	760	None	1	raised	160	1213.4	1215	600	Debris tests with pier nose changes
D_760a_PN2_1	760	None	2	raised	160	1213.4	1215	600	Changed breasting wall to semi-circular profile
D_760a_PN1_1	760	None	1	raised	160	1213.4	1215	600	Repeat test with new breasting wall
D_760a_PN3_1	760	None	3	raised	160	1213.4	1215	600	
D_760a_PN4_1	760	None	4	raised	160	1213.4	1215	600	
D_760a_PN2_TRa_1	760	A	2	raised	160	1213.4	1215	600	Debris barrier tests
D_760a_PN2_TRb_1	760	B	2	raised	160	1213.4	1215	600	
D_760a_PN2_TRc_1	760	C	2	raised	160	1213.4	1215	600	
D_760a_PN2_TRd_1	760	D	2	raised	160	1213.4	1215	600	Flushing of debris rack investigated (closing diversion)
D_760b_PN2_1	760	None	2	closed	0	1210	1210	760	Shut diversion
D_760b_PN3_1	760	None	3	closed	0	1210	1210	760	
D_1240_PN3_1	1240	None	3	raised	600	1210	1213.15	640	
D_1240_PN2_1	1240	None	2	raised	600	1210	1213.15	640	
D_1240_PN2_TRd_1	1240	D	2	raised	600	1210	1213.15	640	Flushing of debris rack investigated (closing diversion)
D_1240_PN3_TRc_1	1240	C	2	raised	600	1210	1213.15	640	Flushing of debris rack investigated (closing diversion)
D_1240b_PN3_TRc_1	1240	C	2	raised	600	1212.57	1210	640	
D_320_PN2_1	320	None	2	raised	160	1211.05	1215	160	
D_320_PN3_1	320	None	3	raised	160	1211.05	1215	160	
D_320_PN3_TRd_1	320	D	3	raised	160	1211.05	1215	160	
D_320_PN3_TRc_1	320	C	3	raised	160	1211.05	1215	160	

Table 7. Testing program for Test Series D – debris tests with high flood flows.

Test	Target Flow (m^3/s)	Diversion Inlet		Service Spillway		
		Gate Setting	Target Flow (m^3/s)	24m Left Crest Gate Elevation	18m Right Crest Gate Elevation	Target Flow (m^3/s)
E_60_1	60	closed	0	1210	1210	60
E_160_1	160	closed	0	1210	1210	160
E_320A_1	320	raised	160	1211.05	1215	160
E_320B_1	320	closed	0	1210	1210	320
E_760A_1	760	raised	600	1213.4	1215	160
E_760B_1	760	closed	0	1210	1210	760
E_1240A_1	1240	raised	600	1210	1213.15	640
E_1240B_1	1240	raised	600	1212.57	1210	640

Table 8. Testing program for Test Series E – clear water tests.

Test	Service Spillway			
	24m Left Crest Gate Elevation	18m Right Crest Gate Elevation	Target Flow (m^3/s)	Actual Flow (m^3/s)
F_60_1211	1211.05	1211.05	60	75
F_180_1211			180	181
F_320_1211			320	313
F_480_1211			480	464
F_640_1211			640	624
F_1000_1211			1000	894
F_60_1212	1212	1212	60	72
F_180_1212			180	180
F_320_1212			320	313
F_480_1212			480	455
F_640_1212			640	694
F_60_1213p15	1213.15	1213.15	60	63
F_180_1213			180	161
F_320_1213			320	281
F_480_1213			480	436
F_60_1214	1214	1214	60	46
F_180_1214			180	139
F_320_1214			320	263
F_480_1214			480	332
F_180_1215	1215	1215	180	99
F_60_1215			60	44

Table 9. Testing program for Test Series F – service spillway rating curve development.

Test	Target Flow (m^3/s)	Diversion Inlet		Service Spillway		
		Gate Setting	Target Flow (m^3/s)	24m Left Crest Gate Elevation	18m Right Crest Gate Elevation	Target Flow (m^3/s)
G_320_TRe_1	320	raised	160	1211.05	1215	160
G_760_TRe_1	760	raised	600	1213.4	1215	160
G_1240_TRe_1	1240	raised	600	1210	1213.15	640

Table 10. Testing program for Test Series G – debris tests with a large floodplain debris barrier.

Test	Target Flow (m^3/s)	Diversion Inlet		Service Spillway		
		Gate Setting	Target Flow (m^3/s)	24m Left Crest Gate Elevation	18m Right Crest Gate Elevation	Target Flow (m^3/s)
H_320_TRe_1	320	raised	160	1211.05	1215	160
H_505a_TRe_1	505	raised	600	1212	1215	160
H_505b_TRe_1	505	raised	600	1215	1211.05	160
H_760a_TRe_1	760	raised	600	1213.4	1215	160
H_760b_TRe_1	760	raised	600	1215	1213.15	160
H_1240_TRe_1	1240	raised	600	1210	1213.15	640

Table 11. Testing program for Test Series H – debris tests with a large floodplain debris barrier.

5 RESULTS AND DISCUSSION

5.1 Test Series A – Clear Water Tests

Test series A (TSA) focused on observing the flow characteristics within the model at five flow conditions (60 m^3/s, 160 m^3/s, 320 m^3/s, 760 m^3/s and 1240 m^3/s) without any debris or sediment. The test program for TSA is summarized in Table 4. The gate settings for each flow condition were specified by Stantec and were intended to divert the desired amount of flow through the diversion channel, with the remainder passing through the service spillway to the natural river channel. The instrumentation within the model was laid out following Instrumentation Layout 2 as shown in Figure 74. A summary of the measured water levels for all five flow conditions is provided in Table 12. Drogues and coloured dye were introduced into the model in order to visualize flow pathways through the structures and circulation zones within the model. The drogues and dye were tracked via overhead video cameras, overhead time-lapse still photography, and hand-held photography and video.

Test Name	Target Q	Div. Q	MC Q	Diversion channel WL						Main Channel WL											Secondary Channel WL	
				6	17	10	12	13	Weir	1	16	4	7	8	9	18	11	14	15	Weir	2	5
	cms	cms	cms	m	m	m	m	m	m	m	m	m	m	m	m	m	m	m	m	m	m	m
A_60_2	60	3	69	11.32	10.40	10.42	10.39	10.42	10.40	13.18	11.96	11.35	11.14	11.47	11.49	11.05	10.55	10.65	10.59	10.62	13.19	12.80
A_160_1	160	6	165	12.12	10.51	10.49	10.44	10.48	10.45	13.64	12.23	12.12	11.81	11.86	11.77	11.75	11.08	11.29	11.25	11.27	13.70	12.80
A_320_1	320	165	156	13.01	11.86	11.81	11.75	11.78	11.77	14.14	12.96	13.05	12.76	13.01	12.89	11.53	11.19	11.24	11.20	11.22	14.13	12.82
A_760_2	760	585	174	15.11	14.67	14.51	14.43	14.46	14.44	15.53	15.42	15.42	15.39	15.47	15.32	11.70	11.27	11.35	11.30	11.33	15.49	15.44
A_1240_1	1240	620	615	15.12	14.81	14.68	14.58	14.58	14.58	15.87	15.63	15.67	15.18	15.39	14.76	13.26	12.06	12.52	12.50	12.51	15.77	15.76

Table 12. Water level summary for the clear water tests.

5.1.1 *60 m^3/s*

The gate configurations for the 60 m^3/s test were as follows:

- Sluiceway gate – fully raised
- Left hand side service spillway Obermeyer gate – fully lowered (elev. 1210 m)
- Right hand side service spillway Obermeyer gate – fully lowered (elev. 1210 m)
- Diversion inlet gates – fully lowered (Note: diversion inlet gates were not modelled in this phase of the study. The upstream water level was not high enough to overtop the diversion inlet crest.)

For the 60 m^3/s flow condition, all of the flow passed through the sluiceway and service spillway. The water levels upstream of the diversion inlet gates (measured at WP6) were low enough that the water did not overtop the 1211.5 m elevation of the diversion inlet apron. The water level in the sluiceway (measured at WP7) was lower compared to the water flowing through the service spillway (measured at WP8 and WP9), indicating faster moving water through the sluiceway. The service spillway tail-water elevation of 1210.55 m (measured at WP11), closely matched the target tail-water elevation of 1210.50 m provided by Stantec.

Figure 83 shows a summary of the flow pathways that were observed using floating drogues. Drogues placed in the main river channel (locations A and B) reached and flowed along the straight retaining wall between the diversion inlet gates and the sluiceway until they passed through the sluiceway. Drogues placed in the secondary channel (locations D and E) passed through the left hand side (LHS) and right hand side (RHS) of the service spillway, and drogues placed between the two channels (location C) passed through the LHS of the service spillway.

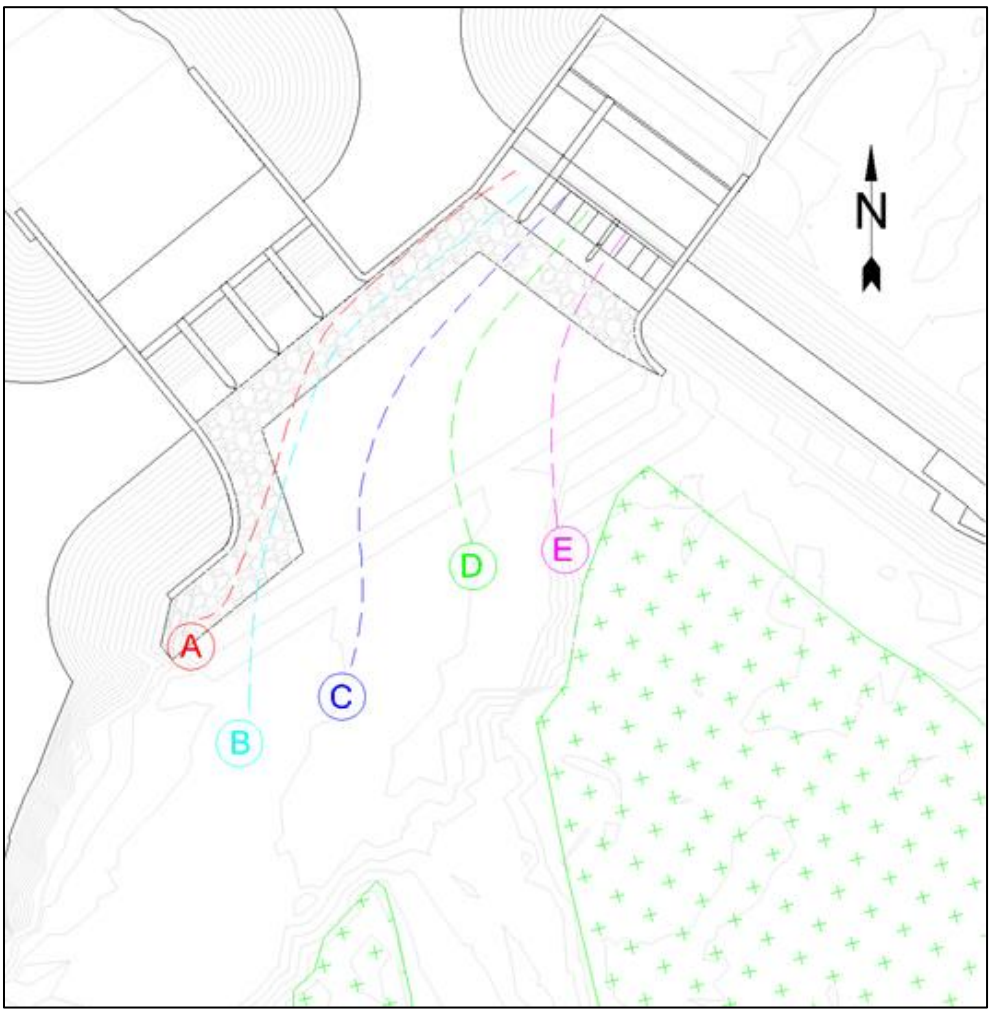

Figure 83. Flow pathways for the 60 m^3/s flow condition.

5.1.2 *160 m^3/s*

The gate configurations for the 160 m^3/s test were as follows:

- Sluiceway gate – fully raised
- Left hand side service spillway Obermeyer gate – fully lowered (elev. 1210 m)
- Right hand side service spillway Obermeyer gate – fully lowered (elev. 1210 m)
- Diversion inlet gates – fully lowered

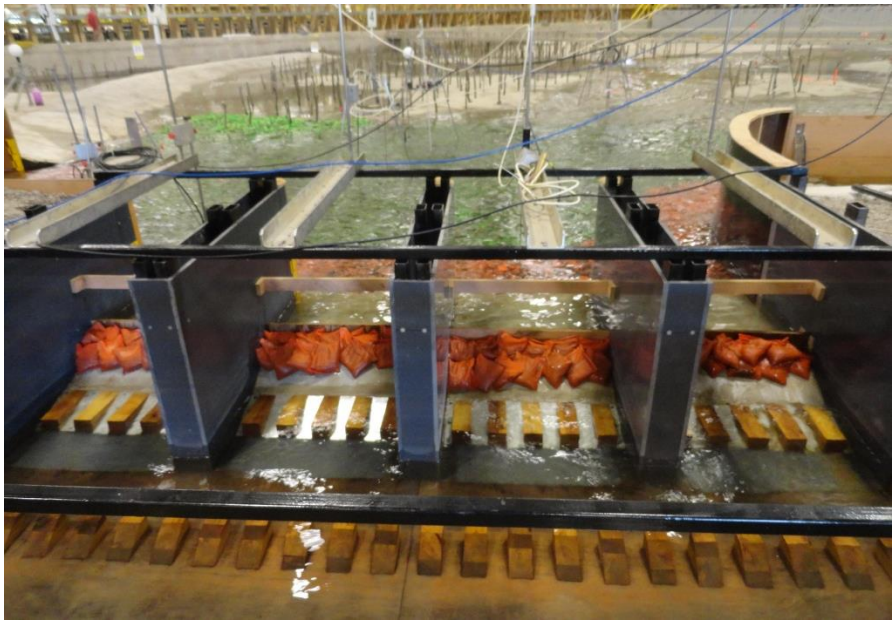

Figure 84. Blockage of the diversion channel inlet for 160 m^3/s flow condition.

Similar to the 60 m^3/s flow condition, the intention for the 160 m^3/s flow condition was to have the entire 160 m^3/s flow pass through the sluiceway and service spillway. Instead of modelling the diversion inlet gates, the flow through the diversion inlet was blocked by inserting wooden slats and sandbags into each bay opening (as shown in Figure 84).

The water levels measured in the sluiceway (WP7) and service spillway (WP8 and WP9) were much closer in elevation for this flow case, varying by only 0.09 m. The measured tail-water elevation of 1211.08 m (WP11) closely matched the target tail-water elevation of 1211.10 m provided by Stantec.

Figure 85 shows a summary of the flow pathways that were observed by deploying drogues in the model at various points. The drogues followed similar flow paths as observed during the 60 m^3/s flow condition. Drogues inserted in the main channel (points A and B) travelled through the sluiceway while those released in the secondary channel (points C and D) travelled through the LHS service spillway (from point C) and the RHS service spillway (from point D).

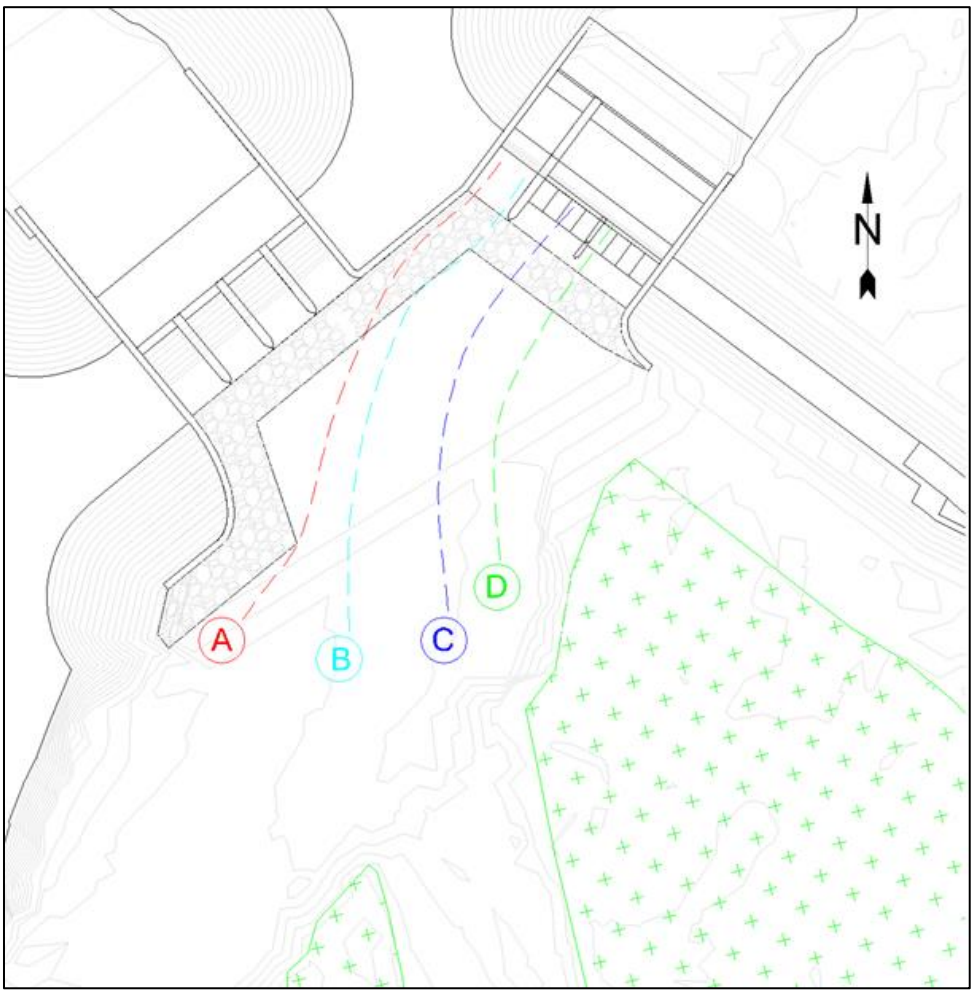

Figure 85. Flow pathways for the 160 m^3/s flow condition.

5.1.3 *320 m^3/s*

The gate configurations for the 320 m^3/s test were as follows:

- Sluiceway gate – set to an elevation of 1212.1 m
- Left hand side service spillway Obermeyer gate – set to an elevation of 1212 m
- Right hand side service spillway Obermeyer gate – set to an elevation of 1212 m
- Diversion inlet gates – fully raised

The gate settings specified by Stantec for the 320 m^3/s flow condition were intended to divert 160 m^3/s through the diversion channel, with the remainder passing through the service spillway to the downstream river channel. The measured flow split in the model was close to the intended targets, with 165 m^3/s passing through the diversion inlet structure and 156 m^3/s flowing through the service spillway/sluiceway. It was observed during testing that the sluiceway gate setting provided by Stantec (1212.1 m) did not have an influence on the flow travelling through the sluiceway. Even though the water level approximately 12m upstream of the sluiceway gate was measured at 1212.76 m (WP7), the flow accelerated substantially as it entered the sluiceway and the local water level

decreased accordingly. This allowed the flow to travel below the sluiceway gate without touching it, as shown in Figure 86 below.

Figure 86. Unobstructed flow passing under the sluiceway gate (320 m^3/s).

There was an uneven flow distribution through the four diversion inlet gate bays, with progressively lower flows moving from east to west (see Figure 87). This was evident from the position and strength of the hydraulic jumps immediately downstream from each of the diversion inlet bays. The hydraulic jumps for the two western bays were smaller and occurred closer to the concrete crest, while the hydraulic jumps for the two eastern bays were larger and occurred further downstream from the sill crest; indicating greater discharge.

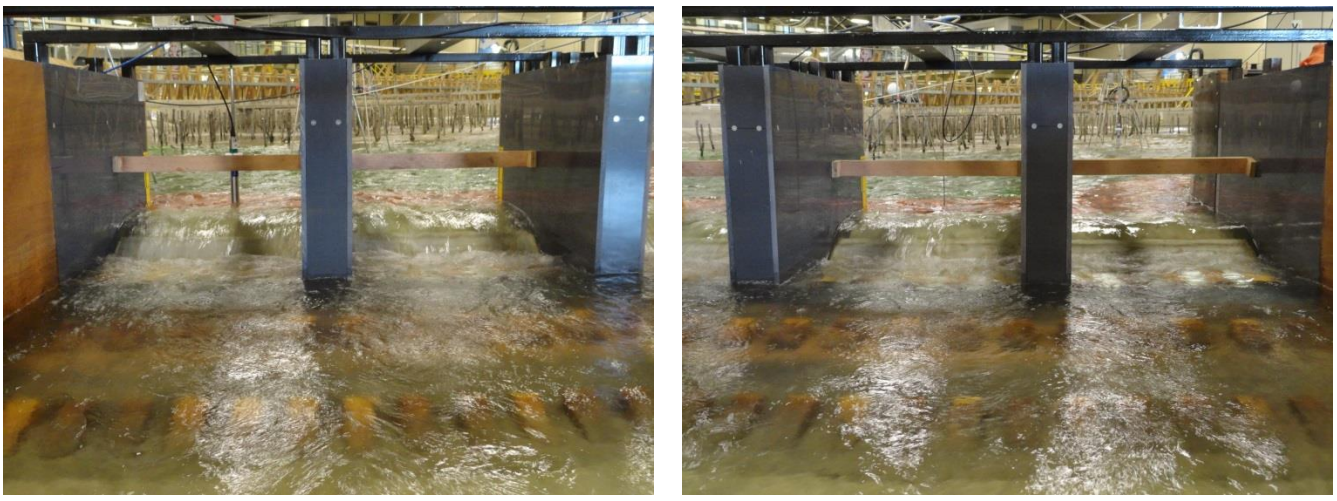

Figure 87. Flow through the diversion inlet viewed from downstream - two eastern bays (left) and two western bays (right).

The measured tail-water elevation of 1211.81 m (WP10) in the diversion channel closely matched the target tail-water elevation specified by Stantec of 1211.80 m. Similarly, the measured tail-water elevation of 1211.19 m (WP11) in the river channel closely matched the 1211.1 m target.

Figure 88 shows a summary of the flow pathways that were observed using drogues released into the model at various points. Drogues placed in the main channel (locations A, B and C) passed through the three western diversion inlet bays. Drogues placed near the western retaining wall (location A) floated along the curved retaining wall and entered the RHS of the western diversion inlet bay, demonstrating low energy flow through the western bay. The approximate flow split line in the floodplain is shown in Figure 88. All flow to the west of the split travelled down the diversion and all flow to the east of the split passed through the sluiceway or service spillway. Drogues released north of the small tree island (location D) travelled through the eastern diversion inlet bay and were influenced by the flow coming from the secondary channel. Drogues released at locations E and F travelled through the sluiceway and service spillway, respectively.

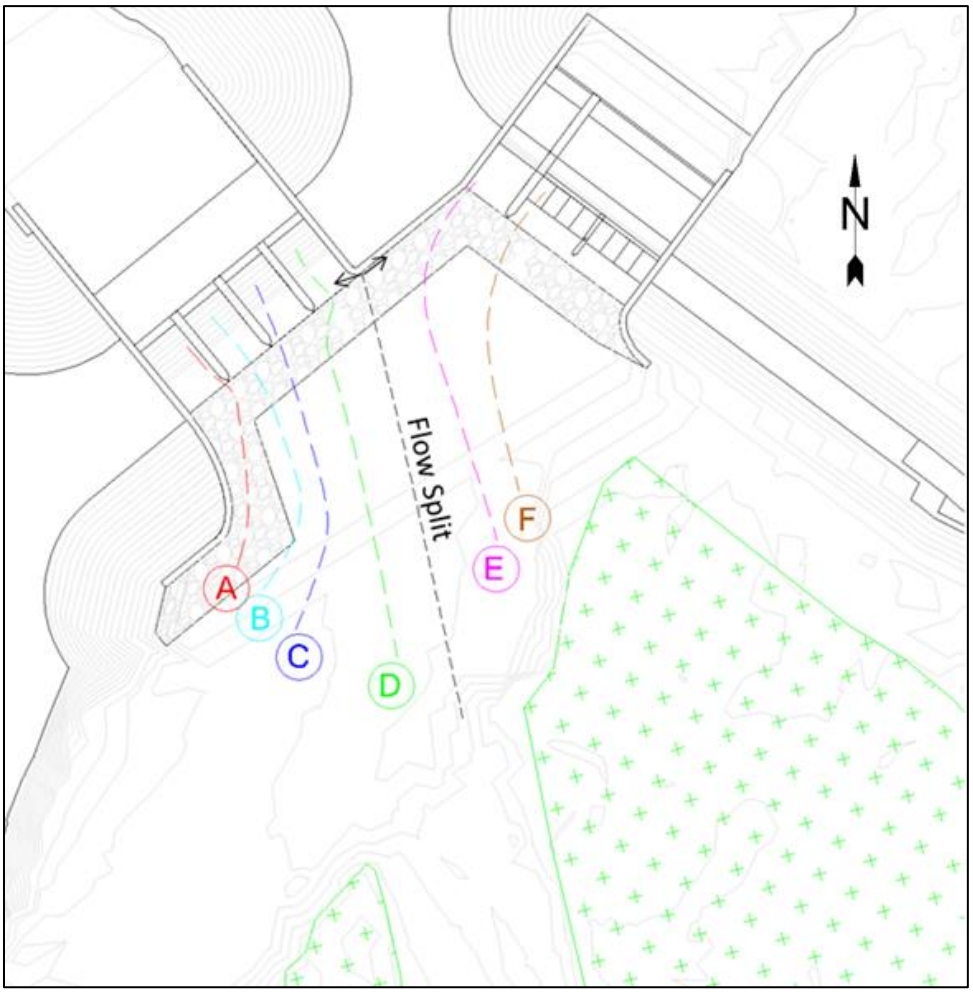

Figure 88. Flow pathways for the 320 m^3/s flow condition.

5.1.4 *760 m^3/s*

The gate configurations for the 760 m^3/s test were as follows:

- Sluiceway gate – set to an elevation of 1210.7 m
- Left hand side service spillway Obermeyer gate – set to an elevation of 1214 m (fully raised)
- Right hand side service spillway Obermeyer gate – set to an elevation of 1214 m (fully raised)
- Diversion inlet gates – fully raised

The target flow split for the 760 m^3/s flow condition was to have 600 m^3/s discharge passing through the diversion channel and 160 m^3/s in the downstream river channel, a ratio of 3.75:1. The gate settings specified by Stantec produced a flow split that closely matched the targets; with 585 m^3/s measured through the diversion and 174 m^3/s measured through the service spillway/sluiceway, a discharge ratio of 3.36:1.

The sluiceway gate was set at an elevation of 1210.7 m, which created approximately 4.7 m of head on the upstream side of the sluiceway gate (see Figure 89). An uneven flow distribution was observed flowing over the Obermeyer gates within the service spillway. The left hand side of the service spillway appeared to be passing more flow compared to the right hand side. This imbalance in the service spillway flow distribution may be a result of the recirculation zone that was observed near the curved wall on the RHS of the service spillway.

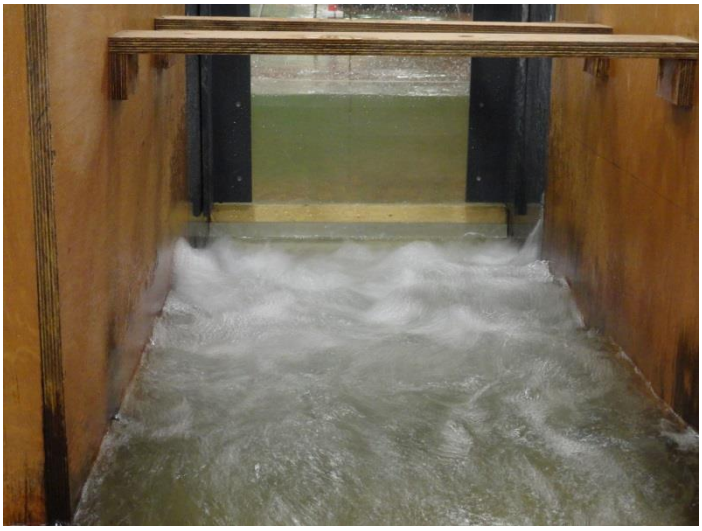

Figure 89. Supercritical flow passing under the sluiceway gate viewed from downstream (with approximately 4.7 m of head on the upstream side of the gate).

The flow through the four diversion inlet bays was more evenly distributed for this condition compared to the 320 m^3/s flow scenario. The hydraulic jumps downstream of the diversion inlet gates all appeared relatively uniform in strength and location, as shown in Figure 90.

Figure 90. Turbulent flows downstream of diversion inlet gates.

The tail-water elevation measured in the diversion channel, 1214.51 m (WP10), closely matched the 1214.50 m target elevation specified by Stantec. Similarly, the tail-water elevation measured in the main channel, 1211.27 m (WP11), closely matched the 1211.1 m target.

Figure 91 shows a summary of the flow pathways that were observed by releasing drogues into the model at various locations in the upstream floodplain. Drogues placed in the main channel (locations A and B) travelled through the two western diversion inlet bays. Drogues placed at location A tended to hug the curved retaining wall. Drogues released along the western side of the large treed area (locations C, D and E) all flowed through the two eastern diversion inlet bays. The flow split line for this flow condition was located much closer to the sluiceway compared to the 320 m^3/s flow condition. The larger flow draw from the diversion (~600 m^3/s) directed all flow from the main and secondary upstream river channels through the diversion channel, while the sluiceway and service spillway only received flow from the northern part of the treed area beside the floodplain berm. Drogues released at location F travelled west across the opening of the service spillway until they hit the retaining wall between the diversion inlet and sluiceway, before eventually making their way through the sluiceway. Drogues released near the floodplain berm (location G) would travel past the RHS of the service spillway before moving downstream through the LHS. One drogue released on the flow split line travelled along the line to the retaining wall where it was trapped in a small recirculating eddy that formed very close to the wall.

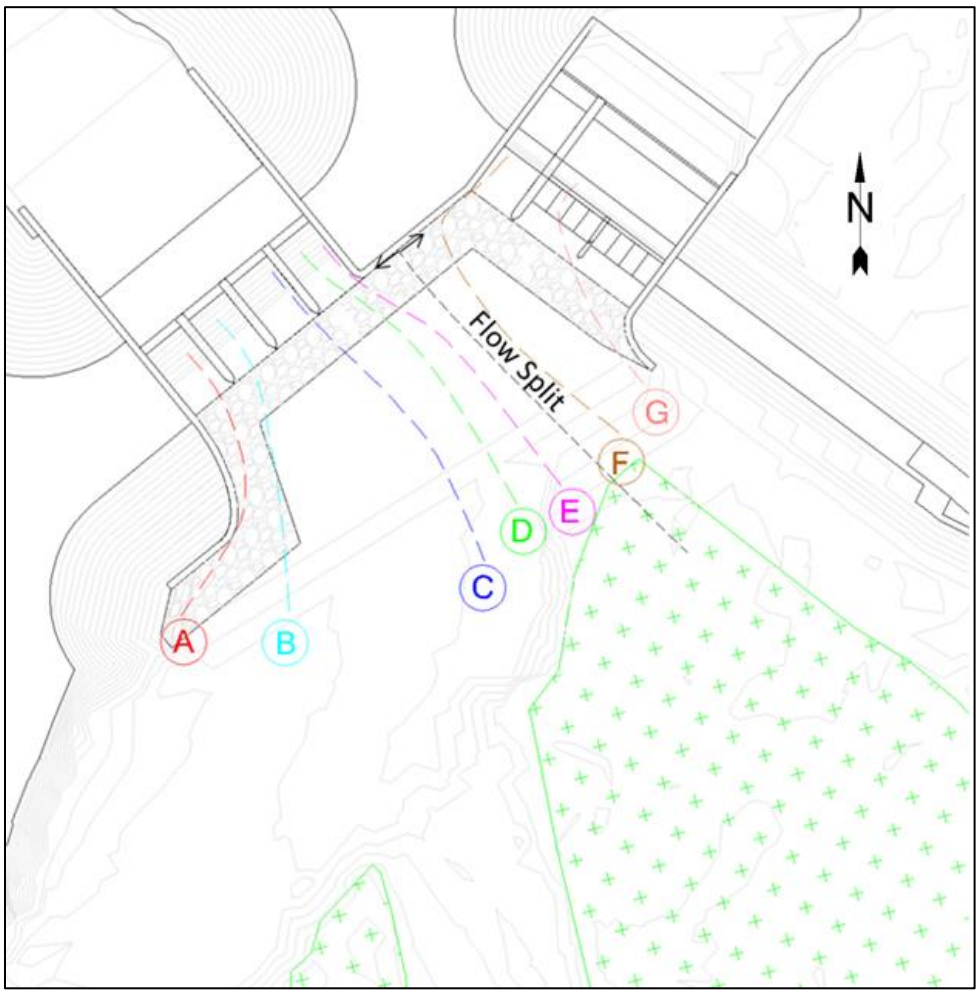

Figure 91. Flow pathways for the 760 m^3/s flow condition.

5.1.5 *1240 m^3/s*

The gate configuration for the 1240 m^3/s test was as follows:

- Sluiceway gate – fully raised
- Left hand side service spillway Obermeyer gate – set to an elevation of 1211.8 m
- Right hand side service spillway Obermeyer gate – set to an elevation of 1211.8 m
- Diversion inlet gates – fully raised

The target flow split for the 1240 m^3/s flow condition was to have 600 m^3/s passing through the diversion and 640 m^3/s passing downstream through the natural river channel, equivalent to a 48:52 ratio. The discharge measurements with this setup indicated a 50:50 flow split with 620 m^3/s and 615 m^3/s passing through the diversion channel and downstream river channel, respectively.

For these conditions the water level was slightly lower in the RHS of the service spillway than in the LHS, suggesting lesser discharge passing through the RHS. This was due in part to the flow re-circulation caused by the flow spilling over the curved RHS retaining wall /abutment. The upstream flow travelling roughly parallel to the floodplain berm would accelerate in wrapping around the upstream end of the RH side wall, creating a zone of flow recirculation beside the RH side wall (see

Figure 92). Some rip-rap was displaced below the zone of local flow acceleration and recirculation, near the interface between the rip-rap and the concrete apron.

Figure 92. Local flow acceleration and recirculation at the right hand side of the service spillway.

An uneven flow distribution was observed within the four diversion inlet bays for this condition, with the western (left) bay conveying lesser flow compared to the other three bays. This was evident as the hydraulic jump that formed downstream from the inlet in the other three bays was not observed in the western (left) bay. Similar to the 320 m^3/s flow condition (and unlike the 760 m^3/s flow condition) the flow arriving from the west side of the main channel separated off of the curved retaining wall and travelled away from the western diversion inlet bay.

The tail-water elevation of 1214.68 m (WP10) measured in the diversion channel closely matched the target of 1214.50 m. A tail-water elevation of 1212.06 m (WP11) was recorded downstream of the service spillway, which was lower than the 1212.6 m target predicted by Stantec.

Figure 93 shows a summary of the flow pathways that were observed by tracking drogues released into the model at various locations. Drogues released in the main channel (locations A and B) travelled through the three western diversion inlet bays. Drogues released in the secondary channel (location C) travelled through the eastern diversion inlet bay; which was also the bay with the most flow. Drogues released at location D travelled through the sluiceway while drogues released at the north end of the large treed area (location E) passed through the LHS of the service spillway. Drogues released beside the berm (location F) tended to wrap along the curved retaining wall on the RHS of the service spillway before passing through the RHS. The approximate location of the dividing line between the flow passing through the diversion inlet and the flow moving down the river channel is sketched in Figure 93. All flow arriving from the main and secondary upstream river channels flowed through the diversion channel while the sluiceway and service spillway were fed by flow coming from the treed floodplain and along the floodplain berm.

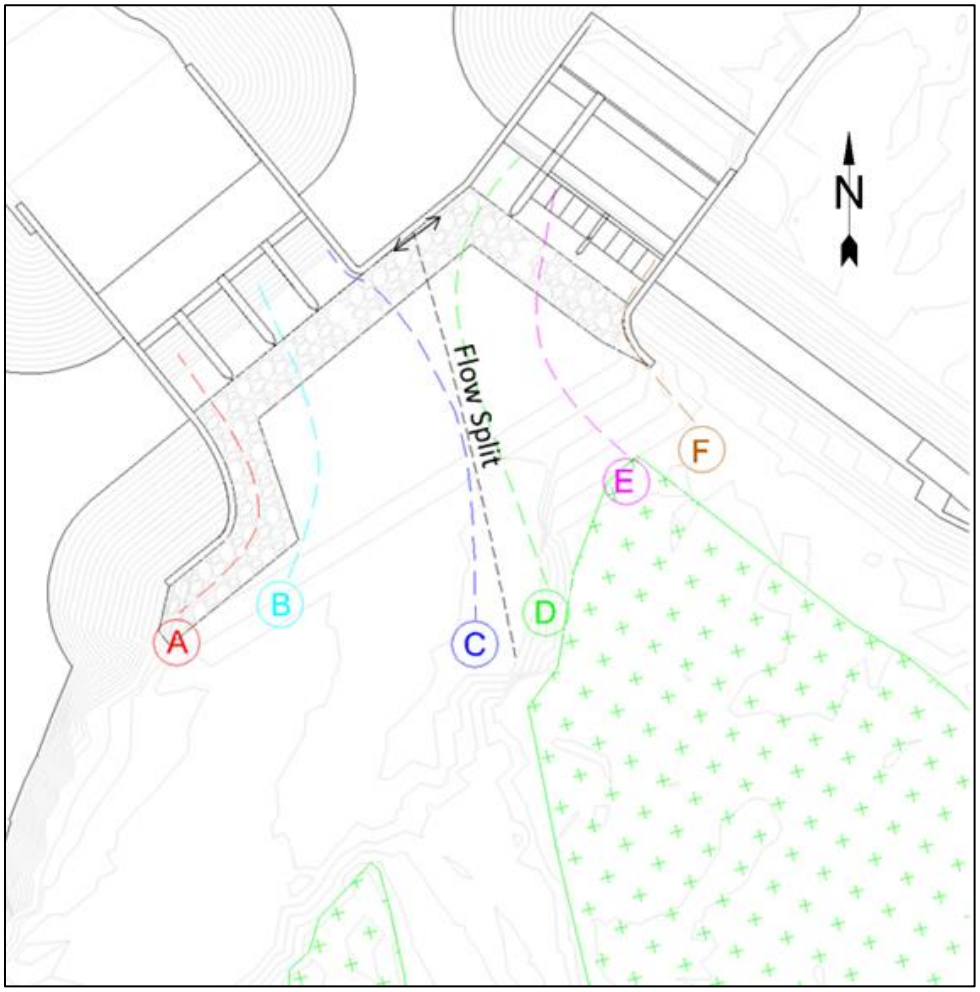

Figure 93. Flow pathways for the 1240 m^3/s flow condition.

5.2 Test Series B – Debris Tests

Test series B (TSB) investigated the interaction of water-borne woody debris with the two flow control structures, for both the 760 m^3/s and 1240 m^3/s flow conditions. The test program for TSB is summarized in Table 5. One set of gate settings was modelled with the 1240 m^3/s flood (the same settings modelled in TSA), while two different gate settings were studied with the 760 m^3/s flood. In one case the same settings modelled in TSA were used, while for the second case, the situation in which the service spillway Obermeyer gates were lowered to 1211.8 m (the setting used with the 1240 m^3/s flow condition) was modelled. Model scale woody debris simulating uprooted conifer trees was introduced into the upstream flow at specific locations and the interaction of the debris with the structures was observed and recorded. The model debris was introduced in several ways: as individual trees released in series, as small rafts comprised of 10 trees arranged in random patterns, and as larger rafts comprised of 40 model trees arranged randomly. The final step in each debris test was to load the model with numerous model trees (approximately 100 trees in 60 seconds) released in three locations (main channel, secondary channel and a point between the two; see Figure 94).

As described in Section 3.4.4, actual tree branches complete with bark, bends and knots were harvested for use in the model. Roughly 60% of the debris pieces had a small wooden “X” fixed at one end to simulate a root ball, while the remainder were rootless. The debris was tracked through the model via overhead video camera, overhead time-lapse still photography and handheld camera photos and videos.

Figure 94. Debris loading locations for 100 trees in 60 seconds.

5.2.1 *760 m^3/s*

The debris generally followed the streamlines that had been mapped out using drogues and dye during test series A. Single trees were able to pass through the diversion inlet bays as long as they were oriented with the flow. Since the width of each diversion inlet bay was less than the length of the trees, the trees tended to catch on the piers whenever they approached a diversion inlet bay sideways. Trees with a root ball were more frequently caught than trees without root balls. Individual trees would sometimes rotate around the point of contact and then pass safely through the diversion. In other cases, the trees would end up spanning the width of the bay between two adjacent piers. Once one tree was caught on the piers it caused a snowball effect and the single tree would catch multiple trees regardless of their orientation (see Figure 95). Most of the trees in the larger rafts were caught on the piers with only a few individual trees passing through the diversion inlet bays.

Figure 95. Single trees (left) and a 40-tree raft (right) caught on the diversion inlet piers.

Individual trees frequently became snagged on the Obermeyer service spillway gates. Trees with roots were snagged more frequently than trees without roots. Trees without roots were sometimes able to pass over the gates and move downstream, however, some of the passing trees became trapped in the roller that formed immediately downstream of the gates. The head over the Obermeyer gates for the 760 m^3/s flow was not deep enough to pass much debris unobstructed. As at the diversion channel, once a single tree caught on the gate, the single tree would catch other trees causing a build-up that grew over time as more trees arrived from upstream (see

Figure 96).

Figure 96. Woody debris caught on the Obermeyer gate and trapped in the downstream roller.

In the last debris test conducted for this flow condition, 122 trees were released into the upstream flow at a steady rate over 72 (model scale) seconds. Initially, some of the trees passed through the diversion inlet bays as long as they were aligned with the flow. However, once a single tree caught on the piers it trapped the majority of the following trees causing a large raft to form in front of the piers. Of the 122 trees released, 20 trees passed through the diversion inlet bays, while 102 were retained on the diversion inlet piers (16% passing rate). A further 80 trees were added to the existing debris raft/jam to create a large debris raft comprised of approximately 180 trees (see Figure 97). This large debris raft/jam decreased the flow through the diversion channel by approximately 100 m^3/s (~18% reduction).

Figure 97. Debris jam of approximately 180 trees.

Lowering both of the Obermeyer gates to 1211.8 m elevation increased the rate at which debris was able to pass through the service spillway. For this gate arrangement the combined discharge was 783 m^3/s, with 448 m^3/s passing through the diversion and 335 m^3/s passing through the service spillway, a 57:43 split. With more flow going down the sluiceway/ service spillway than before (335 m^3/s compared to 160 m^3/s for the higher gate setting) more trees were directed towards the service spillway (and away from the diversion channel) and the higher head above the Obermeyer gates allowed more of the trees, but not all, to pass through without getting caught on the gate crests. As before, longer trees and trees with roots were more frequently snagged, either on the gate crest or by spanning across adjacent piers (see Figure 98).

Figure 98. Debris caught in the service spillway/sluiceway with lower (1211.8m) Obermeyer gate setting.

5.2.2 *1240 m^3/s*

Although the flow for the 1240 m^3/s condition was much more evenly distributed between the two structures, the debris behaviour at the upstream face of both structures was similar to that observed for the 760 m^3/s flow condition. Single trees passed through the diversion inlet bays until one was caught on the piers, which caused the subsequent trees to become snagged leading to formation of sizeable debris raft at the pier noses (see Figure 99).

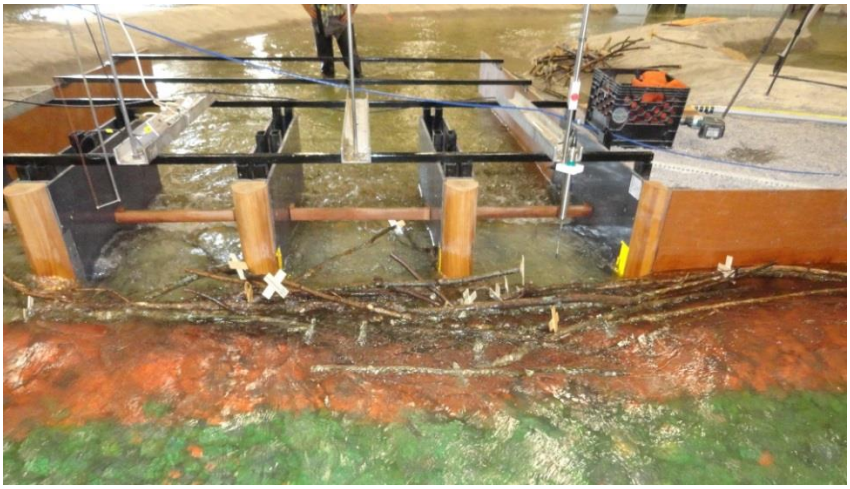

Figure 99. Collection of debris snagged on the diversion inlet piers.

Single trees generally were able to pass over the service spillway Obermeyer gates due to the greater flow and higher head. All of the single trees placed in the flow upstream of the service spillway were able to orient themselves with the flow and pass safely over the gate crest. However, a portion of the

trees that made it over the Obermeyer gates became trapped in the downstream roller. The rafts of trees that were released into the upstream flow were not able to orient themselves with the flow direction and therefore got caught in the service spillway, particularly between the two piers (see Figure 100).

Figure 100. Tree raft snagged on piers in the service spillway.

Following these tests with individual trees and tree rafts, the model was loaded with approximately 100 trees released steadily over 60 (model scale) seconds. This triggered the formation of a large debris jam at the entrance of the diversion channel. An additional 100 trees were added to the debris jam to create a jam comprised of approximately 200 trees (see Figure 101). This debris jam decreased the flow passing through the diversion channel by approximately 60 m^3/s (10%).

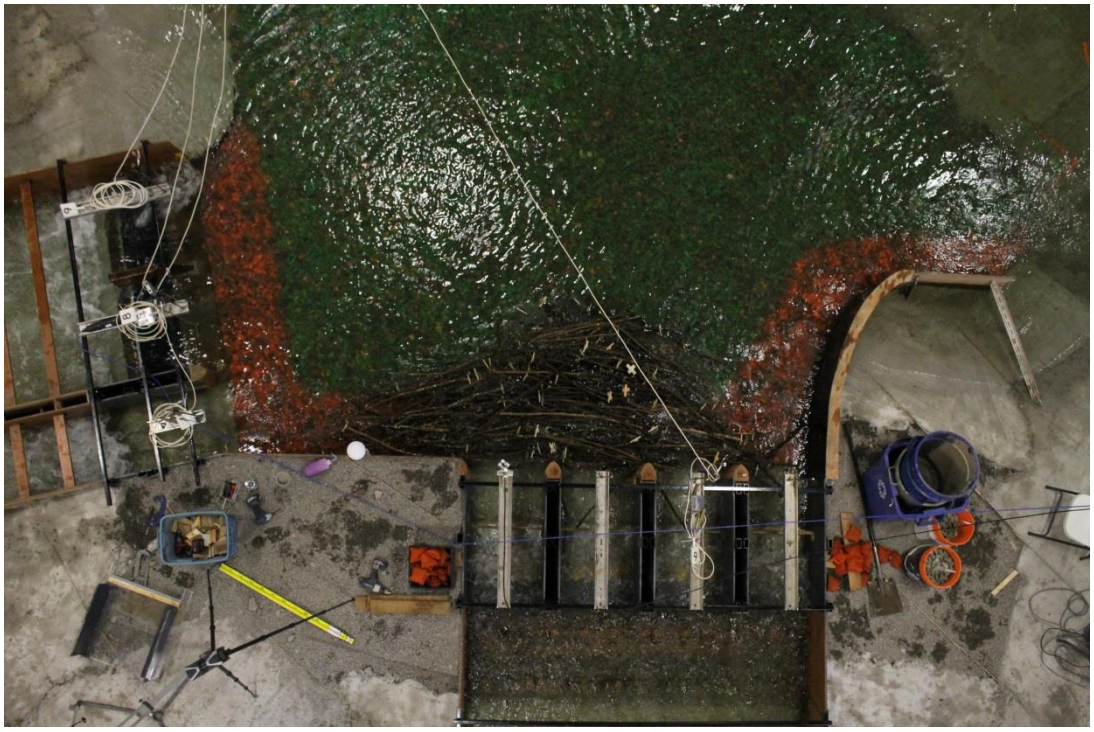

Figure 101. Debris jam of approximately 200 trees.

5.3 Task 2: Test Series C – Sediment Tests

The behaviour of riverine sediments at the three higher flow conditions (320 m^3/s, 760 m^3/s and 1240 m^3/s) was studied in Test Series C (TSC). The test program for TSC is summarized in Table 6. The granular material used in the physical model is described in Section 3.2.3. It is worth repeating that the model sediments were selected to represent the behaviour of the courser materials found on the riverbed at the site. The fact that the finer sediments were not represented in the physical model should be kept in mind when reviewing the results presented below.

For these tests the upstream riverbed was preloaded with sediment (see Figure 102), and additional sediment was delivered through sediment spreaders installed in the upstream part of the model as described in Section 3.4.5. One spreader was operated in the main upstream channel for the experiment with 320 m^3/s discharge, two spreaders were operated in the main and secondary upstream channels during the experiment with 760 m^3/s discharge, and three spreaders were operated during the 1240 m^3/s flow experiment. The sediment in the forebay area (the area immediately upstream from the two structures) was not re-shaped between each experiment, so the final bedforms at the end of the 1240 m^3/s flow experiment were the result of erosion, transport and deposition accumulated during each flow condition. The sediment in the river channels further upstream was re-shaped (through a combination of shovelling and raking) between each test to smooth out irregularities and achieve a quasi-uniform preloading condition. The spreaders were re-loaded with additional sediment between each experiment.

Figure 102. Initial sediment preloading in the upstream (left) and forebay (right) areas.

Before the first test and after each subsequent test, the model was drained and a 3D laser scanner (described in Section 3.5.3) was used to document the shape of the mobile riverbed in the forebay area. For each survey, at least four scans from four different points of view were recorded. The information from each scan was then combined to create a single 3D point cloud describing the shape/geometry of the riverbed in the forebay area. The bed elevations defined by the point cloud were then mapped onto a high-resolution rectangular grid. Elevation data from successive surveys could then be differenced to define the changes that occurred during each experiment, as well as the cumulative changes overall. Finally, a series of maps was prepared to illustrate the riverbed morphology and morphology changes observed in the physical model. Figure 103 shows the initial condition of the mobile bed in the forebay area before the first experiment. As with all the images presented in this report derived from the laser scans, the elevations in Figure 103 are in model scale meters with the basin floor as the reference datum (0m elevation). In addition to the laser scans, multiple video clips and photographs were recorded to document the appearance of the mobile bed sediments before and after each experiment.

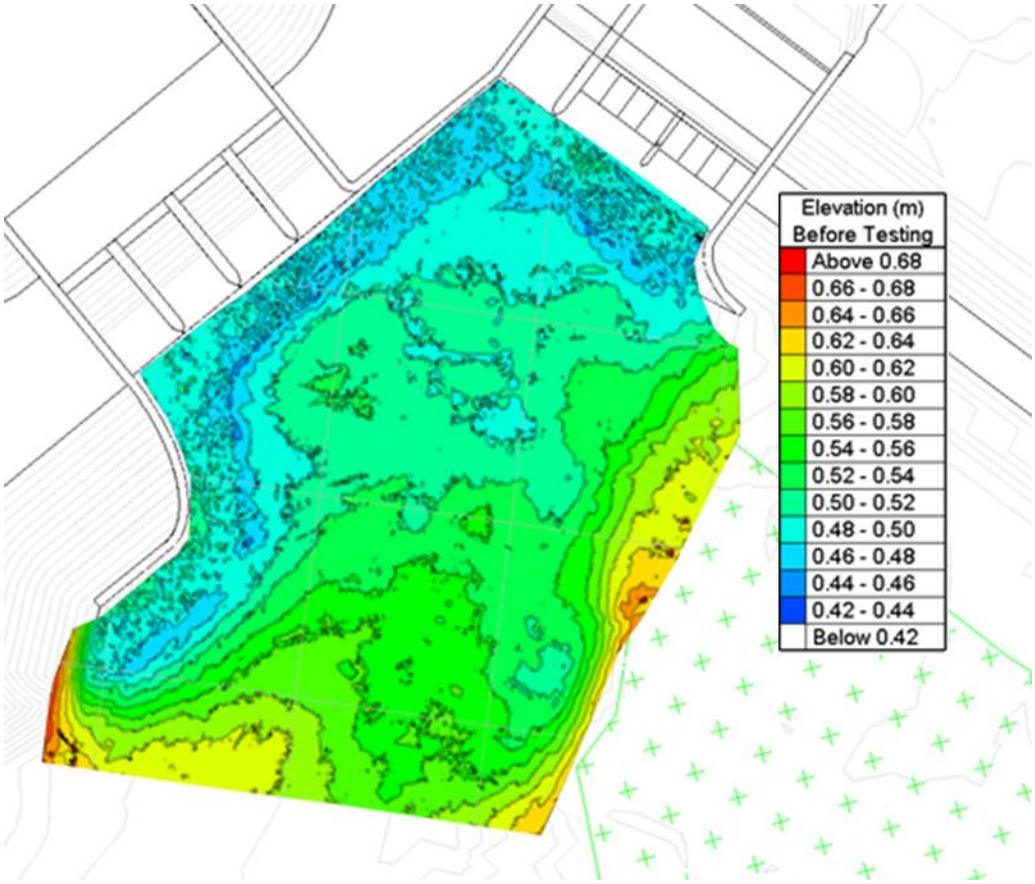

Figure 103. Initial elevation of the mobile bed in the forebay area.

5.3.1 ***320 m^3/s***

The structure gate settings for the experiment with 320 m^3/s discharge were as described in Section 5.1.3. The battery-powered sediment spreader was fully loaded and positioned in the far upstream part of the main river channel and the spreader opening was set to the "small" setting, corresponding to a target delivery rate of approximately 283 kg/s at full scale. The spreader was turned on only after first verifying that the 320 m^3/s flow condition was achieved. With the hopper full, the small spreader opening caused the spreader to seize. To rectify this, the opening was switched to the "medium" setting and the spreader was then operated continuously for 48 minutes (190 full scale minutes) until the sediment hopper was empty. The spreader was estimated to have delivered 1800 kg of sediment over 48 minutes, for a rate of 0.625 kg/s at model scale, or 640 kg/s at full scale.

The 320 m^3/s flow was able to mobilize and transport sediments from the main and secondary upstream channels downstream into the forebay area. However, no sediment deposition was observed on top of the riprap immediately upstream of each flow control structure. The sediment that had been placed on the bottom of the river channels was eroded in locations of greater flow velocity, exposing the underlying concrete bathymetry (see Figure 104). Some of the material delivered by the spreader was broadcast downstream, however, a pile of sediment also formed directly below the outlet. Every few minutes during the experiment, this lump of sediment was pushed and raked downstream as well as shovelled over to the secondary river channel. The sediment

in the secondary channel was quickly transported downstream and was continually re-placed with sediment shovelled from the main channel. The flow in the main river channel was also sufficient to mobilize and transport sediment downstream.

Figure 104. Erosion of sediment in secondary upstream flow channel (circled)

Figure 105 and Figure 106 shows conditions in the forebay area at the end of testing. A large elongated lobe of deposition formed extending all the way from the downstream end of the secondary (right) river channel (where it transitions to the forebay area) to the edge of the riprap in front of the diversion inlet structure. A second lobe of deposition formed in the lower part of the main channel that extended into the upstream part of the forebay area. A zone of erosion formed between these deposition lobes, roughly where the flows from the main and secondary channels joined each other and mixed together (see Figure 106). No sediment was observed passing through either structure at this flow rate and no sediment was observed downstream of either structure once the model was drained.

Figure 105. Deposition and erosion in the forebay area after 320 m^3/s flow condition.

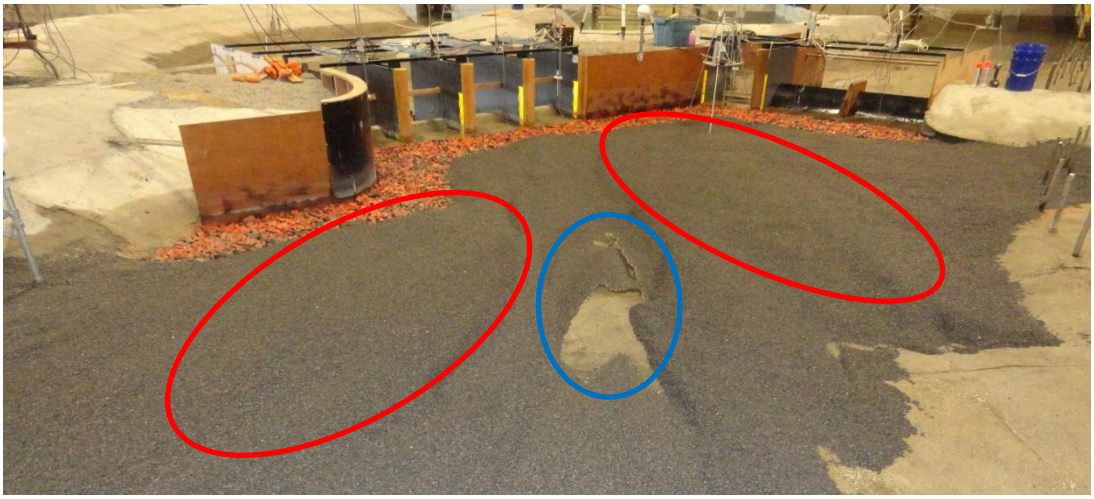

Figure 106. Riverbed morphology in the forebay area following the 320 m^3/s flow condition; deposition zones in red, erosion zones in blue

The map of bed elevation in the forebay area derived from the 3D laser scans taken after the experiment is presented in Figure 107, while Figure 108 shows the change in bed elevation due to the 320 m^3/s flood. In Figure 108 hot colours (oranges and reds) indicate deposition and cool colours indicate erosion. (Note that all elevations in these figures are in model scale meters.) These images clearly show the zone of erosion that formed between the two large lobes of deposition. The scan data indicates that the elongated right dune reached a height of 1.6m (0.1m model scale) above the surrounding bed elevation while the left dune was slightly lower.

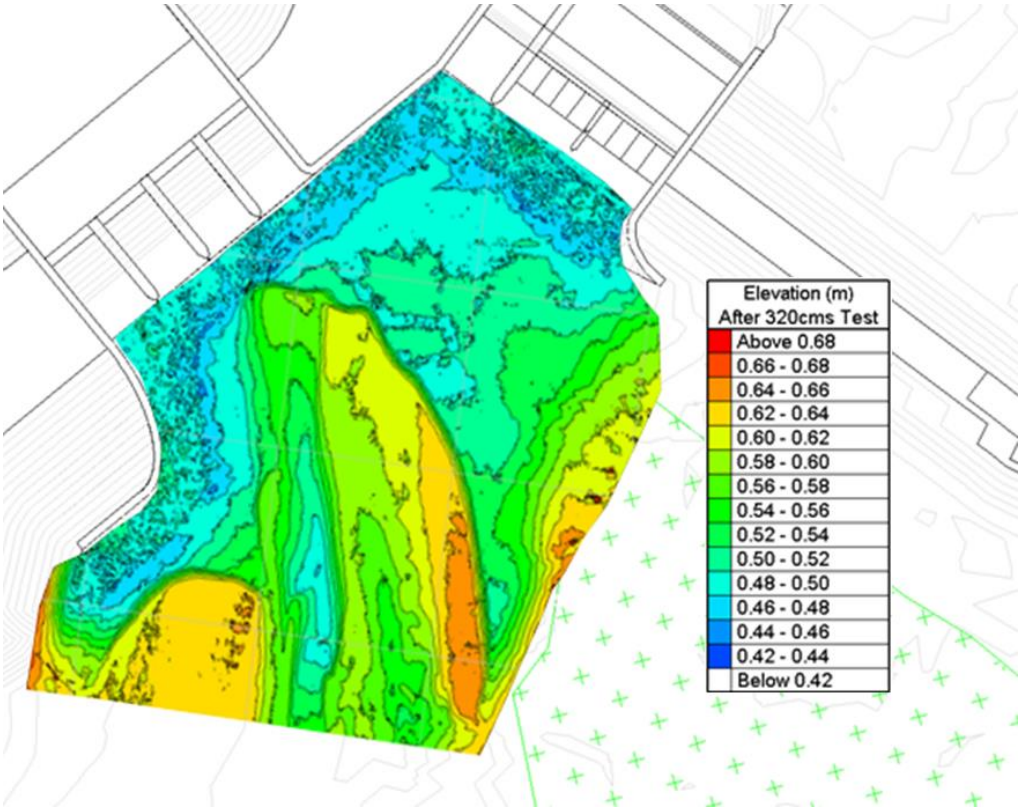

Figure 107. Bed elevation in the forebay area after 320 m^3/s flow condition.

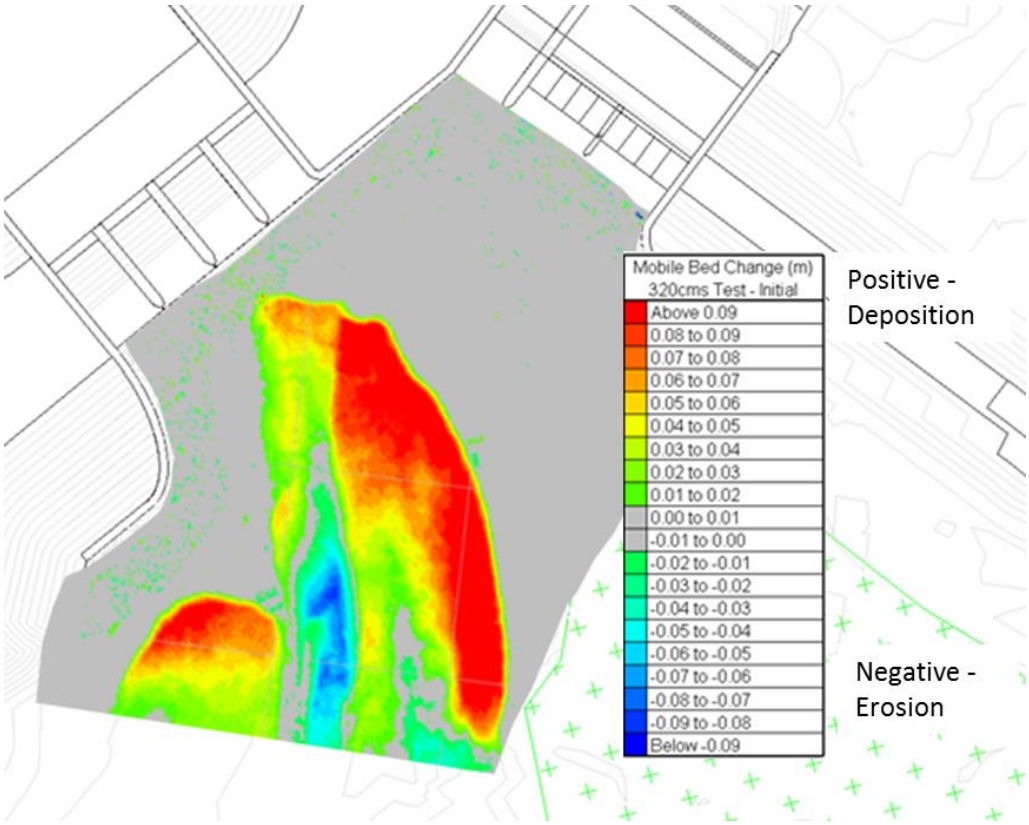

Figure 108. Change in bed elevation in the forebay area during the 320 m^3/s flow condition.

5.3.2 *760 m^3/s*

In preparation for the next experiment with 760 m^3/s discharge, the main and secondary upstream river channels were again pre-loaded with sediment while the sediment in the forebay area was left untouched. The new sediment was placed to achieve a smooth transition between existing and new material; hence the sediment depth was not always spatially uniform. Moreover, a pilot channel was formed in the bed of the main river channel as seen in Figure 109.

The battery-powered spreader was re-filled with new sediment and moved to the upstream part of secondary channel, and the larger B750 spreader was filled and positioned in the upper part of the main flow channel (see Figure 109). The opening for the B750 spreader was set to the small setting and the opening for the battery powered spreader was set to the medium opening (to avoid seizing the spreader) providing an expected full scale loading rate of approximately 720 kg/s for the B750 spreader and 500 kg/s for the battery powered spreader.

The structure gate settings were set as described in Section 5.1.4. A small section of the retaining wall at the right hand entrance to the service spillway was cut out before testing began to improve flow conditions at the service spillway entrance (see Figure 110). After first verifying that the 760 m^3/s flow condition had been reached, the spreaders were run for 136 mins (34 mins model scale) and 184 mins (46 mins model scale) respectively, until the sediment hoppers were empty

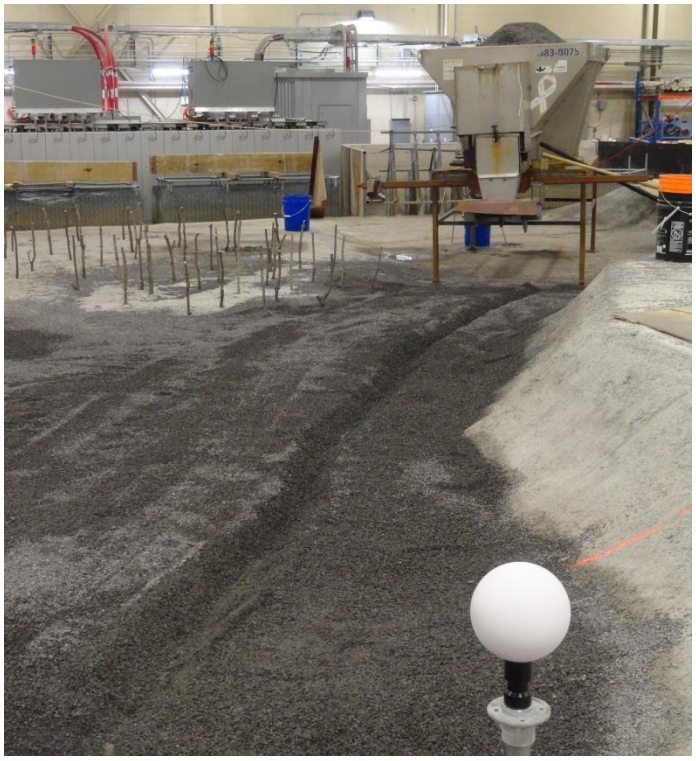

Figure 109. “Pilot channel” formed in the bed of the main river channel.

Figure 110. Cut-out section of retaining wall at RHS of service spillway.

The model sediments were generally much less mobile in this flow condition, due to the deeper water depths and slower velocities that prevailed in many areas. The service spillway gates were raised to divert flows into the diversion inlet channel, which caused the water depths in the forebay area and the upstream channels to be significantly greater than before, with corresponding reductions in flow velocity and bed shear stress. The flow was generally unable to mobilize and transport sediment downstream on its own. Because the flow around the spreaders was unable to transport material on its own, large amounts of sediment would accumulate rapidly below the outlets of both spreaders, significantly more than for the 320 m^3/s flow condition. As before, shovels and rakes were used to move the sediment delivered by the spreaders across the floodplain and downstream into the lower portions of the main and secondary river channels.

Visual observations during and after testing indicated that there was very little sediment transport and virtually no change in the bed morphology in the forebay area (see Figure 111). Almost all of the sediment delivered by the spreaders remained where it had been deposited by raking and shovelling. These visual observations were confirmed by the 3D scanning results shown below in Figure 112 and Figure 113. The scan results showed some minor changes throughout the mobile bed ranging from 80-176mm (5-11mm model scale), but no significant changes to the mobile bed occurred during the 760 m^3/s flow condition.

Figure 111 shows the mobile riverbed in the forebay area at the end of the experiment with the 760 m^3/s flow condition.

Figure 111. Riverbed in the forebay and upstream areas after the 760 m^3/s flow condition.

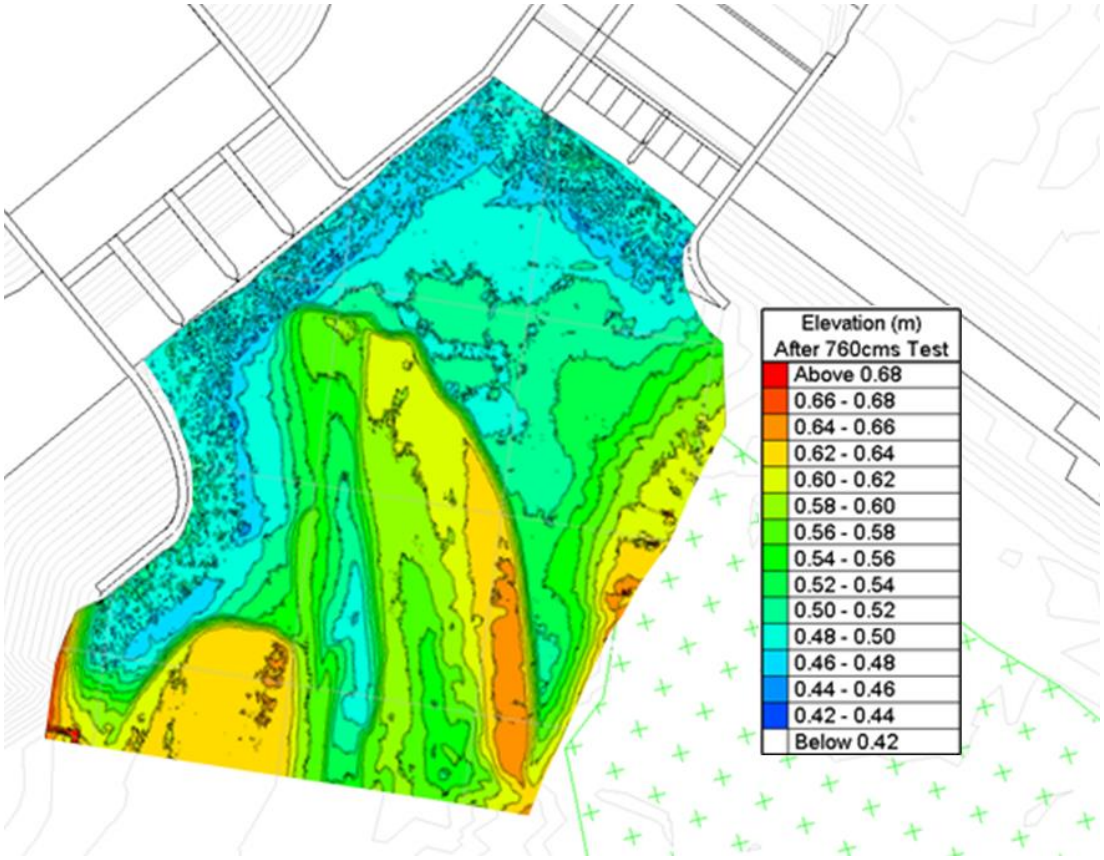

Figure 112. Bed elevation in the forebay area after 760 m^3/s flow condition.

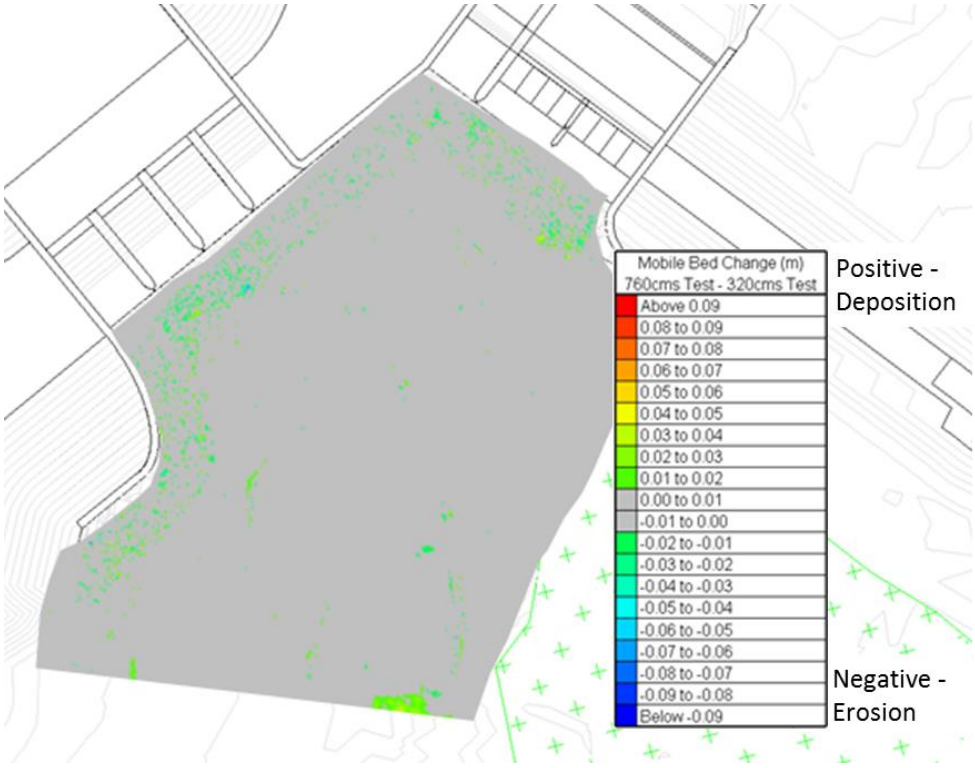

Figure 113. Change in bed elevation in the forebay area during the 760 m^3/s flow condition.

5.3.3 ***1240 m^3/s***

In preparation for the next experiment with 1240 m^3/s discharge, the structure gates were configured as described in Section 5.1.5. Some of the sediment that was deposited in the upstream river channels during the previous test was removed and a quasi-uniform sediment preloading condition was restored (see Figure 114). The sediment in the forebay area was not touched. As before, a small "pilot channel" was formed in the bed of the main (left) upstream flow channel.

Figure 114. Initial upstream mobile bed conditions prior to the 1240 m^3/s flow condition.

A third sediment spreader was added to the model in preparation for the experiment with 1240 m^3/s discharge. The B750 spreader was located in the main channel, the battery powered spreader was set up in the secondary channel and the 3360 spreader was located in between the main and secondary channels. All three hoppers where filled with sediment and the spreader openings were all set to the "medium" setting. The spreader openings provided a full scale loading rate of approximately 1250 kg/s for the B750 spreader, 1280 kg/s for the 3360 spreader and 500 kg/s for the battery powered spreader. Once the 1240 m^3/s flow condition was reached and confirmed, the spreaders were switched on and operated for 57, 54 and 60 model scale minutes respectively (corresponding to 228, 216, and 240 full scale minutes) until the hoppers were empty. The flow was maintained for a further 60 minutes to ensure that any erosion or deposition would be fully developed.

In general, more sediment transport was observed than in the previous test with 760 m^3/s flow rate, but significantly less than what was observed with 320 m^3/s discharge. High water levels and turbid conditions made it difficult to observe whether sediments where being mobilized and transported, and if so, where and to what extent. Sediment delivered by the spreaders tended to pile-up below the spreader outlet and had to be continually raked and shovelled across the floodplain and downstream to distribute it more evenly.

Figure 115 shows the general condition of the riverbed in the forebay area at the end of testing. During the most recent test a sizeable new scour hole was formed beside the edge of the riprap apron protecting the toe of the curved guide wall on the LHS of the diversion inlet structure (see Figure 116). Some of the sediment eroded from this scour hole was deposited on the surrounding riprap apron, while a small quantity was also transported to the downstream side of the diversion inlet structure. The riprap itself did not appear to have been damaged in this area. While the riprap remained stable at the diversion inlet structure, the 1240 m^3/s flood was able to dislodge approximately eighteen 440 kg stones from the riprap on the RHS of the service spillway structure, forming a scour hole in that location, see Figure 117. The 1240 m^3/s flow condition was the only flow condition that transported any appreciable quantity of sediment through the two structures; however, the volume

of sediment passing either structure was very small. Figure 118 shows the small amount of sediment that was discovered beneath the service spillway Obermeyer gates and along the RHS of the river channel downstream of the service spillway.

Figure 115. General view of the mobile bed in the forebay area after the 1240 m^3/s flow condition (new scour hole highlighted).

Figure 116. Scour hole on the upstream side of the diversion inlet structure (left) and corresponding sediment deposition on the downstream side (right).

Figure 117. Scouring of the 440kg rip-rap at RHS of the service spillway inlet.

Figure 118. Sediment deposited downstream of the service spillway structure along the RHS of the channel (left) and underneath the Obermeyer gates (right).

The final bed elevation in the forebay area is shown in Figure 119 while the change in forebay bed elevation due to the 1240 m^3/s flow condition alone is shown in Figure 120. Finally, the cumulative change in forebay bed elevation produced by the three floods is presented in Figure 121. The large elongated lobe of sediment originally deposited in the forebay area during the 320 m^3/s flow condition migrated a bit further downstream (less than 2 full scale meters) so that it now overlaps the upstream edge of the riprap in front of the diversion inlet structure (see Figure 115 and Figure 120). The other large lobe of sediment that had previously formed in the lower part of the left river channel also migrated slightly further downstream. As shown in Figure 120, elevation of these deposits did not appear to change in any significant way.

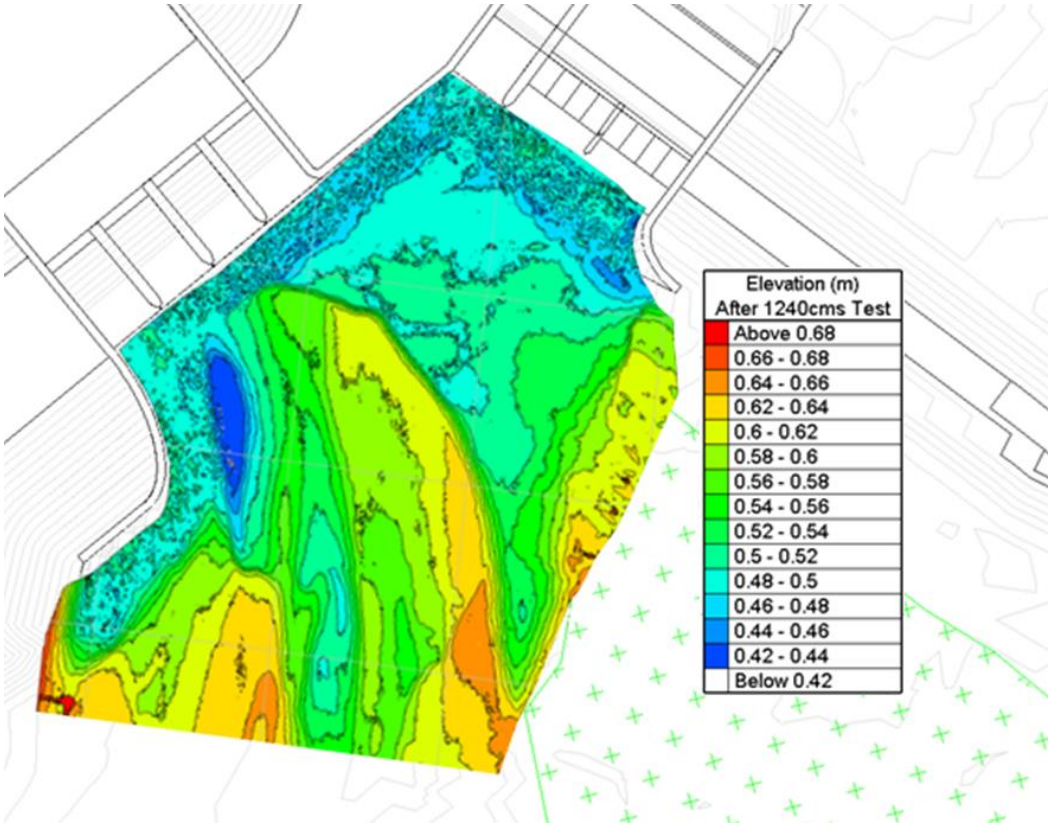

Figure 119. Mobile bed elevation in the forebay area after the 1240 m^3/s flow condition.

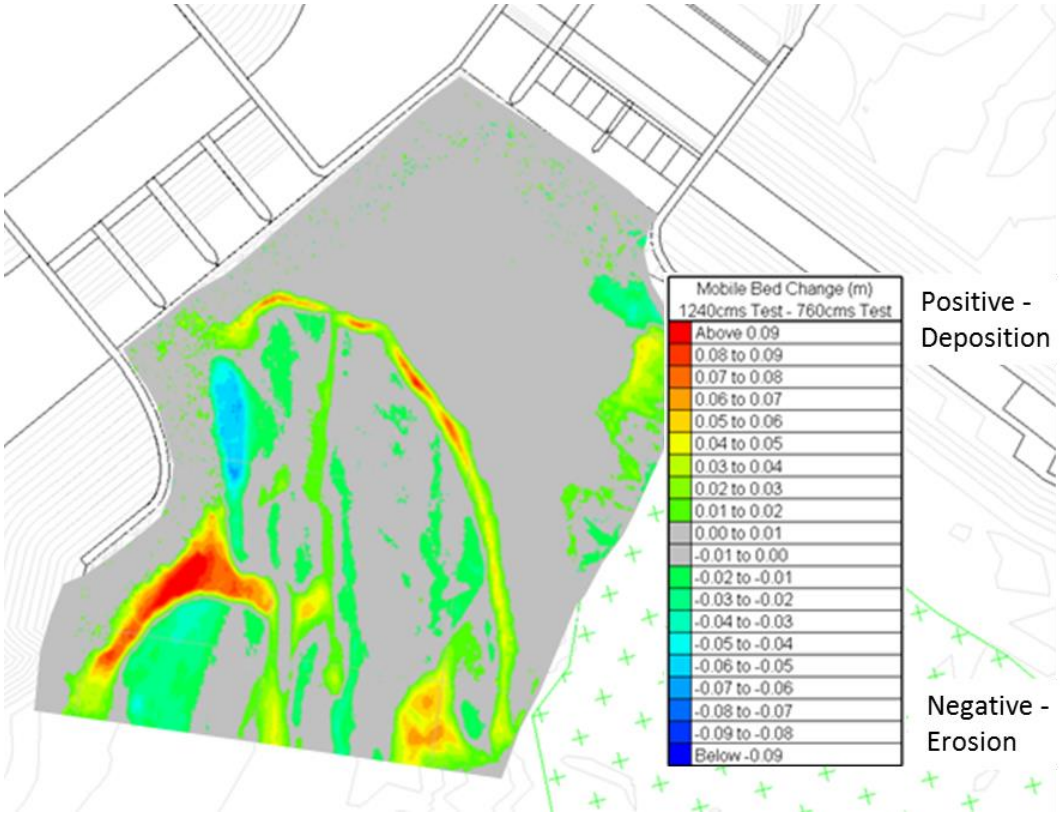

Figure 120. Change in bed elevation during the 1240 m^3/s flow condition.

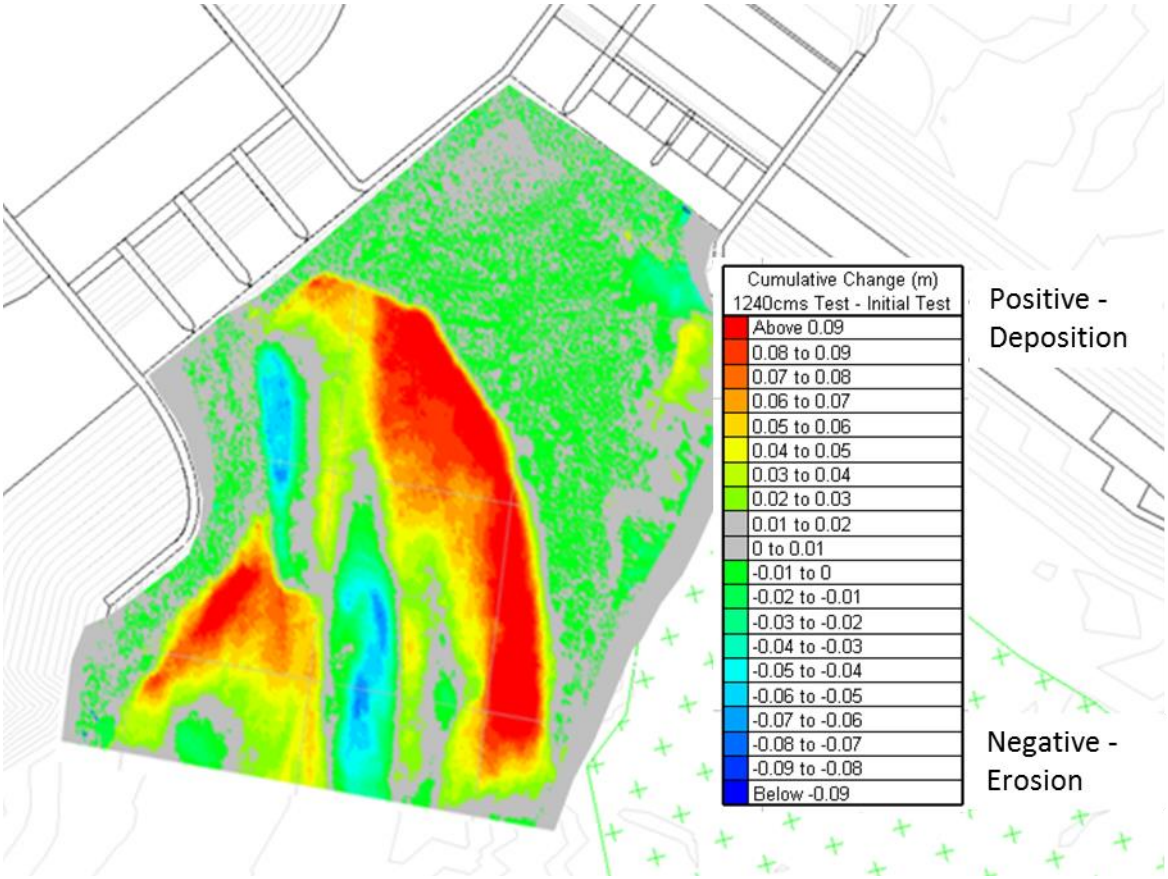

Figure 121. Cumulative change bed elevation during experiments with 320, 760 and 1240 m^3/s discharge.

5.4 Test Series D

Test series D (TSD) investigated the revised design for the diversion inlet and service spillway with a focus on how woody debris impacted the re-designed structures at the higher flood flow conditions (320 m^3/s, 760 m^3/s and 1240 m^3/s). The test program for TSD is shown in Table 7, and the order of the tests was chosen to investigate the 760 m^3/s flow event first and most thoroughly, followed by the 1240 m^3/s and 320 m^3/s floods. The tests investigated the performance of four different pier noses at the diversion inlet (identified by PN1-4 in the test name) as well as four different debris barrier designs in front of the diversion inlet (identified by TRa-d). The designs of the pier noses and debris barriers as well as their model representations are discussed in Section 3.4.3.3 and 3.4.3.4, respectively. The Obermeyer gate settings on the service spillway were prescribed by Stantec and intended to direct a target flow down the diversion and service spillway channels based on a given flood flow condition. The procedure for each of the debris tests was similar – for each combination of pier nose and debris barrier, model tree debris was added at specific points in the upstream floodplain in combinations of single debris loads (single trees from one to four trees at a time), or rafts of 10, 40, and 100 trees. The fate of the debris was tracked thorough the model via overhead video camera, overhead time-lapse still photography, and isometric view video cameras.

Observations were made on the performance of the various pier noses, debris barriers, as well as the fate of the debris as it passed through the diversion inlet and service spillway structures.

5.4.1 *760 m^3/s*

The test settings for the 760m^3/s flow investigated the diversion inlet gate in the fully raised position, and the service spillway Obermeyer gates set to 1213.4m on the 24m wide left-hand side (LHS) and 1215m on the 18m wide right-hand side (RHS). Model tree debris was inserted into the model in one of seven locations (A-G) as shown in Figure 122 during the tests. A summary of the behaviour of the debris, and the performance of the structural features of the diversion inlet and service spillway are discussed in the following sections.

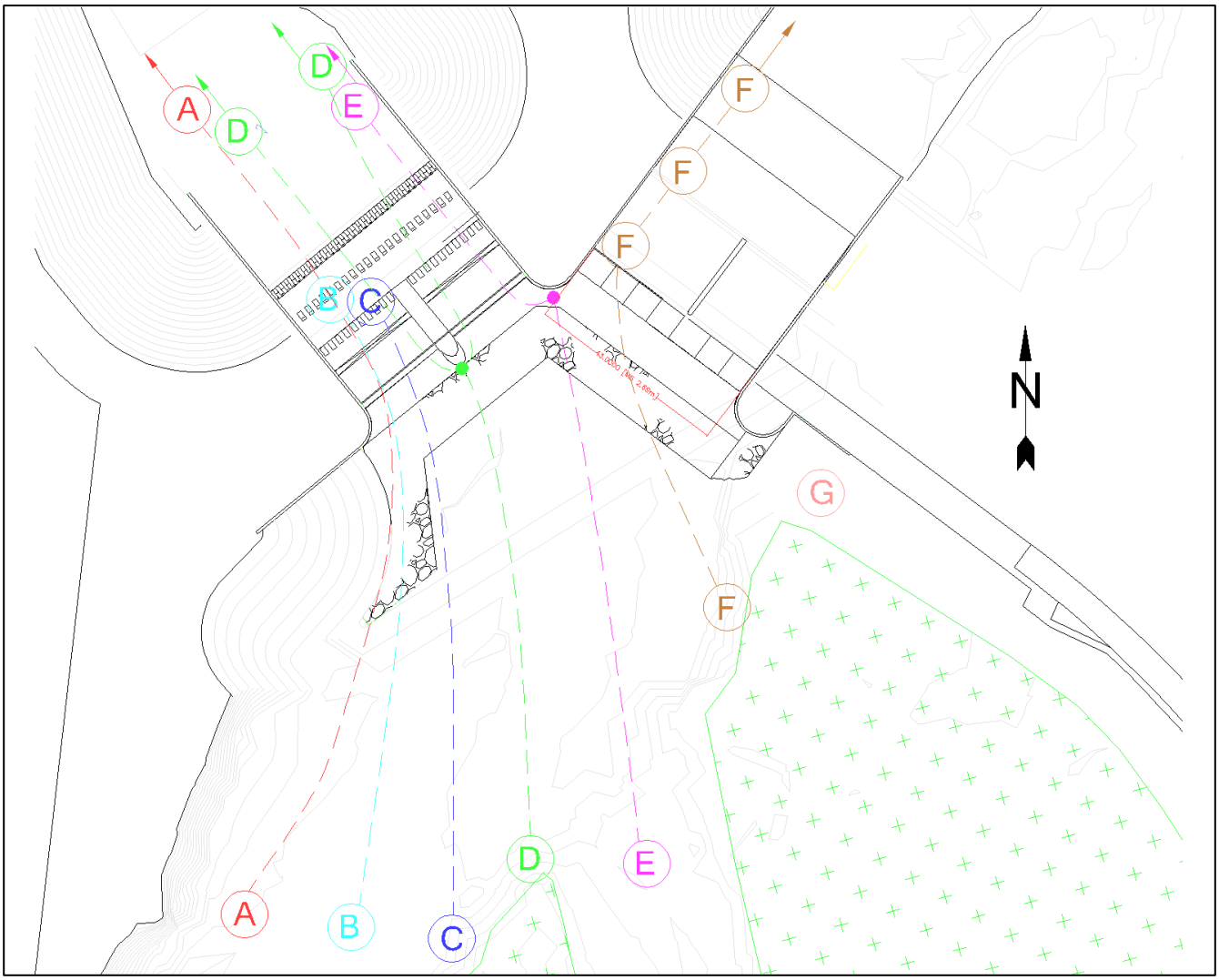

Figure 122. Debris pathways for TSD, 760 m^3/s flow conditions with the diversion inlet gates open.

5.4.1.1 Pier Nose 1

The pier nose 1 design drawings are shown in Section 3.4.3.3, and the main characteristics feature a curving arrow-head plan-shape with the apex of the point being 3.5m upstream of the front of the diversion/breast wall. Figure 123 shows pictures of the flow conditions at the diversion inlet and the service spillway. There was a slight wake on the RHS of the diversion inlet stemming from pier nose 1, however the hydraulic jump was relatively stable on both sides of the pier. On the service spillway, water barely spilled over the RHS gate as it was set to 1215m, and the waterfall was more energetic on the LHS.

Figure 123. Flow conditions at the structure during the 760 m^3/s event with the Obermeyer gates set to 1213.4m (LHS) and 1215m (RHS). Left - facing southwest at the diversion, right - facing southeast at the service spillway.

Debris was deployed at several points in the floodplain and tracked through the model. Again, refer to Figure 122 for the debris insertion locations and pathways, and Table 13 presents a summary the debris tests for pier nose 1. Model trees placed in the main river channel west of the small island of trees (locations A-C) passed through the LHS of the diversion, while debris inserted to the north of the small tree island (D) or in the secondary channel (E) passed through the RHS of the diversion. A percentage of the trees were caught in the pier nose, particularly those from the larger debris rafts (packs of 10 and 40 trees). The trees and their roots were caught on the pier nose itself as well as the breast wall (see Figure 124). The close proximity of the pier nose apex and the breast wall provided an area where a piece of debris could bridge and catch at two points simultaneously. The model representation of the breast wall was simply a flat piece of plywood set to the correct elevation. The sharp edges of the model plywood breast wall likely contributed to catching onto the root wads. Since the prototype breast wall is curved, the model breast wall was replaced with a 4” diameter (model scale) section of pipe after this test series (see Figure 125).

Debris Type	Starting Location	Debris Pathways							Notes
		Debris Barrier	Pier Nose 1	Diversion LHS	Diversion RHS	Center Wall	Service Spillway LHS	Service Spillway RHS	
Singles	A	NA	-	100%	-	-	-	-	
	B	NA	-	100%	-	-	-	-	trees stuck in hydraulic jump
	C	NA	-	100%	-	-	-	-	trees stuck in hydraulic jump
	D	NA	stalls	50%	50%	-	-	-	
	E	NA	-	-	100%	stalls	-	-	
	F	NA	-	-	-	-	100%	-	trees stuck in waterfall
Rafts of 10	B	NA	-	100%	-	-	-	-	
	D	NA	20%	40%	40%	-	-	-	caught on pier nose and breasting wall
	E	NA	-	-	100%	stalls	-	-	
Rafts of 40	B	NA	50%	45%	5%	-	-	-	caught on pier nose and breasting wall
	D	NA	100%	-	-	-	-	-	caught on previous debris
	E	NA	-	-	100%	stalls	-	-	breaks up previous debris raft
Continuous	All	NA	~10%	~50%	~40%	stalls	-	-	caught on pier nose and breasting wall

Table 13. Debris behaviour for 760 m^3/s with Pier Nose 1 installed in the diversion.

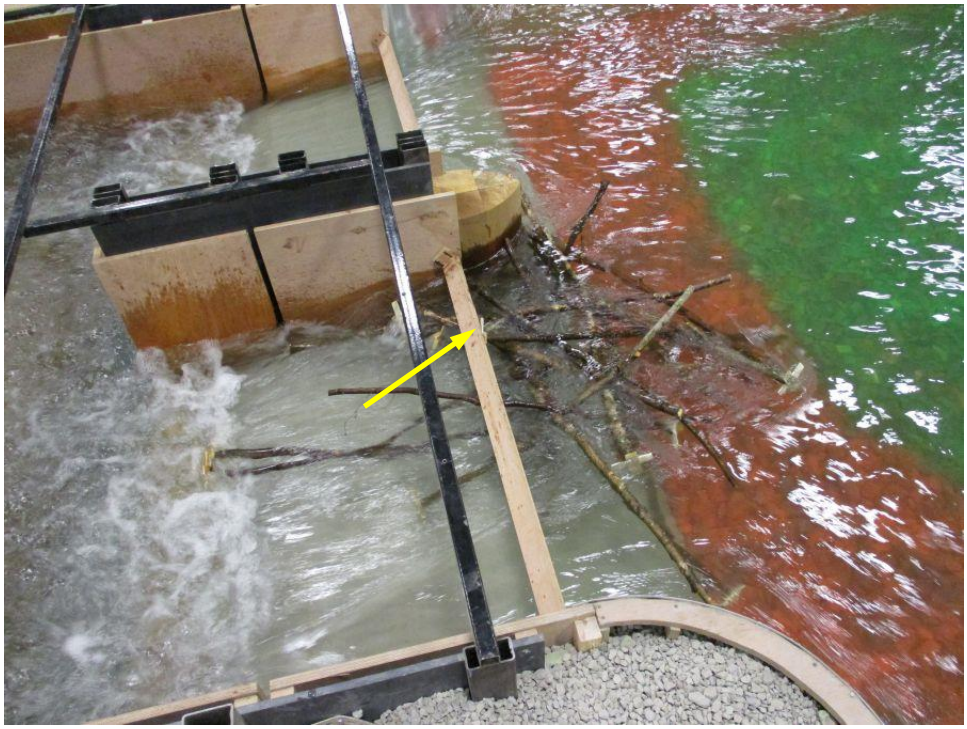

Figure 124. Debris collecting on Pier Nose 1 and root wads catching on the breast wall (arrow).

Figure 125. Flat breast wall on Pier Nose 1 (left) and curved breast wall (right) used for all future debris tests (Pier Nose 2 shown).

5.4.1.2 Pier Nose 2

Design sketches for pier nose 2 are shown in Section 3.4.3.3. This structure re-uses the nose from pier nose 1 however the apex of the pier nose was offset 6m upstream placing it 9.5m upstream of the breast wall (see Figure 125 for a comparison). Figure 126 presents the flow conditions at the diversion channel and the service spillway. The flow conditions in each section of the diversion inlet were similar - there was a slight wake on the RHS of the diversion inlet stemming from pier nose 2, however the hydraulic jump was relatively stable on both sides of the pier. On the service spillway the flow patterns were the same as with pier nose 1 - water trickled over the higher RHS gate, and the waterfall was more energetic on the LHS.

Figure 126. Flow conditions at the structure during the 760 m^3/s event with the Obermeyer gates set to 1213.4m (LHS) and 1215m (RHS) and Pier Nose 2 installed. Left - facing southwest at the diversion, right - facing southeast at the service spillway.

As before, debris was deployed at several points in the floodplain and tracked through the model. Again, refer to Figure 122 for the debris insertion locations and pathways and Table 14 shows a summary of the debris behaviour and performance of the structures in the model with pier nose 2 installed in the diversion. Pier nose 2 was much more effective at passing the debris as no trees remained stuck on the pier during the testing (they only stalled on the pier nose for a short time). Since the apex of pier nose 2 was 6m further upstream than pier nose 1, and the breast wall now a truer curved representation of the prototype, the trees from these debris tests pivoted around the pier nose and passed through the diversion inlet without catching on the breast wall (see Figure 127).

Debris Type	Starting Location	Debris Pathways							Notes
		Debris Barrier	Pier Nose 2	Diversion LHS	Diversion RHS	Center Wall	Service Spillway LHS	Service Spillway RHS	
Singles	A	NA	-	100%	-	-	-	-	25% stuck in hydraulic jump
	C	NA	-	50%	50%	-	-	-	no trees caught on pier nose
	E	NA	-	-	100%	stalls	-	-	~50% stuck in hydrauic jump
	F	NA	-	-	50%	stalls	50%	-	all trees stuck in jump or waterfall
Rafts of 10	A	NA	-	100%	-	-	-	-	10% stuck in hydraulic jump
	D	NA	stalls	20%	80%	-	-	-	trees pass through
	E	NA	-	-	100%	stalls	-	-	trees pass through
Rafts of 40	B	NA	-	100%	-	-	-	-	5% stuck in hydraulic jump
	D	NA	stalls	-	100%	-	-	-	10% stuck in hydraulic jump
	E	NA	-	-	100%	stalls	-	-	trees pass through

Table 14. Debris behaviour for 760 m^3/s with Pier Nose 2 installed in the diversion.

Figure 127. Debris pivoting around Pier Nose 2 while passing through the diversion.

5.4.1.3 Pier Nose 1 (with curved breast wall)

Debris Type	Starting Location	Debris Pathways							Notes
		Debris Barrier	Pier Nose 1	Diversion LHS	Diversion RHS	Center Wall	Service Spillway LHS	Service Spillway RHS	
Rafts of 40	D	NA	30%	35%	35%	-	-	-	some debris caught on pier nose

Table 15. Debris behaviour for 760 m^3/s with Pier Nose 1 installed in the diversion inlet (repeat test with the curved breast wall).

Pier nose 1 was re-installed on the model to see if the new curved breast wall improved its performance. Table 15 shows the fate of a 40-tree raft released from the central channel in the floodplain (position D). Less debris was collected on the pier nose than with the original pier nose 1, suggesting the new breast wall offered some improvement, but it did not perform as well as pier nose 2. A percentage of the debris still remained caught on the nose and bridged over to the breast wall (see Figure 128).

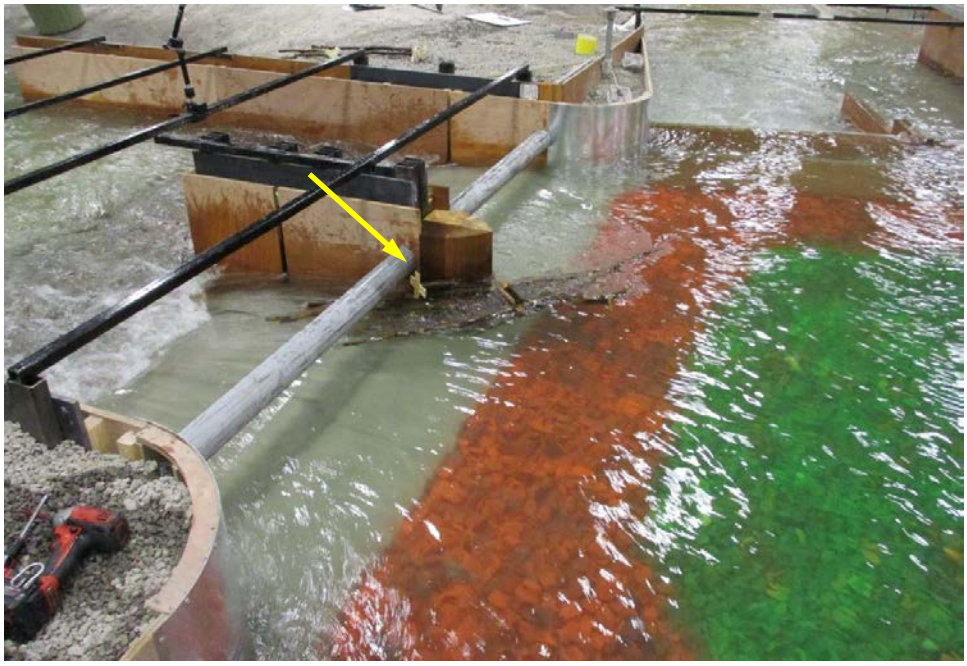

Figure 128. Debris collecting on Pier Nose 1 and root wads catching on the curved breast wall (arrow).

5.4.1.4 Pier Nose 3

Design sketches for pier nose 3 are shown in Section 3.4.3.3. This nose featured the same curved arrowhead plan-shape of pier nose 1 and 2, however the profile is set on an adverse 1:4 slope. Therefore the apex is 8m upstream of the breast wall at the top of the pier nose and 6m upstream of the breast wall at the base. Figure 129 shows pictures of the flow conditions at the diversion inlet with pier nose 3 installed. The flow conditions at the diversion inlet and the service spillway were similar to those seen with pier nose 2.

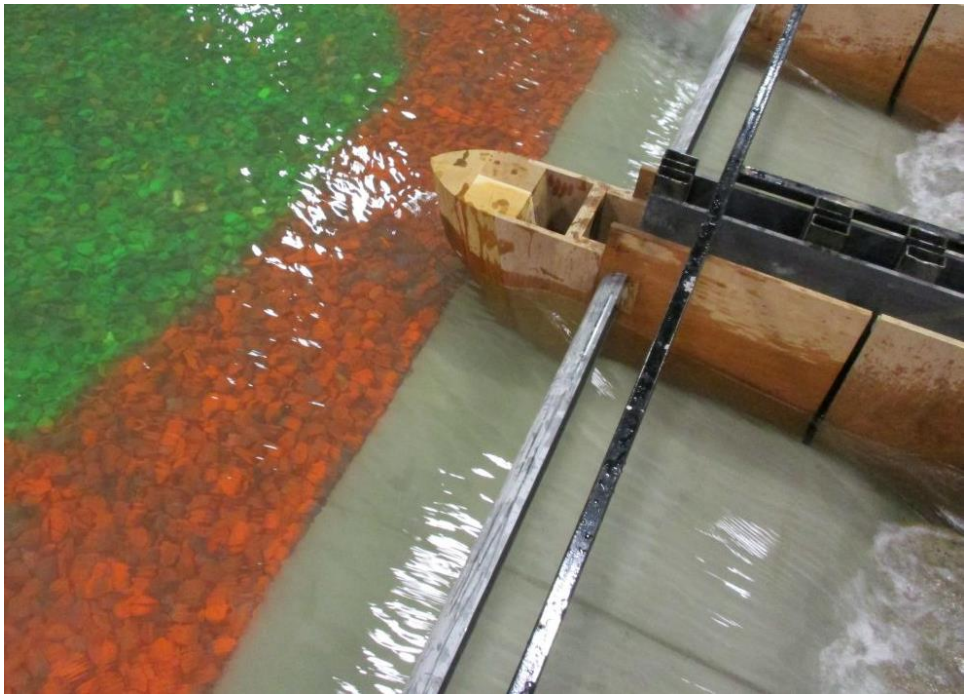

Figure 129. Flow conditions at the diversion inlet with Pier Nose 3 installed.

As before, debris was inserted at several points in the floodplain and tracked through the model. Again, refer to Figure 122 for the debris insertion locations and pathways. Table 16 shows a summary of the debris behaviour and performance of the structures in the model with pier nose 3 installed in the diversion. Pier nose 3 outperformed pier nose 1, and was similar to pier nose 2 (the nose being further upstream and away from the breast wall) in terms of its ability to pass debris through the diversion. However, material released at the north of the small tree island (location) collected on pier. Since the nose had an adverse slope, debris rode down the face of the nose and became wedged below the water surface (see Figure 130).

Debris Type	Starting Location	Debris Pathways							Notes
		Debris Barrier	Pier Nose 3	Diversion LHS	Diversion RHS	Center Wall	Service Spillway LHS	Service Spillway RHS	
Rafts of 10	A	NA	-	100%	-	-	-	-	trees pass through
	C	NA	-	100%	-	-	-	-	trees pass through
	D	NA	90%	5%	5%	-	-	-	caught on pier nose
	E	NA	-	-	98%	stalls	2%	-	cleared trees caught on pier nose
Rafts of 40	D	NA	stalls	50%	50%	-	-	-	trees pass through

Table 16. Debris behaviour for 760 m^3/s with Pier Nose 3 installed in the diversion.

Figure 130. Debris caught on Pier Nose 3.

5.4.1.5 Pier Nose 4

Designs for pier nose 4 are shown in Section 3.4.3.3 and it featured a semi-circular and narrower outer nose section that rose at a 2:1 slope. The bottom and top ends of the pier nose are 12m and 1m upstream of the breast wall, respectively. Figure 129 shows pictures of the flow conditions at the diversion inlet with pier nose 4 installed. The wake pattern emanating from the pier nose was rougher and more turbulent than that seen with any of the other pier noses, but otherwise the flow conditions at the diversion inlet and the service spillway were similar to those seen previously.

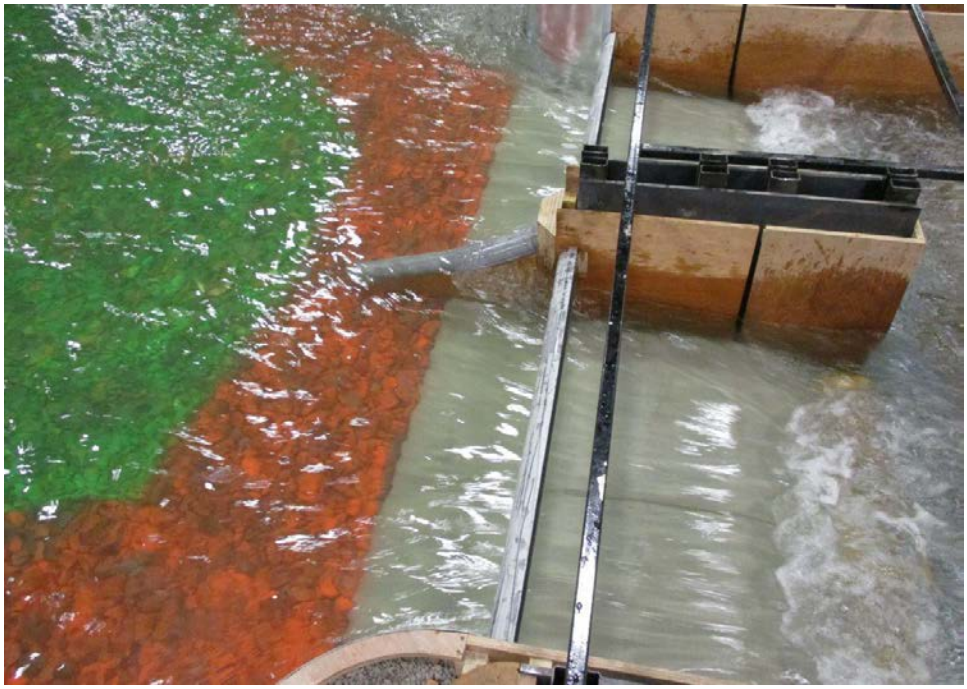

Figure 131. Flow conditions at the diversion inlet with Pier Nose 4 installed.

As before, debris was inserted at several points in the floodplain and tracked through the model. Again, refer to Figure 122 for the debris insertion locations and pathways. Table 17 shows a summary of the debris behaviour and performance of the structures in the model with pier nose 4 installed in the diversion. The sloping pier nose 4 was not effective at passing the tree debris. The trees rode up the sloping nose, and became stuck either directly on the nose or wedged against the breast wall (see Figure 132).

Debris Type	Starting Location	Debris Pathways							Notes
		Debris Barrier	Pier Nose 4	Diversion LHS	Diversion RHS	Center Wall	Service Spillway LHS	Service Spillway RHS	
Rafts of 10	A	NA	-	100%	-	-	-	-	trees pass through
	B	NA	-	100%	-	-	-	-	trees pass through
	C	NA	-	-	100%	-	-	-	trees pass through
	E	NA	-	-	100%	-	-	-	5% stuck in hydraulic jump
	F	NA	-	-	20%	80%	-	-	cleared trees caught on center wall
Rafts of 40	D	NA	90%	-	10%	-	-	-	caught on pier nose
	D	NA	100%	-	-	-	-	-	caught on previous debris

Table 17. Debris behaviour for 760 m^3/s with Pier Nose 4 installed in the diversion.

Figure 132. Debris caught on Pier Nose 4.

5.4.1.6 Debris Barrier A, Pier Nose 2

Figure 133. Debris barrier A.

The performance of four debris barriers fronting the diversion inlet was also investigated in test series D, and Section 3.4.3.4 shows the designs and layout of the different barriers. Debris barrier A featured four 600mm piles on 5m spacing across both of the diversion inlet bays spanning from the pier nose to the curved outer retaining walls (see Figure 133). Table 18 shows a summary of the

debris behaviour and performance of this debris barrier (refer to Figure 122 for a schematic showing the debris insertion points and pathways). Single trees from the individually deployed woody debris runs were able to pass through the debris barrier and pass through the diversion, but all of the rafted debris elements were retained on the barrier. At the end of the testing a large debris pile remained on the barrier (see Figure 134), and the 24m (LHS) Obermeyer gate was lowered from 1213.4m to 1210m in an effort to flush the trees from the face of the debris barrier. Only two of the trees were released and the vast debris raft remained intact on the debris barrier. The debris build-up the diversion inlet caused more flow to pass through the service spillway (a re-direction of approximately 40m^3/s).

Debris Type	Starting Location	Debris Pathways							Notes
		Debris Barrier A	Pier Nose 2	Diversion LHS	Diversion RHS	Center Wall	Service Spillway LHS	Service Spillway RHS	
Singles	A	50%	-	50%	-	-	-	-	passing tree stuck in hydraulic jump
	C	100%	-	-	-	-	-	-	caught in debris barrier
	E	100%	-	-	-	-	-	-	caught in debris barrier
Rafts of 10	A	100%	-	-	-	-	-	-	caught on previous debris
	D	100%	-	-	-	-	-	-	caught on previous debris
	E	100%	-	-	-	-	-	-	caught on previous debris
Rafts of 40	A	100%	-	-	-	-	-	-	dropping Obermeyer gate did not budge the debris

Table 18. Debris behaviour for 760 m^3/s with Debris Barrier A and Pier Nose 2 installed in the diversion.

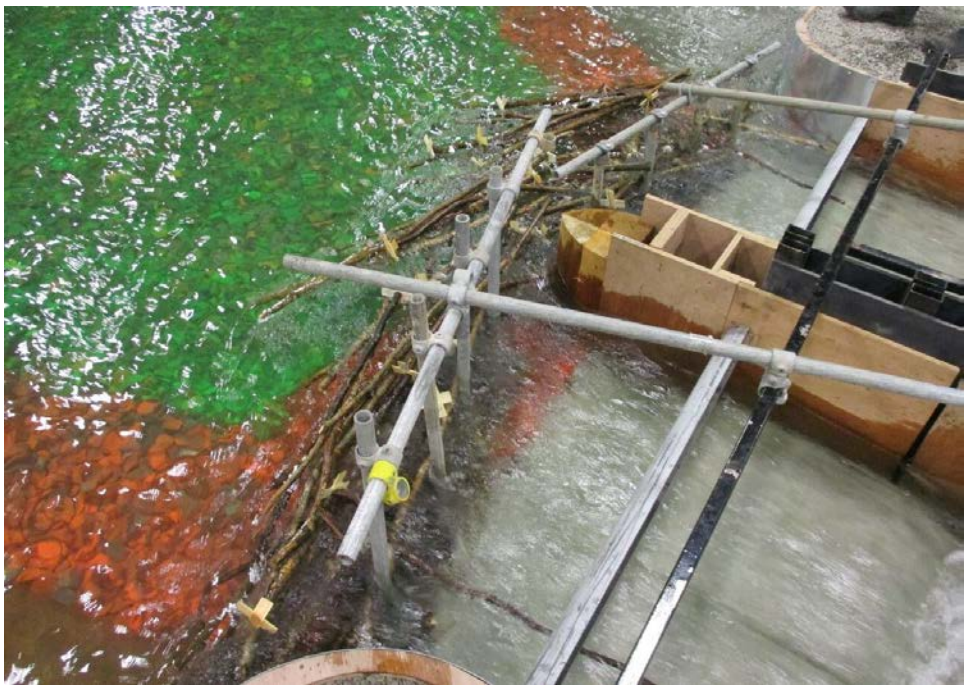

Figure 134. Debris caught on Debris Barrier A.

5.4.1.7 Debris Barrier B, Pier Nose 2

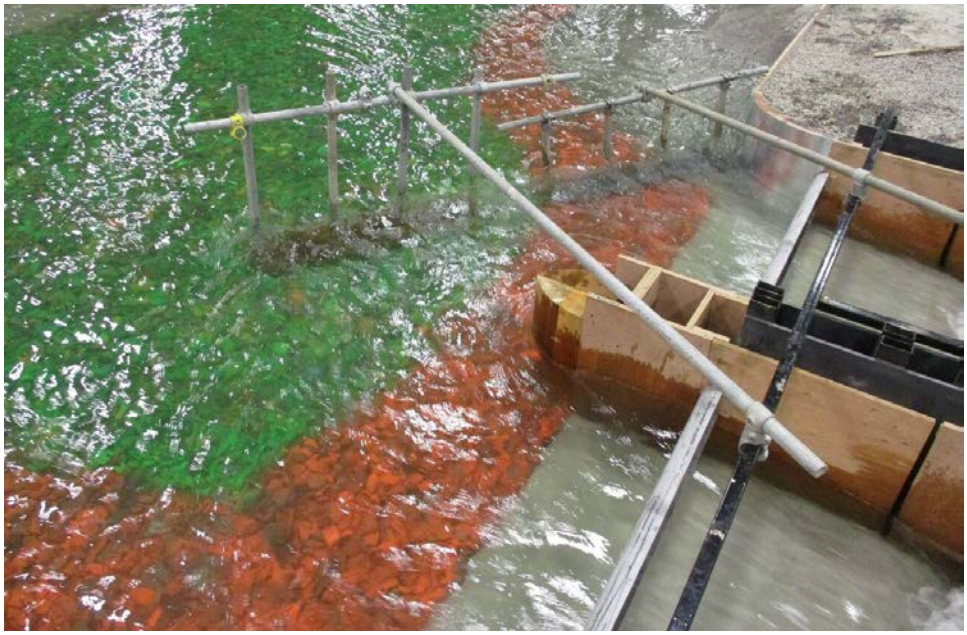

Figure 135. Debris barrier B.

Debris Barrier B utilized the same structure used previously (eight piles at 5m spacing) but the piles were aligned all in one row and set at an angle to the diversion inlet structure (see Figure 135 and refer to section 3.4.3.4 for the design and layout of the barrier). Table 19 shows a summary of the debris behaviour and performance of the debris barrier (refer to Figure 122 for a schematic showing the debris insertion points and pathways). This debris barrier was not as effective as barrier A, as some of the trees released from in front of the small island of trees and in the secondary channel (locations D and E) travelled around the end of the barrier and passed through the diversion. As the debris raft grew in front of the barrier the effective end point shifted to the east as more and more debris piled up in this direction (see Figure 136).

Debris Type	Starting Location	Debris Pathways							Notes
		Debris Barrier B	Pier Nose 2	Diversion LHS	Diversion RHS	Center Wall	Service Spillway LHS	Service Spillway RHS	
Singles	A	50%	-	50%	-	-	-	-	passing tree passed through the model
	C	75%	-	25%	-	-	-	-	caught in debris barrier
	E	50%	-	-	50%	-	-	-	passing tree passed through the model
Rafts of 10	A	90%	-	-	-	-	-	-	caught on previous debris
	D	90%	-	-	-	-	-	-	caught on previous debris
	E	0%	-	-	100%	-	-	-	20% stuck in hydraulic jump
Rafts of 40	A	100%	-	-	-	-	-	-	caught in debris barrier
	E	40%		-	60%	-	-	-	passing trees passed through the model

Table 19. Debris behaviour for the 760 m^3/s flow with Debris Barrier B and Pier Nose 2 installed in the diversion.

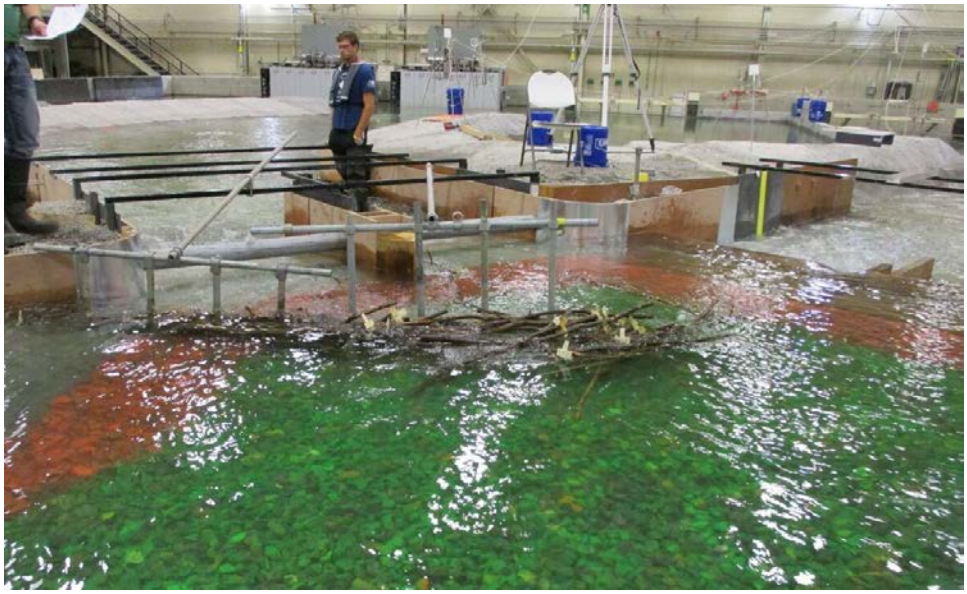

Figure 136. Debris caught on Debris Barrier B.

5.4.1.8 Debris Barrier C, Pier Nose 2

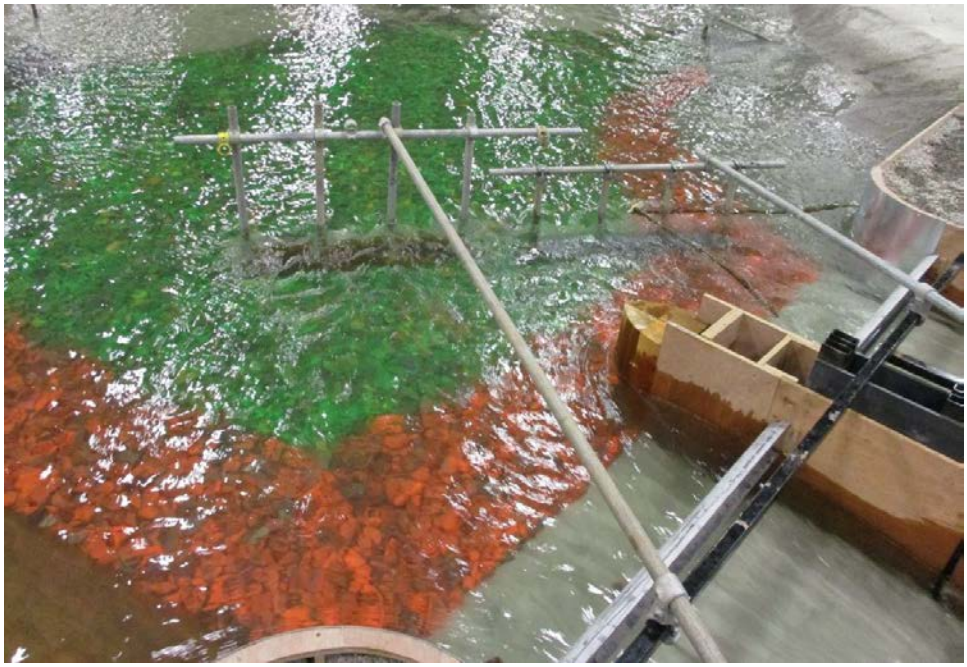

Figure 137. Debris barrier C.

Debris Barrier C utilized the same barrier structure and alignment angle used previously (8 piles at 5m spacing) but the piles were shifted along the alignment toward the southeast end point and leaving a larger gap at the left hand retaining wall of the diversion inlet (see Figure 137 and refer to section 3.4.3.4 for the design and layout of the barrier). Table 20 shows a summary of the debris behaviour and performance of the debris barrier (refer to Figure 122 for a schematic showing the debris insertion points and pathways). As with barrier B the trees released from in front of the small island of trees and in the secondary channel (locations D and E) travelled around the right-hand end of the

barrier and passed through the diversion. As before, the debris raft caught on the barrier grew in length shifting the effective end point of the barrier towards the service spillway, however debris from the secondary floodplain channel still passed around the debris/barrier and passed through the diversion inlet (see Figure 138).

Debris Type	Starting Location	Debris Pathways							Notes
		Debris Barrier C	Pier Nose 2	Diversion LHS	Diversion RHS	Center Wall	Service Spillway LHS	Service Spillway RHS	
Singles	A	75%	-	25%	-	-	-	-	passing tree passed through the model
	C	75%	-	25%	25%	-	-	-	caught in debris barrier
	E	0%	-	-	100%	-	-	-	passed through model
Rafts of 10	A	100%	-	-	-	-	-	-	caught in debris barrier
	C	100%	-	-	-	-	-	-	caught in debris barrier
	E	0%	-	-	100%	-	-	-	trees pass through model

Table 20. Debris behaviour for 760 m^3/s with Debris Barrier C and Pier Nose 2 installed in the diversion.

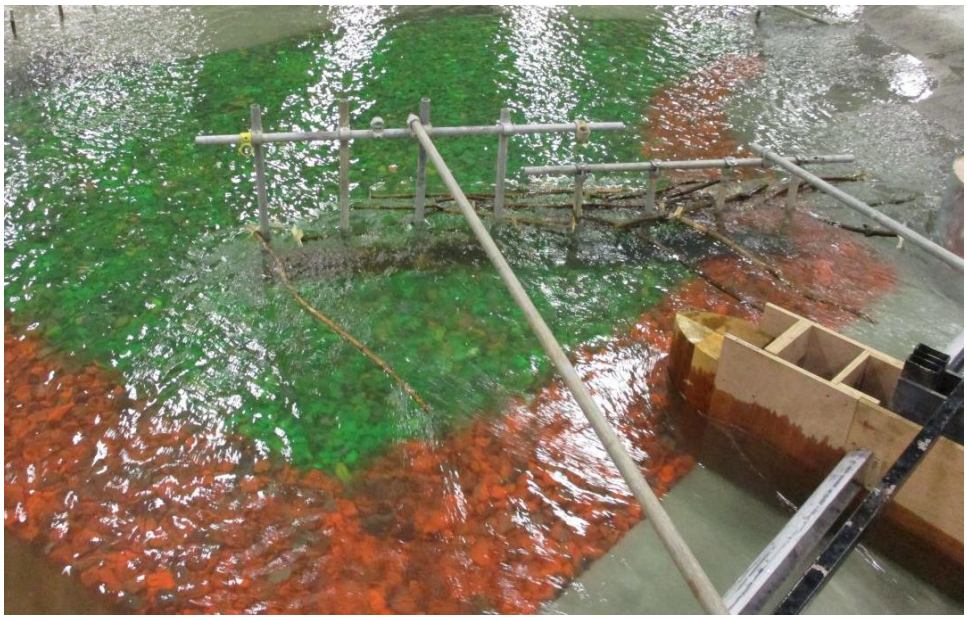

Figure 138. Debris caught on and passing around the end of Debris Barrier C.

5.4.1.9 Debris Barrier D, Pier Nose 2

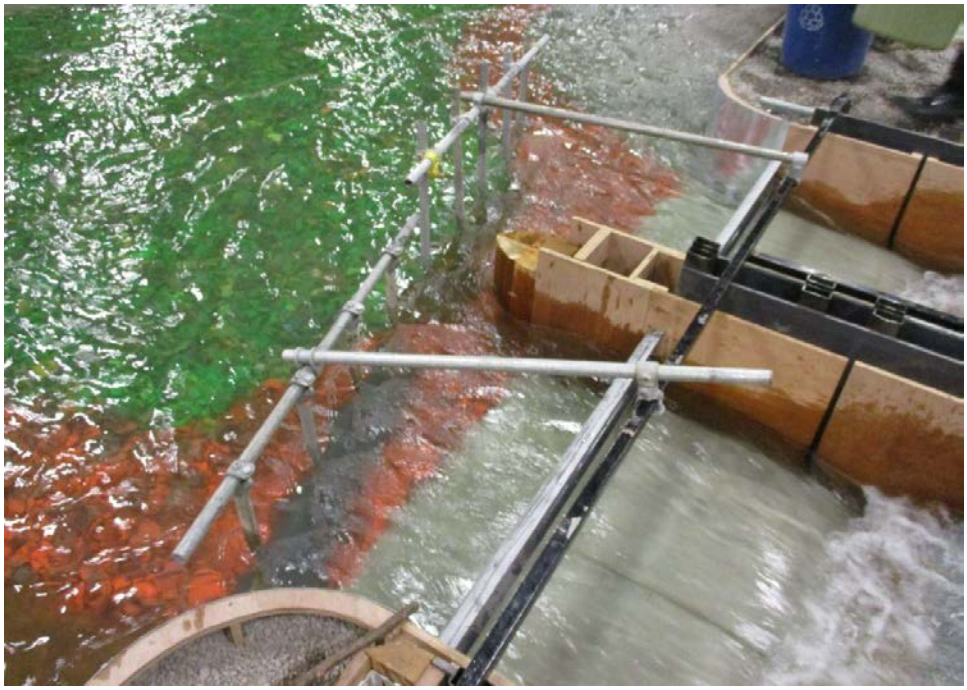

Figure 139. Debris barrier D.

Debris Barrier D utilized a similar barrier structure as before (piles spaced at 5m) however an additional pile was inserted giving nine piles for a 45m total barrier length. The barrier was angled such that it covered the RHS of the diversion inlet entirely and a portion of the LHS (see Figure 139 and refer to section 3.4.3.4 for the design and layout of the barrier). Table 21 shows a summary of the debris behaviour and performance of debris barrier D (refer to Figure 122 for a schematic showing the debris deployment points and pathways). Since the west end of the debris rack did not completely shelter the LHS of the diversion, debris inserted at location A in the main channel bypassed the barrier and passed through the LHS of the diversion. Otherwise, the barrier was effective at collecting the debris at locations B-E. A raft of debris was allowed to collect on the debris barrier and the diversion inlet gates were closed to investigate if the debris could be pulsed off the barrier and pass through the service spillway (see Figure 140). This was successful as only a small percentage (4%) of the trees remained on the barrier after closing the diversion.

Debris Type	Starting Location	Debris Pathways							Notes
		Debris Barrier D	Pier Nose 2	Diversion LHS	Diversion RHS	Center Wall	Service Spillway LHS	Service Spillway RHS	
Singles	A	0%	-	100%	-	-	-	-	passed through model
	B	100%	-	-	-	-	-	-	caught in debris barrier
	C	100%	-	-	-	-	-	-	caught in debris barrier
	D	100%	-	-	-	-	-	-	caught in debris barrier
	E	100%	-	-	-	-	-	-	caught in debris barrier
Raft of 50	On Debris Barrier D	4% remained	-	-	-	-	96%	-	A raft of 50 trees were placed on the barrier, the diversion gates were shut, debris raft "pulsed" off the barried and passed through spillway

Table 21. Debris behaviour for 760 m^3/s with Debris Barrier D and Pier Nose 2 installed in the diversion.

Figure 140. Debris caught on Debris Barrier D , the diversion inlet was closed and LHS Obermeyer gate was lowered to pulse the trees off the barrier.

5.4.2 *760 m^3/s – Diversion inlet Closed*

Pier nose 3's performance was investigated with the diversion inlet gates closed and both of the service spillway Obermeyer gates set to fully open (1210m). As before, the model tree debris was inserted into the model in one of six locations as shown in Figure 141 during the tests.

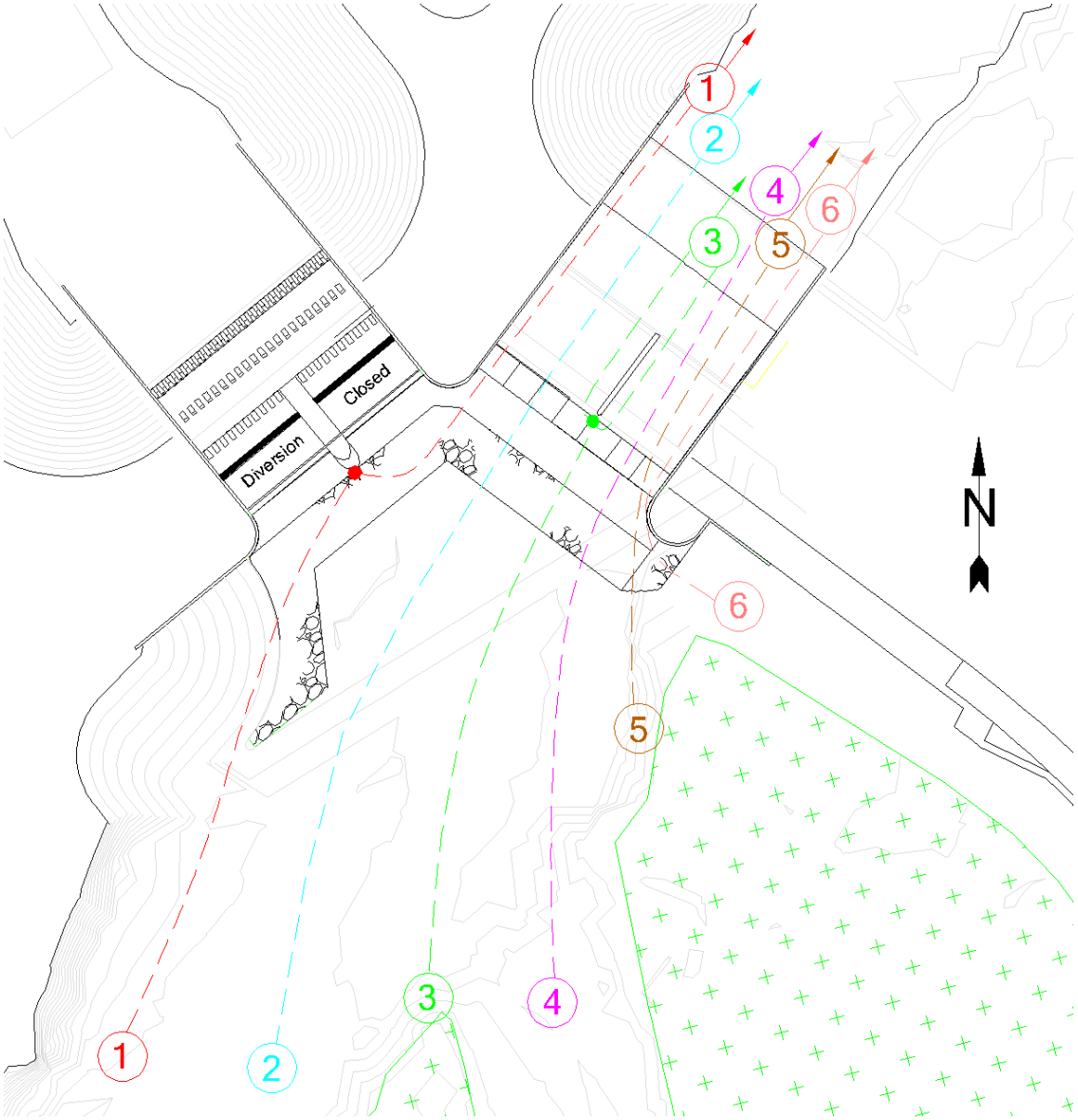

Figure 141. Debris pathways for TSD, 760 m^3/s flow conditions with the diversion inlet gates closed.

5.4.2.1 Pier Nose 3

The split point for the debris to pass down either the LHS or RHS of the service spillway was to the north of the small island of trees in the floodplain (location 3 in Figure 141). The debris did not get caught on the central pier between the Obermeyer gates. With the flood flow restricted entirely to the service spillway, the flow patterns were fairly energetic, and the hydraulic jump on the RHS was relatively unstable as the wake from the central pier combined with the wake emanating from the circular retaining wall on the RHS of the service spillway (see Figure 142).

Debris Type	Starting Location	Debris Pathways							Notes
		Debris Barrier	Pier Nose 3	Diversion LHS	Diversion RHS	Center Wall	Service Spillway LHS	Service Spillway RHS	
Rafts of 10	1	NA	-	-	-	-	100%	-	passed through model
	2	NA	-	-	-	-	100%	-	passed through model
	3	NA	-	-	-	-	50%	50%	passed through model
	4	NA	-	-	-	-	-	100%	passed through model
	5	NA	-	-	-	-	-	100%	passed through model
	6	NA	-	-	-	-	-	100%	passed through model
Rafts of 40	3	NA	-	-	-	-	-	100%	passed through model

Table 22. Debris behaviour for 760 m^3/s with Pier Nose 3 installed in the diversion.

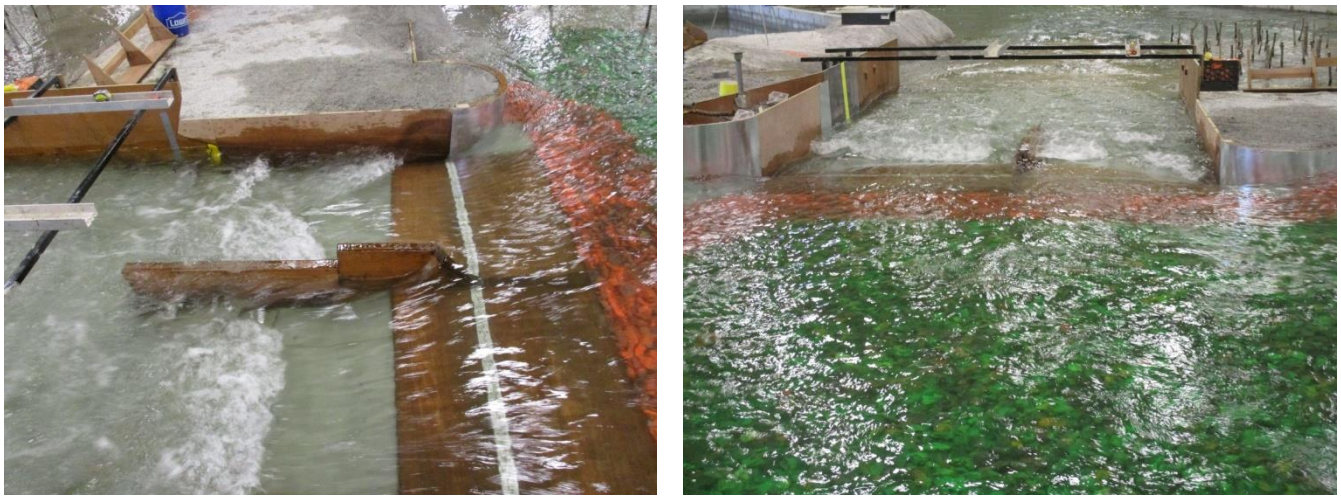

Figure 142. Flow patterns generated in the service spillway with the diversion inlet gates closed at 760m^3/s.

5.4.3 *1240 m^3/s*

The gate settings for the 1240m^3/s flow investigated the diversion inlet gate in the fully raised position, and the service spillway Obermeyer gates set to 1210m on the 24m wide left-hand side (LHS) and 1213.15m on the 18m wide right-hand side (RHS). These settings were intended to direct 640m^3/s through the service spillway and 600m^3/s through the diversion. Model tree debris was inserted into the model in one of seven locations (A-G) as shown in Figure 143 during the tests. Based on the results of the tests at 760m^3/s, only pier noses 2 and 3 were considered for further investigation. A summary of the behaviour of the debris, and the performance of the structural features of the diversion inlet and service spillway are discussed in the following sections.

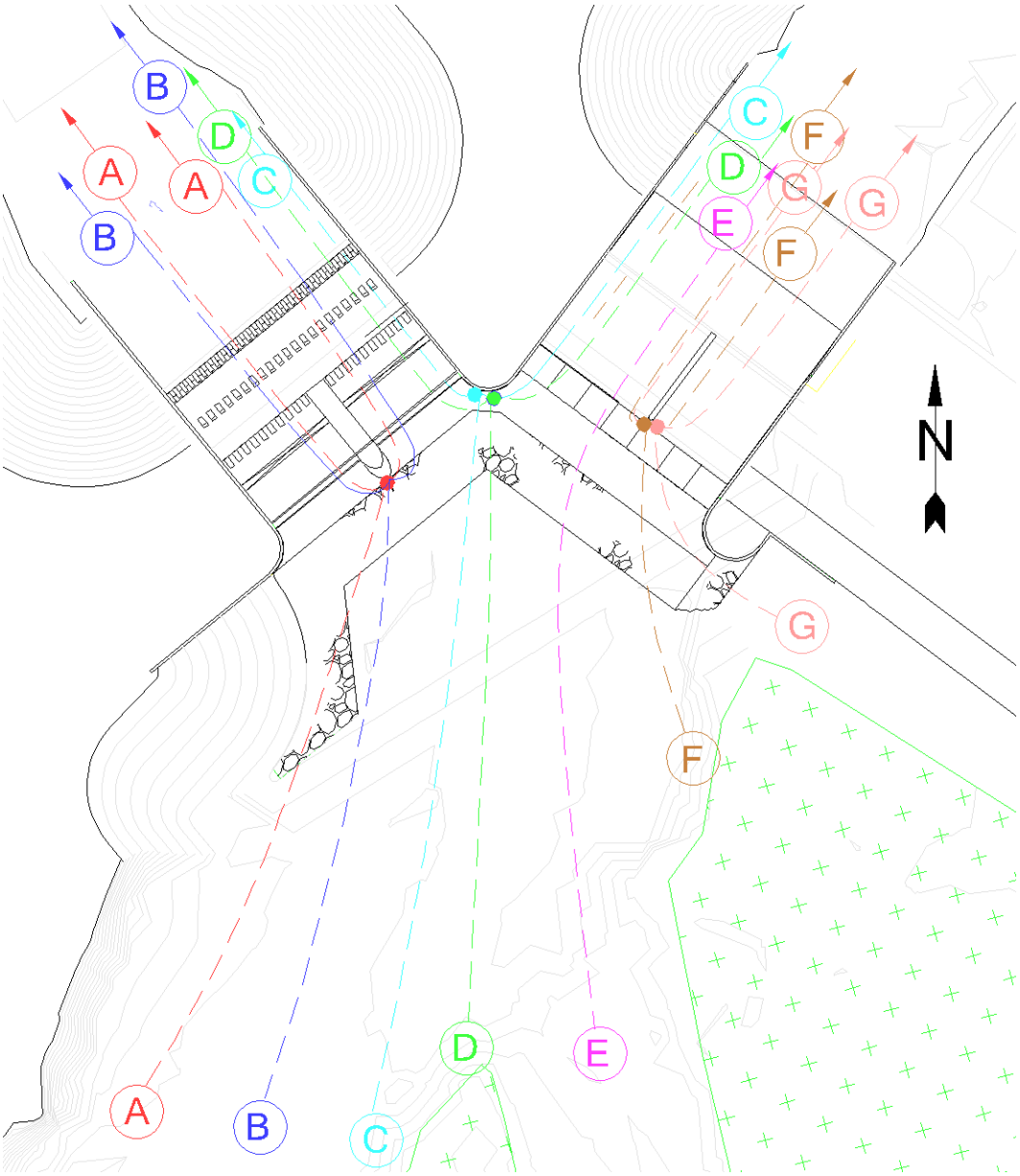

Figure 143. Debris pathways for the 1240 m^3/s flow conditions with the diversion inlet gates open.

5.4.3.1 Pier Nose 3

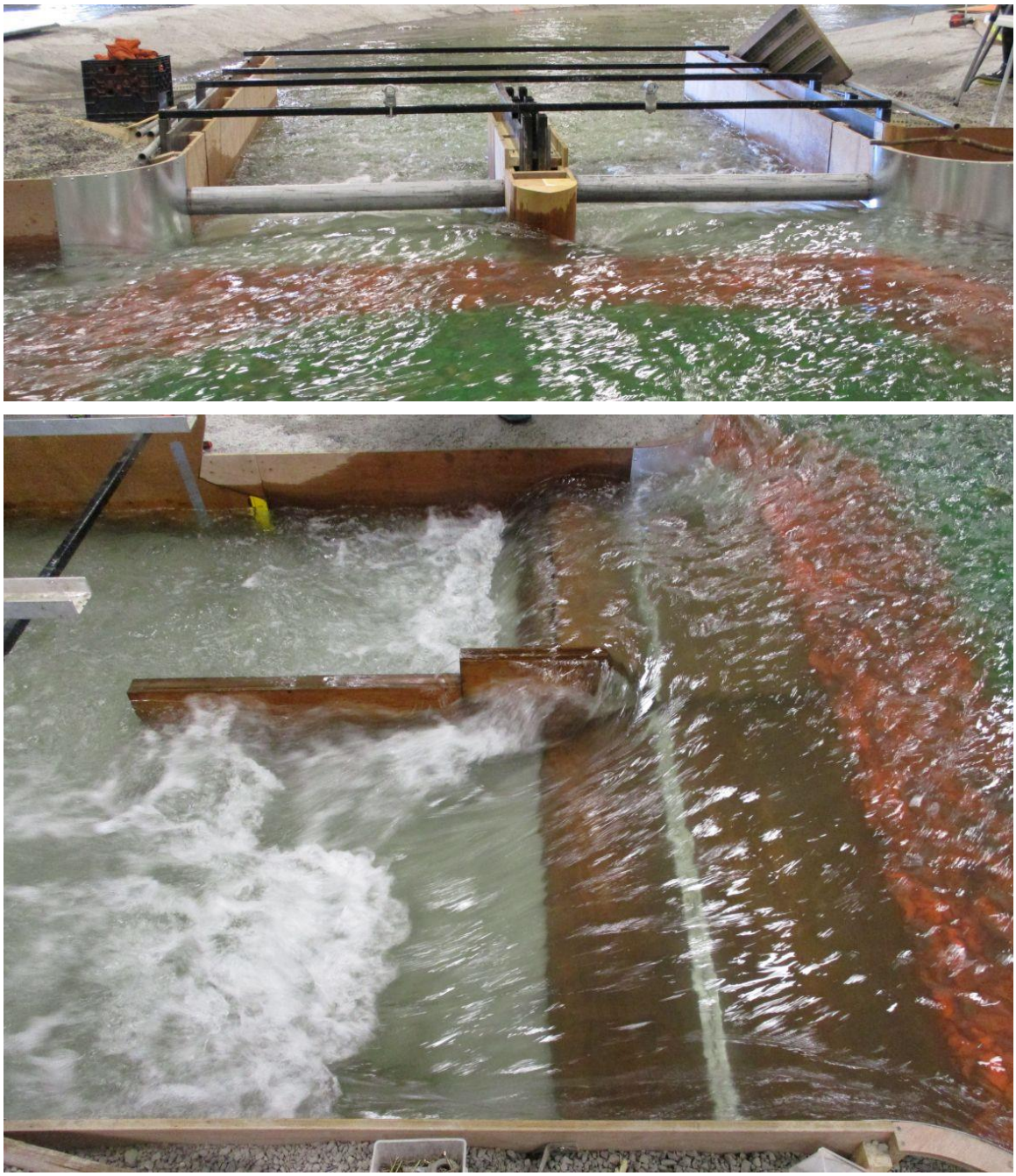

Figure 144. Flow conditions at the structure during the 1240 m^3/s event. Top – facing downstream at the diversion, bottom - facing southeast at the service spillway.

The flow conditions through both the diversion inlet and the service spillway were very energetic for the 1240m^3/s flood condition. Deep wakes stemmed from the LHS entrance wall and pier nose at the diversion inlet (see the top photograph in Figure 144). The hydraulic jump on the LHS of the service spillway was more unstable than the RHS, as the flows were higher and also the wake generated by the central pier affected the location of the jump (see Figure 144 – bottom). Debris was inserted at

several points in the floodplain and tracked through the model (see Figure 143 for the insertion points and pathways). Table 23 shows a summary of the debris behaviour and performance of the model with pier nose 3 installed in the diversion. In general, the pier nose passed most of the debris through the diversion, with only a small portion of the trees of the 40-pack raft getting caught (see Figure 145).

Debris Type	Starting Location	Debris Pathways							Notes
		Debris Barrier	Pier Nose 3	Diversion LHS	Diversion RHS	Center Wall	Service Spillway LHS	Service Spillway RHS	
Singles	A	NA	-	100%	-	-	-	-	trees pass through
	B	NA	-	100%	-	-	-	-	trees pass through
	C	NA	-	-	50%	-	50%	-	trees pass through
	E	NA	-	-	-	-	100%	-	trees pass through
	F	NA	-	-	-	-	50%	50%	trees pass through
Rafts of 10	A	NA	-	100%	-	-	-	-	trees pass through
	B	NA	-	50%	50%	-		-	trees pass through
	D	NA		-	50%	-	50%	-	trees pass through
	E	NA	-	-	-	-	100%	-	trees pass through
	F	NA	-	-	-	-	100%	-	trees pass through
	G	NA	-	-	-	-	50%	50%	trees pass through
Rafts of 40	A	NA	10%	45%	45%	-	-	-	some wedged on pier nose
	D	NA	-	-	50%	-	50%	-	trees pass through
	F	NA	-	-	-	-	100%	-	trees pass through

Table 23. Debris behaviour for 1240 m^3/s with Pier Nose 3 installed in the diversion.

Figure 145. Debris caught on Pier Nose 3.

5.4.3.2 Pier Nose 2

Figure 146. Wake emanating from pier nose 2 during the 1240 m^3/s event.

The flow conditions through both the diversion inlet and the service spillway were similar for pier nose 2 and pier nose 3. The wake cast from pier nose 2 appeared to be slightly deeper and more turbulent (see Figure 146). As before, debris was inserted at several points in the floodplain and tracked through the model (see Figure 143 for the insertion points and pathways). Table 24 shows a summary of the debris behaviour and performance of the model with pier nose 2 installed in the diversion. When debris came from the left hand side of the main floodplain channel (location A) a small portion was caught on the pier nose (see Figure 147).

Debris Type	Starting Location	Debris Pathways							Notes
		Debris Barrier	Pier Nose 2	Diversion LHS	Diversion RHS	Center Wall	Service Spillway LHS	Service Spillway RHS	
Singles	A	NA	25%	75%	-	-	-	-	trees caught on pier nose
	C	NA	-	-	100%	-	-	-	trees pass through
	D	NA	-	-	50%	25%	25%	-	trees stuch on center wall
	E	NA	-	-	-	-	100%	-	trees pass through
Rafts of 10	A	NA	20%	40%	40%	-	-	-	some wedged on pier nose
	C	NA	-	-	100%	-		-	trees pass through
	D	NA		-	50%	-	50%	-	10% stuck in hydraulic jump on SS-RHS
Rafts of 40	A	NA	5%	45%	50%	-	-	-	some wedged on pier nose
	D	NA	-	50%	50%	-	-	-	trees pass through

Table 24. Debris behaviour for 1240 m^3/s with Pier Nose 2 installed in the diversion.

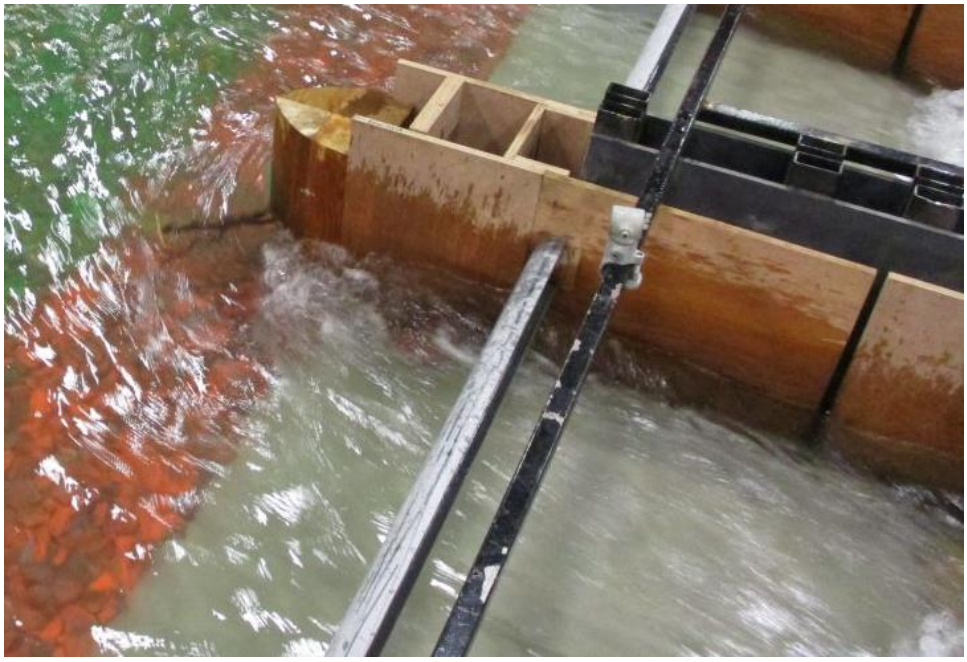

Figure 147. Debris caught on Pier Nose 2.

5.4.3.3 Debris Barrier D, Pier Nose 2

Debris Barrier D was re-installed in front of the diversion inlet and its performance at 1240m^3/s was investigated (refer to section 3.4.3.4 for the design and layout of the barrier). As seen in previous tests with this barrier, since the west end did not completely shelter the LHS of the diversion, debris inserted at location A in the main channel bypassed the barrier and passed through the LHS of the diversion. Otherwise, the barrier was effective at collecting the debris at locations B-E. A raft of debris was allowed to collect on the debris barrier and the diversion inlet gates were closed to investigate if the debris could be pulsed off the barrier and pass through the service spillway (see Table 25 and Figure 148). This was successful as only a small percentage (8%) of the trees remained on the barrier after closing the diversion. It should be noted that the gates cannot be operated in this manner for an extended period of time without overtopping the auxiliary spillway.

Debris Type	Starting Location	Debris Pathways							Notes
		Debris Barrier D	Pier Nose 2	Diversion LHS	Diversion RHS	Center Wall	Service Spillway LHS	Service Spillway RHS	
Raft of 50	On Debris Barrier D	8% remained	-	-	-	-	92%	-	A raft of 50 trees were placed on the barrier, the diversion gates were shut, debris raft "pulsed" off the barried and passed through the spillway

Table 25. Debris behaviour for 1240 m^3/s with Debris Barrier D and Pier Nose 2 installed in the diversion.

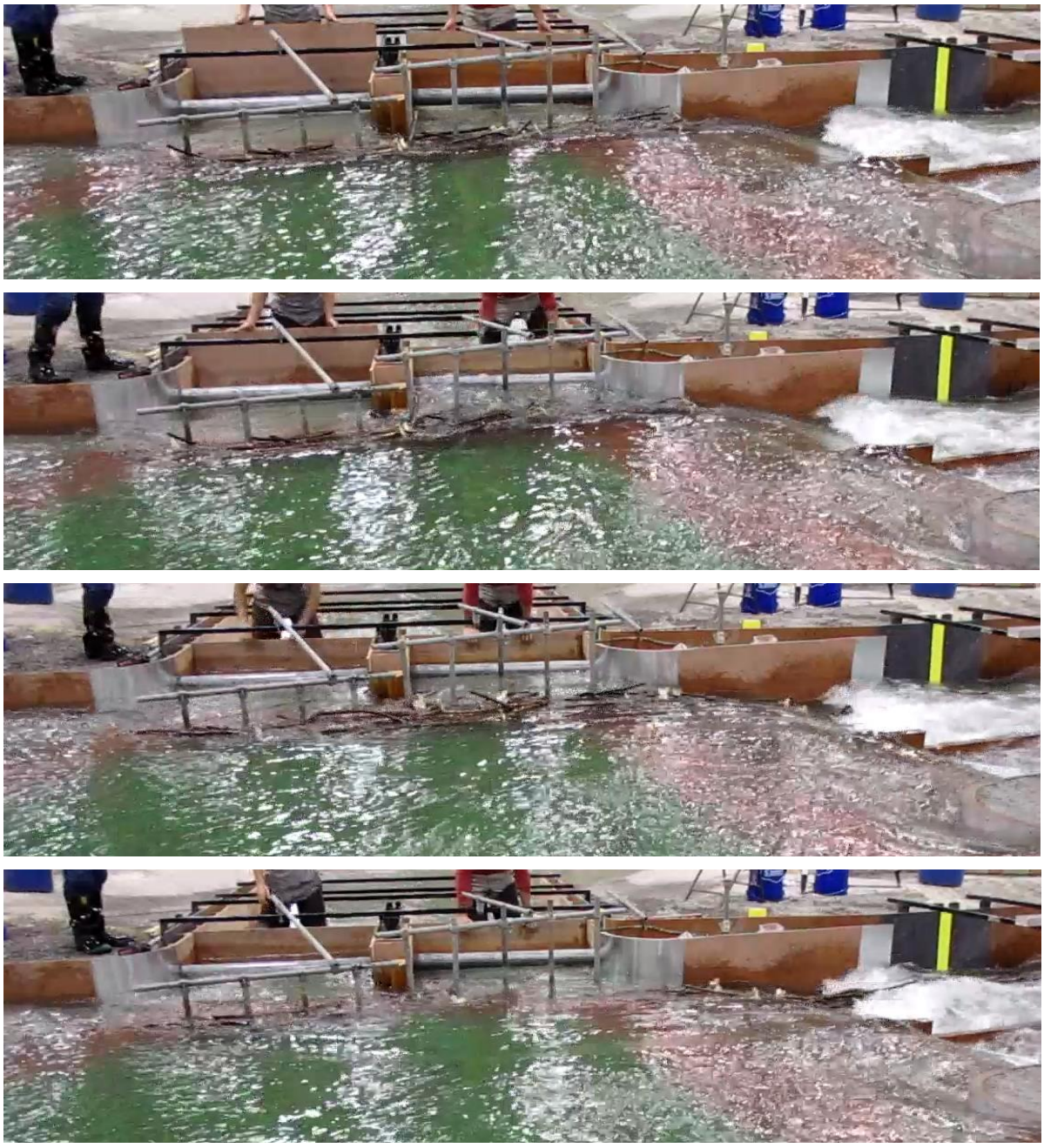

Figure 148. Diversion inlet gates being closed and the trees being removed from the barrier.

5.4.3.4 Debris Barrier C, Pier Nose 3

The performance of Debris Barrier C and Pier Nose 3 under a flood flow of 1240m^3/s was investigated (refer to section 3.4.3.4 for the design and layout of the barrier). For this test, approximately 80 trees were already in place on the barrier from the previous tests run at 320m^3/s flow. The flow was increased to 1240m^3/s and only three trees were removed from the debris raft collected on the barrier (see Figure 149). Additional debris was then inserted in the model in locations D, E, F, and G and the debris paths through the model were noted (see Figure 143 for the debris insertion locations

and Table 26 for the performance of the barrier). The debris bypassed the barrier and passed through the service spillway.

Debris Type	Starting Location	Debris Pathways							Notes
		Debris Barrier C	Pier Nose 3	Diversion LHS	Diversion RHS	Center Wall	Service Spillway LHS	Service Spillway RHS	
Singles	D	Pre-loaded	-	-	-	-	100%	-	trees pass through
	E	Pre-loaded	-	-		-	100%	-	trees pass through
	F	Pre-loaded	-	-	-	-	-	100%	trees pass through
	G	Pre-loaded	-	-	-	-	-	100%	trees pass through

Table 26. Debris behaviour for 1240 m^3/s with Debris Barrier C and Pier Nose 3 installed in the diversion.

Figure 149. Debris collected on barrier C at the start of the tests.

5.4.4 ***320 m^3/s***

The gate settings for the TSD 320m^3/s flow utilized the diversion inlet gate in the fully raised position, and the service spillway Obermeyer gates set to 1211.05m on the 24m wide left-hand side (LHS) and 1215m on the 18m wide right-hand side (RHS). The setting was intended to direct 160m^3/s through the service spillway and 160m^3/s through the diversion. Model tree debris was inserted into the model in one of seven locations (i-vii) as shown in Figure 150 during the tests. Based on the results of the tests at 760m^3/s and 1240m^3/s, only pier noses 2 and 3 and debris barriers C and D were investigated. A summary of the behaviour of the debris, and the performance of the structural features of the diversion inlet and service spillway are discussed in the following sections.

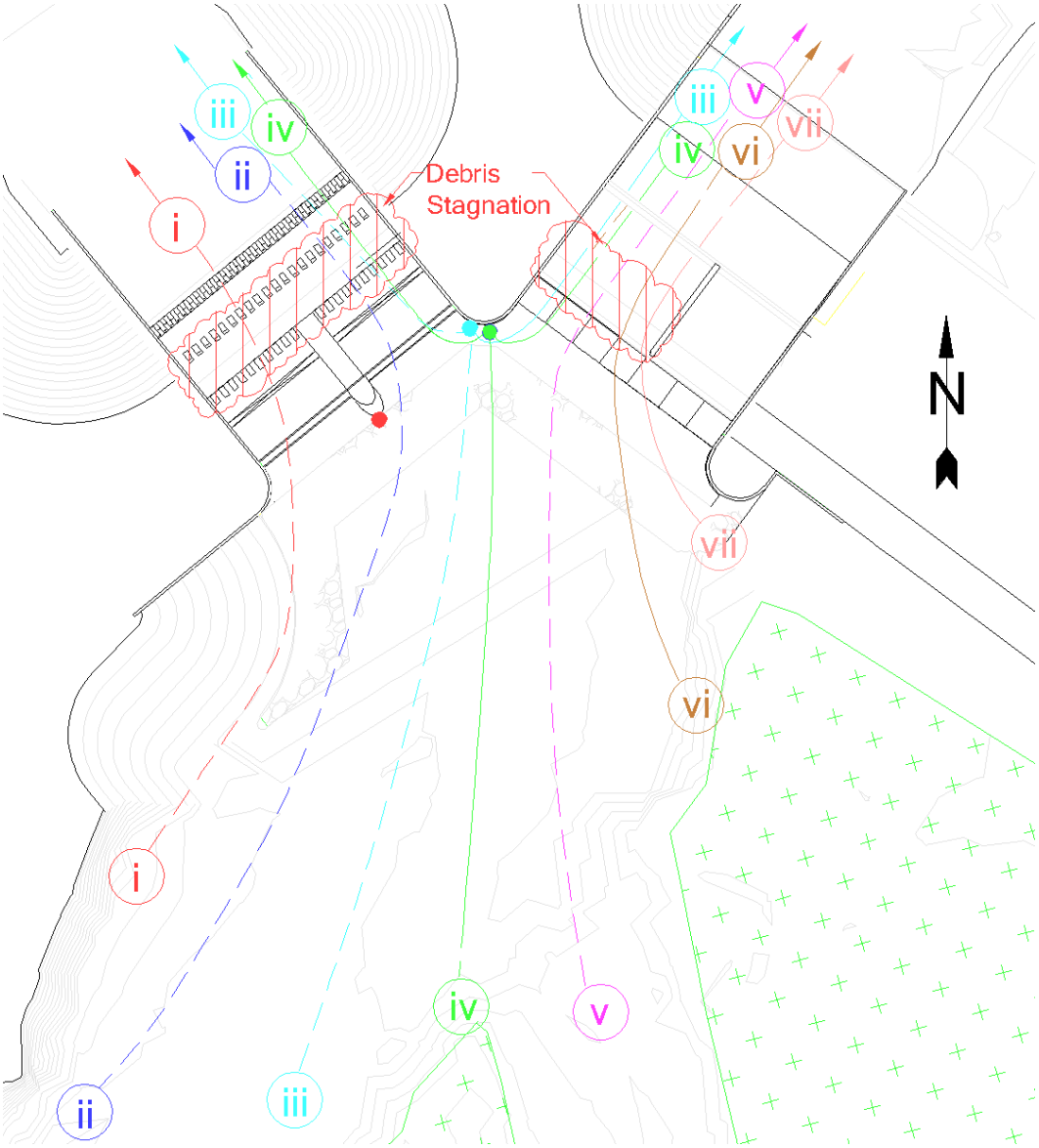

Figure 150. Debris pathways for the 320 m^3/s flow conditions.

5.4.4.1 Pier Nose 2

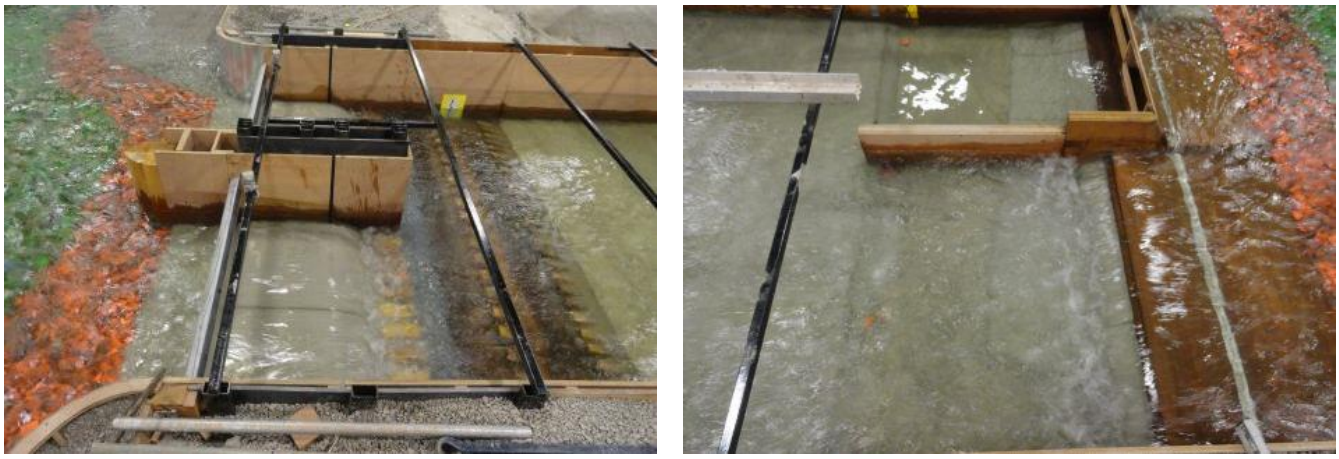

Figure 151. Flow conditions at the structure during the 320 m^3/s event. Top – facing southwest at the diversion, bottom - facing southeast at the service spillway.

The flow conditions through both the diversion inlet and the service spillway were relatively benign for the 320m^3/s flood condition. The flow depth through the diversion inlet and the chute blocks was shallow, and the hydraulic jump downstream of the LHS service spillway gate had little energy (see Figure 151). Debris was deployed at several points in the floodplain and tracked through the model (see Figure 150 for the insertion points and pathways). Table 27 shows a summary of the debris behaviour and performance of the structures in the model with pier nose 2 installed in the diversion. In general, the debris passed by the pier nose relatively unobstructed. However, there was often insufficient energy or depth to pass the debris over the chute blocks on the diversion inlet or through the hydraulic jump on the service spillway (see Figure 152). Of note, the tree debris stuck in the chute blocks in the diversion inlet often piled up where the diversion inlet gates would be closing, which may affect the gate operation (yellow arrow in Figure 152). At the end of the tests with the debris still caught in the structures, the LHS Obermeyer gate was raised to force all the flow through the diversion. The tree debris that was stuck in the hydraulic jump of the diversion inlet slowly floated down the channel, but the increased flow through the diversion inlet did not release the debris caught in the diversion inlet chute blocks.

Debris Type	Starting Location	Debris Pathways							Notes
		Debris Barrier	Pier Nose 2	Diversion LHS	Diversion RHS	Center Wall	Service Spillway LHS	Service Spillway RHS	
Singles	i	NA	-	100%	-	-	-	-	trees stuck in chute blocks
	ii	NA	-	-	50%	-	50%	-	trees stuck in chute blocks (Div) or waterfall (SS)
	iii	NA	-	-	50%	-	50%	-	trees stuck in chute blocks (Div) or waterfall (SS)
	iv	NA	-	-	-	-	100%	-	trees stuck in waterfall
	v	NA	-	-	-	-	100%	-	trees stuck in waterfall
	vi	NA	-	-	-	-	100%	-	trees stuck in waterfall
Rafts of 10	ii	NA	pause	-	100%	-	-	-	trees caught on chute blocks (blocking gates)
	iv	NA	-	-	80%	pause	20%	-	trees stuck in chute blocks (Div) or waterfall (SS)
	v	NA		-	-	-	100%	-	trees stuck in waterfall, knock other trees free

Table 27. Debris behaviour for 320 m^3/s with Pier Nose 2 installed in the diversion.

Figure 152. Debris caught in the structures during the 320m^3/s flow condition with pier nose 2.

5.4.4.2 Pier Nose 3

The flow conditions through the diversion inlet and service spillway were unchanged with pier nose 3 installed. As before, the flow depth through the diversion inlet and the chute blocks was shallow, and the hydraulic jump downstream of the LHS service spillway gate had little energy. Debris was inserted at several points in the floodplain and tracked through the model (see Figure 150 for the insertion points and pathways). Table 28 shows a summary of the debris behaviour and performance of the

structures in the model with pier nose 3 installed in the diversion. No debris was caught on the pier nose. As with the other 320m^3/s test, there was often insufficient energy to pass the debris over the chute blocks on the diversion, or fully through the hydraulic jump on the service spillway (see Figure 153). Of note, the tree debris stuck in the chute blocks in the diversion inlet often piled up where the diversion inlet gates would be closing, which may affect the gate operation (yellow arrow in Figure 153).

Debris Type	Starting Location	Debris Pathways							Notes
		Debris Barrier	Pier Nose 3	Diversion LHS	Diversion RHS	Center Wall	Service Spillway LHS	Service Spillway RHS	
Singles	ii	NA	-	50%	50%	-	50%	-	trees stuck in chute blocks
	iii	NA	-	-	-	-	100%	-	10% of trees stuck in waterfall
	iv	NA	-	-	-	50%	50%	-	trees stuck on center wall and in SS-LHS waterfall
	v	NA	-	-	-	-	100%	-	trees pass through the model
Rafts of 10	i	NA	-	100%	-	-	-	-	trees pause on chute blocks, then pass
	iii	NA	-	-		pause	100%	-	90% of trees stuck in waterfall
	iv	NA	-	-	90%	pause	10%	-	trees stuck in chute blocks (Div) or waterfall (SS)
	v	NA		-	-	-	100%	-	trees stuck in waterfall, knock other trees free
Rafts of 40	iv	NA	-	-	-	-	100%	-	10% stuck in waterfall
	v	NA	-	-	5%	3%	92%	-	8% of trees stuck in waterfall

Table 28. Debris behaviour for 320 m^3/s with Pier Nose 3 installed in the diversion.

Figure 153. Debris caught in the structures during the 320m^3/s flow condition with pier nose 3.

5.4.4.3 Pier Nose 3 and Debris Barrier D

Debris Barrier D was re-installed in the model (refer to section 3.4.3.4 for the design and layout of the barrier) and debris was inserted into the model floodplain (refer to Figure 150 for a schematic showing the debris insertion points and pathways). The debris barrier was loaded with approximately 80 trees and the diversion inlet gates were closed to investigate if the debris collected on the barrier

would drift off and pass through the service spillway. After closing the diversion inlet gates the debris did not immediately flush off the barrier. However, as more debris was added to the floodplain approximately 50% of the debris was eventually released from the barrier and flowed through the LHS of the service spillway (see Figure 154 and Table 29)

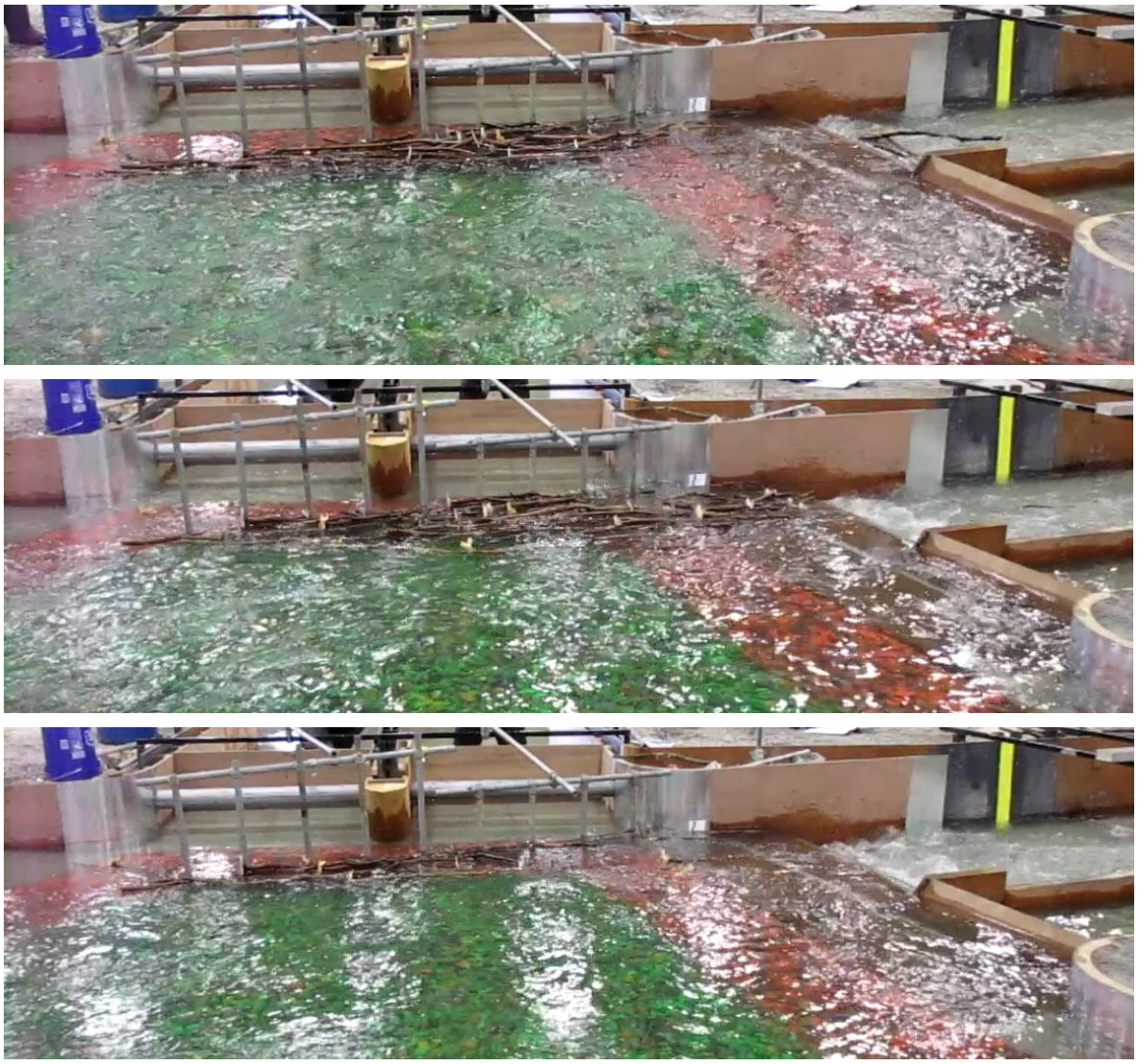

Figure 154. After closing the diversion inlet (top), and continuing to feed the upstream floodplain with trees (middle), 50% the debris caught on the debris barrier was eventually flushed through the service spillway (bottom).

Debris Type	Starting Location	Debris Pathways							Notes
		Debris Barrier D	Pier Nose 3	Diversion LHS	Diversion RHS	Center Wall	Service Spillway LHS	Service Spillway RHS	
Raft of ~80	On Debris Barrier D	50% remained	-	-	-	-	50%	-	A raft of 80 trees were placed on the barrier, the diversion gates were shut, 50% of the debris drifted off the barrier and passed through spillway

Table 29. Debris behaviour for 320 m^3/s with Pier Nose 3 and debris barrier D installed in the model.

5.4.4.4 Pier Nose 3 and Debris Barrier C

Debris Barrier C was re-installed in the model (refer to section 3.4.3.4 for the design and layout of the barrier) and debris was inserted into the model floodplain (refer to Figure 150 for a schematic showing the debris insertion points and pathways). The debris barrier was effective at blocking tree debris from the left-hand side of the floodplain (locations i, ii, iii, and iv), but debris placed at locations v, vi and vii bypassed the barrier and flowed into the service spillway. Figure 155 and Table 30 illustrate the debris behaviour and summarize the performance of the debris barrier for this flow rate.

Figure 155. Model trees collecting on debris barrier C during the 320m^3/s flow.

Debris Type	Starting Location	Debris Pathways							Notes
		Debris Barrier C	Pier Nose 3	Diversion LHS	Diversion RHS	Center Wall	Service Spillway LHS	Service Spillway RHS	
Singles	i-iv	100%	-	-	-	-	-	-	trees restrained by debris barrier
	v-vi	0%	-	-	-	-	100%	-	some trees caught in waterfall

Table 30. Debris behaviour for 320 m^3/s with Pier Nose 3 installed in the diversion.

5.5 Test Series E – Clear Water Tests

Clear water testing was performed on the model with the modified layout of the diversion inlet and service spillway (see Section 3.4.3.2 for the design modifications to these structures). Similar to the clear water tests in TSA, TSE focused on observing the flow characteristics within the model at five flow conditions (60 m^3/s, 160 m^3/s, 320 m^3/s, 760 m^3/s and 1240 m^3/s) without any debris or sediment, and used the full suite of water level gauges and velocity probes in the model. Note, pier nose 2 was installed on the diversion inlet pier for the TSE tests. The test program for TSE is shown in Table 8. The various gate settings prescribed by Stantec were intended to split the incoming flow down the diversion channel and service spillway such that target flows are met for each flood flow condition. The instrumentation within the model was laid out following Sensor Layout 5 as described in 3.5. Since the flow patterns and debris pathways for the modified service spillway and diversion inlet were well documented in TSD, drogues and coloured dye injections were not undertaken in this test series. A summary of the water level information gathered during the tests is presented in Table 31. Note, the water level information for the gauges is stated above the 1200m elevation - for example, an elevation of 11.30m in the table corresponds to a water level elevation of 1211.30m at that location.

Test Name	Target Q	Total Q	Div. Q	MC Q	Sensor layout	Diversion channel WL							Main Channel WL										Secondary Channel WL	
						6	7	17	10	12	13	Weir	1	16	4	8	9	18	11	14	15	Weir	2	5
	cms	cms	cms	cms		m	m	m	m	m	m	m	m	m	m	m	m	m	m	m	m	m	m	m
Clear water testing																								
E_60_1	60	68	-	68	5	11.30	11.26	11.61	11.58	11.55	11.56	11.55	13.24	11.97	11.03	11.11	11.10	11.05	10.73	10.61	10.63	10.62	13.09	12.48
E_160_1	160	160	-	160	5	12.07	12.04	11.64	11.61	11.58	11.59	11.59	13.59	12.15	11.77	11.78	11.80	11.71	11.18	11.23	11.26	11.24	13.66	12.49
E_320a_1	320	325	172	153	5	12.97	13.17	11.95	11.83	11.80	11.81	11.80	14.03	13.05	12.89	13.03	13.02	11.59	11.23	11.19	11.22	11.20	14.05	12.69
E_320a_2	320	327	174	154	5	12.99	13.17	11.96	11.84	11.80	11.83	11.81	14.04	12.95	12.92	13.04	13.04	11.60	11.24	11.19	11.22	11.21	14.06	12.71
E_320b_1	320	275	-	275	5	12.70	12.75	10.90	10.88	10.84	10.86	10.85	14.05	12.89	12.51	12.44	12.44	12.32	11.66	11.86	11.90	11.88	14.07	12.70
E_320b_2	320	276	-	276	5	12.71	12.76	10.90	10.88	10.84	10.86	10.85	14.05	12.88	12.52	12.45	12.44	12.32	11.71	11.86	11.90	11.88	14.07	12.70
E_760a_1	760	766	575	191	5	15.27	15.25	14.64	14.43	14.41	14.39	14.40	15.74	15.66	15.42	15.55	15.55	11.62	11.44	11.41	11.44	11.42	15.72	15.65
E_760b_1	760	710	-	710	5	14.99	14.67	11.90	11.87	11.84	11.85	11.85	15.23	15.07	14.57	14.24	14.17	13.46	12.55	12.74	12.78	12.76	15.18	15.05
E_1240a_1	1240	1275	607	668	5	15.45	15.43	14.76	14.56	14.54	14.51	14.53	16.05	15.84	15.42	15.22	15.34	13.19	12.38	12.71	12.71	12.71	15.99	15.82
E_1240b_1	1240	1286	611	675	5	15.43	15.38	14.78	14.58	14.55	14.53	14.54	16.03	15.81	15.37	15.51	14.87	13.38	12.35	12.72	12.75	12.74	15.97	15.80

Table 31. Water level summary for test series E clear water tests.

5.5.1 *60 m^3/s*

The gate configuration for the 60 m^3/s test was as follows:

- Diversion inlet gates were fully lowered (closed). Note: the diversion inlet gates were not installed as the water levels were not high enough to overtop the concrete crest.
- Left hand side service spillway Obermeyer gate – fully lowered (elev. 1210 m).
- Right hand side service spillway Obermeyer gate – fully lowered (elev. 1210 m).

The water levels recorded in the model for the 60 m^3/s flow condition are summarized in Table 31. All of the flow passed through the service spillway. The water levels upstream of the diversion inlet gates (measured at WP6 and WP7) were low enough that the water did not enter the structure (crest elevation 1211.5m). The water levels measured in and around the service spillway were reasonably close to those seen with the previous design (TSA) and the tail-water elevation of 1210.73 m

(measured at WP11) was reasonably close to the target tail-water elevation of 1210.50 m provided by the Stantec numerical model.

5.5.2 *160 m^3/s*

The gate configuration for the 160 m^3/s test was as follows:

- Diversion inlet gates were fully lowered (closed).
- Left hand side service spillway Obermeyer gate – fully lowered (elev. 1210 m).
- Right hand side service spillway Obermeyer gate – fully lowered (elev. 1210 m).

Figure 156. Diversion inlet structure (left) and service spillway (right) during the 160 m^3/s flow condition.

Similarly to the 60 m^3/s flow condition, the 160 m^3/s flow condition had all of the flow passing through the service spillway (refer to Table 31 for the flow splits and the water levels). Flow was blocked from travelling through the diversion channel by inserting wooden drop gates into each bay opening. The water levels in the service spillway (WP7 and WP8) were very close (11.78m and 11.80m). The tail-water elevation of 1211.18 m (WP11) was reasonably close to the target tail-water elevation of 1211.10 m provided by Stantec.

5.5.3 *320 m^3/s – Case (a), diversion inlet gates open.*

The gate configuration for the Case (a) 320 m^3/s test was as follows:

- Diversion inlet gates were fully raised (open).
- Left hand side service spillway Obermeyer gate set to 1211.05 m.
- Right hand side service spillway Obermeyer gate set to 1215 m.

Figure 157. Flow through the diversion inlet structure (left) and service spillway (right) during the 320 m^3/s case (a) flood condition.

The gate settings did a reasonable job of splitting the incoming 320 m^3/s flow between the diversion inlet and service spillway (172 m^3/s and 153 m^3/s, respectively). Refer to Table 31 for the flow splits and the water level measurements made in the model. As was seen in TSA, there was a slightly uneven flow distribution through the diversion inlet gate bays with the RHS seeing higher water levels (1213.17 m vs 1212.97 m). The tail-water elevation of 1211.83 m (WP10) in the diversion channel closely matched the target tail-water elevation provided by Stantec of 1211.80 m. Similarly, the service spillway tail-water elevation of 1211.23 m (WP11) was reasonably close to the target 1211.1 m, and the flow through the service spillway was evenly distributed between the LHS and RHS.

5.5.4 *320 m3/s – Case (b), diversion inlet gates closed.*

The gate configuration for the Case (b) 320 m^3/s test was as follows:

- Diversion inlet gates were fully lowered (closed).
- Left hand side service spillway Obermeyer gate set to 1210 m.
- Right hand side service spillway Obermeyer gate set to 1210 m.

Figure 158. Flow through the service spillway during the 320 m^3/s case (b) flood condition with the diversion inlet closed.

The flow through the service spillway was fairly evenly distributed between the RHS and LHS as the water levels measured at the structure were 1212.44 m and 1212.45 m, respectively. Closing the diversion inlet gates raised the tail-water elevation downstream of the service spillway by 0.48 m to 1211.7 m.

5.5.5 *760 m^3/s – Case (a), diversion inlet gates open.*

The gate configuration for the Case (a) 760 m^3/s test was as follows:

- Diversion inlet gates were fully raised (open).
- Left hand side service spillway Obermeyer gate set to 1213.4 m.
- Right hand side service spillway Obermeyer gate set to 1215 m.

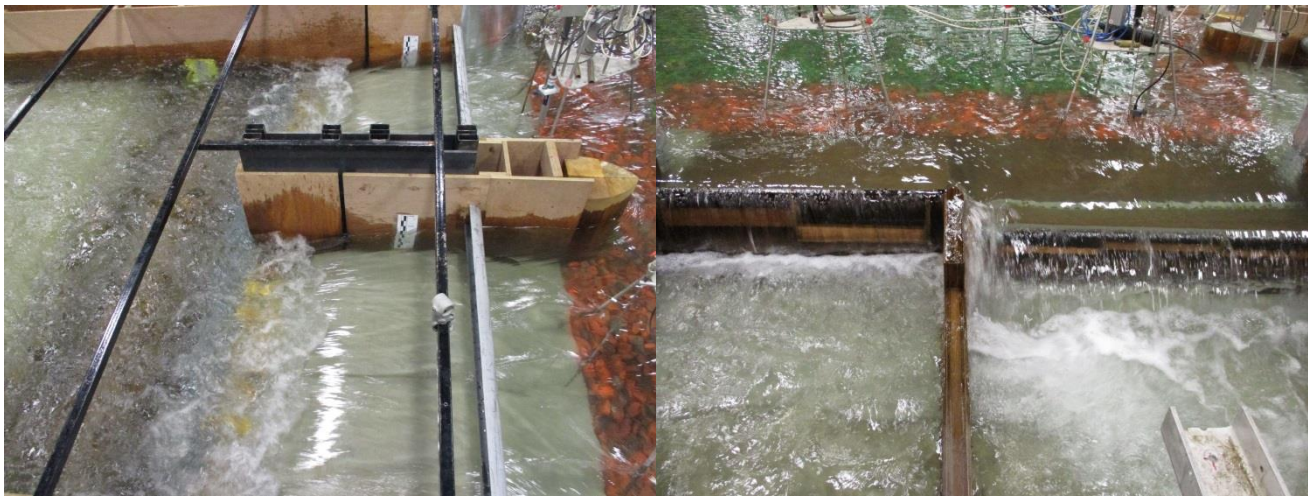

Figure 159. Flow through the diversion inlet structure (left) and service spillway (right) during the 760 m^3/s case (a) flood condition.

The target flow split for the 760 m^3/s flow condition is to have 600 m^3/s in the diversion channel and 160 m^3/s in the main channel. The gate settings provided by Stantec provided a flow split that reasonable matched the targets; the recorded flow over the diversion channel weir was 575 m^3/s and the recorded flow over the main channel weir was 191 m^3/s (the total flow was 766 m^3/s - refer to Table 31 for the flow splits and the water levels). The head at the upstream end of the each bay of the diversion inlet (WP6 and WP7) were very even between the LHS and RHS (1215.27 m and 1215.25 m). This was also the case upstream of the service spillway (WP8 and WP9 each read 1215.55 m). The flow barely crested the RHS crest gate on the service spillway (elevation 1215 m).

5.5.6 *760 m^3/s – Case (b), diversion inlet gates closed.*

The gate configuration for the Case (b) 760 m^3/s test was as follows:

- Diversion inlet gates were fully lowered (closed).
- Left hand side service spillway Obermeyer gate set to 1210 m.
- Right hand side service spillway Obermeyer gate set to 1210 m.

As described in Section 5.4.2, with the diversion inlet gate closed the 760 m^3/s flow through the service spillway was fairly energetic and turbulent (see Figure 160). The hydraulic jumps on both the LHS and RHS were influenced by the wakes emanating from the circular abutment wall on the RHS and the central dividing pier on the LHS. Figure 161 shows the relatively unstable hydraulic jump on the RHS with a closer look at the depth of the wake stemming from the RHS circular abutment wall at the entrance of the structure. Table 31 presents the water level information for the various gauges. This data shows slightly more head on the LHS (WP8 – 1214.24 m) than on the RHS (WP9 – 1214.17 m) of the service spillway. The currents downstream of the service spillway were observed to be relatively higher along the training wall on the LHS indicating a potential for scour and erosion at this location.

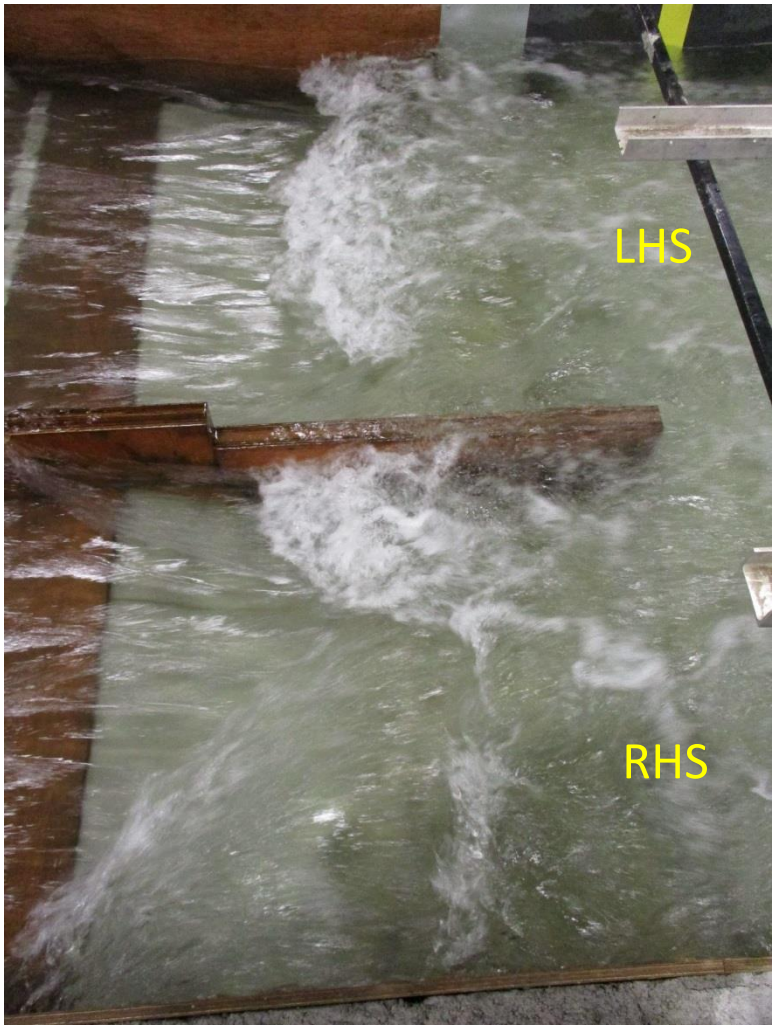

Figure 160. Flow through the service spillway (right) during the 760 m^3/s case (b) flood condition with the diversion inlet closed.

Figure 161. Flow through the diversion inlet structure (left) and service spillway (right) during the 760 m^3/s case (b) flood condition.

5.5.7 *1240 m^3/s – Case (a)*

The gate configuration for the Case (a) 1240 m^3/s test was as follows:

- Diversion inlet gates were fully raised (open).
- Left hand side service spillway Obermeyer gate set to 1210 m.
- Right hand side service spillway Obermeyer gate set to 1213.15 m.

Figure 162. Flow through the diversion inlet structure (left) and service spillway (right) during the 1240m^3/s case (a) flood condition.

The target flow split for the 1240 m^3/s flow condition sent 600 m^3/s through the diversion channel and 640 m^3/s through the main channel service spillway. The gate settings provided by Stantec provided a flow split that matched the targets very well; the recorded flow over the diversion channel weir was 607 m^3/s and the recorded flow over the main channel weir was 668 m^3/s (the total flow was 1275 m^3/s - refer to Table 31 for the flow splits and the water levels). The water level in the LHS of the service spillway (WP8) was slightly lower compared to the right hand side (WP9), while the water levels were relatively even across the diversion inlet structure. The flow through the diversion inlet appeared to be relatively even and the hydraulic jump was stable (see the left hand side of Figure 162). In the service spillway there was much more flow through the LHS since the Obermeyer gates were lower leading to relatively higher velocities than the RHS. The hydraulic jump was influenced by the wake stemming from the central pier between the service gates (see the right side

of Figure 162). High velocities were observed along the LHS training wall of the service spillway indicating the potential for erosion or scour at this location. The modification to the RHS retaining wall, changing the plan shape to a circular design, showed an improvement on the entrance flows over the straight wall design used in test series A-C (see Figure 163).

Figure 163. Wakes generated by the retaining wall on the RHS of the service spillway – left: straight wall of the initial design, right – circular design for TSD-H.

5.5.8 *1240 m^3/s – Case (b)*

The gate configuration for the Case (b) 1240 m^3/s test was as follows:

- Diversion inlet gates were fully raised (open).
- Left hand side service spillway Obermeyer gate set to 1212.57 m.
- Right hand side service spillway Obermeyer gate set to 1210 m.

The target flow split for the 1240 m^3/s flow condition is to have 600 m^3/s in the diversion channel and 640 m^3/s in the main channel. For this test case the gate settings provided by Stantec provided a flow split that matched the targets very well; the recorded flow over the diversion channel weir was 611 m^3/s and the recorded flow over the main channel weir was 675 m^3/s (the total flow was 1286 m^3/s - refer to Table 31 for the flow splits and the water levels). Again, the water level in the LHS of the service spillway (WP8) is slightly lower compared to the RHS (WP9), while the water levels were relatively even across the diversion inlet structure (WP's 6 and 7). The flow through the diversion inlet bays appeared to be relatively even and the hydraulic jump was stable (see the left hand side of Figure 164). In the service spillway there was more flow through the RHS since the Obermeyer gates were lower here. The hydraulic jump was influenced by the wake stemming from the circular retaining wall (see the right side of Figure 164). Again, modifying the RHS retaining wall to a circular design showed an improvement on the entrance flows. The wake from this retaining wall is shown in Figure 165, along with the wake stemming from the pier nose in the diversion.

Figure 164. Flow through the diversion inlet structure (left) and service spillway (right) during the 1240 m^3/s case (b) flood condition.

Figure 165. Wakes generated by the retaining wall on the RHS of the service spillway (left), and the RHS of the diversion inlet stemming from pier nose 2 (right).

5.6 Test Series F – Rating Curves

Test series F investigated the water level elevation at the upstream end of the service spillway for various flows and settings on the Obermeyer gates. Rating curves were developed that relate the water level elevation (stage) to the flow discharge for an array of gate settings. Both of the Obermeyer gates on the left and right side of the service spillway were set to the same elevation for each test. The instruments were arranged in Sensor Layout 5 and their location can be seen in Figure 77. Only the flow over the service spillway was of interest during this test series, therefore the diversion inlet gates were closed. The data measured by the water level probes just upstream of the service spillway were used (WP8 and WP9) and their rating curve information is given in Table 32 and Figure 166. Note that the water level information is given in metres above the 1200m elevation, therefore a water level of 11.94m corresponds to a water level elevation of 1211.94m.

Test Name	Spillway Flow Q	WP8	WP9
	cms	m	m
Gates at 1211.05m			
F_60_1211_1	75	11.94	11.92
F_180_1211_1	181	12.71	12.67
F_320_1211_1	313	13.47	13.39
F_480_1211_1	464	14.12	14.01
F_640_1211_1	624	14.56	14.56
F_1000_1211_2	894	15.46	15.35
Gates at 1212m			
F_60_1212_1	72	12.79	12.78
F_180_1212_1	180	13.59	13.54
F_320_1212_1	313	14.35	14.28
F_480_1212_1	455	14.99	14.85
F_640_1212_1	694	15.85	15.82
Gates at 1213.15m			
F_60_1213p15_1	63	13.75	13.73
F_180_1213_1	161	14.50	14.48
F_320_1213_1	281	15.22	15.18
F_480_1213_2	436	15.86	15.83
Gates at 1214m			
F_60_1214_2	46	14.35	14.33
F_180_1214_1	139	15.18	15.15
F_320_1214_1	263	15.90	15.85
F_480_1214_1	332	16.21	16.17
Gates at 1215m			
F_180_1215_1	99	15.87	15.85
F_60_1215_1	44	15.37	15.36

Table 32. Rating curve data for the service spillway Obermeyer gates. Note the water level probe information is given in elevation above 1200m.

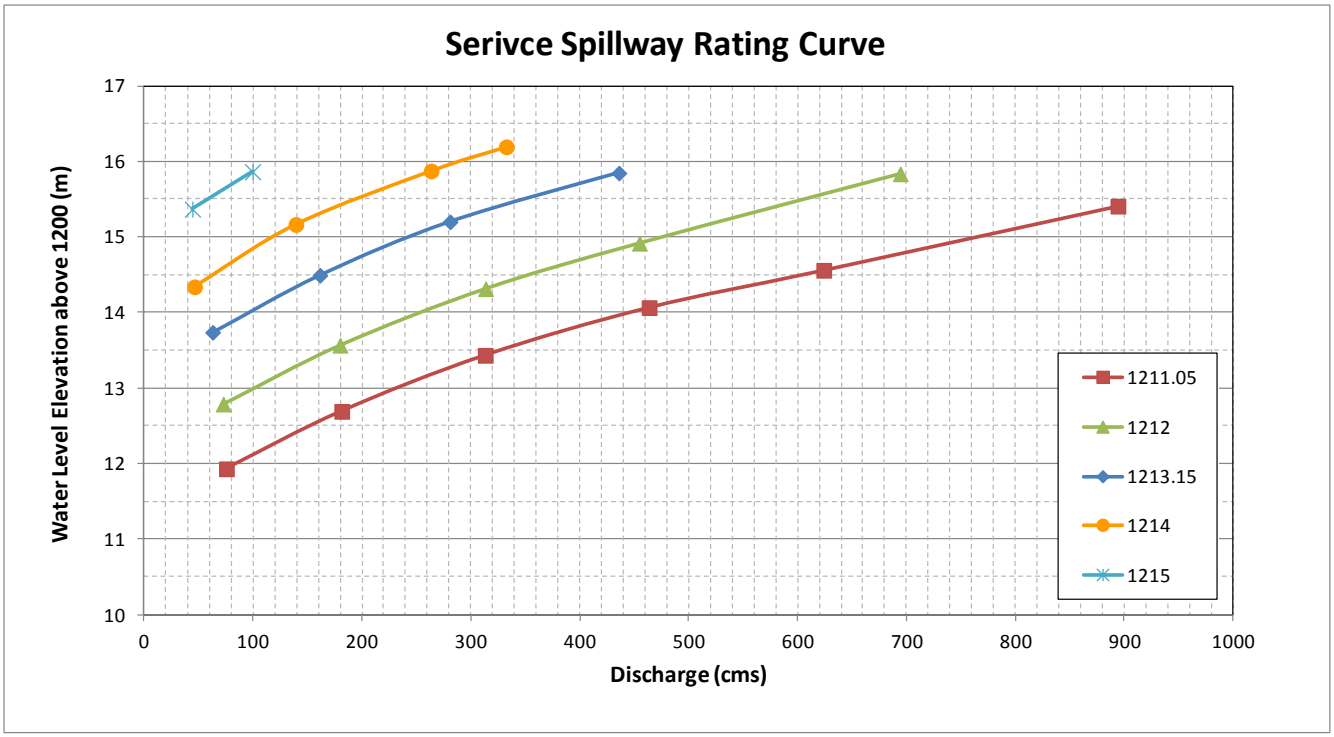

Figure 166. Rating curves for the service spillway Obermeyer gates - upstream water level elevation versus discharge for the various gate setting elevations.

5.7 Test Series G

Test series G (TSG) focused on testing the revised designs for the diversion inlet and service spillway with a large debris barrier installed in the upstream floodplain. Debris barrier E was much longer than any of the previous debris barriers as it extended approximately 175m upstream of the diversion inlet structure (refer to Section 3.4.3.4 for a full description of its design). The test program for TSG is shown in Table 10. The Obermeyer gate settings were prescribed by Stantec and intended to direct a target flow through the diversion inlet and service spillway channels based on a given upstream flood flow condition. As in previous debris test series, model tree debris was added at specific points in the floodplain in combination of single debris loads, or rafts of 4, 10, and 40 trees. The fate of the debris was tracked thorough the model via overhead video camera, overhead time-lapse still photography, and profile view video cameras. Pier nose 3 was installed on the model diversion inlet for all TSG tests.

5.7.1 *320 m^3/s*

The gate settings for the 320m^3/s flow utilized the diversion inlet gate in the fully raised position, and the service spillway Obermeyer gates set to 1211.05m on the 24m wide left-hand side (LHS) and 1215m on the 18m wide right-hand side (RHS). The setting was intended to direct 160m^3/s through the service spillway and 160m^3/s through the diversion. Again, model tree debris was inserted into the model in one of seven locations (1-7) as shown in Figure 167 during the tests. Table 33 shows a summary of the debris behaviour at this flow condition. For ease of description, debris barrier E was

divided into legs AB, BC and CD as shown in the figure. Debris inserted into the left hand side of the western floodplain (locations 1 and 2) collected on leg AB and the debris tended to tumble along the barrier coming to rest at point B. Here, debris would collect and protrude out into the river beyond point B. When larger rafts of trees originated at location 2 the debris rafts bridged across from the debris barrier (at point B) to the standing forest in the floodplain, thus blocking the river channel (see Figure 168). At the end of the tests at 320m^3/s, there was some debris caught in the barrier on leg AB, but legs BC and CD were clear of debris. In general the debris from locations 3-7 would pass through the LHS of the service spillway. Some of the single debris entries would remain caught in the hydraulic jump beyond the service spillway gate, but this debris would eventually be knocked downstream by later debris passing over the crest gates. Large rafts of debris tended to pass all the way through the structure and not hang at the hydraulic jump.

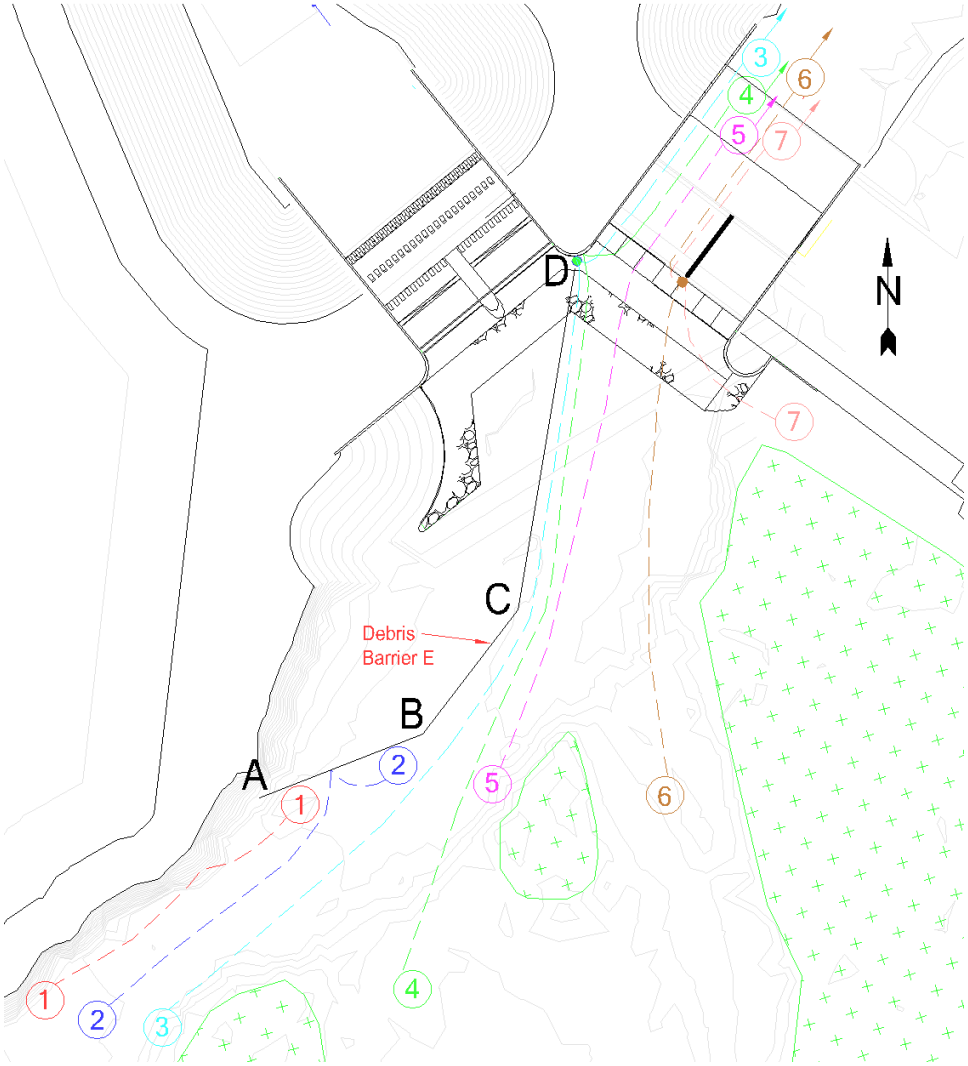

Figure 167. Debris pathways for TSG, 320 m^3/s flow conditions with debris barrier E.

Debris Type	Starting Location	Debris Pathways					Notes
		Debris Barrier E Leg AB	Debris Barrier E Leg BC	Debris Barrier E Leg CD	Service Spillway LHS	Service Spillway RHS	
Singles	1	100%	-	-	-	-	Caught in leg AB
	2	100%	-	-	-	-	Caught in leg AB, extending past point B into river
	3	-	-	-	100%	-	25% stuck in hydraulic jump
	4	-	-	-	100%	-	25% stuck in hydraulic jump
	5	-	-	-	100%	-	50% stuck in hydraulic jump
	6	-	-	-	100%	-	50% stuck in hydraulic jump
	7	-	-	-	100%	-	25% stuck in hydraulic jump, knock others through
Rafts of 10	1	100%	-	-	-	-	Caught in leg AB and on river floor
	2	100%	-	-	-	-	Caught in leg AB, extending past point B into river
	5	-	-	-	100%	-	50% stuck in hydraulic jump
	6	NA	-	-	100%	-	trees cleared out those stuck in hydraulic jump
Rafts of 40	2	50%	-		50%	-	10% stuck in hydraulic jump
	6	-	-	-	100%	-	trees pass through

Table 33. Debris behaviour for 320 m^3/s with debris barrier E installed in the upstream floodplain.

Figure 168. Debris being caught on the barrier and protruding out into the river (left), and this phenomenon continuing to bridge across the river against the standing trees producing a jam (right).

5.7.2 *760 m^3/s*

The gate settings for the 760m^3/s flow utilized the diversion inlet gate in the fully raised position, and the service spillway Obermeyer gates set to 1213.4m on the 24m wide left-hand side (LHS) and 1215m on the 18m wide right-hand side (RHS). The setting was intended to direct 160m^3/s through the service spillway and 600m^3/s through the diversion. Again, model tree debris was inserted into the model in one of seven locations (1-7) as shown in Figure 169 during the tests. Table 34 shows a summary of the debris behaviour at this flow condition. The relatively larger amount of flow passing through the diversion inlet (and through the barrier) compared to that passing through the service spillway drew the woody debris into the debris barrier much more than the other flow conditions. Debris originating from the left hand side of the western floodplain (locations 1, 2 and 3) collected on barrier leg AB. On almost the entire floodplain the debris was sucked into and pinned up against the debris barrier by the flow being directed into the diversion. Only debris inserted in the model near the floodplain berm at the RHS of the service spillway (location 7) had a significant portion pass

through the service spillway. At the end of the tests much debris remained on the barrier on all three legs (see Figure 170).

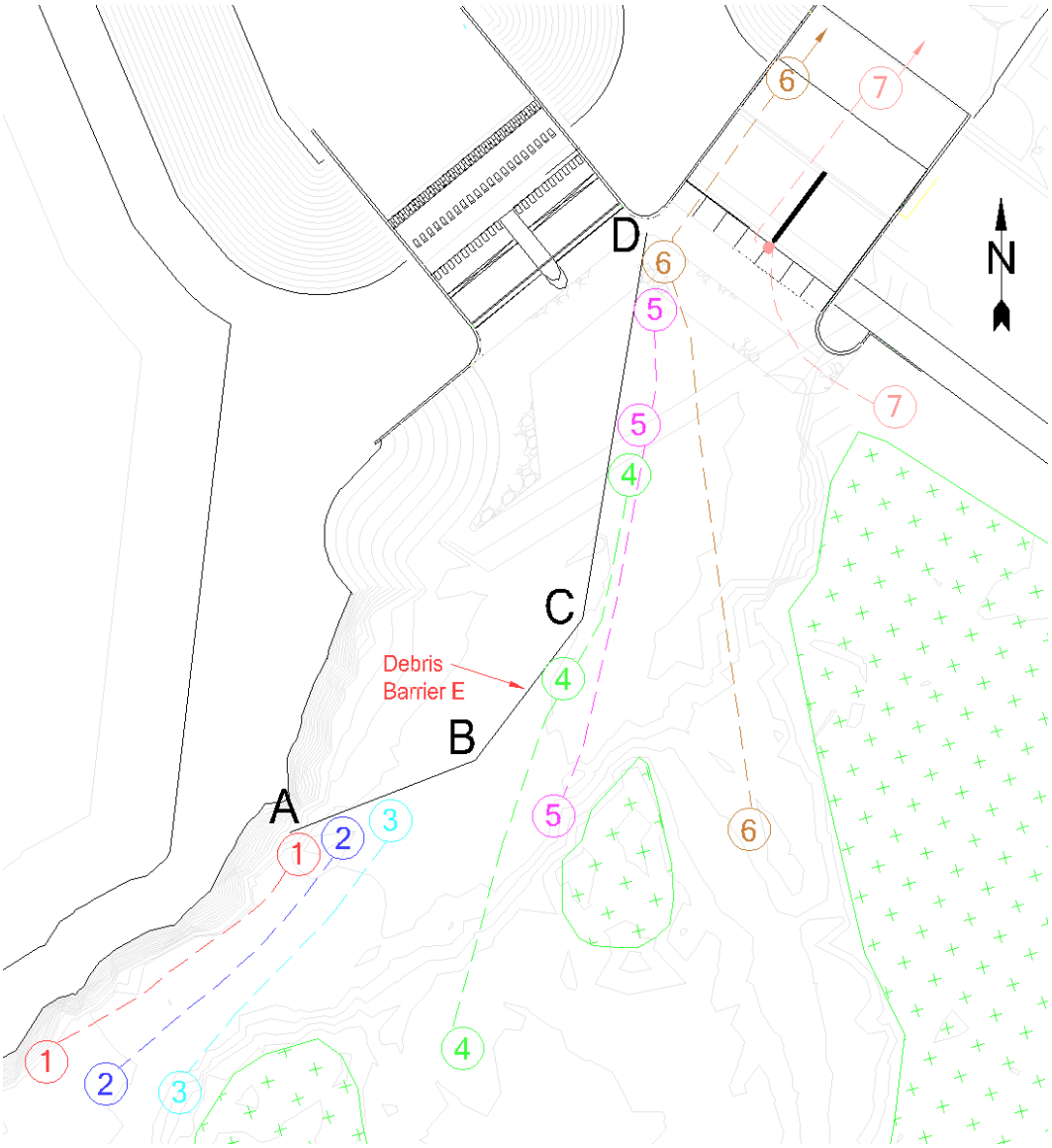

Figure 169. Debris pathways for TSG, 760 m^3/s flow conditions with debris barrier E.

Debris Type	Starting Location	Debris Pathways					Notes
		Debris Barrier E Leg AB	Debris Barrier E Leg BC	Debris Barrier E Leg CD	Service Spillway LHS	Service Spillway RHS	
Singles	1	100%	-	-	-	-	Caught in leg AB
	2	100%	-	-	-	-	Caught in leg AB
	3	100%	-	-	-	-	Caught in leg AB
	4	-	75%	25%	-	-	Caught in leg BC and CD
	5	-	-	75%	25%	-	25% stuck in hydraulic jump, knock others through
	6	-	-	50%	50%	-	50% stuck in hydraulic jump, knock others through
	7	-	-	-	100%	-	25% stuck in hydraulic jump, knock others through
Rafts of 10	1	100%	-	-	-	-	Caught in leg AB
	2	100%	-	-	-	-	Caught in leg AB, extending past point B into river
	4	-	100%	-	-	-	Caught in leg BC
	5	-	-	100%	-	-	10% stuck in hydraulic jump
	6	-	-	25%	75%	-	25% stuck in hydraulic jump
	7	-	-	-	100%	-	40% stuck in hydraulic jump
Rafts of 40	2	100%	-		-	-	Caught in leg AB
	4	-	-	-	100%	-	Pulled some of the trees off the barriers at BC
	6	-	-	75%	25%	-	25% of trees pass through

Table 34. Debris behaviour for 760 m^3/s with Pier Nose 3 installed in the diversion.

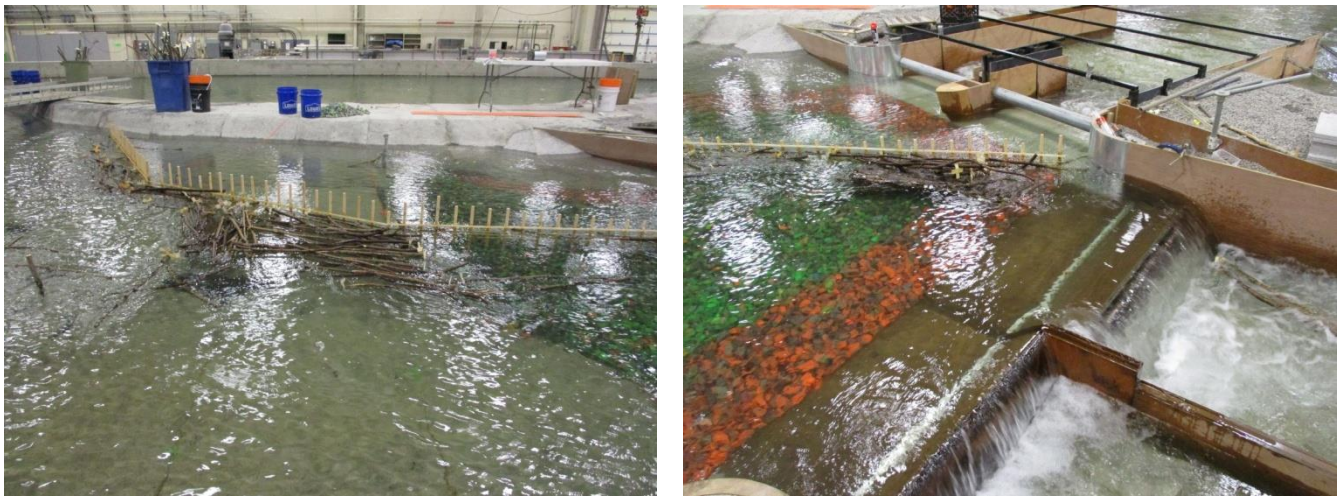

Figure 170. Debris left on barrier at the end of the 760m^3/s tests for leg AB and BC (left) and at the end of the barrier on leg CD (right).

5.7.3 *1240 m^3/s*

The gate settings for the 1240m^3/s flow utilized the diversion inlet gate in the fully raised position, and the service spillway Obermeyer gates set to 1210m on the 24m wide left-hand side (LHS) and 1213.5m on the 18m wide right-hand side (RHS). The setting was intended to direct 640m^3/s through the service spillway and 600m^3/s through the diversion. Model tree debris was inserted into the model in one of seven locations (1-7) as shown in Figure 171 during the tests. Table 33 shows a summary of the debris behaviour at this flow condition. Again, for ease of description, debris barrier E was divided into legs AB, BC and CD. Debris inserted into the left hand side of the western floodplain (locations 1 to 4) collected on leg AB and along this leg debris tended to tumble along the barrier to point B and extended into the river. When larger rafts of trees originated at location 4 the debris rafts bridged across from the debris barrier (at point B) to the standing forest in the floodplain,

thus blocking the river channel (see Figure 172, left). At the end of the tests at 1240m^3/s, there was debris caught in the barrier at the B and C vertices (see Figure 172, right). The model tree debris rafts ran along the straight legs of the barrier and then became trapped as the raft pivoted around the corners at points B and C. Leg CD was clear of model debris at the end of the tests.

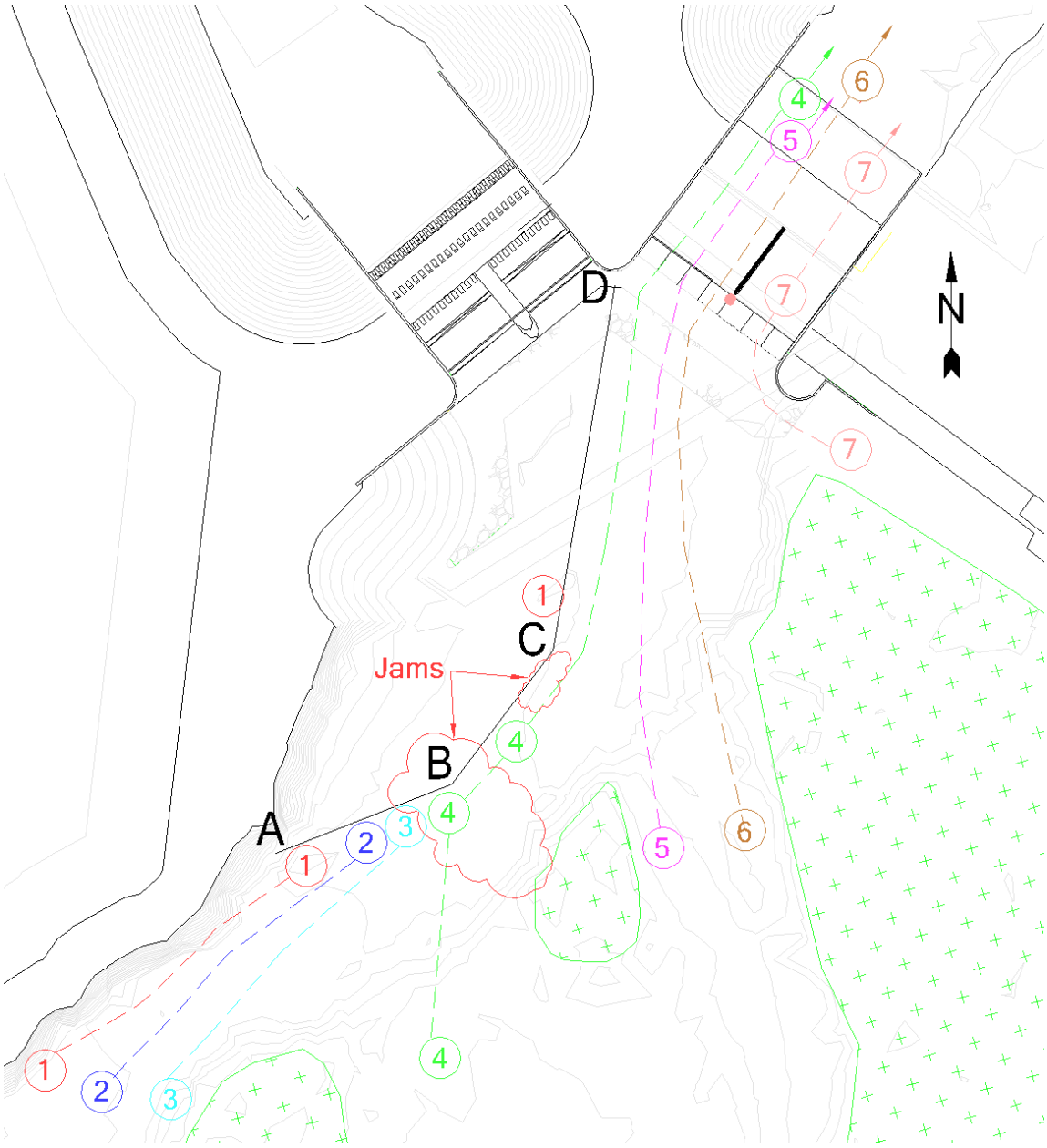

Figure 171. Debris pathways for TSG, 1240 m^3/s flow conditions with debris barrier E.

Debris Type	Starting Location	Debris Pathways					Notes
		Debris Barrier E Leg AB	Debris Barrier E Leg BC	Debris Barrier E Leg CD	Service Spillway LHS	Service Spillway RHS	
Singles	1	100%	-	-	-	-	Caught in leg AB
	2	100%	-	-	-	-	Caught in leg AB
	3	100%	-	-	-	-	Caught in leg AB
	4	50%	50%	-	-	-	Caught in leg AB and BC
	5	-	-	-	100%	-	Trees pass through
	6	-	-	-	100%	-	Trees pass through
	7	-	-	-	-	100%	Trees pass through
Rafts of 10	1	100%	-	-	-	-	Caught in leg AB
	2	100%	-	-	-	-	Caught in leg AB
	4	-	-	20%	80%	-	80% pass through the spillway
	5	-	-	-	100%	-	Trees pass through
	6	-	-	-	100%	-	Trees pass through
	7	-	-	-	50%	50%	50% stuck on pier divider, 50% pass through the spillway
Rafts of 40	2	100%	-		-	-	Caught in leg AB
	4	35%	-	-	65%	-	Trees bridge across barrier to the stand of trees in the floodplain, jam
	6	-	-	-	100%	-	100% of trees pass through

Table 35. Debris behaviour for 1240 m^3/s with debris barrier E installed in the upstream floodplain.

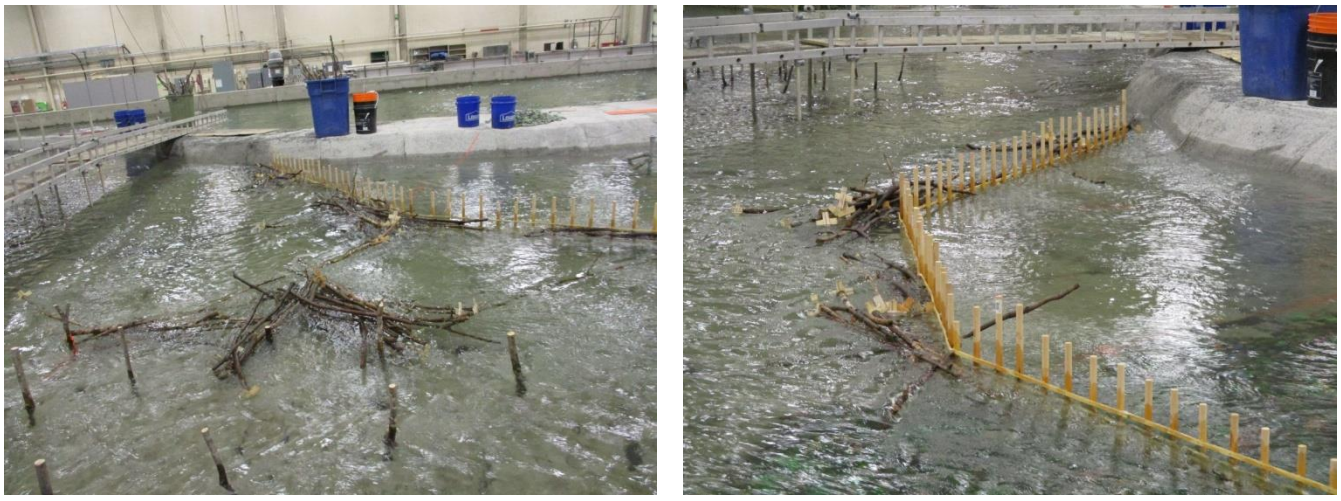

Figure 172. Left - Debris being caught on the barrier and protruding out into the river and this phenomenon continuing to bridge across the river against the standing trees producing a jam. Right – debris trapped in the barrier at the end of the tests.

5.8 Test Series H

Test series H (TSH) revised the upstream debris barrier tested in TSG by having the plan-shape remain closer to the left hand side of the river (and not protrude out into the river channel flow as much). Also, additional horizontal guide rails were added to tighten the spacing to every 0.5m from 1213m to 1216m (refer to Section 3.4.3.4 for a full description of the design). The test program for TSH is shown in Table 11. The Obermeyer gate settings were prescribed by Stantec and intended to direct a target flow down the diversion inlet and service spillway channels based on a given flood flow condition. The procedure for each of the debris tests was similar – model tree debris was added at specific points in the floodplain in combination of single debris loads, or rafts of 2, 10, and 40 trees.

The fate of the debris was tracked thorough the model via overhead video camera, overhead time-lapse still photography, and profile view video cameras. Pier nose 3 was installed on the model diversion inlet for all tests.

5.8.1 *320 m^3/s*

The gate settings for the 320m^3/s flow utilized the diversion inlet gate in the fully raised position, and the service spillway Obermeyer gates set to 1211.05m on the 24m wide left-hand side (LHS) and 1215m on the 18m wide right-hand side (RHS). These settings were intended to direct 160m^3/s through the service spillway and 160m^3/s through the diversion, which was close to the measurements made in the model (178m^3/s in the diversion and 142m^3/s through the main channel). Again, model tree debris was inserted into the model in one of seven locations (1-7) as shown in Figure 173 during the tests. Table 36 shows a summary of the debris behaviour at this flow condition. For ease of description, debris barrier E was divided into legs AB, BC and CD. Debris inserted into the left hand side of the western floodplain (locations 1 and 2) bounced along leg AB before coming to rest close to point B. At other debris deployment locations, the model trees would often catch in the debris barrier at leg CD. During the deployment of the rafts of ten debris units, the trees bridged across from the barrier and jammed at the LHS of the service spillway. This jam did not permit the passage of any further debris causing a larger jam by the end of the tests at this flow rate (see Figure 174).

At the end of the debris tests, with the large debris raft (~130 trees) caught in front of the diversion inlet and service spillway, efforts were made to drop the diversion inlet gates as well as the LHS Obermeyer gate to try and clear the debris from the barrier. The diversion inlet gates were lowered first and the Obermeyer gate second and 5-10 trees drifted off the jam at the barrier and they passed through the LHS. Another diversion inlet gate raise/lowering sequence removed another 10 trees from the barrier. The diversion inlet gates were then raised and the LHS Obermeyer gate was raised to allow some backwater head to build up in front of the service spillway. The diversion inlet gates were then closed and the LHS Obermeyer gate lowered and the entire jam of trees caught was pulsed off the debris barrier and the trees passed through the LHS of the service spillway. However, the rate of closure of the diversion inlet gates was likely much quicker than that which could be performed in the prototype. This rapid gate closure led to a wave emanating from the gates that dynamically removed debris from the barrier. Later in TSH sensitivity tests were performed to investigate the effects of lower diversion inlet gate closure rates on clearing the debris jams at the barrier.

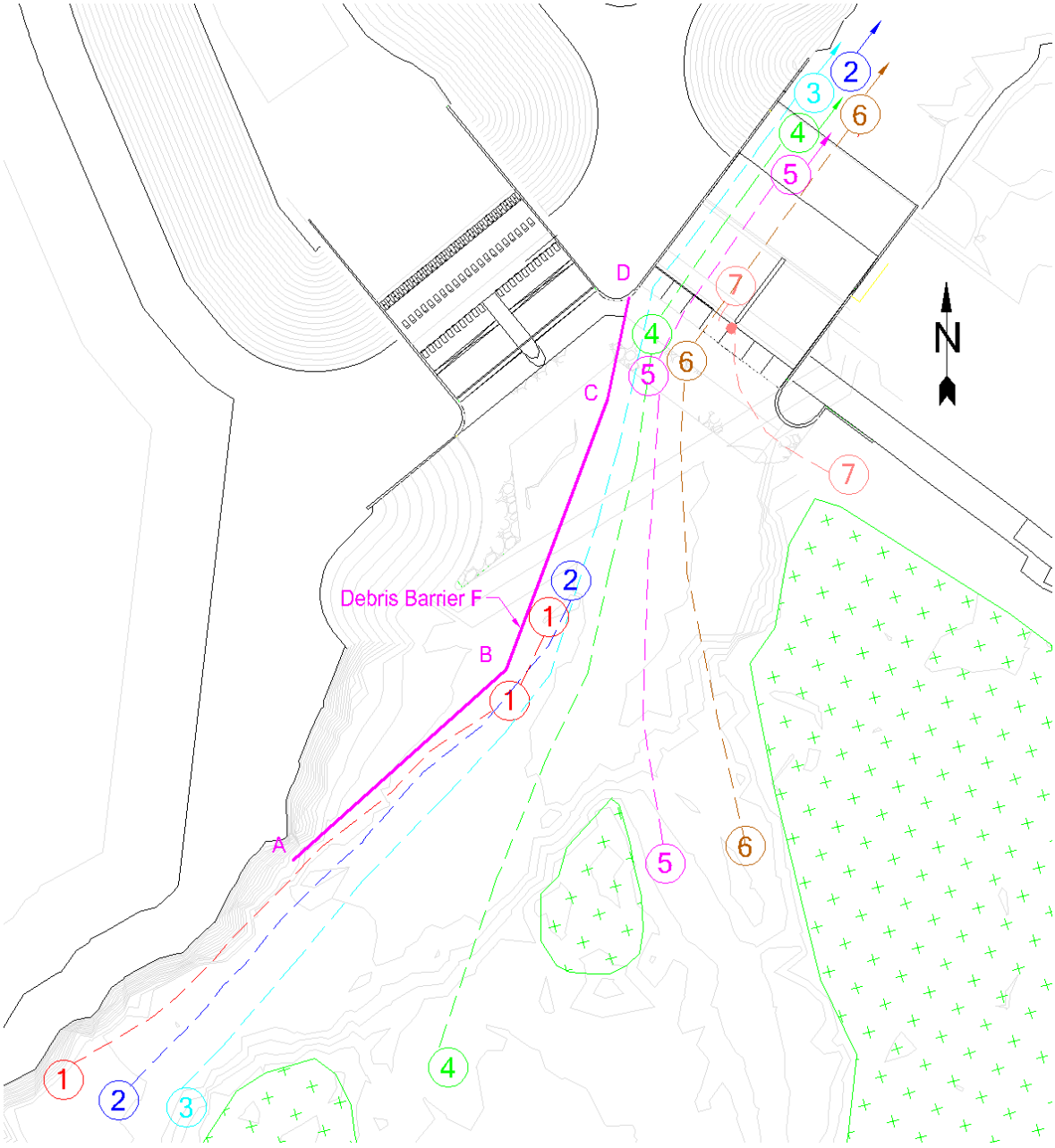

Figure 173. Debris pathways for TSH, 320 m^3/s flow conditions with debris barrier F.

Debris Type	Starting Location	Debris Pathways					Notes
		Debris Barrier F Leg AB	Debris Barrier F Leg BC	Debris Barrier F Leg CD	Service Spillway LHS	Service Spillway RHS	
Singles	1	100%	-	-	-	-	50% caught in leg AB, 50% pass through
	2	-	50%	-	50%	-	50% caught in leg BC, 50% pass through
	3	-	-	50%	50%	-	50% caught in the hydraulic jump
	4	-	-	100%	-	-	Caught in leg CD
	5	-	-		100%	-	50% stuck in hydraulic jump
	6	-	-		100%	-	50% stuck in hydraulic jump
	7	-	-		100%	-	50% stuck in hydraulic jump
Rafts of 10	1	-	10%	-	90%	-	Debris that passes clears out those caught in the hydraulic jump
	2	-	10%	30%	60%	-	Debris that passes clears out those caught in the hydraulic jump
	4	-	-	50%	50%	-	Those caught in the barrier bridge across the SS-LHS - raft jam
	5	-	-	90%	10%	-	Caught in the debris jam at the Service Spillway
	6	-	-	100%	-	-	Caught in the debris jam at the Service Spillway
Rafts of 40	2	-	-	100%	-	-	Caught in the debris jam at the Service Spillway
	4	-	-	100%	-	-	Caught in the debris jam at the Service Spillway
	6	-	-	100%	-	-	Caught in the debris jam at the Service Spillway

Table 36. Debris behaviour for 320 m^3/s with debris barrier F installed in the upstream floodplain.

Figure 174. Debris being caught at the downstream end of the barrier and bridging across the LHS of the service spillway to start a jam (left), and the jam building through the testing program (right).

5.8.2 *500 m^3/s*

There were two tests with different gate settings for the 500m^3/s flow conditions. Case (a) had the RHS Obermeyer gate raised, and case (b) had the LHS Obermeyer gate raised.

5.8.2.1 Case a – Obermeyer gates set to 1212m (LHS) and 1215m (RHS)

The case (a) gate settings for the 500m^3/s flow utilized the diversion inlet gate in the fully raised position, and the service spillway Obermeyer gates set to 1212m on the 24m wide left-hand side (LHS) and 1215m on the 18m wide right-hand side (RHS). The total flow through the river floodplain was 516m^3/s and the flow splits through the diversion inlet and the service spillway were 331m^3/s and 185m^3/s, respectively. Again, model tree debris was inserted into the model in one of seven locations (1-7) as shown in Figure 175 during the tests. Table 37 shows a summary of the debris behaviour at

this flow condition. For ease of description, debris barrier F was divided into legs AB, BC and CD. Debris inserted into the left hand side of the western floodplain (locations 1 to 4) was trapped on the barrier along leg AB and created a debris jam at point B. Some of the debris in the jam eventually drifted off and collected on the barrier at the downstream end (leg CD). At other debris deployment locations, the model trees would often catch in the debris barrier at leg CD, and a second debris jam was created in front of the LHS of the service spillway (see Figure 176).

At the end of the tests, the upstream debris jam consisted of approximately 90 trees (see Figure 176, left) and the downstream jam was slightly smaller (~ 35 trees - see Figure 176, right). Gate operations were undertaken to try and remove the trees from the barrier. Initially the LHS Obermeyer gate was lowered to 1210m and this removed approximately 20 of the 35 trees from the jam close to the diversion inlet and passed them through the LHS of the service spillway. The diversion inlet gates were then closed and the other 15 trees drifted off the debris barrier and through the LHS as well. As the backwater effect raised the water level in the upstream floodplain, the large raft at Point B on the barrier moved slightly downstream and away from the barrier. The diversion inlet gates were then opened and approximately 60% of this jam floated downstream and through the LHS of the service spillway.

An observation was made that the rate of the diversion inlet gate closure in the model was likely faster than what could be achieved in the prototype, and this rapid closure created a relatively short wave that can more effectively pulse the debris from the barrier. A separate test was commissioned where a debris jam (roughly 40 trees) was allowed to form at the downstream end of the barrier (in front of the diversion inlet at leg CD) and the diversion inlet gates were lowered at rate specified by Stantec (0.3m per minute, full scale) which represented typical drop gate closure rates. The pulsing wave emanating from the rapid diversion inlet gate closure that was observed in the previous tests did not form. After approximately 8mins (full scale) the debris jam at the downstream end of the barrier was dislodged and flowed over the LHS Obermeyer gate. The LHS gate was still at 1212m elevation when the debris was passed. The debris that had collected further upstream in the barrier (on leg A B) was not dislodged when the diversion inlet gates were closed. The LHS Obermeyer gate was lowered to 1210m and this debris jammed still remained on the barrier at point B.

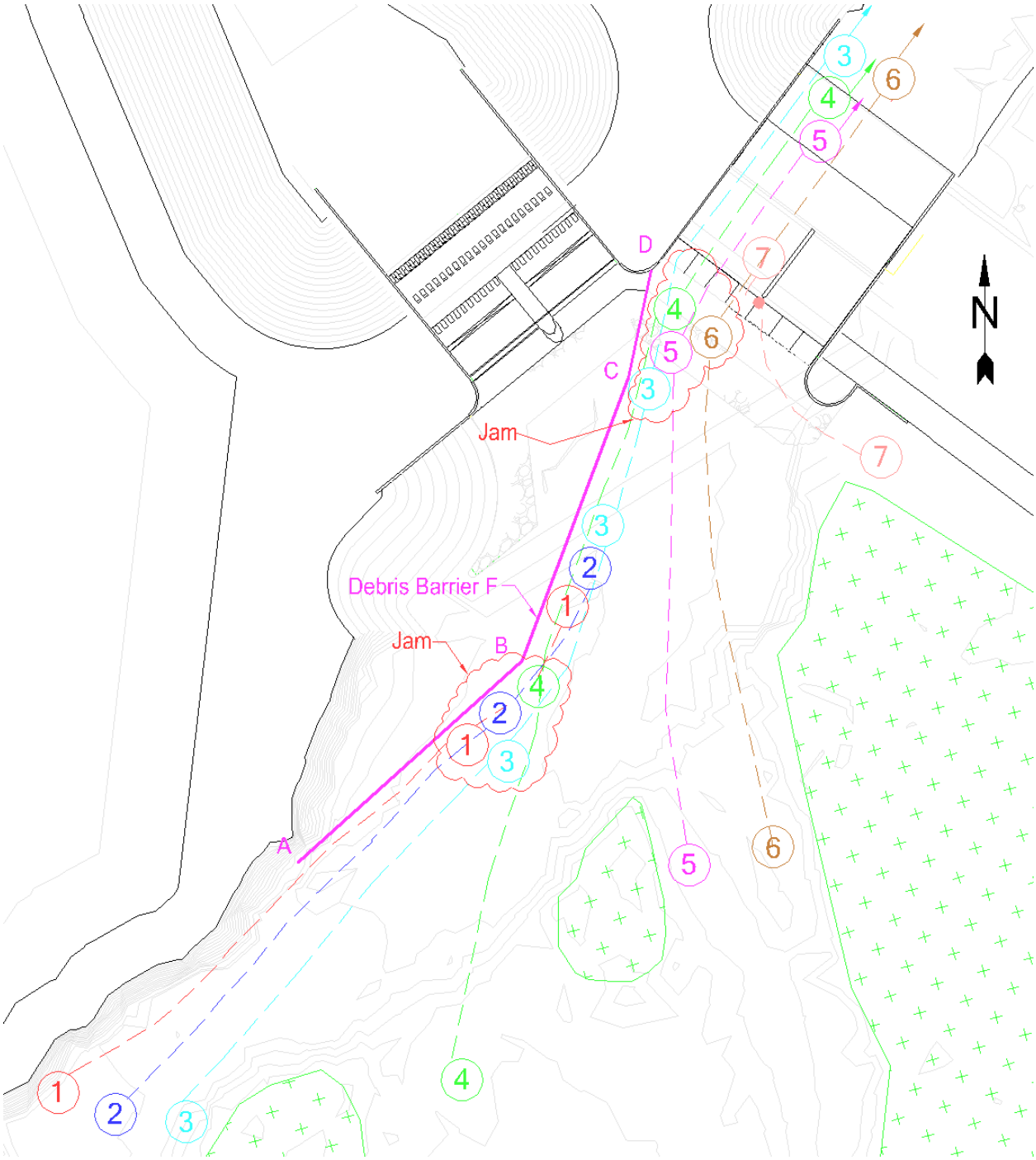

Figure 175. Debris pathways for TSH, 500m^3/s flow conditions with debris barrier F.

Debris Type	Starting Location	Debris Pathways					Notes
		Debris Barrier F Leg AB	Debris Barrier F Leg BC	Debris Barrier F Leg CD	Service Spillway LHS	Service Spillway RHS	
Singles	1	100%	-	-	-	-	Caught in leg AB
	2	50%	-	-	50%	-	50% caught in leg AB, 50% pass through
	3	50%	-	-	50%	-	50% caught in the hydraulic jump
	4	50%	50%	-	-	-	Caught in leg AB and BC
	5	-	-	-	100%	-	Trees pass thorugh
	6	-	-	-	100%	-	Trees pass thorugh
	7	-	-	-	100%	-	50% stuck in hydraulic jump
Rafts of 10	1	10%	10%	-	80%	-	40% caught in the hydraulic jump
	2	80%	-	20%	-	-	Caught on barrier and also at the SS-LHS gate
	4	20%	-	80%	-	-	Caught on barrier and also at the SS-LHS gate
	5	-	-	10%	90%	-	50% caught in the hydraulic jump
	6	-	-	-	100%	-	Trees pass thorugh
Rafts of 40	2	98%	2%	-	-	-	Large jam at leg AB
	4	100%	-	-	-	-	Caught in the debris jam at point B
	6	-	-	100%	-	-	Caught on leg CD and the SS-LHS gate

Table 37. Debris behaviour for TSH, 500m^3/s flow conditions with debris barrier F.

Figure 176. Debris caught on the upstream end of the barrier (leg AB) and protruding out into the river (left), debris caught at the downstream end of the barrier (leg BC) and on the LHS Obermeyer gate (right).

5.8.2.2 Case b – Obermeyer gates set to 1215m (LHS) and 1211.05m (RHS)

A separate case was run for the 500 m^3/s flow condition with the Obermeyer gates at the service spillway reversed – the LHS was higher (1215m) and the RHS was lower (1211.05m). This setting created a stagnation zone at the downstream end of the debris barrier in front of the raised gate on the LHS and caused more debris to collect in this location. However, the large debris jam that occurred at the upstream end of the debris barrier (leg AB) for case (a) was not as large (see Figure 177).

Figure 177. Debris caught on the upstream end of the barrier (leg AB) at the end of the Case B tests (left) and at the downstream end of the barrier (leg BC) in front of the raised LHS Obermeyer gate (right).

At the end of the tests, there was a large debris jam of approximately 130 trees collected at the downstream end of the barrier in front of the raised LHS Obermeyer gate, and a smaller number of trees (~10) caught in the upstream barrier in leg AB. Gate operations were then undertaken to try and remove the trees from the barrier. The LHS Obermeyer gate was lowered and almost all the trees from the downstream jam passed through the LHS of the service spillway. Only seven trees remained caught around the central pier between the Obermeyer gates (see Figure 178). The small number of trees in the upstream portion of the barrier (leg AB) were not affected by the any gate operations and remained caught in the upstream barrier.

Figure 178. Debris remaining caught on the dividing pier after lowering the Obermeyer gates after all of the gate operations of the 500m^3/s Case B flow condition.

5.8.3 *760 m^3/s*

As with the 500m^3/s tests, there were two tests with different gate settings for the 760m^3/s flow conditions. Case (a) had the RHS Obermeyer gate raised, and case (b) had the LHS Obermeyer gate raised.

5.8.3.1 Case a – Obermeyer gates set to 1213.4m (LHS) and 1215m (RHS)

The diversion inlet gate was in the fully raised position, and the service spillway Obermeyer gates were set to 1213.4m on the 24m wide left-hand side (LHS) and 1215m on the 18m wide right-hand side (RHS) for the case (a) tests. The setting was intended to direct 160m^3/s through the service spillway and 600m^3/s through the diversion, and this was represented well in the model (563m^3/s through the diversion inlet and 188m^3/s through the service spillway). Again, tree debris was inserted into the model in one of seven locations (1-7) as shown in Figure 179 during the tests. Table 38 shows a summary of the debris behaviour at this flow condition. The relatively larger amount of flow passing through the diversion inlet (behind the barrier) compared to the service spillway drew the woody debris into the debris barrier much more than the other flow conditions. Debris originating from the left hand side of the western floodplain (locations 1, 2 and 3) collected on leg AB. On almost the entire floodplain (locations 1-6) the debris was sucked into and pinned up against the debris barrier by the flow. Only debris inserted in the model near the floodplain berm at the RHS of the service spillway (location 7) had a significant portion pass through the service spillway. At the end of the tests much debris remained on the barrier on all three legs (see Figure 180).

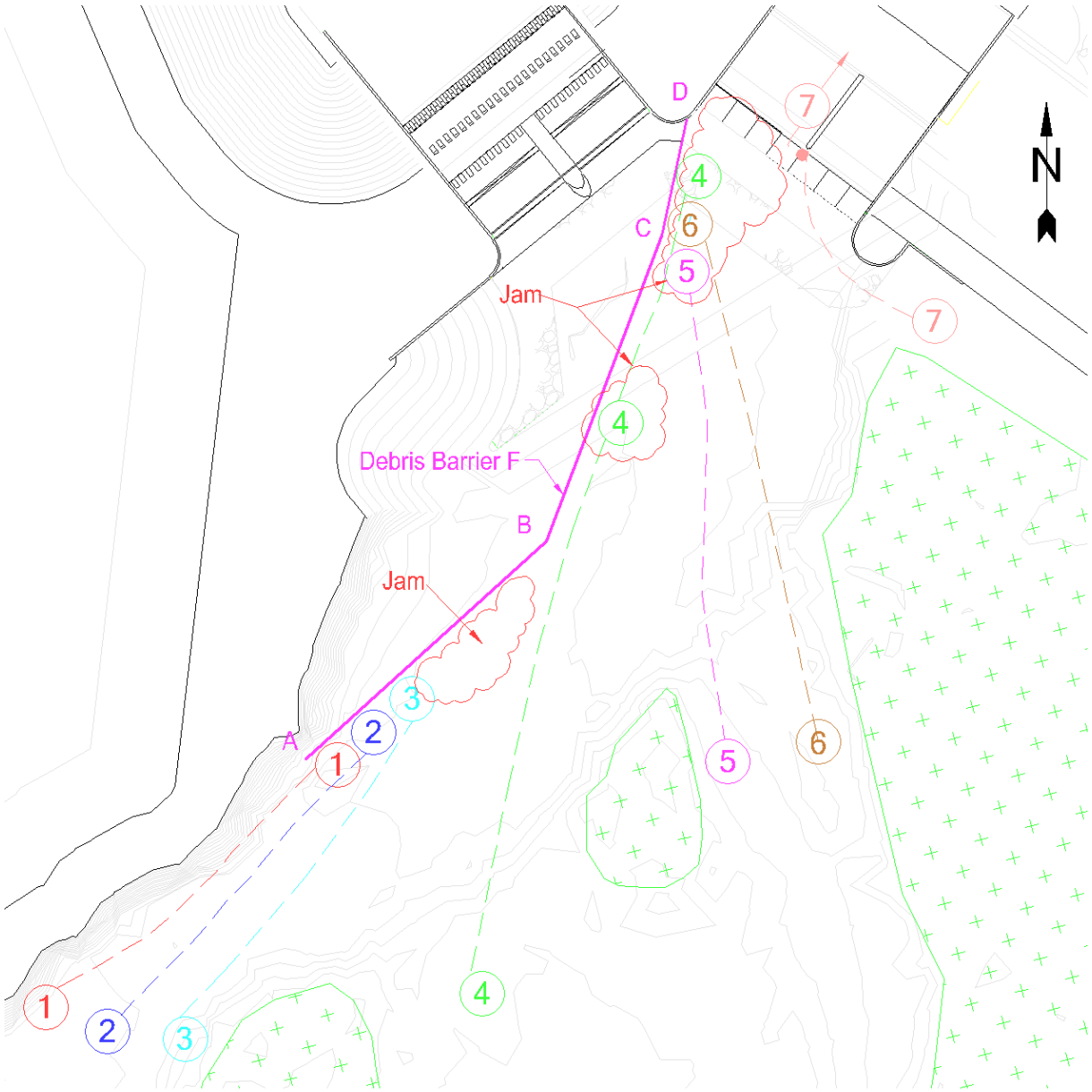

Figure 179. Debris pathways for TSH, case (a) 760 m^3/s flow conditions with debris barrier F.

Debris Type	Starting Location	Debris Pathways					Notes
		Debris Barrier F Leg AB	Debris Barrier F Leg BC	Debris Barrier F Leg CD	Service Spillway LHS	Service Spillway RHS	
Singles	1	100%	-	-	-	-	Caught in leg AB
	2	100%	-	-	-	-	Caught in leg AB
	3	100%	-	-	-	-	Caught in leg AB
	4	-	-	100%	-	-	Caught in leg CD
	5	-	-	100%	-	-	Caught in leg CD
	6	-	-	100%	-	-	Caught in leg CD
	7	-	-	-	100%	-	Trees pass thorugh
Rafts of 10	1	100%	-	-	-	-	Caught in leg AB
	2	50%	-	50%	-	-	Caught in leg AB and CD
	4	-	100%	-	-	-	Caught in leg BC
	5	-	-	100%	-	-	Caught in debris jam at spillway
	6	-	-	100%	-	-	Caught in debris jam at spillway
	7	-	-	100%	-	-	Caught in debris jam at spillway
Rafts of 40	2	100%	-	-	-	-	Caught in leg AB
	4	-	100%	-	-	-	Caught in leg BC and creates a jam
	6	-	25%	75%	-	-	Caught on leg BC and the jam at the spillway

Table 38. Debris behaviour for 760 m^3/s case (a) with debris barrier F installed in the upstream floodplain.

Figure 180. Debris left on barrier at the upstream end (left) and at the end of the barrier bridging across to the central pier in the service spillway (right).

At the end of the 760m^3/s case (a) debris tests, with the large debris raft (~100 trees) caught in front of the diversion, efforts were made to drop the diversion inlet gates as well as the LHS Obermeyer gate to try and clear the debris jam. The diversion inlet gates were lowered first and some of the debris that was caught on the Obermeyer gate was freed. Also the jams further upstream on the barrier at AB and BC floated off of the debris barrier and came further downstream. After lowering the Obermeyer almost all (~90%) of the debris trapped on the debris barrier was freed and passed through the LHS of the service spillway.

Another test was run where a similar 100-tree debris raft was allowed to build at the downstream end of barrier in front of the diversion inlet and service spillway. Then only the LHS Obermeyer gate was lowered (the diversion inlet remained open). This cleared all the debris from the barrier and passed them through the LHS of the diversion.

Yet another gate operation test was commissioned where the debris jam (roughly 100 trees) was again allowed to form at the downstream end of the barrier (in front of the diversion) and the diversion inlet gates were lowered at a specified rate (0.3m per minute, full scale) which represents typical drop gate closure rates. The pulsing wave that more rapid gate closures created in earlier tests did not occur. After approximately 8mins (full scale) approximately 75% the debris caught in the barrier was dislodged and flowed over the LHS Obermeyer gate. The LHS gate was still at 1213.4m elevation when this debris was passed. However, the flood level rose on the floodplain until it overtopped the flood berm during this gate operation. The LHS Obermeyer gate was lowered and the debris that remained on the barrier was flushed through the LHS of the service spillway.

5.8.3.2 Case b – Obermeyer gates set to 1215m (LHS) and 1213.15m (RHS)

A separate case was run for the 760m^3/s flow condition with the Obermeyer gates at the service spillway reversed – the LHS was higher (1215m) and the RHS was lower (1213.15m). In the model these gate settings produced a flow split of 553m^3/s through the diversion inlet and 200m^3/s through the service spillway. Again, with the relatively larger amount of flow directed towards the diversion inlet (and through the debris barrier) all of the debris deployed in the upstream floodplain at locations 1-6 from Figure 179 were trapped in the debris barrier. Raising the Obermeyer gate on the LHS of the service spillway, instead of the RHS as it was in case (a), served to trap even more debris as a large stagnation zone in front of the raised gate was created. At the end of the case (b) tests there were debris jams along all three legs (AB, BC, CD) of debris barrier F (see Figure 181).

Figure 181. Debris caught on the upstream end of the barrier (left) and at the downstream end of the barrier (right) in front of the raised LHS Obermeyer gate at the end of the tests.

After the debris had been deployed in the model a large debris jam of approximately 120 trees collected at the downstream end of the barrier in front of the diversion inlet and the raised LHS

Obermeyer gate, and a smaller number of trees (roughly 30) were caught in the upstream barrier in leg AB. A number of gate operations were then undertaken to try and remove the trees from the barrier. The LHS Obermeyer gate was lowered to 1210m and approximately 80 trees that were at the downstream end of the barrier drifted off and passed through the LHS of the service spillway. The diversion inlet gates were then lowered at the prescribed drop gate rate of 0.3m per minute (full scale) and none of the debris on the barrier was dislodged. The RHS Obermeyer gate was then lowered to 1210m and roughly 15 trees were removed from the downstream debris jam and passed through the LHS of the service spillway. Figure 182 shows photographs of these gate operations. Approximately 60 trees remained caught on the debris barrier after all gate operations had concluded.

Figure 182. Gate operations to removed trees caught in debris barrier F. Left – dropping the LH Obermeyer gate to 1210 removed ~80 trees from the barrier. Right – lowering the diversion inlet gates and the RH Obermeyer gate removed ~15 trees from the barrier.

5.8.4 *1240 m^3/s*

The gate settings for the 1240m^3/s flow utilized the diversion inlet gate in the fully raised position, and the service spillway Obermeyer gates set to 1210m on the 24m wide left-hand side (LHS) and 1213.5m on the 18m wide right-hand side (RHS). The setting was intended to allow 640m^3/s through the service spillway and 600m^3/s through the diversion, and these targets were reasonably produced in the model (584m^3/s through the diversion inlet and 654m^3/s through the service spillway). Model tree debris was inserted into the model in one of seven locations (1-7) as shown in Figure 183 during the tests. Table 39 shows a summary of the debris behaviour at this flow condition. For ease of description, debris barrier F was divided into legs AB, BC and CD. Debris inserted into the left hand side of the western floodplain (locations 1, 2 and 3) collected on leg AB and along this leg debris tended to tumble along the barrier coming to rest at point B. Very little debris collected on legs BC and CD during the tests. At the end of the tests, the debris jam at point B was comprised of about 50 trees, and there were 5 trees snagged in the barrier in front of the diversion inlet structure (see Figure 184).

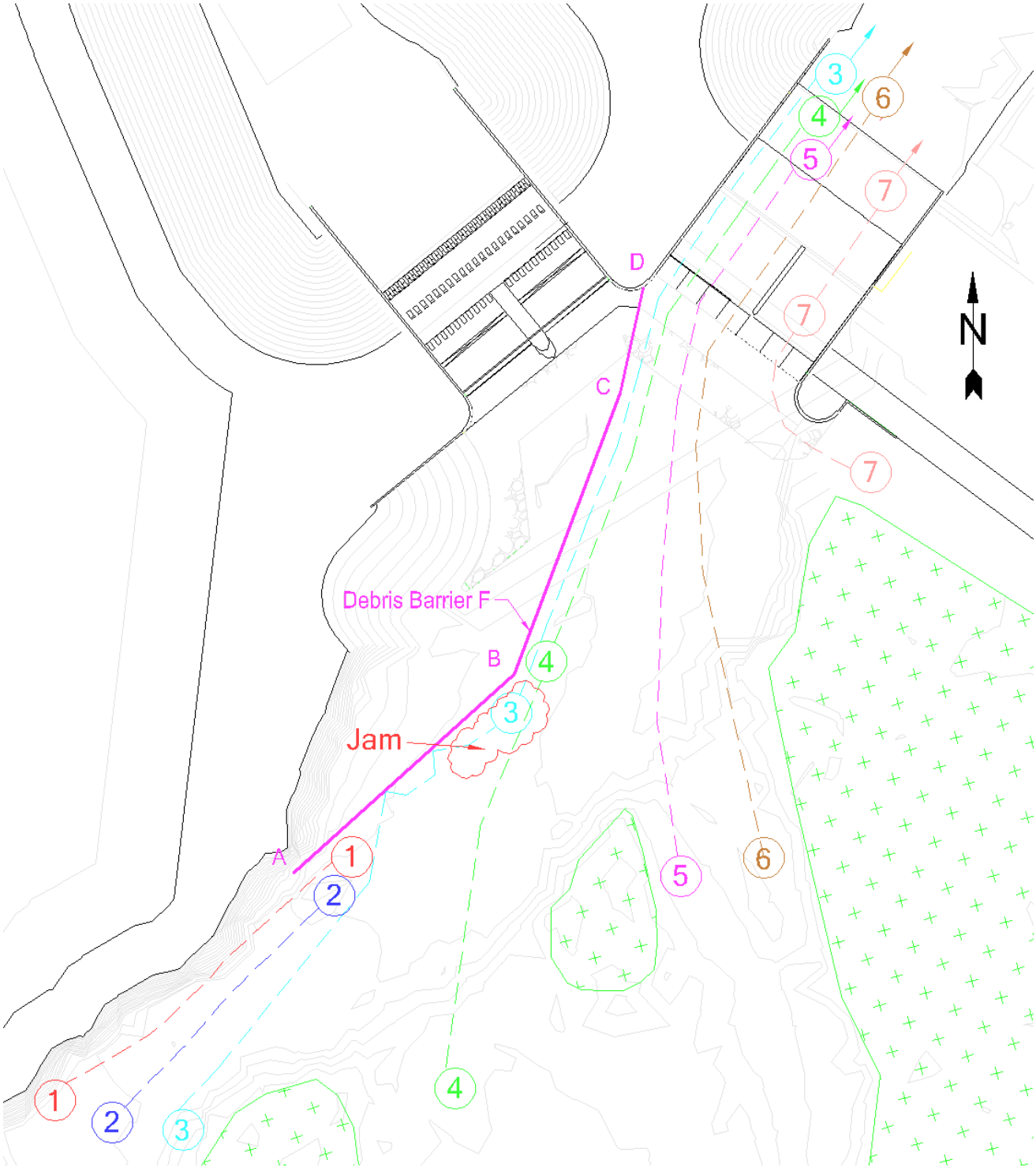

Figure 183. Debris pathways for TSH, 1240 m^3/s flow conditions with debris barrier F.

Debris Type	Starting Location	Debris Pathways					Notes
		Debris Barrier F Leg AB	Debris Barrier F Leg BC	Debris Barrier F Leg CD	Service Spillway LHS	Service Spillway RHS	
Singles	1	100%	-	-	-	-	Caught in leg AB
	2	100%	-	-	-	-	Caught in leg AB
	3	50%	-	-	50%	-	Caught in leg AB or passed through SS-LHS
	4	50%	-	-	50%	-	Caught in leg AB and BC
	5	-	-	-	100%	-	Trees pass through
	6	-	-	-	100%	-	Trees pass through
	7	-	-	-	-	100%	Trees caught in hydraulic jump
Rafts of 10	1	100%	-	-	-	-	Caught in leg AB
	2	100%	-	-	-	-	Caught in leg AB
	4	-	-	20%	80%	-	80% pass through the spillway
	5	-	-	-	100%	-	Trees pass through
	6	-	-	-	100%	-	Trees pass through
	7	-	-	-		100%	20% stuck on pier divider, 60% caught in hydraulic jump
Rafts of 40	2	100%	-		-	-	Caught at point B on leg AB
	4	10%	-	-	90%	-	Most of the trees pass through the spillway
	6	-	-	-	100%	-	100% of trees pass through

Table 39. Debris behaviour for 1240 m^3/s with debris barrier F installed in the upstream floodplain.

Figure 184. Debris jam at point B (left) and debris caught in the barrier in front of the diversion inlet structure (right) at the end of the TSH tests at 1240m^3/s.

6 ACKNOWLEDGEMENTS

The authors wish to thank and acknowledge the efforts of all NRC staff who contributed to the success of this study. In particular, the authors wish to thank Alistair Rayner, Brian Perry, Yvan Brunet, David Hnatiw, John Marquardt, Bill Gow, and Nathalie Brunette for their technical support during the construction, setup and operation of the model.

The authors also thank Rick Lux, John Menninger, Matt Wood, George Sabol, and Steve Abt from the Stantec project team, as well as Syed Abbas from Alberta Transportation, for their many important contributions to the study described in this report.

7 REFERENCES

Dean, R.G., 1985. Physical Modeling of Littoral Processes. (In *Physical Modeling in Coastal Engineering*, edited by R.A. Dalrymple), published by A.A. Balkema, Boston, USA.

Funke, E.R. and E.P.D. Mansard, 1984. *The NRCC Random Wave Generation Package*, NRC Technical Report TR-HY-002, Ottawa, Canada.

Hughes, S.A., 1993. *Physical Models and laboratory Techniques in Coastal Engineering*. published by World Scientific, New Jersey, USA.

IAHR/PIANC, 1986. *List of Sea State Parameters*. Supplement to Bulletin 52, P.I.A.N.C.

Miles, M.D., 1989. *User Guide for GEDAP Version 2.0 Wave Generation Software*. NRC Technical Report LM-HY-034. Ottawa, Canada.

Miles, M.D., 1990. *The GEDAP Data Analysis Software Package*. NRC Technical Report TR-HY-030. Ottawa, Canada.

Miles, M.D., 1997. *GEDAP Users Guide for Windows NT*. NRC Technical Report HYD-TR-021. Ottawa, Canada.

Vanoni, V.A., 1975. *Sedimentation Engineering*. American Society of Civil Engineers, Manual No. 54.

8 APPENDIX A – ELECTRONIC ARCHIVE

See electronic archive.